

THE UNIVERSITY OF HULL

The Design, Synthesis and Mesomorphic Properties of
Discotic Liquid Crystals

being a Thesis submitted for the Degree of Doctor of Philosophy

in the University of Hull

by

Philip Jeffrey Stackhouse MChem(Hons) PGDip AMBCS AMInstP MRSC

July 2008

Summary of Thesis Submitted for the Degree of Ph.D.

by

Philip Jeffrey Stackhouse MChem(Hons) PGDip AMBCS AMInstP MRSC

on

The Design, Synthesis and Mesomorphic Properties of Discotic Liquid Crystals

Discotic liquid crystal research is now more than 30 years old, however it is still early days compared with the well-established area of calamitic liquid crystal research which dates back for more than a century. Since the 1990's there has been great deal of interest in discotic liquid crystal research, due to applications such as discotic compensation films for enhancing liquid crystal display (LCD) viewing angles and exciting new potential applications such as organic semi-conductors and photovoltaics.

The work contained in this thesis can be broken down into three major areas: investigation of synthetic methodologies of hexasubstituted triphenylene-based discotic liquid crystals, examination of structure-property relationships within novel triphenylene-based discotic liquid crystalline materials, and the design and mesomorphic properties of novel disc-shaped molecular architectures.

The investigation of the synthetic methodologies of triphenylene-based liquid crystals examined two main areas of the synthesis of triphenylene-based discotic materials: iodination reactions to generate valuable intermediates, and the oxidative strategies and methods for the generation of hexasubstituted triphenylenes. These investigations have revealed that careful control over reaction conditions can offer great selectivity in the synthesis of halogenated intermediates for the synthesis of triphenylene-based liquid crystals and that electron rich intermediate species offer the greatest scope for the synthesis of hexasubstituted triphenylenes in good yield and purity.

The determination of structure-property relationships within triphenylene-based discotic liquid crystals has examined various peripheral substituents and various near-core modifications to the conventional discotic liquid crystal.

A small number of novel spiral-shaped materials have been synthesised, which have revealed interesting mesomorphic properties. These materials have shown the ability to self-organise in such a manner as to fill free space around central disc units so as to generate columnar mesophases in materials which would not otherwise be expected to exhibit mesomorphism.

Acknowledgements

I wish to thank my supervisor, Dr Mike Hird for his guidance, support, encouragement and enthusiasm throughout my Ph.D. programme. I am extremely grateful for the many insightful discussions that we have had on various aspects of chemical synthesis, liquid crystal research and his advice concerning the preparation of various poster presentations, papers and this thesis.

I would also especially like to thank all members past and present of the Liquid Crystals & Advanced Organic Materials research group at the University of Hull, both past and present, especially Dr R. Lewis, Mrs J. Haley, Dr K. Fergusson, Dr C. Wilson, Dr D. Wilson, Dr G. Mehl, Dr D. Lacey, Dr L. Cseh, Dr R. McDonald, Mr I. Radini, and Dr A. Stipetic for their expertise, encouragement, support, friendship and countless discussions on both chemistry and non-chemistry related matters! I also wish to thank Mr C. Hope of the Inorganic and Magnetic Materials research group for his friendship and similar discussions on chemistry (and non-chemistry) related issues.

I would like to express my gratitude to Miss E. Wong, and Mr C. Hine for their valuable assistance during their final year research projects.

This programme of research would not have been possible without the financial support of the EPSRC and the excellent facilities and staff of the Department of Chemistry at the University of Hull, for all of which I am extremely grateful. I especially wish to thank the technical staff of the Department of Chemistry for their assistance regarding various analytical measurements.

Finally I would like to express my eternal gratitude to my family, particularly my parents. Without their constant, unwavering and unconditional support my education, and consequently this programme of research and indeed this thesis, would not have been possible.

Many thanks to you all, for you are truly the *sine qua non*.

Publications and Presentations

The following publications and presentations have included work which is contained within this thesis:

- P.J. Stackhouse and M. Hird, “Influence of Branched Chains on the Mesomorphic Properties of Symmetrical and Unsymmetrical Triphenylene Discotic Liquid Crystals”, *Liq. Cryst.*, 2008, **35**, 5, 597-607.
- P.J. Stackhouse, “Synthesis and Properties of Triphenylene Discotic Liquid Crystals”, *Departmental Research Colloquia*, University of Hull, 2007.
- P.J. Stackhouse and M. Hird, “Synthesis and Properties of Novel Symmetrical and Unsymmetrical Hexa-substituted Triphenylenes”, *21st Annual British Liquid Crystal Society Conference*, Sheffield, 2007.
- P.J. Stackhouse and M. Hird, “Synthesis and Properties of Novel Spiral-shaped Molecular Architectures”, *Dendrimer Soft Self-assembly Systems DENSOM Euro-conference*, Oberni, France, 2006.
- P.J. Stackhouse and M. Hird, “Synthesis and Properties of Novel Spiral-shaped Molecular Architectures”, *20th Annual British Liquid Crystal Society Conference*, York, 2006.
- P.J. Stackhouse and M. Hird, “Selected Methodologies for the Synthesis of Disc-shaped Systems”, *20th Annual British Liquid Crystal Society Conference*, York, 2006.

Contents

1	Introduction	1
1.1	History of Liquid Crystal Research	1
1.2	Introduction to Liquid Crystals	4
1.2.1	Calamitic and Bent-core Systems	9
1.2.1.1	Nematic Phase (N)	11
1.2.1.2	Smectic Phases (Sm)	11
1.2.1.3	Bent-core Liquid Crystals	13
1.2.2	Chirality	14
1.2.2.1	Chirality in Liquid Crystals	15
1.2.3	Discotic Liquid Crystals	21
1.2.3.1	Background	21
1.2.3.2	Mesomorphism in Disc-shaped Structures	21
1.2.3.3	Structure-property Relationships of Disc-shaped Systems	29
1.3	Identification and Characterisation of Mesophase Morphology	34
1.3.1	Polarised Optical Microscopy (POM)	34
1.3.2	Differential Scanning Calorimetry (DSC)	35
1.3.3	X-Ray Diffraction (XRD)	36
1.4	Applications of Liquid Crystals	37
1.4.1	Chiral Nematic and Temperature Sensitive Materials	37
1.4.2	Liquid Crystal Displays	38
1.4.3	Electricity Conduction and Generation	42
2	Aims and Objectives	46
3	Experimental	50
3.1	Instrumentation and Materials	50
3.1.1	Nuclear Magnetic Resonance Spectroscopy (NMR)	50
3.1.2	Gas Chromatography (GC)	51
3.1.3	Mass Spectrometry (MS)	51
3.1.4	Elemental Analysis (EA)	51
3.1.5	High Performance Liquid Chromatography (HPLC)	51
3.1.6	Polarised Optical Microscopy (POM)	52

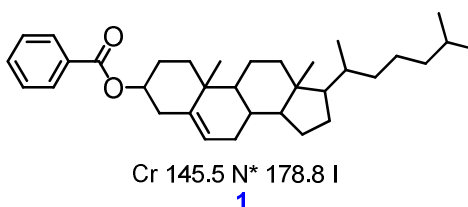
3.1.7	Differential Scanning Calorimetry (DSC)	52
3.1.8	Column Chromatography	52
3.1.9	Thin Layer Chromatography (TLC)	53
3.2	Schemes	54
3.3	Experimental Procedures	69
3.4	Discussion of Synthetic Routes and Methodologies	121
3.4.1	Benzene-based Disc-shaped Systems	121
3.4.2	Iodination Reactions to Generate Valuable Intermediates	123
3.4.3	Spiral-shaped Systems	125
3.4.4	Synthesis of Alkoxytriphenylenes	128
3.4.5	Triphenylene-banana Combinations	134
3.4.6	Terminal Acetylenes	136
3.4.7	Cyclohexanes	137
3.4.8	Esters and Ethers of Triphenylene	138
3.4.9	Coupling Reactions	140
4	Results and Discussion	141
4.1	Investigation of Synthetic Methodologies	141
4.1.1	Iodination Reactions	141
4.1.2	Synthesis of Hexaalkoxytriphenylenes	145
4.2	Mesomorphic Properties of Materials	153
4.2.1	Spiral-shaped	153
4.2.2	Triphenylene-based Materials	160
4.2.2.1	Unbranched Open Alkoxy Chains	160
4.2.3	End-group Modifications of Hexa-substituted Triphenylenes	164
4.2.3.1	Branched Alkoxy Chains	164
4.2.3.2	Terminal Acetylenes	170
4.2.3.3	Cyclohexanes	178
4.2.3.4	Ethers	182
4.2.3.5	Terminal Fluoro Substituents	184
4.2.4	Near-core Modifications of HAT6	187
4.2.4.1	Acetylenes	187
4.2.4.2	Miscellaneous Near-core Modifications	191

5	Conclusions and Summary.....	198
5.1	Synthetic Methodologies.....	198
5.1.1	Iodination Reactions.....	198
5.1.2	Synthesis of Hexaalkoxytriphenylenes	198
5.2	Mesomorphic Properties of Materials	200
5.2.1	Spiral-shaped.....	200
5.2.2	Triphenylene-based Materials.....	200
5.2.2.1	Unbranched Open Alkoxy Chains	200
5.2.3	End-group Modifications of Hexa-substituted Triphenylenes.....	201
5.2.3.1	Branched Alkoxy Chains	201
5.2.3.2	Terminal Acetylenes	202
5.2.3.3	Cyclohexanes	203
5.2.3.4	Ethers	203
5.2.3.5	Terminal Fluoro Substituents.....	204
5.2.4	Near-core Modifications of HAT6.....	204
5.2.4.1	Acetylenes.....	204
5.2.4.2	Miscellaneous Near-core Modifications.....	204
6	References.....	206

1 Introduction

1.1 History of Liquid Crystal Research

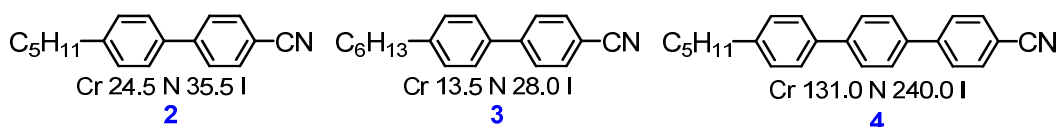
During the 19th century researchers began reporting unusual “double melting” and “double refracting” phenomena.¹ One such early discovery was by Virchow in 1855 whilst working with nerve fibre Myeline,² which was later reported by Mettenheimer to be double refracting¹ and another discovery by Heintz in 1855, who noticed that stearin melted to a cloudy fluid at 52 °C, which became opaque at 58 °C, and a clear liquid at 62.5 °C.^{1, 3} These observations probably marked the discovery of liquid crystalline substances, but they were not recognised as such. In 1888 a botanist, Reinitzer, noticed that cholesteryl benzoate (**1**), melted to a “turbid but absolutely fluid liquid” at 145.5 °C which “suddenly became clear” at 178.8 °C.^{1, 4, 5}



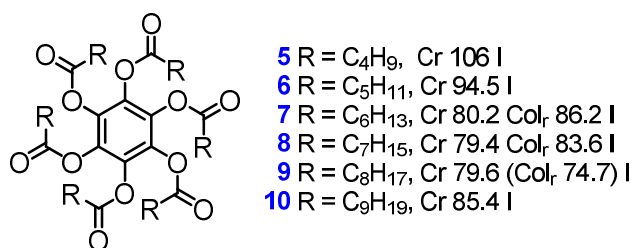
Reinitzer, upon discovering the unusual melting behaviour of compound **1**, contacted a physicist, Lehmann, who had developed a polarising microscope. Lehmann discovered that compound **1** was exhibiting a uniform phase of matter, eliminating the possibility of solid and liquid phases occurring simultaneously. Lehmann subsequently authored a paper entitled “*Über fließende Krystalle*” (“On flowing Crystals”), which inspired the use of the term “liquid crystals”.^{6, 7} From this point on there was an interest in liquid crystals, albeit mostly academic in nature. Some research did occur, however, and the most prolific researcher of the time was Vorländer, who undertook a vast programme of research (more than 2000 compounds) which was aimed at determining basic structure-property relationships in liquid crystals.^{8, 9} Vorländer’s research led to many interesting new discoveries *e.g.* the understanding that molecular shape was important to liquid crystal phase generation, room temperature liquid crystalline materials, and ‘banana’ liquid crystals, since several compounds he synthesised exhibited banana phases, although they were not recognised as such at the time.^{10, 11}

Friedel, who believed the term “liquid crystal” to be misleading, introduced the term mesomorphic and a new classification system of liquid crystals in 1922.¹² Optical microscopy had revealed that there was more than one type of mesomorphism and hence Friedel proposed the terms: nematic, smectic, and cholesteric, which have since been refined, however they are still broadly in use today.¹²⁻¹⁴

Between 1920 and 1940 the first X-ray experiments were conducted upon mesomorphic materials which provided a definitive model of mesophase structure.¹⁵ By the end of World War II, however, liquid crystal research had virtually disappeared, in part due to the lack of perceived applications and reductions in funding.^{8, 13} During the 1960’s and 1970’s, however, there was a resurgence of liquid crystal research due to the lure of new applications. This research period was dominated by Gray who made many discoveries, e.g. the first stable room temperature nematic liquid crystal that could be used in a display device (e.g. 2-4), and with Goodby, the current classification of smectics (into true smectics: A, B, C, F and I and crystal smectics: B, E, G, H, J, and K).^{8, 9, 16-18}



During the 1960’s and 1970’s the increase in liquid crystal research brought about further theories regarding the molecular shape of liquid crystals, including the theory that disc-shaped molecules could exhibit mesomorphism.¹³ Such mesomorphism had actually already been observed by Backer and Van der Baan when they synthesised hexa-*n*-alkanoates of benzene (1937)¹⁹ and Eaborn and Jackson when they synthesised diisobutylsianediol (1952)^{20, 21}. However, the mesomorphic behaviour of these compounds were not recognised until the 1980’s.²¹



The first recognised reports of disc-shaped compounds to exhibit mesomorphic behaviour came in 1977 when Chandrasekhar, working with hexa-esters of benzene (*e.g.* compounds **5-10**), noted that they could form columnar mesophase structures.^{22, 23} Since the discovery of mesomorphic behaviour in disc-shaped architectures by Chandrasekhar, such mesomorphic behaviour has been reported in more than three thousand different compounds and based upon more than fifty different core units.^{24, 25} A large portion of this research has occurred within the last few years, since it has been driven, in part, by the use of discotic compensation films in opto-electronic devices and the lure of potential new technologies, such as organic semi-conductors and organic solar cells (described in Section 1.4).²⁴

1.2 Introduction to Liquid Crystals

Prior to Reinitzer's momentous discovery of liquid crystalline phases, states of matter were restricted to: solid, liquid and gas (Figure 1.1). The crystalline (solid) state is the most ordered of the states of matter, with long range positional and orientational ordering of the constituent molecules, which vibrate around a central point. Upon heating a crystalline solid the thermal energy imparted increases the motions of the molecule until the motions are sufficient to break the forces of attraction which hold the crystalline solid together and the material melts into the liquid phase. In the liquid phase, the constituent molecules are free to rotate, vibrate and flow; they no longer possess any positional or orientational ordering, and thus are described as isotropic (from the Greek 'isos' meaning equal, since the liquid phase has the same physical properties when measured from any direction). Heating material in the liquid phase causes further increases in the vibrations and motions of the molecules until such time that the material reaches its boiling point, and boils to the gaseous phase. In the gaseous phase, the most disordered of the phases of matter, there are fewer constituent molecules in a given volume than any of the other states of matter.

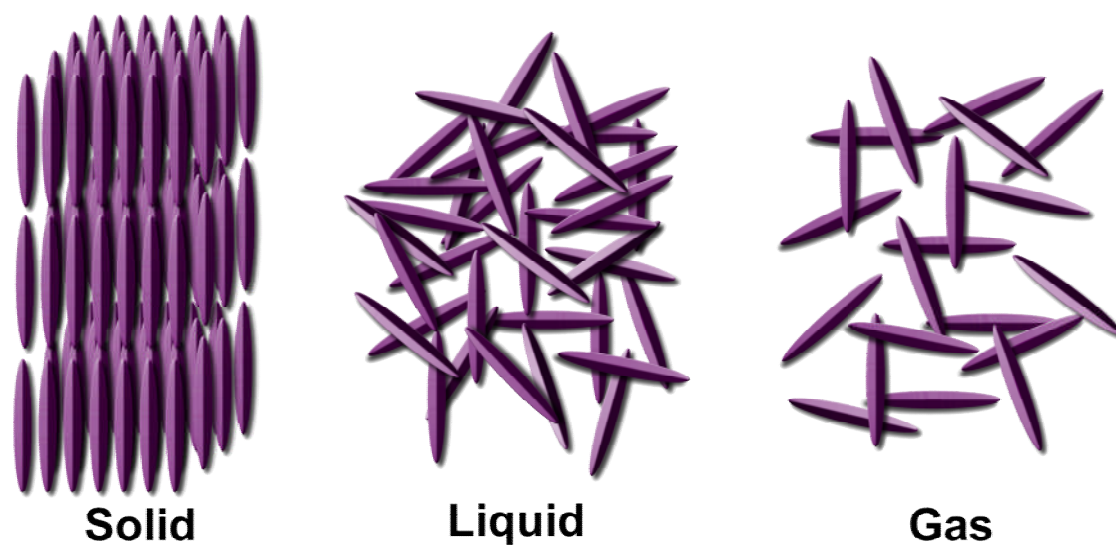


Figure 1.1: Molecular arrangements within the three common states of matter

This simplistic view is not universal, however, carbon dioxide, for example, does not exhibit the liquid phase; it bypasses the liquid phase and sublimates (*i.e.* changes directly from the solid to the gaseous state upon heating). Other physical properties of materials

do not follow this simplistic pattern either, for example deoxyribonucleic acid (DNA) has the ability to self organise when it replicates, which is not a property which is possible in the crystalline solid or isotropic liquid states.²⁶ Cell membranes consist of a lipid bilayer, which also cannot follow this simplistic pattern, since if skin cell membranes were in the crystalline state then movement would be impossible and if they existed in the isotropic liquid state then there would be no cohesive force holding a person together, and thus people would exist as puddles.^{26, 27} Cell membranes and DNA, therefore, exhibit some of the physical properties that are usually associated with a crystalline solid and those of an isotropic liquid simultaneously, thus they exhibit an intermediate phase of matter.^{27, 28} Clearly DNA and cell membranes are significantly different than cholesteryl benzoate (**1**, mentioned earlier) which exhibited an intermediate phase of matter in between the solid and liquid phases upon heating, this is due to the wide ranging nature of the materials termed as ‘liquid crystals’.¹³

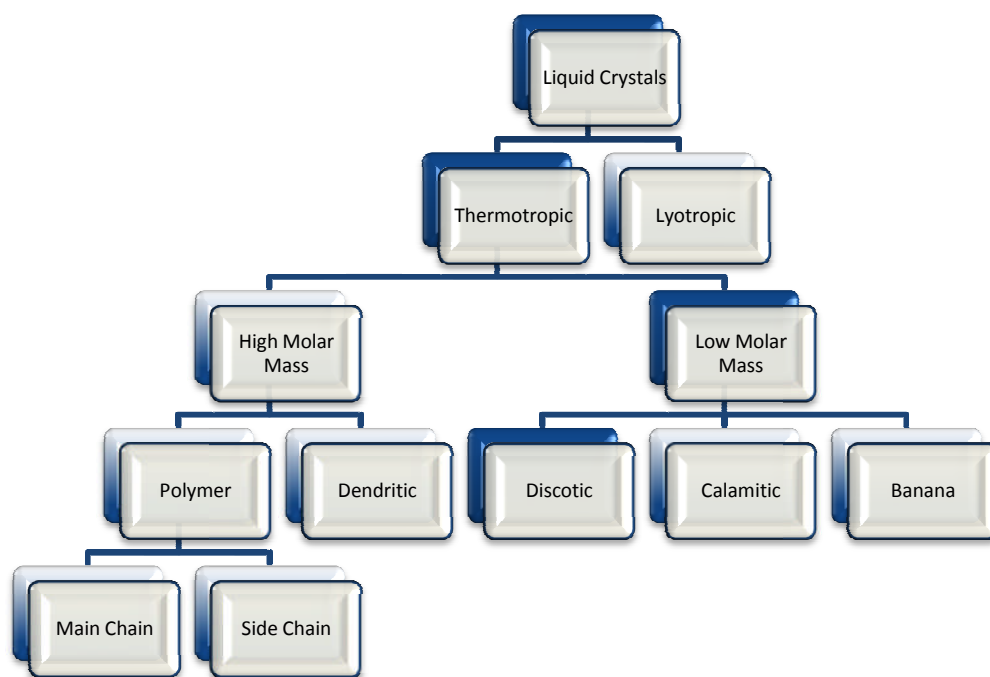


Figure 1.2: Classification of liquid crystals

Figure 1.2 shows a breakdown of the classifications of liquid crystals. The main two types of liquid crystals are lyotropic (from the Greek ‘*luein*’ meaning ‘to loosen’) and thermotropic (from the Greek ‘*thermos*’ meaning ‘hot’).^{14, 29} The mesomorphic behaviours of lyotropic liquid crystals are controlled by the concentration of a material

in a solvent,^{14, 29} examples of which include DNA, cell membranes, and soap.²⁷ The mesomorphic behaviours of thermotropic liquid crystals, however, are controlled by temperature.^{14, 29} The classification of thermotropic liquid crystals can be further subdivided into high molar mass and low molar mass materials. This thesis is concerned with low molar mass thermotropic liquid crystals, and thus will concentrate on such from this point on.

Liquid crystalline behaviour can arise from various different types of molecule; however, the molecular shape (as defined by the volume of space in which the molecule rotates or vibrates) is, as was noted by Vorländer, extremely important. Generally, the shape of a molecule that can give rise to liquid crystalline behaviour will usually be: rod-like (calamitic, from the Greek ‘*kalami*’ meaning ‘reed’)¹⁸, disc-like (discotic)³⁰, banana-like (calamitic, but with a bent core)³¹, wedge-shaped¹³, or ‘T’-shaped¹³.

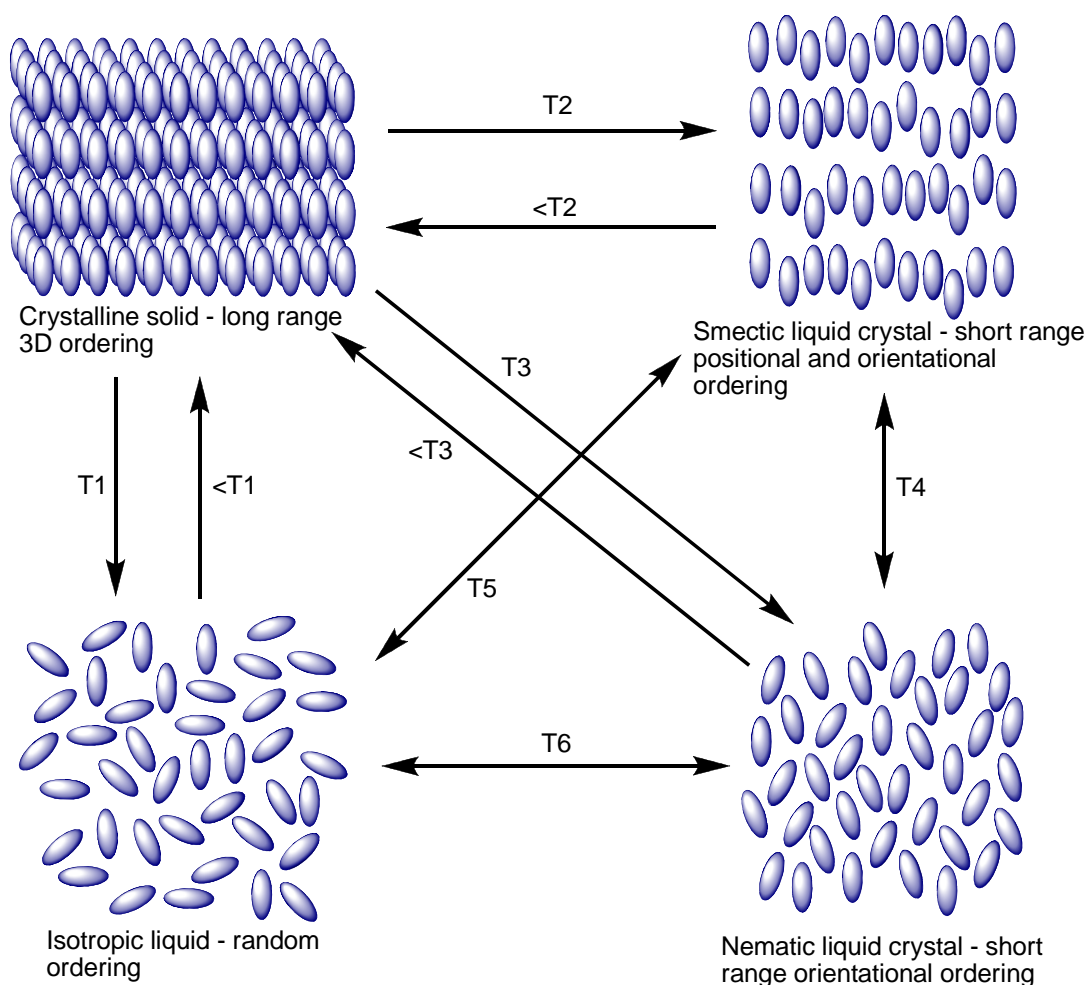


Figure 1.3: Possible transitions of thermotropic calamitic liquid crystals

Since mesomorphic (from the Greek '*mesos*', meaning 'middle') behaviour occurs in between that of the perfectly ordered crystalline solid and the completely disordered isotropic liquid, the possible transitions that mesogenic compounds exhibit becomes somewhat more complex than the simple solid/liquid/gas transitions described earlier. Figure 1.3 illustrates some of the possible phase transitions that a calamitic liquid crystal can undergo. If the compound is non-mesogenic, then the material will melt to the isotropic liquid (T1), and the material will recrystallise at a temperature lower than the melting point ($<T1$), due to supercooling (metastable molecular state, whereby due to kinetic motion the molecules do not fall into the crystalline state)^{32, 33}. Upon heating if the energy imparted is sufficient for the molecules to break the terminal forces of attraction, but not lateral attractions (T2, due to stronger lateral attractions), a layered structure forms (smectic liquid crystal, described in greater detail in Section 1.2.1), and the molecules will statistically 'point' in the same direction (possess orientational order). The preferred direction in which the molecules will tend to align themselves is known as the 'director' (n).¹⁴ Upon heating of the material (T4), the lateral forces of attraction are broken, and the layered structure breaks down, but orientational order remains (nematic liquid crystal, described in greater detail in Section 1.2.1). Heating the material to the point where the orientational order is lost (T6) the material forms the isotropic liquid (termed the 'clearing point').¹⁴ Liquid crystal transitions (*e.g.* T4, T5 and T6), do not undergo the process of supercooling, and thus are said to be 'reversible' (within *ca* 0.5 °C).¹³ Since not every material exhibits all of the possible mesophases, a mesogenic compound can undergo transition straight from the crystalline solid to the nematic phase (T3), or clear into the isotropic liquid phase from a smectic phase (T5). If the aforementioned phase transitions occur at a temperature above the melting point of the material, then the transition is termed 'enantiotropic' (from the Greek '*enantios*', meaning 'opposite').¹⁴ If the phase transition occurs at a temperature *below* the melting point of the material but prior to recrystallisation (*i.e.* due to supercooling), then the transition is said to be 'monotropic'.¹⁴

The thermal behaviour is not the only unusual behaviour of liquid crystals. Due to the nature of the mesophases, which possess some level of order (orientational or positional), they are anisotropic fluids.²⁸ It is easy to understand how this anisotropy can arise, since the molecules themselves are anisotropic, Figure 1.4 shows an example of a calamitic liquid crystalline compound and a discotic liquid crystalline compound, and

shows how the length of the compounds and the width of the compounds are significantly different.²⁸

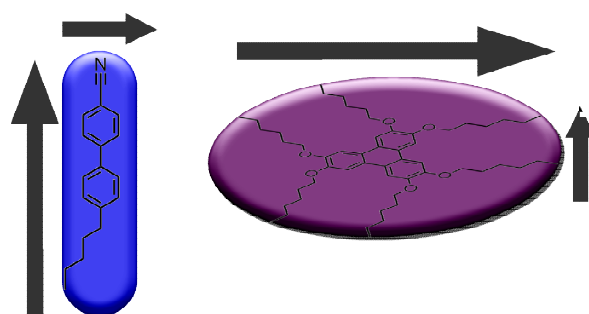


Figure 1.4: Molecular anisotropy

Molecular anisotropy leads to many other forms of anisotropic behaviour. One such anisotropic behaviour of liquid crystals is in the optical behaviour of the material. Such optical anisotropy is known as ‘birefringence’.¹³

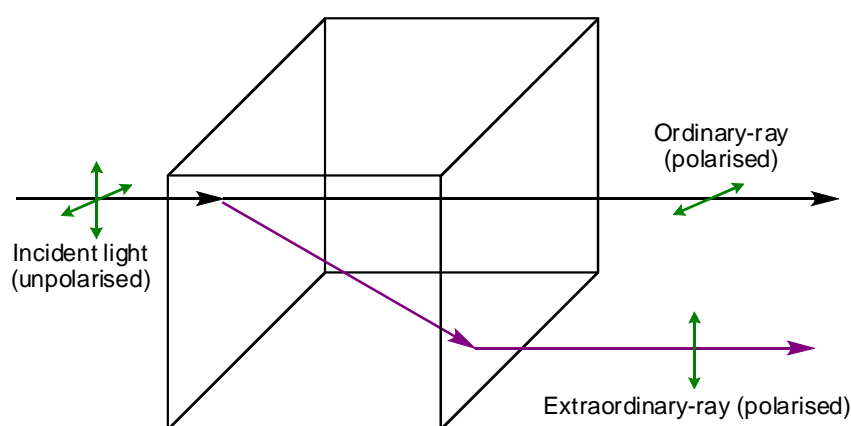


Figure 1.5: Behaviour of light travelling through a birefringent medium

The phenomenon of birefringence is well known in solid materials, where anisotropy is common, and the process is essentially the same in liquid crystals. Light can be thought of as a transverse wave of electromagnetic energy which is made up of fluctuating electric and magnetic fields, which are perpendicular to one another.³⁴ When light enters a birefringent substance (Figure 1.5), the light is broken up into its constituent components, one of which will travel parallel to the director, and the other will travel perpendicular director.³⁴ Thus, since the molecules in the material are anisotropic (Figure 1.4), the two constituent components of the light (the fast, “ordinary” or “o” ray,

and the slow “extraordinary” or “e” ray) travelling through the material will travel at different velocities, thus when the two waves are recombined as they exit the material they are no longer in phase with one another.³⁵

The refractive indices of the ordinary ray and extraordinary ray can be calculated, thus:

$$n_o = \frac{c}{v_{\perp}} \qquad n_e = \frac{c}{v_{\parallel}}$$

where c is the speed of light through a vacuum and v is the velocity of light travelling perpendicular (\perp), or parallel (\parallel) to the orientation of the molecules through which the light is travelling.³⁵ Hence, the birefringence of a material can be calculated, thus:

$$\Delta n = n_e - n_o \quad 35-37$$

For calamitic materials the value of the birefringence is typically positive, however for discotic materials, this value is usually negative, since the molecules are arranged in an orientation which is perpendicular to that of calamitic molecules (*i.e.* the long and short axes are reversed, see Figure 1.4).³⁸ This reversal of the effect upon birefringence has important implications upon the applications of liquid crystals in optoelectronic devices, and is elaborated further in Section 1.4.

Another physical property that is crucially affected by the anisotropic nature of liquid crystals is the dielectric permittivity (ϵ).³⁶ The dielectric permittivity of a compound is a measure of interaction of a permanent or induced electrical dipole of the compound with an electrical field, thus compounds which contain groups which induce strong dipoles, such as cyano or fluoro substituents, will interact strongly with an applied electric field.^{13, 34} The anisotropic nature of liquid crystalline materials means that the permittivity of a compound will be different when measured perpendicular (\perp), or parallel (\parallel), to the director. Thus the dielectric anisotropy is calculated as follows:

$$\Delta\epsilon = \epsilon_{\parallel} - \epsilon_{\perp} \quad 13, 34, 36$$

The dielectric anisotropy of a material is highly important for display devices, where the ability to switch the orientation of a molecule, and to do so at high speed when an electrical field is applied, is essential. Thus, large magnitudes (either positive or negative depending on the application) of $\Delta\epsilon$ are extremely important.^{13, 34}

1.2.1 Calamitic and Bent-core Systems

Calamitic liquid crystals were the first thermotropic mesogenic materials to be discovered and, as already been mentioned, it was soon noted that there was more than one type of mesophase.¹² Indeed, there is a rich polymorphism that can be exhibited by

materials which are in between the crystalline and liquid phases. The most observed of these mesophases are the nematic and (various) smectic phases (as represented in Figure 1.6).¹³

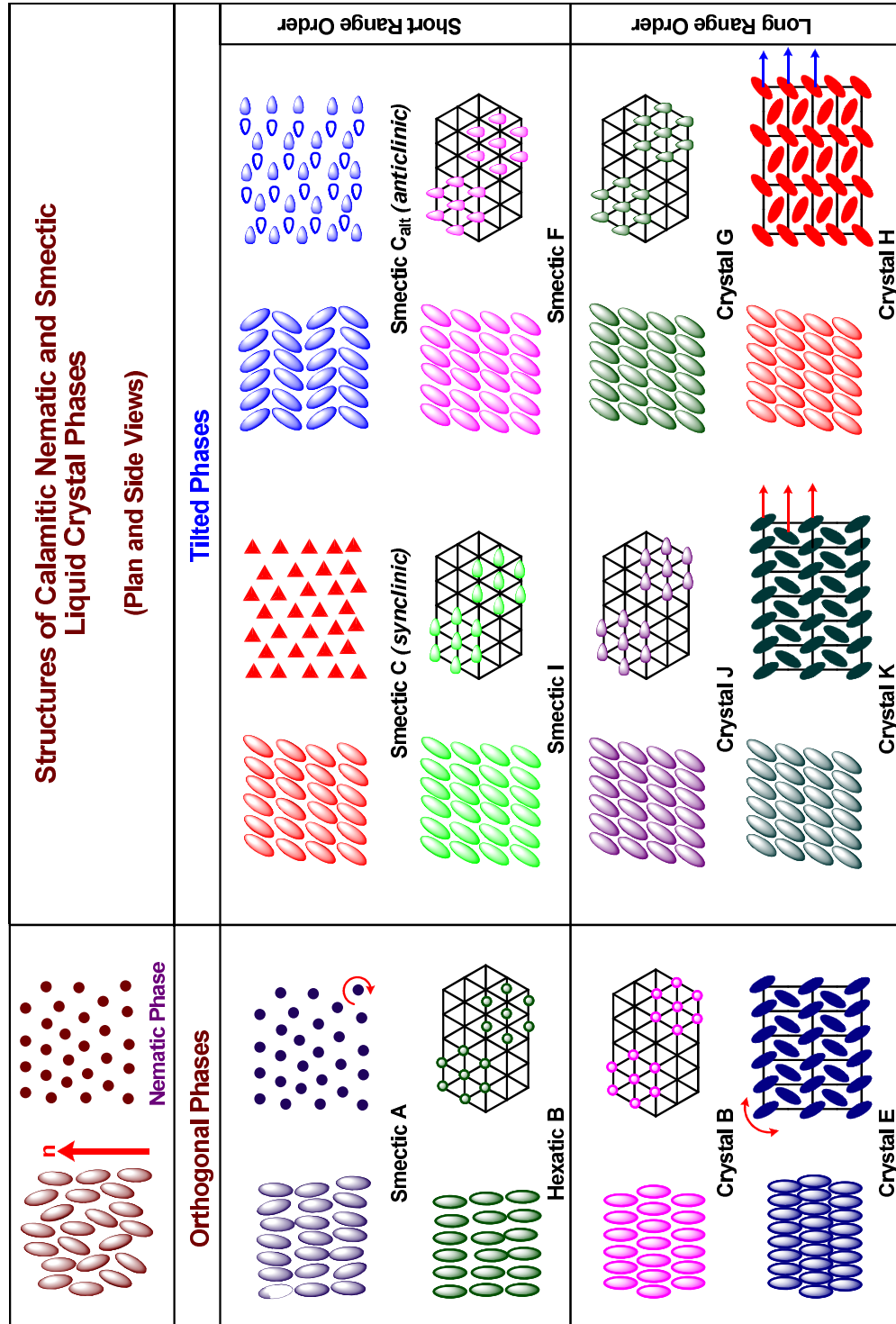


Figure 1.6: Representation of the nematic and smectic phases, modified from reference³⁹

1.2.1.1 Nematic Phase (N)

The nematic mesophase (from the Greek '*nêma*' meaning 'thread', since thread-like textures are observed during optical microscopy) is the least ordered, and the simplest of all mesophases.¹³ Molecules in the nematic mesophase are, on average, orientationally ordered, *i.e.* they point in the same direction (along the director, *n*), and they possess no long-range positional order (Figure 1.7).^{13, 14} Due to the uniaxial nature of the ordering in the nematic phase, only one nematic phase is possible.¹³ Molecules in the nematic phase possess $D_{\infty h}$ spatial symmetry.¹⁴

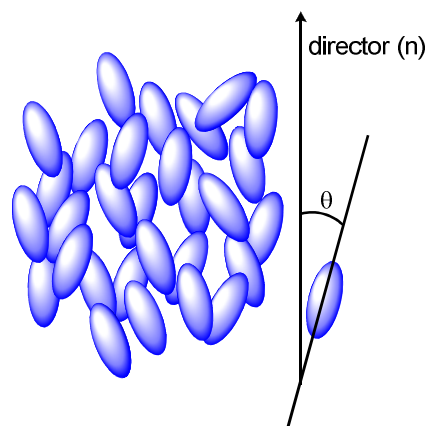


Figure 1.7: Molecular organisation in the nematic mesophase

The extent of orientational order of a mesophase can be expressed in terms of the *order parameter* ($\langle P_2 \rangle$), and is calculated as follows:

$$\langle P_2 \rangle = \frac{3 \langle \cos^2 \theta \rangle - 1}{2}$$

where $\langle \rangle$ denotes an average over many molecules at the same time, an order parameter of $P_2 = 1$ denotes a perfectly ordered system, and $P_2 = 0$ indicates an extremely disordered system.^{13, 14}

For the nematic mesophase, typical values for the order parameter are approximately 0.4-0.7.¹³

1.2.1.2 Smectic Phases (Sm)

Smectic mesophases (from the Greek '*smêchô*' meaning 'soap', since smectic-like phases were first observed in soap) were named in the order in which they were discovered, hence the first smectic discovered was termed smectic A, the second smectic B, *etc.*¹³ Smectic mesophases possess both orientational and (some) positional

ordering.¹⁴ This short-range positional ordering permits polymorphism within the classification of smectics, since there are many ways in which positional ordering can be achieved in a layered structure. The smectic phases have since been sub-divided into the “true smectics” (A, B, C, I, and F), which are mesophases with layered structures and liquid-like properties (*i.e.* liquid crystals), and the crystal “pseudo smectics” (B, E, G, J, K), which are mesophases which possess long-range positional molecular ordering and three-dimensional correlation between layer stacks, but possess less order than a crystalline solid (*i.e.* they are “soft” crystals, not liquid crystals).^{8, 14, 29} The two most widely observed smectic mesophases are the smectic A and the smectic C phases.

Smectic A (SmA)

The SmA phase is the least ordered of the smectic mesophases and can be considered to be a two-dimensional liquid.¹⁴ The mesophase consists of layers of molecules, with the long molecular axis perpendicular to the layers (*i.e.* the director is parallel to the layer normal, Figure 1.8), and is characterised as possessing $D_{\infty h}$ spatial symmetry.^{13, 14, 40, 41}

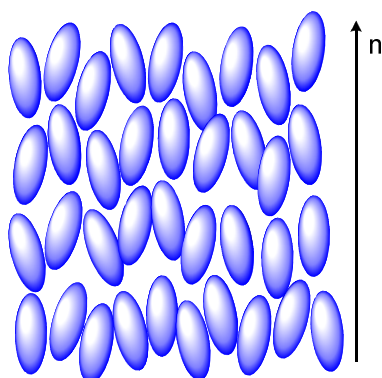


Figure 1.8: Molecular organisation of the SmA mesophase

Smectic C (SmC)

The SmC mesophase is similar to the SmA phase, with molecules arranged into layers and the molecules within each layer are approximately parallel to one another. Unlike the SmA phase, however, the director is tilted with respect to the layer normal, this difference in angle between the director and the layer normal is known as the ‘tilt angle’ (θ , Figure 1.9).^{13, 14, 40, 41} The magnitude of the tilt angle is the same in each individual layer; however, the tilt direction varies randomly between layers.¹⁴ The tilt angle is temperature dependant, and as the temperature increases, the tilt angle decreases, thus a

compound can exhibit both the SmA and SmC mesophases.³⁰ The tilt angle also means that the overall layer spacing is usually less than the overall length of the constituent molecules, thus if the temperature is reduced, the tilt angle increases and the layer spacing decreases.

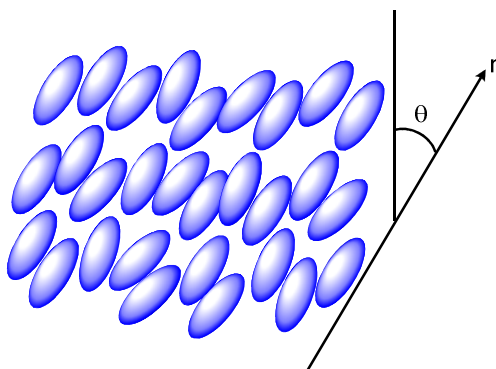


Figure 1.9: Molecular organisation of the SmC mesophase

The SmC phase structure possesses C_{2h} monoclinic spatial symmetry.^{30, 42}

1.2.1.3 Bent-core Liquid Crystals

Recently (1996) it has been recognised that molecules that possess a bent molecular core can exhibit mesomorphism where previously it had been believed that only rod-like and disc-like structures could give rise to mesomorphism.^{43, 44} Such structures were originally investigated by Vorländer, however, the significance of their mesomorphic behaviours was overlooked.¹¹ Today, however, bent-core or banana-shaped, liquid crystals are well-recognised for their mesomorphic properties. To date, eight ‘banana phases’, named B_1 through B_8 , have been discovered and, like smectic mesophases, the ‘B’ nomenclature was derived from the order in which they were discovered.^{44, 45} Of the eight banana phases, the B_1 and B_2 phases are the most-often observed.

B_1 Phase

The B_1 phase is identified *via* a mosaic-like texture during optical microscopy, and possesses liquid-like properties.^{14, 44, 46, 47} Since its initial discovery, the B_1 phase has subsequently been characterised as a columnar (Col) structure, either oblique (Col_{ob}), or rectangular (Col_r) in nature (Col_{ob} and Col_r are further described in Section 1.2.3.2).^{44, 47}

B₂ Phase

The B₂ phase is probably the most commonly observed of all of the B phases. The B₂ phase is a liquid-like mesophase consisting of a layered structure of tilted molecules (Figure 1.10), and as such, is related to the SmC mesophase.^{44, 47} Recently the B₂ phase has been further refined, defining the phase structure as SmCP_A, SmC_SP_A, SmC_AP_A, *etc.* depending upon various factors, including the orientation of molecules within the phase. However, these definitions are beyond the scope of this thesis.^{47, 48}

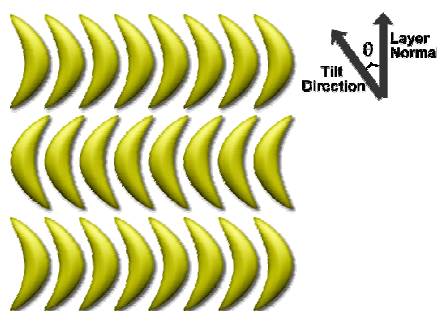


Figure 1.10: Molecular organisation of the B₂ mesophase

1.2.2 Chirality

Chirality is, by definition, the ability to exist as two (left and right) ‘handed’ structural forms.^{32, 33} This definition arises since the simplest and most observed example of chirality is the left and right hands of the human body. Hands are mirror images of one another and as such, the two ‘images’ are non-superposable (*i.e.* when superimposed the images do not coincide throughout their entire extent). In organic chemistry, this phenomenon can arise from having four different substituents bonded to a single carbon atom, a simple example of which is illustrated in Figure 1.11 where, as it can easily be seen, at best only two of the substituents can be matched should the two images be superimposed upon one another.^{49, 50} The two enantiomers of a chiral compound are often referred to as ‘optical isomers’ since they have opposing effects upon the rotation of plane polarised light, *i.e.* if one enantiomer rotates plane polarised light in one direction, then the other enantiomer will rotate light to the same magnitude in the opposite direction.^{49, 50} In a 1:1 ratio (racemic mixture), the optical effects of the two enantiomers will cancel out, and there will be no rotation of the polarised light.^{49, 50}

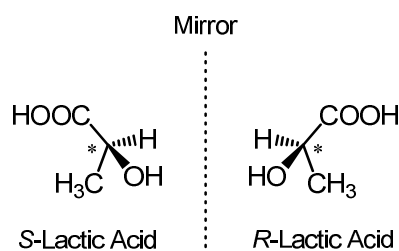


Figure 1.11: Simple example of a chiral compound

The phenomenon of chirality in organic chemistry is often vitally important, which is most easily exemplified by the case of thalidomide. Thalidomide is a chiral compound, and as such exists in two structural forms, one of which is an excellent sedative (the *R*-form) and can be used to great effect in treating a range of conditions, including morning sickness in pregnant women.^{49, 51} The other structural form of thalidomide (the *S*-form), however, has significant teratogenic effects and was responsible for significant birth defects in children of women that took thalidomide during their pregnancies in the 1950's.^{49, 51} Crucially, a single enantiomer of thalidomide will racemise *in vivo* via a presently unknown mechanism, thus the effective use of a single enantiomer is impossible.^{49, 51}

1.2.2.1 Chirality in Liquid Crystals

Chirality has significant influence in organic chemistry; it is no surprise, therefore, that the incorporation of a chiral unit can greatly affect the properties of an observed mesophase. Incorporation of a chiral unit can be accomplished by one of two methods: including a chiral moiety in the molecular structure of a liquid crystalline compound, or doping an achiral liquid crystalline (host) material with a chiral substance (*i.e.* to produce a mixture).¹³

Chiral Nematic (N*)

The chiral nematic mesophase was originally designated as the cholesteric phase, since the mesophase was initially observed in cholesterol derivatives, such as cholesteryl benzoate (**1**).^{13, 14, 29, 37} The term 'chiral nematic', however, is more accurate since it is descriptive of the phase structure, which is a nematic phase that is comprised of chiral materials.^{13, 14, 29, 37} The incorporation of a chiral unit causes a slight and gradual rotation of the director in the chiral nematic phase, and thus a helical structure is

generated.^{13, 14, 37} This effect is illustrated in Figure 1.12, however it should be noted that the illustration is simplified somewhat since the phase does not consist of layers as depicted; rather, it is a continuous change.³⁷

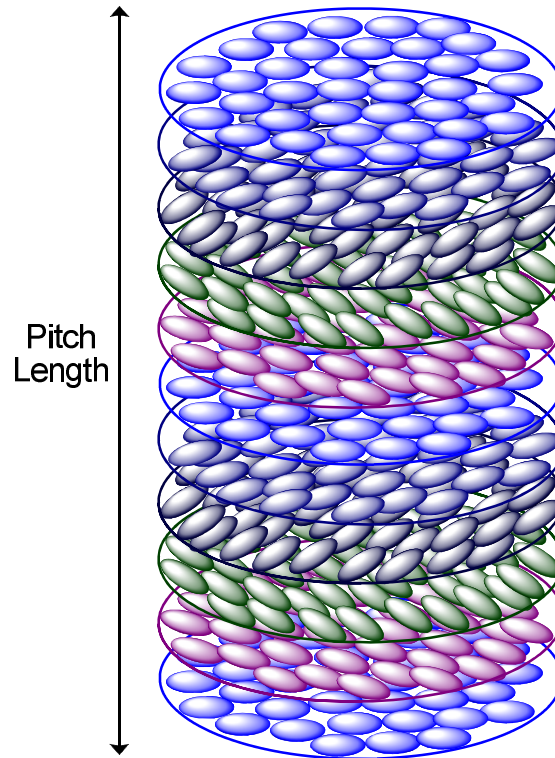


Figure 1.12: Representation of the helical structure of the N* phase

As is depicted in Figure 1.12, the pitch length is the distance required to rotate the director through 360°, although since the direction of the director (+n or -n) is arbitrary, the phase structure effectively repeats itself every 180°. ¹⁴ The pitch length is dictated by several different factors, including the nature of the liquid crystalline material (or chiral dopant) present and, crucially, temperature. ^{13, 37} High temperatures cause the director to rotate to a greater degree, thus reducing the pitch length and creating a tighter pitch and *vice versa*. ^{28, 37} This change in pitch length is highly important, since the pitch length is proportional to the wavelength of reflected electromagnetic energy according to the formula:

$$\lambda = \langle n \rangle P^{14, 37}$$

where λ is the wavelength, $\langle n \rangle$ is the mean refractive index and P is the pitch length. ^{14,}

³⁷

Thus, at an appropriate pitch length, the reflected wavelength of light could be in the visible region, and in addition, as the temperature increases the concurrent reduction in pitch length causes shorter wavelengths of light to be reflected.²⁸ This effect has significant implications for applications of liquid crystals, which are discussed later in Section 1.4.

Chiral Smectic C (SmC*) and Sub-phases

As was previously mentioned the SmC mesophase possesses the C_{2h} point group. When a chiral unit is introduced to the molecule, however, the SmC* loses symmetry operations, and as such is reduced to the C_2 point group (Figure 1.13).^{28, 37, 42} This reduction in symmetry is due, in part, to the packing of the chiral units, whereby they can only pack effectively in the phase structure with like-groups in the same direction.^{28, 37, 42} This enforced packing and reduced symmetry confers a dipole to the phase, since the net polarisation can only act in one axis (Figure 1.13), this effect is termed the ‘spontaneous polarisation’ (Ps).^{28, 37, 42}

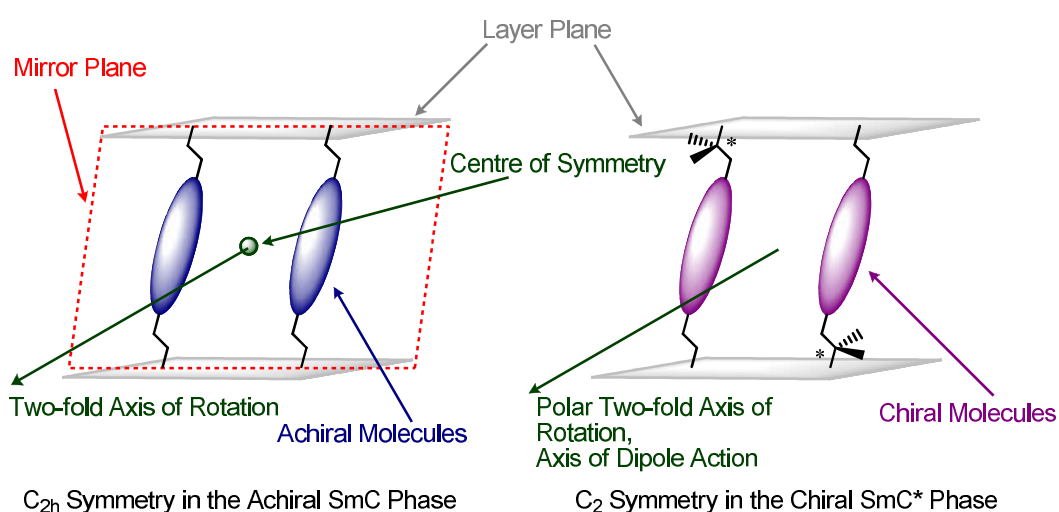


Figure 1.13: Symmetry of the SmC and SmC* phases

Just as the asymmetry in the molecular structure caused a gradual rotation of the director in the chiral nematic phase, the asymmetry in the structure of the smectic C phase also causes a rotation of the director when this asymmetry is translated to the bulk phase structure.^{13, 37, 42} This twist in the director leads to the generation of a helical structure, similar to the chiral nematic phase, although it is inherently more complex

due to the tilted, layered nature of the smectic C phase structure, hence generating the helical chiral smectic C (SmC^*) phase.^{13, 37, 42} This phase structure is illustrated in Figure 1.14, however, for clarity only one molecule per layer is shown, also illustrated is the direction of polarisation which, naturally, rotates just as the director does.^{13, 37, 42} This gradual rotation of the polarisation vector (Figure 1.13) means that the overall polarisation throughout the bulk of the phase cancels itself out, hence the overall polarisation is zero, and hence the SmC^* is classed as ‘helielectric’ rather than ferroelectric.¹³

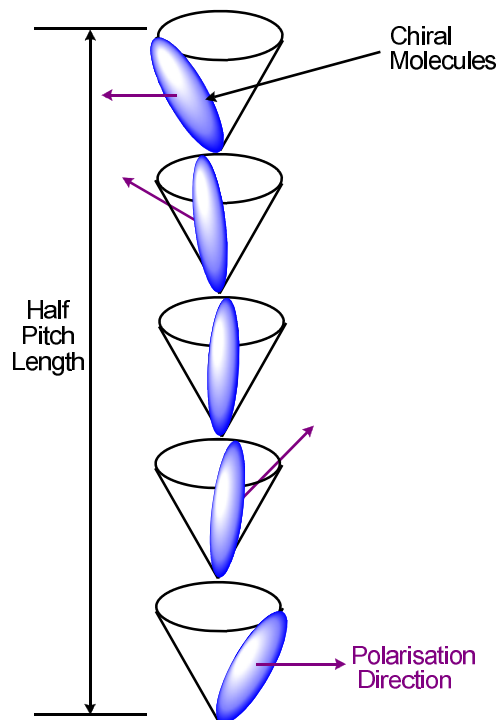


Figure 1.14: Representation of the SmC^* phase

Although the overall polarisation of the SmC^* phase is zero, each layer in the phase structure has a polarisation associated with it. If, therefore, the helical structure of the SmC^* phase is unwound, it is possible to generate a polarised phase since the polarisation is no longer being cancelled out by the constantly changing direction of the polarisation vector.¹³

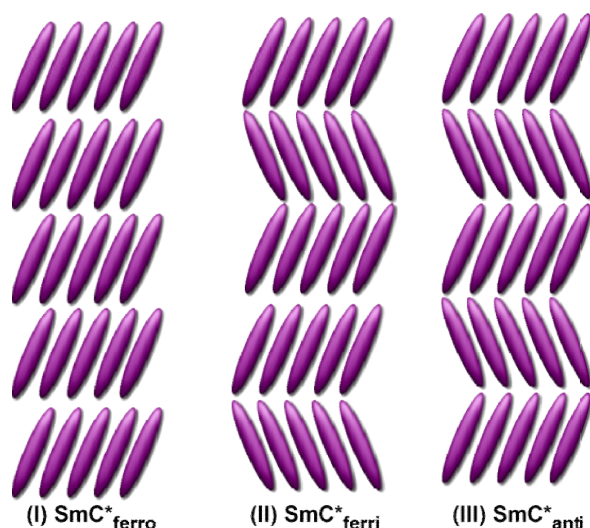
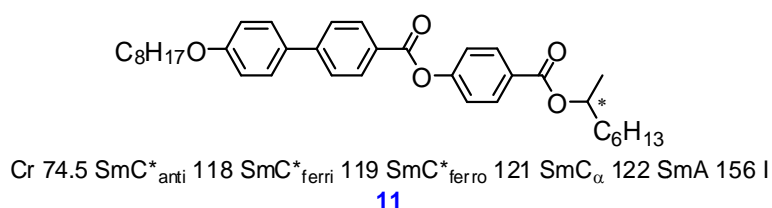


Figure 1.15: Structures of the ferro-, ferri-, and antiferro-electric SmC* phases

Unwinding the helix of the SmC* phase can give rise to three possible sub-phases (Figure 1.15): the ferroelectric (SmC*_{ferro}), the ferrielectric (SmC*_{ferri}), and the antiferroelectric (SmC*_{anti}).^{13, 37} The ferroelectric phase (SmC*_{ferro}, Figure 1.15 I), arises when the tilt direction of the molecules within the layers is the same, thus generating an overall polarisation.^{13, 37} The ferrielectric phase (SmC*_{ferri}, Figure 1.15 II), is an intermediate phase, between the ferro- and antiferro-electric phases. The tilt direction of molecules within the layers of the ferrielectric phase alternates between layers, but not to any equal extent, thus there is a higher proportion of layers pointing in one orientation, leading to an overall polarisation (but lower than that of the corresponding SmC*_{ferro} phase).^{13, 37} The antiferroelectric phase (SmC*_{anti}, Figure 1.15 III), arises when the direction of the tilt of the molecules within the layers alternates diametrically from layer to layer, which leads to a net polarisation of zero, since the polarisation difference between the layers cancels each other out.^{13, 37} It is possible for a single compound to exhibit all of these SmC* sub-phases, as is the case with 1-methylheptyl 4-(4'-octyloxybiphenyl-4-carboxyloxy)benzoate (MHPOBC, **11**).¹³

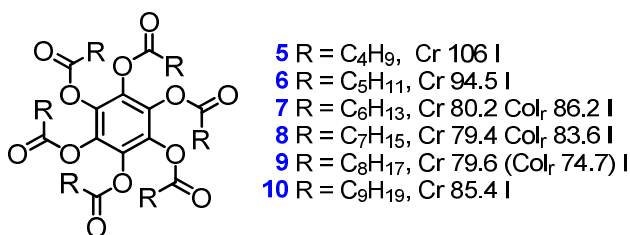


The ferro-, ferri-, and antiferro-electric phases exhibit different properties when exposed to an electrical field, for example, the Ps can couple to a direct current electric field, producing two switched states, and permits the molecules in the phase to rotate relative to the direction of the applied field.¹³ These electronic effects give rise to the possibility of device applications (especially display devices), although the specifics of such devices are beyond the scope of this thesis.

1.2.3 Discotic Liquid Crystals

1.2.3.1 Background

Originally it was believed that only rod-like structures could give rise to mesomorphism. During the 1970's, however, a change in thinking led to the first disc-like structures to be investigated for their mesomorphic properties.^{13, 38} As a consequence, Chandrasekhar discovered the mesomorphic properties of several hexaesters of benzene (compounds **5-10**).²²



The basic thinking behind the theory of why disc-shaped mesomorphism arises is not that dissimilar to that of rod-shaped liquid crystals, in that the mesomorphic behaviour arises since one molecular axis is significantly larger than the others.^{13, 38} This molecular anisotropy was illustrated in Figure 1.4, where it was also shown that the long axis of a disc-shaped system is different than that of a rod-shaped system.

1.2.3.2 Mesomorphism in Disc-shaped Structures

Just as calamitic molecules can exhibit various types of mesomorphism, discotic molecules can also exhibit various different types of mesomorphism. Disc-shaped molecules typically exhibit nematic or columnar mesomorphism, which are comparable to the nematic and smectic phases which are exhibited by calamitic systems.

Discotic Nematic (N_D, or N)

The discotic nematic phase is directly comparable to the nematic phase of calamitic systems. Like its calamitic analogue, the N_D phase is the least ordered and least viscous of all mesophases that can be generated by discotic molecules and possesses the same symmetry (hence the subscript 'D' is somewhat redundant, but is used continuously in this thesis for consistency and completeness).^{13, 14, 30, 52, 53} The phase consists of disc-shaped molecules (or portions of macromolecules) aligned with their symmetry axes

parallel to one another, with a random spatial distribution of their centres of mass (Figure 1.16).^{13, 14, 30, 52, 53} The phase is characterised in the same manner as the N phase of calamitic molecules, *via* a Schleiren texture during optical microscopy, although since the director in the N_D phase is orthogonal to the statistical orientation plane of the molecules (see Figure 1.16), as opposed to parallel to it as in the N phase (see Figure 1.7), optical effects (*e.g.* birefringence) are of opposing vector.^{13, 14, 38, 46} The N_D phase is completely immiscible with the N phase of calamitic molecules (due to the opposing molecular orientation relative to the respective directors), and it is possible to generate the N_D mesophase from non-discotic molecules (*e.g.* some phasmidic compounds, organic salts and oligosaccharides have been shown to exhibit the N_D mesophase).^{13, 14}

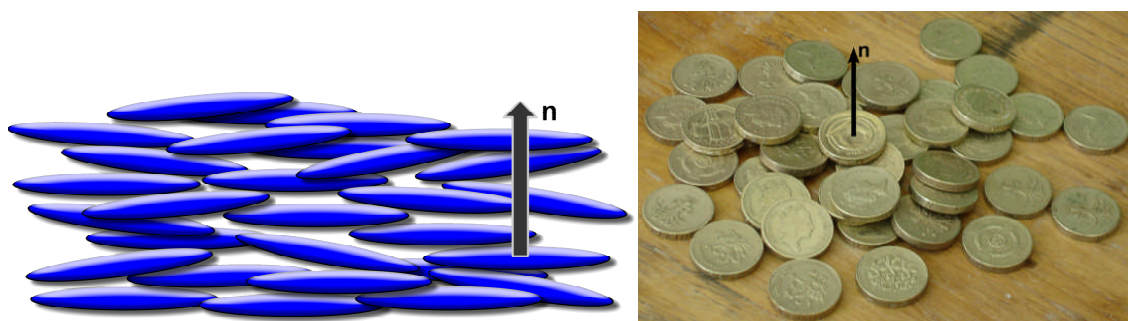


Figure 1.16: Representations of the N_D mesophase of discotic molecules

Chiral versions of this phase have been discovered which, just like its calamitic analogue, possesses a twist to the director, thus generating a helix as is illustrated in Figure 1.17; once again, the diagram is simplified since the phase does not actually consist of layers as depicted, but is rather a continuous phase.^{13, 25, 38} The major difference between the helices of the N_D^* and N^* phases is the orientation of the molecules, since the director of the calamitic and discotic molecules are orthogonal relative to one another (*cf.* Figure 1.7 and Figure 1.16).^{13, 14, 25, 54}

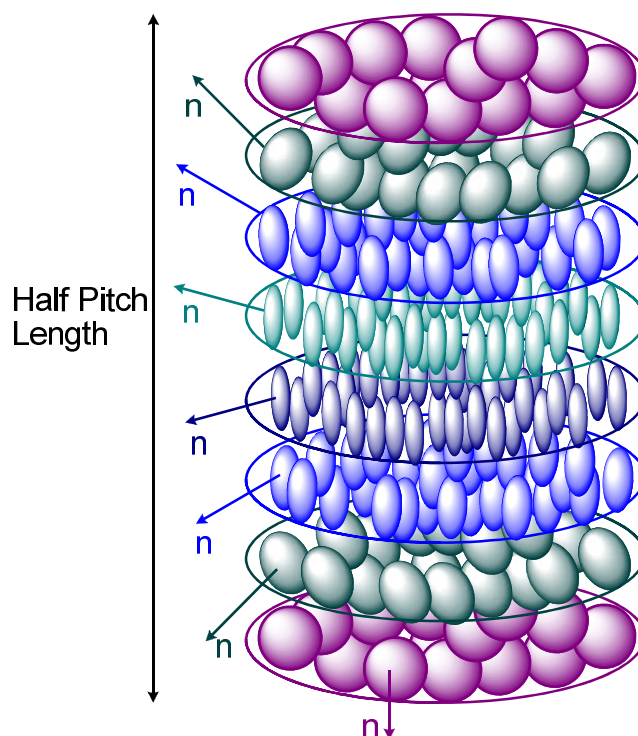


Figure 1.17: Representation of molecular ordering in the N_D^* phase

Columnar Mesomorphism

Columnar mesomorphism, like smectic mesomorphism in calamitic systems, is polymorphic, *i.e.* there are several different types of columnar mesomorphism. The basic columnar structure of any columnar mesophase, however, tends to arise from the same structural effect of the stacking of large core areas on top of one another to form a singular column (this is slightly different for non-discotic materials which form columnar mesophases).^{24, 25, 47, 48} In columnar mesophases, the molecules are stacked in a one dimensional fashion, and often form into a two dimensional lattice of several columns, which lack long-range positional ordering along the columns (although localised effects can lead to occasional short-range positional ordering).^{13, 14, 30, 38} Due to the arrangement of the columnar structures on a two-dimensional lattice, the symmetry classes, which depend on the level of order, permit several different columnar packing possibilities: hexagonal, rectangular, and oblique.^{13, 14, 30, 38}

The individual columns that are formed in a columnar mesophase can exhibit several different levels of order within the columns.²⁴ These levels of order are, however, not discrete since overall the columns are liquid-like, and the levels of order are an artefact of the correlation lengths within the stack of the column *i.e.* the deviation from the perfectly-ordered columnar structure.^{14, 25, 29, 38} These levels of ‘sub-ordering’ can be

affected by temperature, and hence do not reflect a separate state of matter, simply a difference in the correlation lengths within the column.^{14, 24, 25, 29, 38} The main levels of ‘sub-ordering’ that have been identified in columnar structures are (in decreasing levels of order): helical (most often generated from chiral materials), plastic, ordered, and disordered (Figure 1.18).²⁴

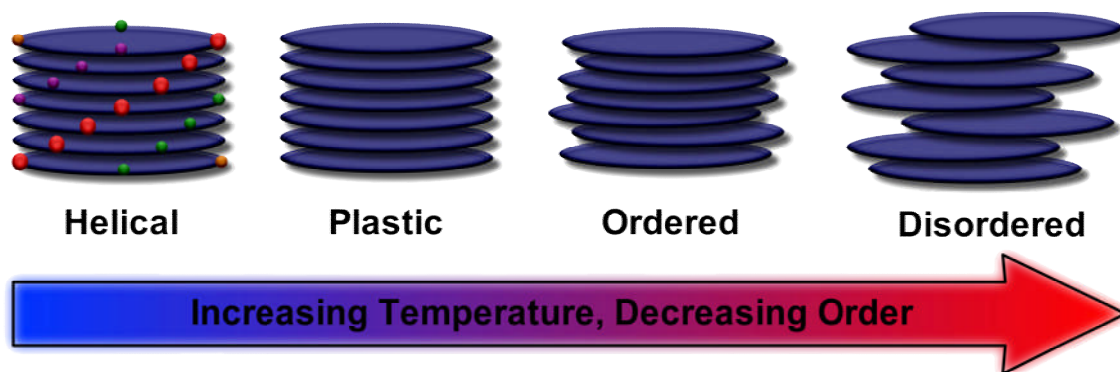


Figure 1.18: Levels of order within a singular column

It was originally believed that only disc-shaped molecules could give rise to such columnar structures, and hence, the classical names for the columnar phases were “discotic” (D) phases.^{13, 29, 52, 53} It has been shown, however, that other molecular architectures can give rise to columnar-style mesomorphism, the most obvious example of which is banana-shaped molecules which exhibit the B₁ mesophase, which is actually a variant of a columnar structure (either rectangular or oblique, as described later in this section).⁴⁷

Columnar Nematic (N_{Col})

The least ordered of all possible arrangements of columnar structures is the columnar nematic. The phase is rarely observed, but is known to comprise of short columns which possess no positional ordering relative to one another, but do possess orientational ordering (Figure 1.19).^{13, 38, 55, 56} Hence, the columns act as the singular ‘building-blocks’ of the nematic phase just as the single molecules do in the nematic or nematic discotic mesophases. The N_{Col} phase possesses the same symmetry as the N_D and N phases and is also characterised in the same manner, *via* Schleioren optical microscopy textures which, since the N_{Col} phase is usually formed from charge-transfer complexes, often exhibit deep colours.^{38, 55, 56}



Figure 1.19: Molecular ordering in the N_{Col} phase

Hexagonal Columnar (Col_h)

The hexagonal columnar mesophase comprises several columns of molecules packed in a hexagonal pattern (Figure 1.20).^{13, 14, 24, 25, 30, 38}



Figure 1.20: Molecular organisation of the Col_h phase

The basic hexagonal columnar phase structure has the following symmetry operations: a singular C_6 axis, six C_2 axes and a σ_h mirror plane (Figure 1.21).^{30, 38} These symmetry operations lead to the hexagonal columnar mesophase possessing the point group D_{6h} .^{14, 30, 38}

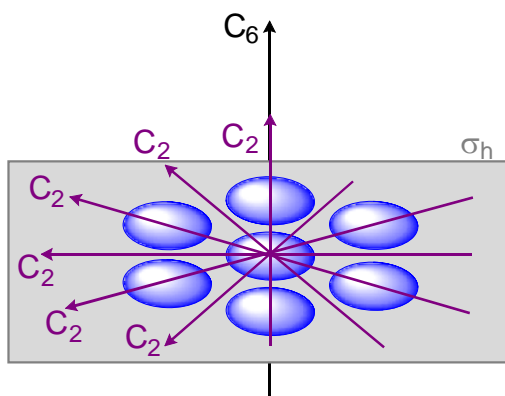
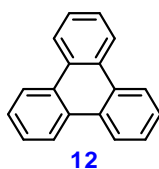


Figure 1.21: Symmetry operations in the Col_h phase

The hexagonal columnar mesophase is probably the most widely observed columnar mesophase. This wide observation of the hexagonal columnar phase is likely due to two major factors: firstly, many molecules that are synthesised are symmetrical, thus they adopt the most efficient packing for a symmetrical disc-shape, which is hexagonal packing; and secondly, the hexagonal columnar is the simplest columnar mesophase into which molecules can pack and as such does not rely on strong intermolecular interactions in order to give rise to the mesophase.^{13, 14, 25, 38, 39, 57} Another reason for the wide observation of the hexagonal columnar mesophase is the proliferation of triphenylene (**12**) derivatives in discotic research, which have a strong tendency to form hexagonal columnar mesophases.²⁴ The wide adoption of research into triphenylene-based discotic liquid crystals is due to device applications such as the wide-view film and organic semi-conductors, which are discussed in Section 1.4.^{24, 58}



Rectangular Columnar (Col_r)

Molecules which form a columnar mesophase, but do not pack into a hexagonal pattern, often pack in a rectangular pattern (Figure 1.22).¹³ Often the reason for the inability of molecules to pack in a hexagonal columnar pattern is due to the tilt of the columns in the phase structure, which is incompatible with hexagonal packing.³⁸ The tilt of the molecules within the mesophase, however, dictates that strong interactions between molecules in the columns exist in the Col_r phase, more so than in the Col_h phase, since the molecules must be able to “recognise” their required orientation with respect to their neighbouring columns.³⁸

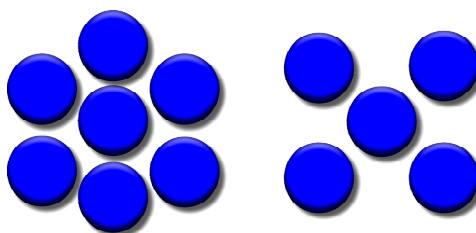


Figure 1.22: Hexagonal and rectangular packing for columnar structures

To date, three variants of the rectangular columnar mesophase have been identified *via* X-ray diffraction studies.^{14, 25, 30, 38} The three variants of the Col_r phase are illustrated in Figure 1.23.^{14, 25, 30, 38} In all three cases of molecular organisation in the Col_r phase, there is liquid-like ordering along the columns and the average orientation of the constituent molecules of the columns is not necessarily normal to the columnar axes.^{14,}

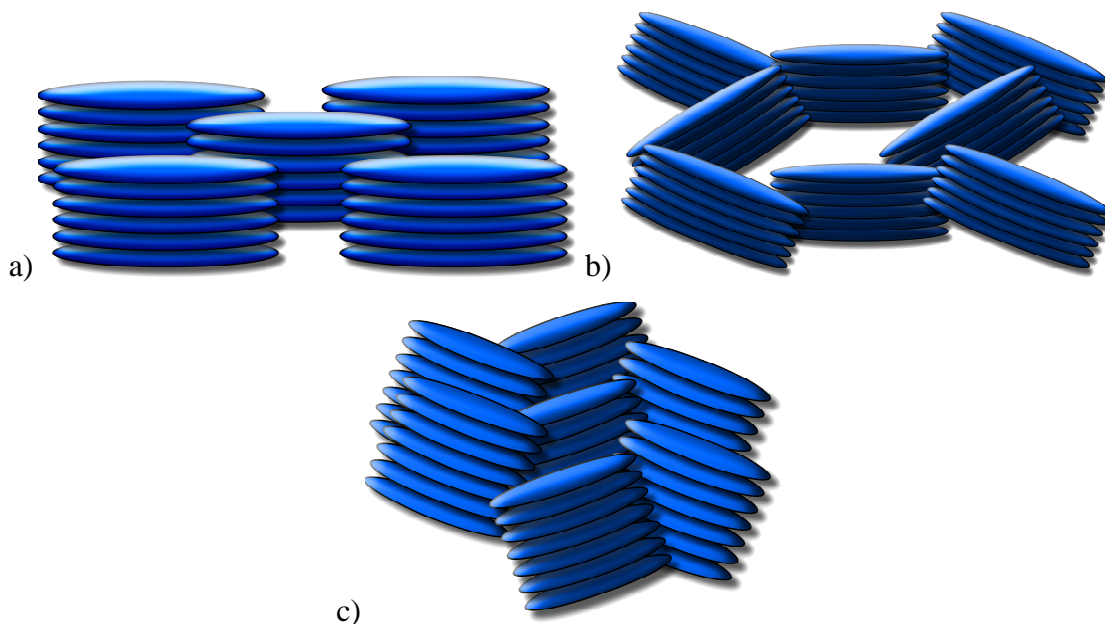


Figure 1.23: Representation of molecular organisation within the Col_r phase variants

Characterisation of the Col_r mesophase can be accomplished *via* optical microscopy, which typically reveals broken fan-shaped and mosaic textures, however identification of the precise variant of the Col_r mesophase (a, b, or c in Figure 1.23) can only be accomplished by detailed X-ray diffraction studies.^{38, 46}

Chiral variations of all three versions of the Col_r phase exist, in which the axis of the constituent molecules of the columns is tilted periodically leading to the tilt direction of the columns varying regularly down the columns (see Figure 1.18).¹⁴

Oblique Columnar (Col_{ob})

The oblique columnar mesophase possesses liquid-like ordering along the columnar axis, and the (usually tilted) columns are arranged oblique with respect to one another.^{14, 25, 30, 38} The phase structure is illustrated in Figure 1.24, showing: a) side view, and b) plan view of molecules in the phase; it should be noted, however, that Figure 1.24 b)

has been simplified to show only the plan views of molecules in the same orientation.^{14, 25, 30, 38} It should also be noted that the average of the planes of the molecules in the Col_{ob} phase is not necessarily normal to the columnar axes.¹⁴

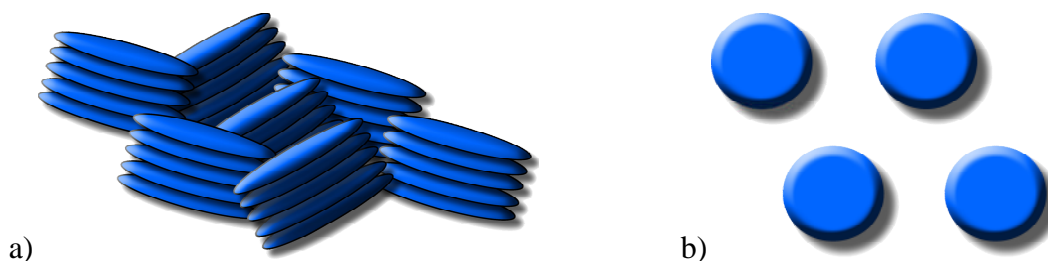


Figure 1.24: Representation of molecular organisation of the Col_{ob} phase

The Col_{ob} phase is the least-observed of all columnar mesophases, since in order to exhibit the phase strong interactions between molecules within the columns is required. However, chiral versions of this phase have also been observed in which the tilt direction of the molecules vary regularly throughout the columns (see Figure 1.18).¹⁴

The Col_{ob} phase can be difficult to characterise *via* optical microscopy as it tends to exhibit optical textures that are virtually identical to the Col_r phase, however characteristic spiral textures are also sometimes observed.^{38, 46}

Lamella Mesophase (D_L)

The lamella mesophase has yet to be fully characterised.³⁸ The phase has been observed to exhibit broken fan-like textures with large domains during optical microscopy, which are visually similar to broken fan-like textures observed in calamitic smectic phases.³⁸ Similarly, X-ray studies have suggested layered structures, which are tilted relative to the layer normal, similar to those of the calamitic smectic C phase.³⁸ Further X-ray evidence has revealed no evidence of a columnar structure (as was previously believed) and that the molecules possess a liquid-like order within the layers.^{38, 59} Thus, it has been suggested that the lamella phase structure (Figure 1.25) is similar to that of a SmC phase, although further study is needed before a definitive structure can be identified.^{38,}

⁵⁹

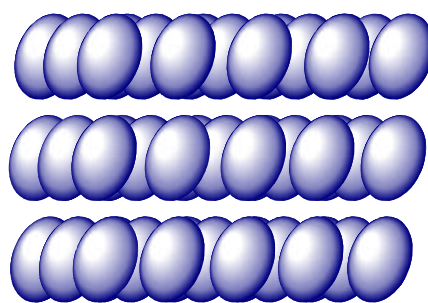


Figure 1.25: Proposed structure of the D_L phase

1.2.3.3 Structure-property Relationships of Disc-shaped Systems

The work of Vorländer at the beginning of the 20th century established that liquid crystalline behaviour stemmed from molecular architectures that were as close to rod-like as possible.⁸ This early work critically established the parallels between anisotropic molecular shape and mesomorphic behaviours. During the 1970's it was established that the anisotropic shape of materials that could give rise to mesomorphism could also come from disc-shaped as well as rod-shaped molecules.²²

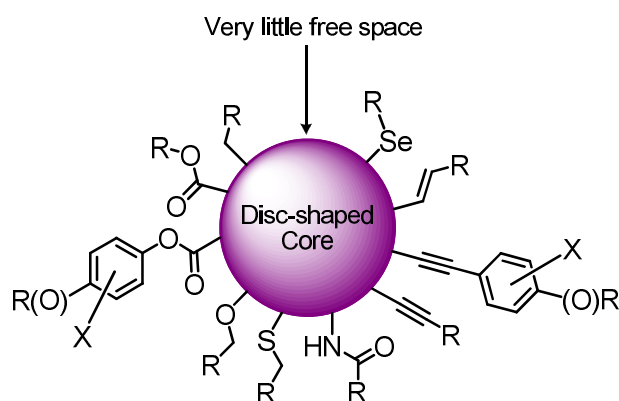


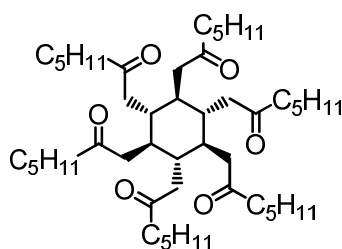
Figure 1.26: General structural template for discotic mesogens

Figure 1.26 shows a general structural template for discotic liquid crystalline materials, which typically consists of a rigid disc-shaped core, with (typically) at least six flexible side chains consisting of five or more atoms which are linked to the central core directly or *via* a linking group (*e.g.* ester, ether or alkyne units).^{13, 25} It is critical that such linking units, side groups and any other substituents that are linked directly to the core expand the overall area of the disc-shape of the molecule, but do not greatly increase the overall height of the disc or lead to the introduction of too much free space.^{13, 25, 56, 60} It

is critical that care is taken in minimising the increase in the height of the disc, since the effect of increasing the height of the disc can prevent effective intermolecular packing which, in turn, prevents the formation of columnar mesophases. However, such modifications can sometimes be beneficial for the generation of the N_D mesophase.^{13, 25, 56}

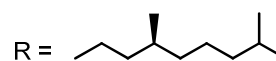
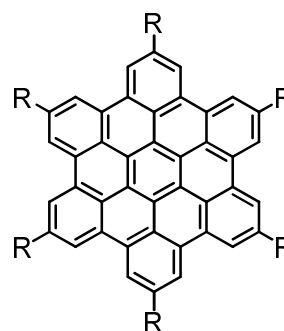
Role of the Discotic Core Unit

The discotic core unit has a critical role to play in the generation of columnar-style mesomorphic behaviour. Indeed, more than 50 disc-shaped core units are known to confer liquid crystalline behaviour (when appropriate peripheral groups are present), which range from simple cyclohexane-based cores (such as compound **13**)^{13, 25}, to significantly more complex cores, such as hexabenzocoronene derivatives (e.g. compound **14**)⁶¹.



Cr 68.5 Col_x 199.5 I

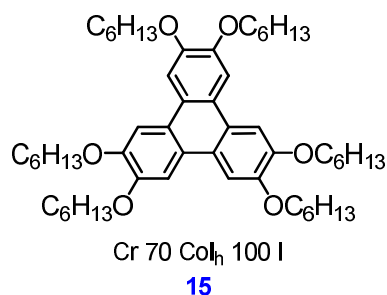
13



Cr 96 Col_h* 430 I

14

The vast majority of discogenic cores, however, share several commonalities which promote columnar phase behaviour. The first example of which comes from compound **13**¹³ which possesses a core which naturally puckers in order to generate the most stable packing model, *i.e.* the core adopts the ideal conformation for the discotic cores to stack better. The second commonality that promotes columnar phase behaviour is illustrated in compounds **14**⁶¹ and **15**⁶² which possess large areas of π -system delocalisation.



The large area of delocalisation of the π -system of compounds **14** and **15** are extremely important to mesophase stability, since the π -orbitals of one molecular core can interact with the π -orbitals of neighbouring core units in the columnar phase structure (see Figure 1.27). This situation arises due to the close contact between aromatic cores in the columnar phase (only *ca* 3-4 Å apart)⁶³, and such π - π interactions stabilise columnar structures, especially in situations where alternating electron deficient and electron rich units are present⁶⁴. This effect is also especially important for the possible formation of organic semi-conductors discussed in Section 1.4.

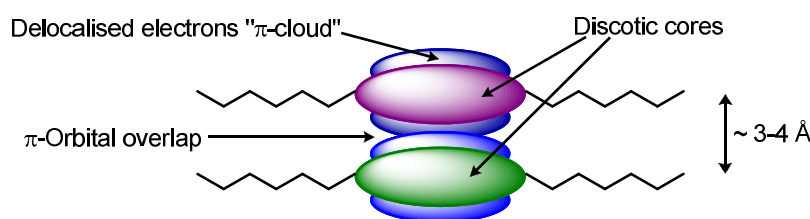
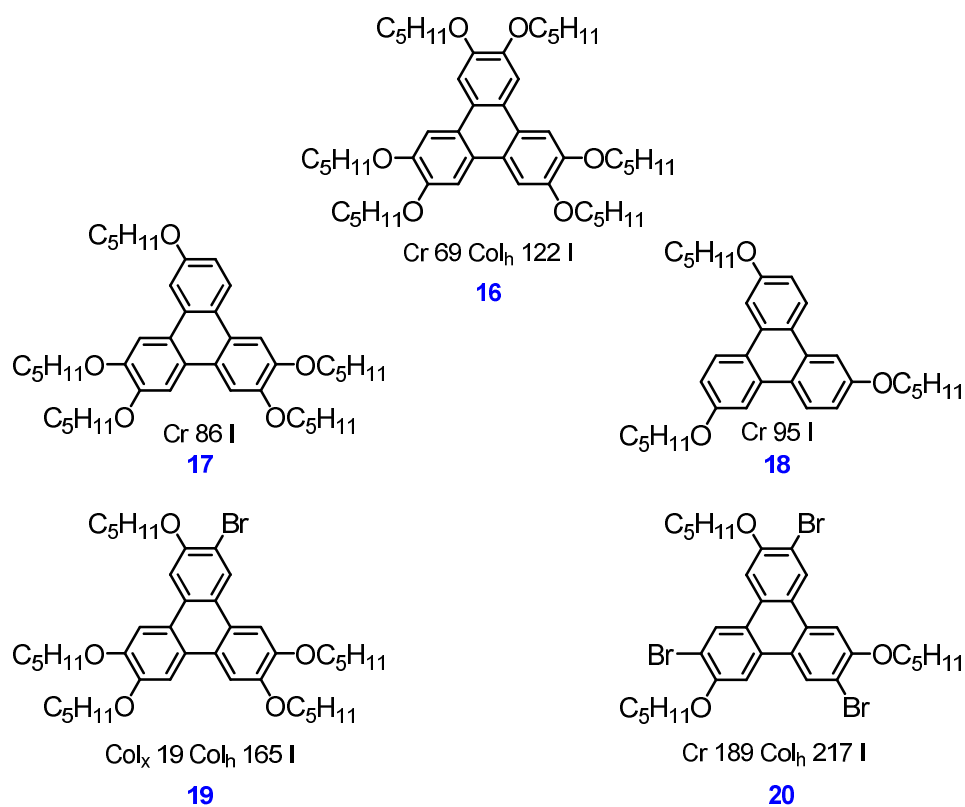


Figure 1.27: Side-on representation of interactions of π -electrons of discotic molecules

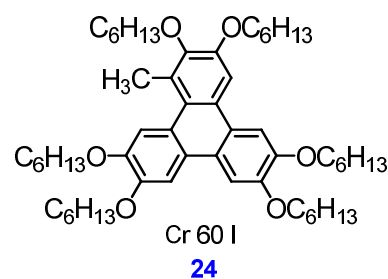
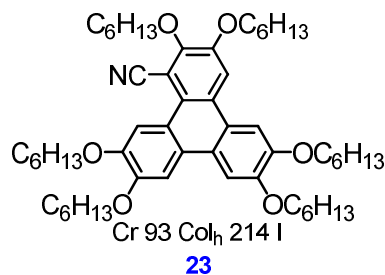
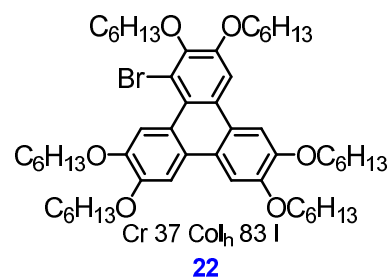
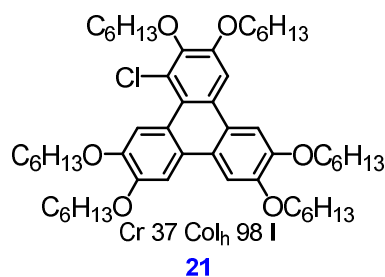
Role of Peripheral Substituents

Discotic core units alone are insufficient to confer mesogenic behaviour; peripheral substituents play a vital role in generating liquid crystalline properties. The absence of appropriate peripheral substituents can prevent mesomorphic behaviour from arising, as illustrated by compounds **16-20**^{60, 65}, where the removal of a singular group from the periphery of the triphenylene core is destructive to columnar phase behaviour, but upon replacing the missing group with another substituent, phase behaviour is restored. This behaviour arises since the peripheral substituent occupies free space around the central core of the disc and thus increases the overall area of the disc, which in turn increases the possibility of mesomorphism arising.



Peripheral groups enhance the overall disc area, however, they also often comprise or include alkyl or alkoxy chains which can reduce the overall rigidity of the molecule and introduce free space around the outer extremity of the central disc.⁶⁰ These factors are highly important as they often reduce the melting points of the materials which permit the observation of the mesophase, which is especially important since many discotic core units possess naturally high melting points as they are comparatively large molecules (*e.g.* compound **12** has a melting point of 199 °C⁶⁶). These factors can also be detrimental as the introduction of free space to a discotic material can disrupt columnar packing and lead to a destabilisation of mesomorphic behaviours.⁶⁰

The spatial effect of a peripheral group around the central disc unit, whilst pivotal in the generation of columnar mesophases, is not the only important factor of peripheral substituents which affects liquid crystal phase behaviour. It is crucial that peripheral substituents are polarisable and enhance the π -system of the core, for instance compounds **21-23**^{62, 67-71} all contain polarisable units, and as such the compounds exhibit mesomorphic behaviour. Compound **24**, however, which contains a non-polarisable substituent, experiences a loss of liquid crystalline behaviour as a consequence.^{67, 72}



Another important factor of peripheral substituents is their steric nature; groups that introduce significant steric disruption (especially near the core) can disrupt columnar packing, which can result in either a loss of liquid crystal phase behaviour, or in less extreme cases, the generation of the N_D phase.⁵⁶ Paradoxically, however, the introduction of bulky peripheral substituents can also enhance liquid crystal phase stability since the bulky unit can fill space around the central disc that is introduced by the peripheral chains, thus leading to a stabilisation of a columnar structure.⁷³ Thus, the introduction of a bulky peripheral substituent often generates a conflict between the steric effect, which reduces the liquid crystal phase stability, and the space filling effect, which enhances liquid crystal phase stability.

1.3 Identification and Characterisation of Mesophase Morphology

There are three essential techniques for the positive identification and characterisation of mesophase morphologies: polarised optical microscopy (POM), differential scanning calorimetry (DSC) and X-ray diffraction (XRD).¹³ Utilisation of one or more of these three methods of identification and characterisation can lead to accurate models of the mesophase morphology and thermal behaviours of a material.

1.3.1 Polarised Optical Microscopy (POM)

POM is one of the most powerful techniques available for swift and definitive identification of mesophase morphology. Indeed, POM can be viewed as the first-line in the identification and characterisation of a mesophase.

By placing a thin film of a material on a microscope slide and placing it in between crossed polarisers, light travelling through the material will be affected by the birefringence of the media.¹³ Consequently when no birefringent media or a non-birefringent media (*e.g.* an isotropic liquid) is present the light will not be affected and hence the light will be blocked by the crossed polarisers and thus appear dark.¹³ When passing through a birefringent material, however, the light is affected to varying degrees based upon several factors *e.g.* the thickness of the sample, the magnitude of the birefringence, the orientation of the director and defects in the structure of the material.¹³ Since the molecular organisation of each phase is unique, each mesophase has a characteristic texture (or textures) associated with it and an experienced researcher can distinguish between the various subtleties of these textures to positively determine mesophase morphology.

The nematic phase is the least viscous and most fluid of all mesophases, which can be demonstrated by ease of displacement of the cover slip during microscopy.¹³ Additionally, nematic mesophases exhibit Schlieren textures (*e.g.* Figure 4.27) and often appear as spherical birefringent droplets against the black background of the optically extinct isotropic liquid.^{13, 38, 46}

The hexagonal columnar mesophase often exhibits one or more of the following optical characteristics: pseudofocal conic textures (*e.g.* Figure 4.22), spherulitic-like textures and straight linear defects (*e.g.* Figure 4.16).^{38, 46} Mosaic and dendritic textures have been observed to be exhibited by the hexagonal columnar mesophase, although these

are rare.^{38, 46} Often the textures of the hexagonal columnar phase grow in from all directions as dendritic or flower-like patterns.^{38, 46}

The optical textures of the rectangular and oblique columnar mesophases are often indistinguishable from one another. Occasionally, however, characteristic spiral textures are exhibited by the oblique columnar phase.^{38, 46} The rectangular and oblique columnar phases often exhibit one or more of the following optical behaviours: broken fan-shaped textures, pseudofocal conic textures and mosaic textures (*e.g.* Figure 4.5).^{38, 46}

1.3.2 Differential Scanning Calorimetry (DSC)

A phase transition occurs when there is a change in the molecular ordering. Any changes in molecular ordering have an associated change in enthalpy. In order for a material to pass from a more ordered to a less ordered state (*e.g.* from a crystal to a mesomorphic state) energy must be imparted to the material in order to break the intermolecular forces of attraction, *i.e.* the process is endothermic.¹³ Conversely, the formation of intermolecular forces, when passing from a less ordered to a more ordered state, is an exothermic process.¹³ DSC measures this energy change by heating a sample and a reference at the same rate over a defined temperature range and monitors the heat flow required to maintain the isothermal conditions of the two furnaces (Figure 1.28).¹³ When endothermic processes occur, increased heat flow to the sample is required, and conversely, when exothermic processes occur, reduced heat flow to the sample is required to maintain the same temperature in the sample and reference furnaces.¹³ This heat flow is then plotted graphically as a thermogram (Figure 1.28).

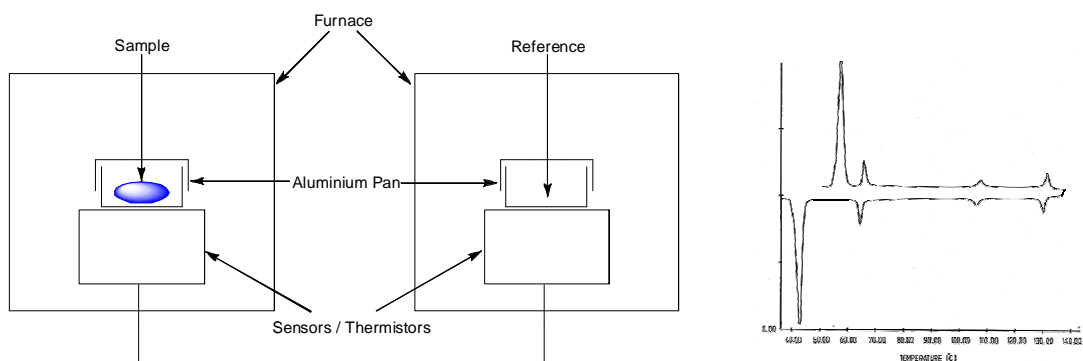


Figure 1.28: Schematic representation of the operation of a DSC and sample thermogram

In a DSC thermogram the first peak is usually the largest and as such represents the process which requires the most amount of energy in order to affect a change in molecular ordering. Hence, this process is usually the melting of a compound from the crystalline phase into either a mesomorphic state or the isotropic liquid. The area beneath the peak is the enthalpy of the transition (ΔH) which corresponds to the difference in the energy of the material before and after the measured transition. This change in enthalpy corresponds to the difference in the level of order of the material before and after the transition.¹³ Hence, the enthalpy of transition for crystal-mesophase transitions are typically large values (*ca* 30-50 kJ mol⁻¹), and mesophase-mesophase transitions are typically small values (usually less than 10 kJ mol⁻¹).¹³ These values can help to give an indication of the level of order, *e.g.* extremely small enthalpies of transition for a mesophase-isotropic liquid transition indicates a very small change in the level of order, indicating a mesophase with a low level of order, *e.g.* nematic phase. However, whilst this information is useful and can be used to give an indication as to the approximate change in the level of order between phases, it cannot be used to identify the mesophase morphology on its own. However, a DSC thermogram does give an excellent indication of the number of mesophases that a compound exhibits and a precise measure of their respective transition temperatures.

1.3.3 X-Ray Diffraction (XRD)

XRD is the ultimate technique in mesophase morphology identification as it provides accurate and direct information regarding molecular positioning and orientation.¹³ Careful analysis of XRD data, therefore, permits the deduction of various important structural features which makes it possible to determine the precise mesophase morphology at a given temperature.

Whilst XRD can provide the most precise information for mesophase identification and characterisation, it requires that the thermal behaviour be well established and, preferably, approximate phase morphology to be known since aligned samples are required.¹³ Hence, XRD can be viewed as the last-line in mesophase characterisation. In many cases where characterisation of the mesophase morphology and thermal behaviour is needed, but precise structural data is not, XRD is not always necessary as POM and DSC can provide sufficient information. For that reason, XRD is not used on any of the materials described in this thesis, and hence, further description of the theories and operating principals of XRD are beyond the scope of this thesis.

1.4 Applications of Liquid Crystals

When considering the applications of liquid crystals, it is easy to become *blasé* and declare that their usage began in the 1970's with the advent of liquid crystal display (LCD) technology. LCD's are, perhaps, the most visible use of liquid crystals, with more LCD's in the world than people and an industry worth in excess of \$60 billion, it is perhaps an understandable misconception that applications of liquid crystals start and end with LCD's.⁷⁴ In actuality, nature has been successfully using liquid crystals for untold millennia for many purposes (*e.g.* cell membranes and DNA, as alluded to previously).⁷⁴ Indeed, human technological use of liquid crystals also predates the LCD, and has been recorded as far back as Babylon in 2800 BC!⁷⁵ Naturally, at the time the concept of 'liquid crystals' had not been conceived of, but nevertheless, the use of soaps and detergents can be traced back to these early beginnings, and it has now been established that such agents are lyotropic liquid crystals.¹³ Presently, after nearly five thousand years of human usage of liquid crystals, new and exciting uses of liquid crystals are being explored, not only in detergents and display devices, but in artificial skin and muscle tissue, electrical conductivity, photovoltaics and holographic data storage!⁷⁴

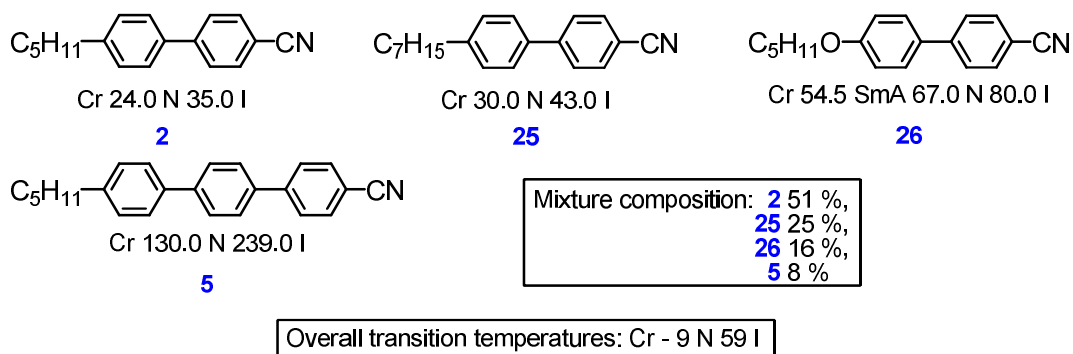
1.4.1 Chiral Nematic and Temperature Sensitive Materials

As was described previously (Section 1.2.2.1) the chiral nematic mesophase, which has a helical structure due to a gradual twist in the director, can reflect light at different wavelengths depending upon the average refractive index and the pitch length of the helical structure. The pitch length of the chiral nematic phase, however, is highly dependent upon temperature; as the temperature increases, the helix begins to shorten, hence the wavelength of the light that is reflected decreases.⁷⁶ Conversely, as the temperature of the chiral nematic phase decreases the pitch length increases, and hence the wavelength of the light that is reflected increases accordingly. Hence, the chiral nematic phase will selectively reflect light from the blue-end of the electromagnetic spectrum when warm, and from the red-end of the spectrum when cold.²⁸ This effect has led to the use of the chiral nematic phase in thermochromic devices, which has been used in many applications, including thermometers and thermal imaging, for which it is especially useful in remote locations where access to medical facilities is difficult, and can be used to detect cancerous tumours and pregnancy.⁷⁶ The thermochromic effect of

the chiral nematic phase has also caused the material to be used for aesthetic reasons, in applications such as paints and dyes for clothing which can change colour depending on temperature, and has even been seen on cars.¹³ It has even been suggested that such thermal imaging could even be useful on aeroplanes and cars to track metal fatigue and damage due to increased temperatures that are sometimes generated by such effects.⁷⁷

1.4.2 Liquid Crystal Displays

LCD's are certainly the most famous application of liquid crystals, especially given the recent proliferation of televisions, computer monitors, mobile phones, laptop computers *etc.* Presently there are many different types of LCD technology including: ferroelectric (FLC), in-plane switching (IPS), twisted nematic (TN) displays, super-twist nematic (STN), and vertically aligned nematic (VAN).⁷⁸ The LCD has become the driving force for much of the liquid crystal research that has occurred in the last 50 years. The basic concept for the first LCDs came about during the 1960's. However, it was not until the groundbreaking work of Gray at the University of Hull in the 1970's that LCD's became practically and commercially viable.¹⁶ The major problems faced by researchers was synthesising materials which exhibited the nematic phase at ambient temperatures, which possessed an appropriate dielectric anisotropy (so the orientation of the molecules could be affected by an electric field) with long lifetimes that were not prone to decomposition.⁷⁸ It is extremely unlikely that a single compound could fulfil all of the exacting requirements (especially since "ambient temperature" must cover a wide temperature range of *ca* -40 °C to +80 °C) of a commercial device, thus a mixture of compounds is invariably used. For example, compounds **2**, **5**, **25** and **26** were used by Gray and co-workers to generate the appropriate properties in an early mixture (E7) for TN devices.^{76, 79}



The basic operating principle of the twisted nematic (TN) display is straightforward, and the majority of LCD's are so based.⁷⁸ In the simplest of these TN devices a nematic liquid crystal is placed in between two indium tin oxide (ITO) electrodes which are coated on parallel glass plates. The glass plates are also coated in a molecular orientation layer (usually polyimide), which is rubbed in a one-dimensional fashion, thus allowing the molecules of the nematic liquid crystal to be aligned homogeneously in the rubbing direction. The rubbed surfaces of the glass plates are then aligned perpendicular to one another, thus the molecular director within the liquid crystalline layer rotates through 90° from top to bottom of the device.^{35, 80, 81} Crossed polarisers are placed either side of the device, and since the molecules in the liquid crystal layer rotate through 90° , so does the light that passes through the device, and hence the area appears bright (Figure 1.29).⁸⁰ When an electrical field is applied to the device, however, the molecules align themselves parallel to the field direction, and hence, light is no longer able to pass through the device and thus the display appears dark (Figure 1.29).⁸⁰ Once the electrical field is removed, the molecules in the liquid crystal layer relax back to the previous 90° twisted orientation and hence the display once again appears bright.^{35, 80, 81}

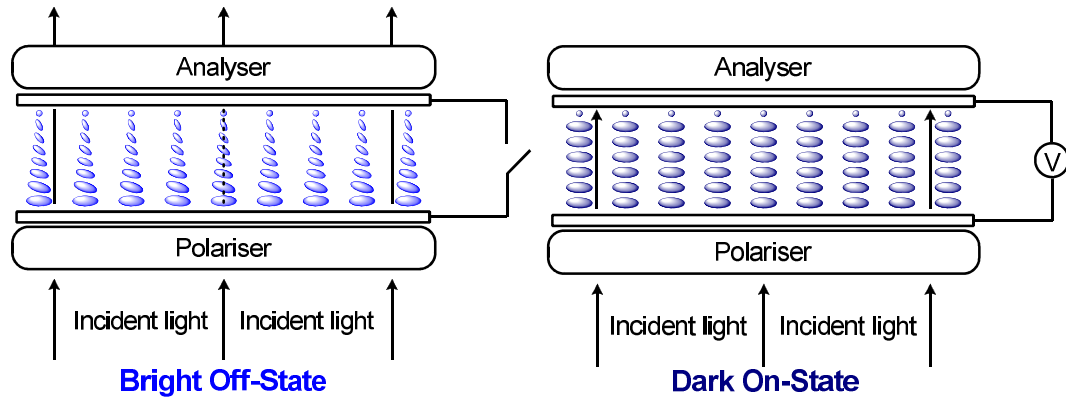


Figure 1.29: Representation of the operation of a TN display

The basic principle of the TN display can be extended to other forms of LCD technology. An example of which is the super-twist nematic (STN) display which operates on the same basic principle as a TN, however greater angles of rotation (180° to 270° are typical values) are used which has the effect of reducing the difference in the 'on-' and 'off-' state voltages.³⁴ This reduction of the difference in voltage in the STN display is highly significant, since it permits greater control of the display, in multiplex-addressing conditions.³⁵

The thin film transistor (TFT) display, utilises the same basic technology as the standard TN display, however the entire display is coated in a single electrode on one side, and on the other side each individual pixel possesses a single transistor which is addressed by a set of narrow electrodes (known as ‘source’ and ‘gate’ lines) which deliver the current flow to each transistor as required (Figure 1.30).^{35, 78, 82}

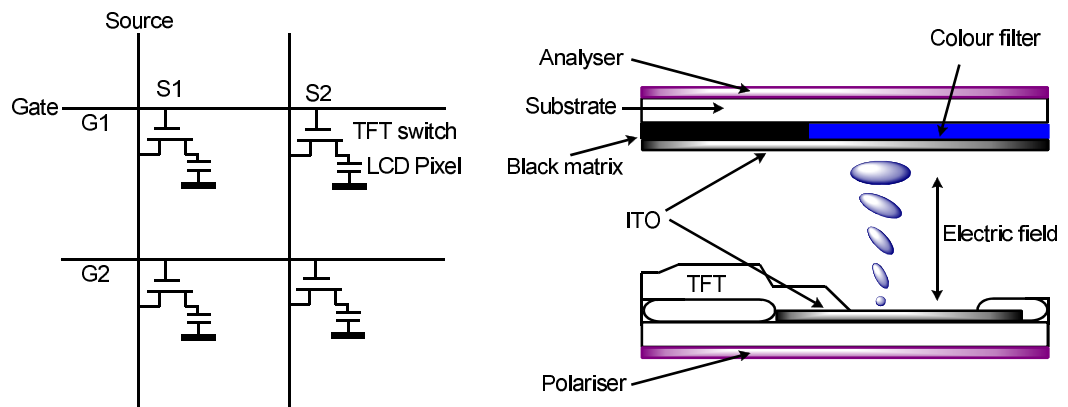


Figure 1.30: Multiplex addressing in TFT displays and structure of a TFT-TN cell

LCD technology offers significant advantages over competing display technologies like the cathode ray tube (CRT), such as: lower power requirements, low mass (offering enhanced portability), and reduced space requirements (can be a flat panel).⁸³ However, the basic technology is not without its disadvantages; one of the most critical of which is the viewing angle of large panel liquid crystal displays, which is reduced due to the birefringent nature of the liquid crystal media through which light is required to travel (Figure 1.5).^{82, 84, 85} Thus one method of countering the reduced viewing angle in an LCD is by affecting the birefringence of the liquid crystalline media. The birefringence can be affected by one of two methods; firstly a nematic liquid crystal with similar dielectric properties and a lower birefringence could be used, although it is difficult to generate such materials, since low birefringent materials are already in use, or secondly by compensating for the birefringence. It was previously mentioned (Section 1.2) that the birefringence of a material was determined by calculating the difference in the refractive index of the extraordinary and ordinary rays thus:

$$\Delta n = n_e - n_o$$

For a uniaxial calamitic nematic liquid crystal, this value invariably turns out to be positive since the optic axis of a calamitic liquid crystal is parallel to the longest

molecular axis. When measuring the birefringence of a discotic nematic, however, since the optic axis is (approximately) perpendicular to the longest molecular axis, the refractive indices are essentially the reverse of those of calamitic molecules, and hence give a negative birefringence (Figure 1.31).^{38, 82, 85}

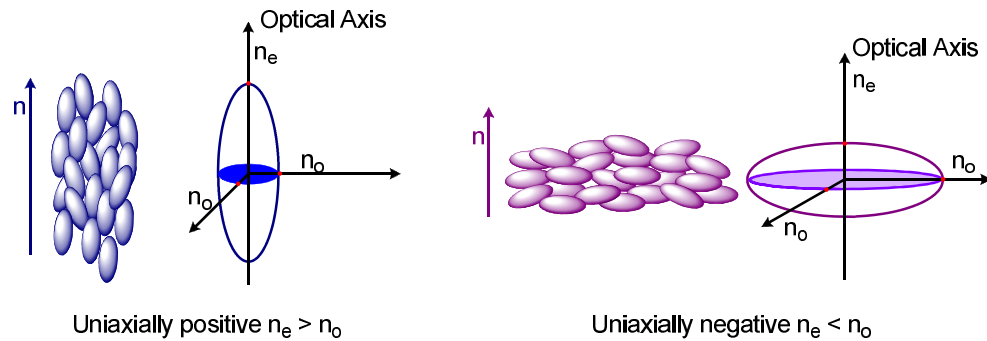


Figure 1.31: Birefringence of calamitic and discotic molecules

The negative birefringence of the discotic nematic mesophase has been exploited by FujiFilm who, in 1996, developed a phase compensation film (“wide view” or “WV” film) that uses triphenylene-based discotic nematic materials of negative birefringence to enhance LCD viewing angles.⁵⁸ Recent enhancements using this technology have added an opposite-twisted discotic liquid crystal film to a TN display (Figure 1.32).⁸⁶

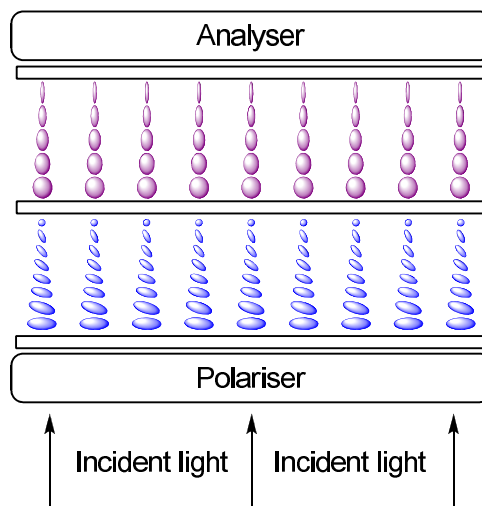


Figure 1.32: TN display birefringence compensated using opposite-twisted discotic films

1.4.3 Electricity Conduction and Generation

In the current age of “green technology”, information technology and the scarcity of raw materials for efficient generation and transportation of “clean” energy, the potential use of liquid crystals as charge transport media and organic solar cells becomes increasingly important. Liquid crystal semiconductors would offer many advantages over conventional organic semiconductors for several reasons, one of the most important of which is in the ability of a liquid crystal semiconductor to “self-repair” since the fluid nature of the liquid crystal phase permits self-organisation which allows defects within the phase structure to be “corrected”.^{87, 88} Discotic liquid crystals currently offer the greatest potential scope for the transport of energy due to the highly ordered nature of the mesophases which they form.²⁴ Within a columnar mesophase there are two possible directions of electron transport: across the columns, or down the columns (Figure 1.33).

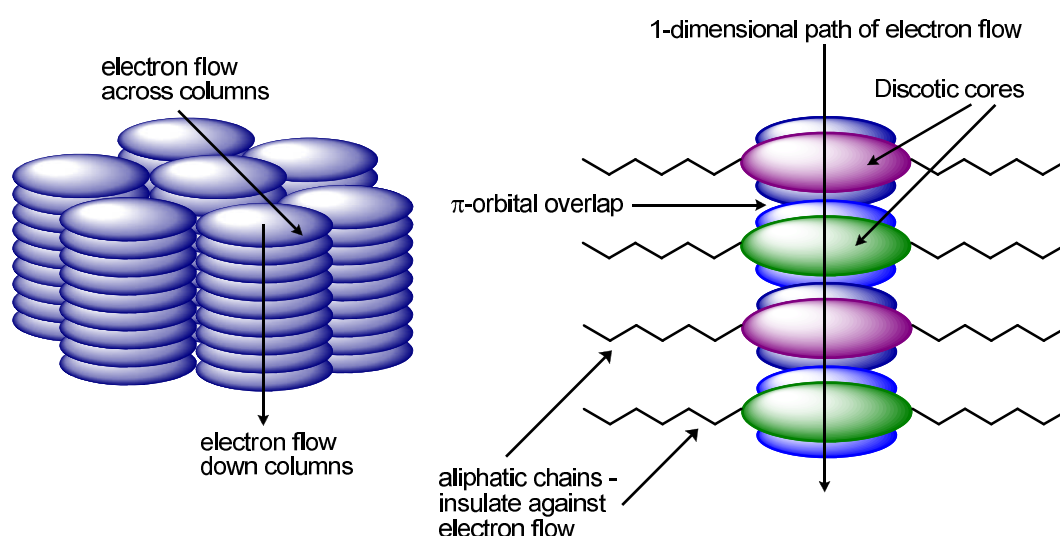


Figure 1.33: Direction of electron flow in columnar mesophases

Of the two possible directions for electron flow in the columnar mesophase (across columns or down them), Figure 1.33 clearly shows that the flow of electrons is most likely to occur down the columns, since the π -orbital overlap of highly conjugated molecules provides a one-dimensional path for electron flow (or positive hole transport) and the peripheral aliphatic chains insulate against electron flow across columns. Indeed, this has been proven experimentally, since electron flow down the column is four orders of magnitude greater than electron flow across the columns.²⁴ Hence, the columnar structures can be considered to be “molecular wires” since they provide a one-

dimensional pathway (along the columnar axis) for the flow of electrons. In addition to this “hopping” mechanism, it has been theoretically predicted that a “band transport” mechanism can also exist in the most ordered columnar mesophases.^{24, 89} Due to the small interdisc distance in a columnar mesophase (*ca* 3-4 Å), overlap of the highest occupied molecular orbitals (HOMO) and, critically, the lowest unoccupied molecular orbitals (LUMO) can occur, hence leading to a conduction band for charge transport along the columnar axis (Figure 1.34).^{38, 90, 91}

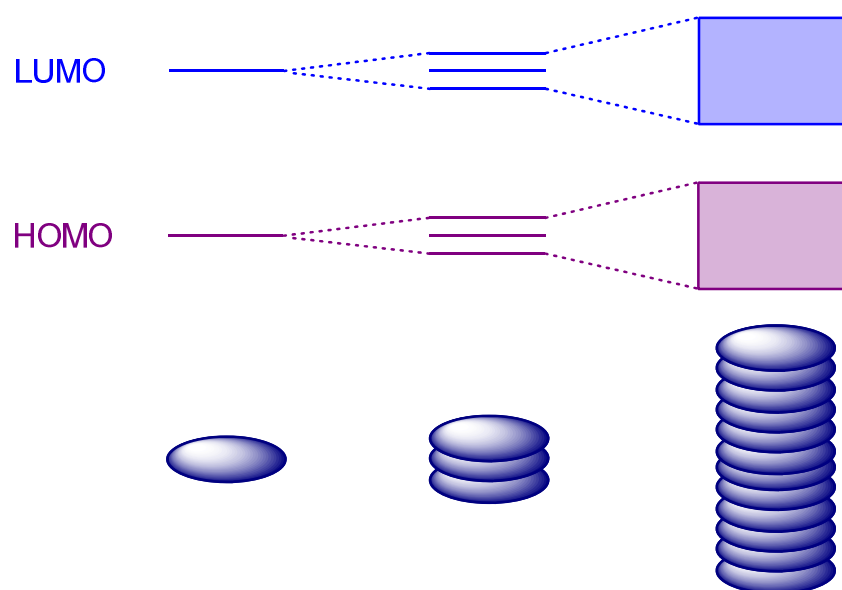


Figure 1.34: Electronic band formation from single molecules to columnar structures

To date, the majority of research into charge transport in discotic liquid crystals has involved triphenylene- or hexabenzocoronene-based materials, since they have a high tendency to form ordered columnar mesophases.⁹²⁻⁹⁵ Such investigations have revealed several important factors which affect the level of conductivity (*i.e.* charge carrier mobility), including: efficacy of charge-carrier injection process, order within the mesophase, structure of the mesophase, and size of the aromatic core of the discogen.^{24, 96, 97} Thus far, low charge carrier mobilities have been a significant problem for charge transport in liquid crystals, however, work in this area is still in its relative infancy and although there is still significant work to be done in this area, many significant breakthroughs have already been made.⁹⁸

Charge transport in discotic liquid crystals also leads to another potential use for discotic liquid crystalline materials, *i.e.* organic solar cells. Currently, high-efficiency flat-panel solar cells are manufactured from inorganic single or polycrystalline silicon-based materials.^{97, 99} This technology, however, is extremely expensive, rendering it unviable for many applications and making it impossible for the technology to compete with more traditional fossil fuel-driven methods of energy generation.^{97, 99} Organic photovoltaic technology, however, is potentially very inexpensive, easy to process, ultra thin, and extremely flexible (whereas the crystalline inorganic competitors would crack).^{97, 99-101} Thus organic photovoltaic technology based upon discotic liquid crystals is extremely attractive, especially in the current world climate of increasing energy demands, decreasing fossil fuel supply and increased need for “clean and green” energy generating solutions and making it, potentially, one of the most important scientific and technological issues of the 21st century.

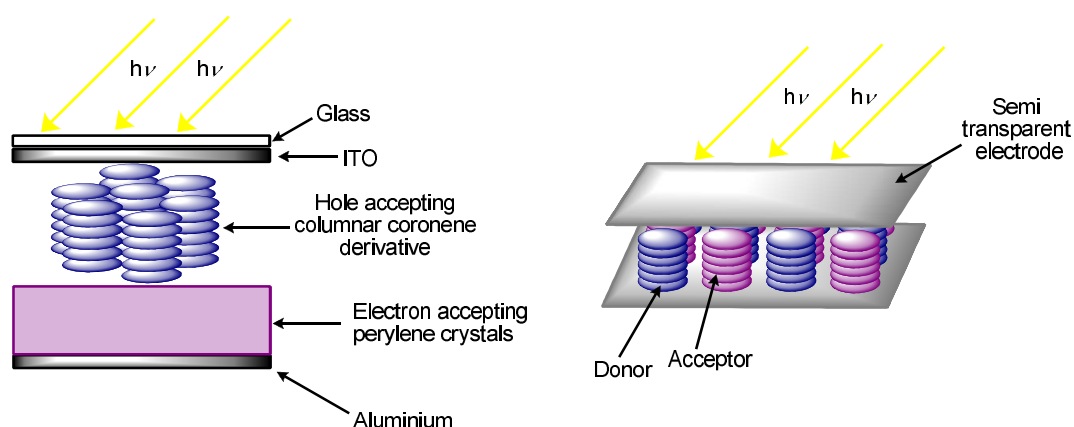


Figure 1.35: Schematic representations of photovoltaic cells containing discotic columnar liquid crystals

Several examples of organic photovoltaic cells have been devised thus far, two of which are illustrated in Figure 1.35.^{98, 99} As can be noted from Figure 1.35, both cells have electron donor and electron acceptor components, which are common features of all organic photovoltaic cells that have been devised to date.⁹⁸ This segregation of donor and acceptor components can be a significant problem since they naturally tend to form columnar structures of alternating donor-acceptor units⁹⁸ within a single stack due to complementary interactions between the π -orbitals of the molecules²⁴. Naturally, such an arrangement, whilst enhancing columnar phase stabilities²⁴, is detrimental to the

charge transport process⁹⁸. Once the device has been appropriately blended, however, the energy level diagram is similar to that illustrated in Figure 1.36¹⁰² whereby the absorption of solar radiation generates electrons and positive holes (due to promotion of electrons from the ground state to the excited state), the charges are then separated and are transported to the anode and cathode as appropriate.^{102, 103}

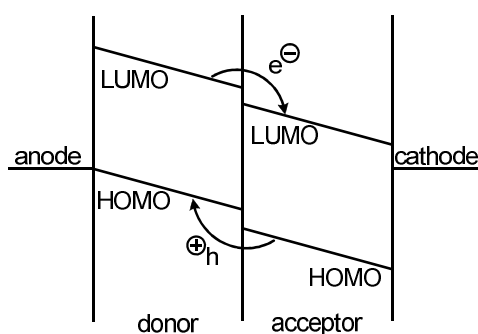


Figure 1.36: Energy level diagram showing charge separation and transport in a blend of an electron donor and acceptor between an anode and cathode

The organic photovoltaic is still a relatively novel idea, and as such there are several problems that still need to be overcome, such as: low quantum efficiencies (*i.e.* the proportion of charges that survive the promotion and transmission processes) although values in excess of 30 % have already been reported, low power conversion efficiencies, narrow light absorption range of organic conductors, high resistivity of organic conductors, low charge mobilities, instability (mechanical and chemical) of some of the compounds in use, and a lack of understanding of the underlying physics of the processes involved.^{24, 89, 97, 98, 101-103}

Despite many of the problems that have been highlighted for organic photovoltaics and organic semiconductors, it remains clear that there is significant scope for the future of these technologies. Future advancements in these areas will, no doubt, be forthcoming which will permit greater understanding of, and consequently, encourage not only the development, but the use of such technologies in the near future.

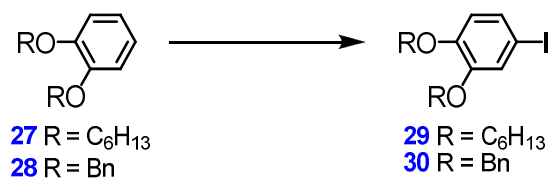
2 Aims and Objectives

Discotic liquid crystal research is now more than thirty years old, however, it is still early days when compared with the well-established area of calamitic liquid crystals. In recent years there has been a significant increase in discotic liquid crystal research due to new applications such as the optical compensation films⁵⁸ for optoelectronic devices and the lure of potential new applications in the areas of organic semiconductors⁹⁸ and photovoltaics⁹⁸. To date, hexa-esters and hexa-ethers of triphenylene are the most widely investigated discotic materials, since they have a tendency to form ordered columnar mesophases, which are of interest for electron transport and they are currently used in optical compensation films.²⁴ The great importance of such materials makes it essential that synthetic strategies and methodologies for the synthesis of hexaalkoxytriphenylenes are fully investigated, and that structure-property relationships in triphenylene-based liquid crystalline materials are further explored.

The synthesis of hexasubstituted triphenylenes can be subdivided into two sections:

a) Halogenation to form valuable intermediate compounds

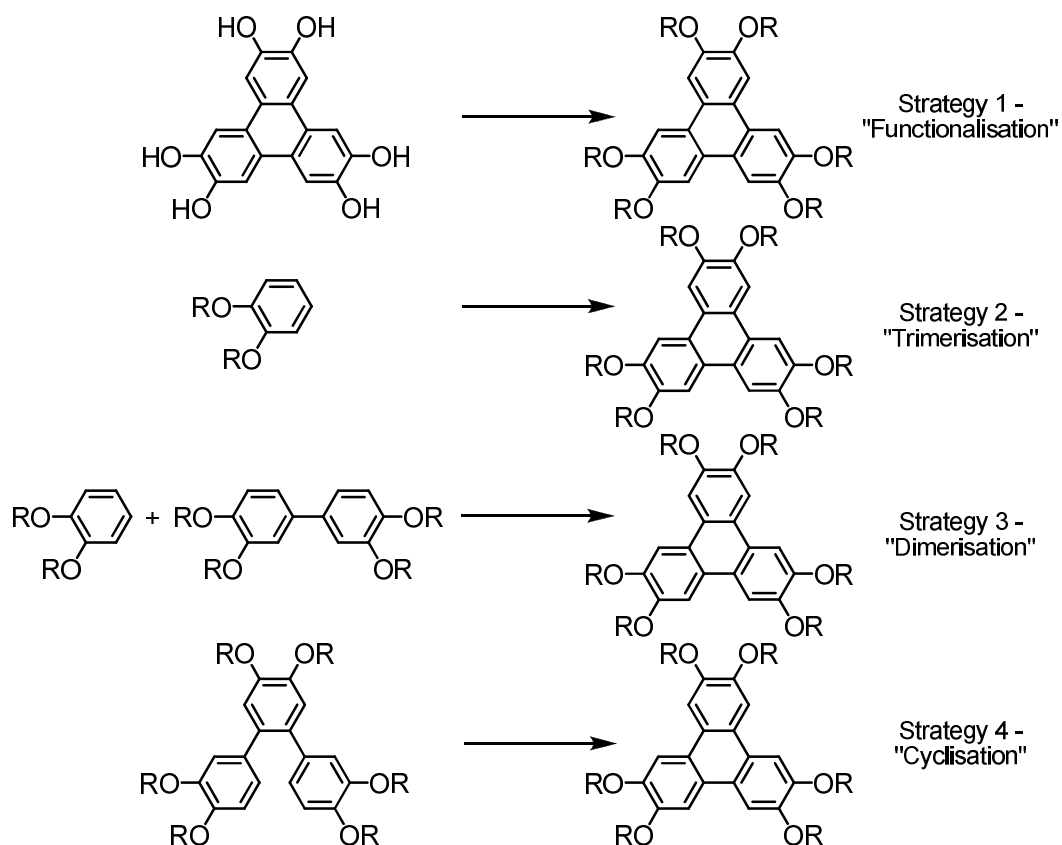
Halogenated moieties are extremely valuable in synthetic organic chemistry. In typical synthetic reactions iodo-substituted materials react at a faster rate than their bromo or chloro analogues.^{49, 104} Thus, it is often advantageous to utilise iodinated materials in preference to bromo or chloro analogues. Thus, the synthesis of several iodinated intermediates was investigated, in order to determine the scope for the generation of 1,2-dialkoxy-4-iodobenzene species (such as compound **29**), which can be used to synthesise more elaborate units subsequently.



b) Oxidative strategies and methods for the formation of the hexaalkoxytriphenylene structure

The seminal work in this area by Cammidge, Boden, Bushby, Borner and Jesudason⁶⁸ has led to a number of different methods for the synthesis of triphenylene.¹⁰⁵ However,

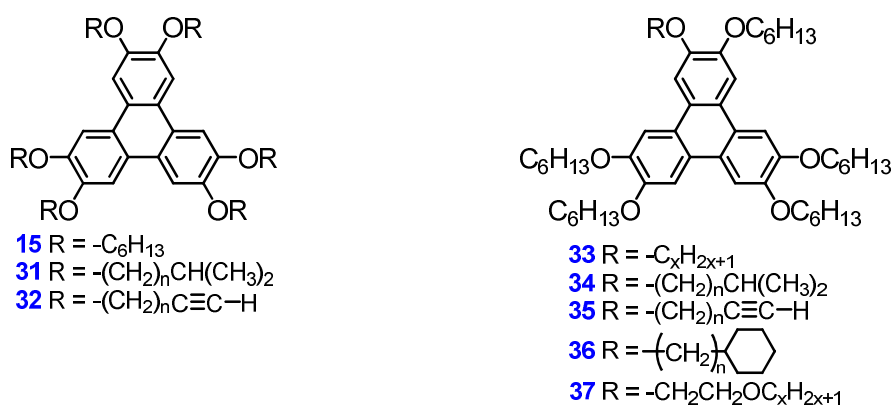
there has been little work which systematically compares the scope and limitations of the various strategies and methods.¹⁰⁵ Thus, it is important to examine the most widely used strategies and methods in order to determine the scope and limitations of such synthesis on the generation of hexa-substituted triphenylene-based materials.



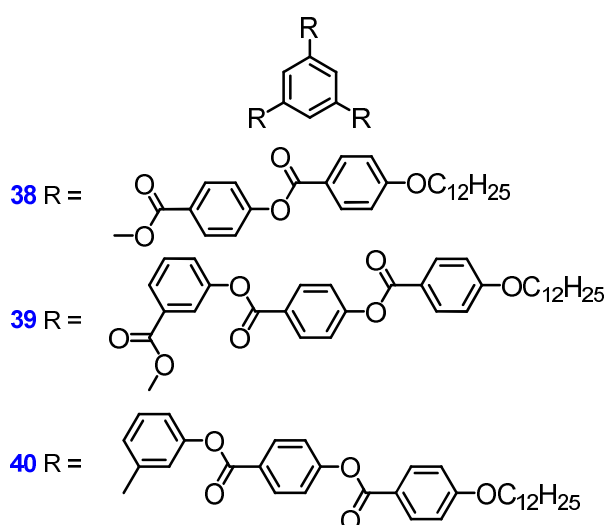
Structural features of triphenylene-based discotic liquid crystals that can be examined for their structure-property relationships include:

- simple unbranched alkoxy chains, which are known compounds (*e.g.* **15**, **33**);
- branched alkoxy chains, to determine their effect upon columnar mesophase stabilities due to their space-filling and steric effects (*e.g.* **31**, **34**);
- terminal acetylenes, to assess the role of π - π interactions, and the space filling and steric effects of the acetylene unit on columnar phase stability (*e.g.* **32**, **35**);
- terminal cyclohexanes, to examine the effect of this bulky unit which can pack effectively, on columnar mesophase stabilities (*e.g.* **36**);
- ethers, to determine the effect of adding an additional oxygen into the peripheral chain, since the oxygen introduces a polar group that allows for the possibility of dipole-dipole interactions, which can affect columnar phase stabilities (*e.g.* **37**);

- terminal fluoro substituents in an alkoxy peripheral chain, to establish the role of the fluorophilic effect upon melting point and mesophase stability;
- near-core modifications to the HAT6 (**15**) structure, to examine the effect upon mesophase stability and morphology of substituting one peripheral unit (alkoxy chain) for a range of other substituents such as acetylene-containing alkyl chains, esters or phenyl rings either directly linked, or attached by a spacer such as ester or acetylene linkages.



This programme of research also aims to investigate a small number of novel molecular architectures for their potential mesomorphic behaviours. An example of a novel molecular architecture that can be investigated for its potential mesomorphic behaviour is that of spiral-shaped molecules such as compounds **38-40**.



Such spiral-shaped materials would not ordinarily be expected to exhibit columnar-type mesomorphism due to the large amount of free space around the central disc, however these compounds have significant flexibility due to the ester linkages, thus the “arms” can fill space around the central disc, hence giving rise to columnar mesomorphism. Compounds **38-40** could also give rise to banana-type mesomorphism since the structures are similar to banana liquid crystals and thus the mesophase morphology is also interesting to investigate.

3 Experimental

3.1 Instrumentation and Materials

All starting materials and solvents were used as purchased from suppliers without further purification. The synthesis of all of the materials used are detailed below, the materials used whereby the synthesis is not detailed below are commercially available and are obtained from the suppliers, with the exceptions of 1,4-difluoro-2,3-dihydroxybenzene (**81**), 1-bromo-4-hydroxybenzene (**141**) and 1-ethynyl-4-hydroxybenzene (**145**), which were obtained from M. Hird, and are used with permission, and tetrakis(triphenylphosphine)palladium(0) which was prepared according to the literature procedure¹⁰⁶. All final products were filtered through Schleicher & Schuell filter papers to remove particulates in addition to the purification techniques described below.

3.1.1 Nuclear Magnetic Resonance Spectroscopy (NMR)

The structures of all compounds prepared were confirmed by NMR using a JEOL JNM ECP400 spectrometer and all chemical shifts reported are given in ppm (δ).

All proton (^1H) NMR spectra were recorded at 400 MHz using tetramethylsilane (TMS, $\delta_{\text{H}} = 0$ ppm) as the internal standard, or where this was not available, the residual protic solvent was used as the internal standard as follows: deuterated chloroform (CDCl_3) $\delta_{\text{H}} = 7.26$ ppm, deuterated dimethylsulfoxide ($\text{SO}(\text{CD}_3)_2$, DMSO- D_6) $\delta_{\text{H}} = 2.05$ ppm, deuterated dichloromethane (CD_2Cl_2) $\delta_{\text{H}} = 5.32$ ppm. All carbon (^{13}C) NMR spectra were recorded at 100.5 MHz, with the central peak of deuterated chloroform (CDCl_3) $\delta_{\text{C}} = 77.00$ ppm used as the internal reference. All fluorine (^{19}F) NMR spectra were recorded at 376 MHz, using trichlorofluoromethane (CFCl_3), $\delta_{\text{F}} = 0$ ppm as the reference.

Splitting patterns of proton signals are described by the following abbreviations:

s	-	singlet	d	-	doublet
t	-	triplet	quart	-	quartet
quint	-	quintet	sext	-	sextet
sept	-	septet	non	-	nonet
dd	-	double doublet	ddd	-	double, double doublet
dt	-	double triplet	m	-	multiplet

3.1.2 Gas Chromatography (GC)

GC was used to monitor the progress of several reactions, and to determine the purity of several commercially available starting materials before use. The system used comprised a Varian CP 3380 gas chromatograph with a Chrompack capillary column with a 10 m long CP-Sil 5 CB stationary phase column with an internal diameter of 0.25 mm and a film thickness of 0.12 μm , a flame ionisation detector (FID – constantly held in an oven at 300 °C) and in conjunction with Varian Star GC workstation software version 5.52.

3.1.3 Mass Spectrometry (MS)

A mass spectrum was recorded for all compounds to confirm the molecular mass of the material. All masses reported are the relative molecular masses (rounded to the nearest integer) and all mass spectra were recorded using either: solid probe electronic ionisation (EI) or matrix assisted laser desorption ionisation (MALDI) techniques.

- a) EI spectra were recorded using a Shimadzu QP5050A quadrupole GC-MS at 70 eV, with the probe at 350 °C and in conjunction with Shimadzu Class-5000 processing software.
- b) MALDI spectra were recorded using a Bruker Reflex IV MALDI-TOF mass spectrometer operating in reflection mode with accelerating voltage in the range of 20-25 kV, using a nitrogen laser providing photons at 337 nm and typically 100-150 laser shots were accumulated and averaged. MALDI mass spectra were processed using Bruker Compass software comprising FlexControl and FlexAnalysis packages.

3.1.4 Elemental Analysis (EA)

Elemental analysis was performed on all final products to determine the relative ratios of carbon and hydrogen in the sample and compared to expected values for the material. All results obtained were within $\pm 0.30\%$ of the expected value, and the analysis was performed using a Fisons EA 1108 CHN analyser.

3.1.5 High Performance Liquid Chromatography (HPLC)

HPLC was used to determine the purity of all final and several intermediate products and to purify several final products.

- a) The analytical system comprised of a Gilson 233XL auto sampler, 321 binary solvent pump, Hewlett Packard 1100 series Diode Array Detector, and a Phenomenex Luna 5 μ m C18(2) column, utilising (typically) 30 % dichloromethane (DCM) / 70 % acetonitrile as eluent.
- b) The preparatory HPLC system comprised a Gilson 233XL auto sampler / fraction collector, 321 binary solvent pump, 151 UV/VIS detector, and a Phenomenex Luna 5 μ m C18(2) column.

3.1.6 Polarised Optical Microscopy (POM)

Melting points, liquid crystal transition temperatures and mesophase morphologies were all determined by polarised optical microscopy using an Olympus BH2 polarising optical microscope, Mettler FP52 and FP82 heating stage and controller. Polarised optical micrographs were obtained using a JVC TK-C1481 colour video camera in conjunction with Mettler Studio Capture software and the polarised microscopy setup.

3.1.7 Differential Scanning Calorimetry (DSC)

Liquid crystal transition and isotropisation temperatures and melting points of all final products were confirmed by DSC, and all temperatures quoted are onset values from the transitions. DSC results were obtained using either:

- a) Mettler DSC822e with STARe software, which was calibrated using indium (melting point onset 156.6 °C, enthalpy 28.45 Jg⁻¹) and zinc (melting point onset 419.47 °C). The calibration of the DSC was checked daily using the indium standard allowing ± 0.3 °C and ± 0.3 Jg⁻¹ experimental error, and using an aluminium standard reference pan.
- b) Perkin Elmer DSC7 calibrated using indium (melting point onset 156.6 °C, enthalpy 28.45 Jg⁻¹) and lead (melting point onset 327.47 °C). The calibration of the DSC was checked daily using the indium standard allowing ± 0.3 °C and ± 0.3 Jg⁻¹ experimental error, and using an aluminium standard reference pan. Data was collected *via* a PC running Pyris software.

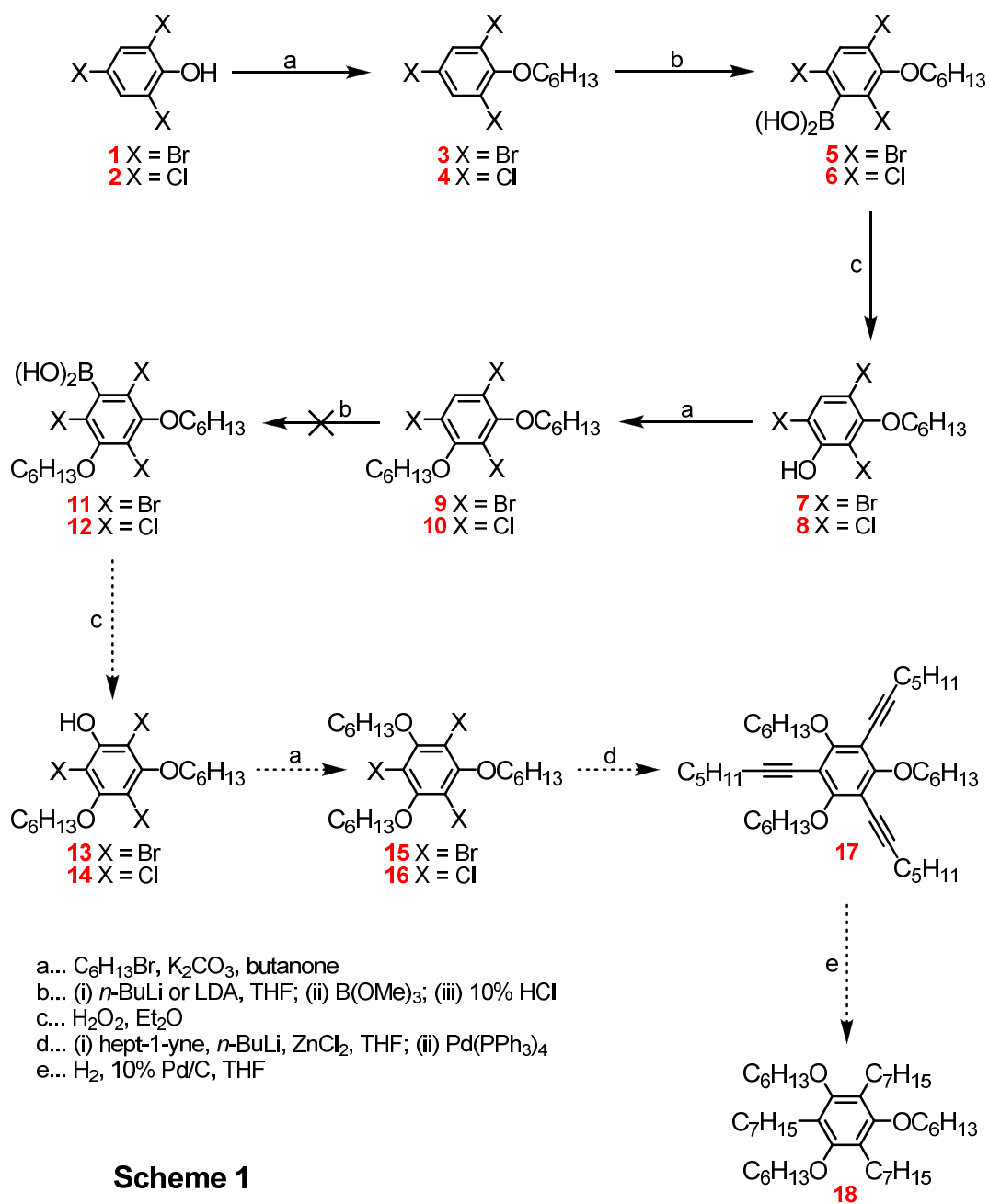
3.1.8 Column Chromatography

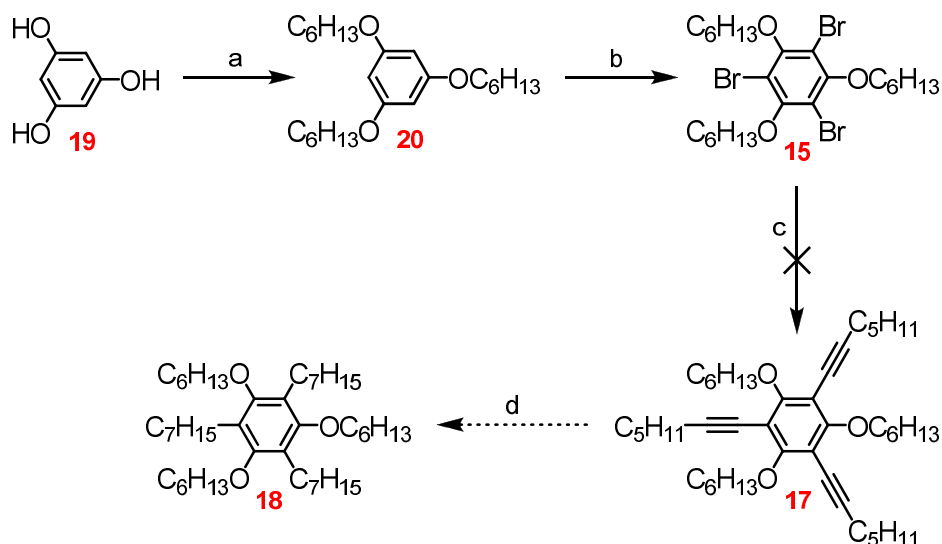
Column chromatography was used to purify many materials using either silica gel (BDH silica gel, average particle size *ca* 65 μ m, particle distribution 35-70 μ m) or alumina (Fluka aluminium oxide, type 507C neutral; 100-125 μ m mesh).

3.1.9 Thin Layer Chromatography (TLC)

TLC was used to monitor the progress of many reactions utilising either: hexane, 4:1 hexane / dichloromethane, 1:1 hexane / dichloromethane, or 100 % dichloromethane as appropriate. TLC was also used in conjunction with column chromatography and to assist in the determination of the purity of materials. The TLC plates used consisted of fluorescent silica gel 60 F₂₅₄ (Merck) on aluminium foil or fluorescent aluminium oxide 60 F₂₅₄ (Fluka) on PET foil and all plates were inspected using ultraviolet light, at a wavelength of both 254 nm and 364 nm.

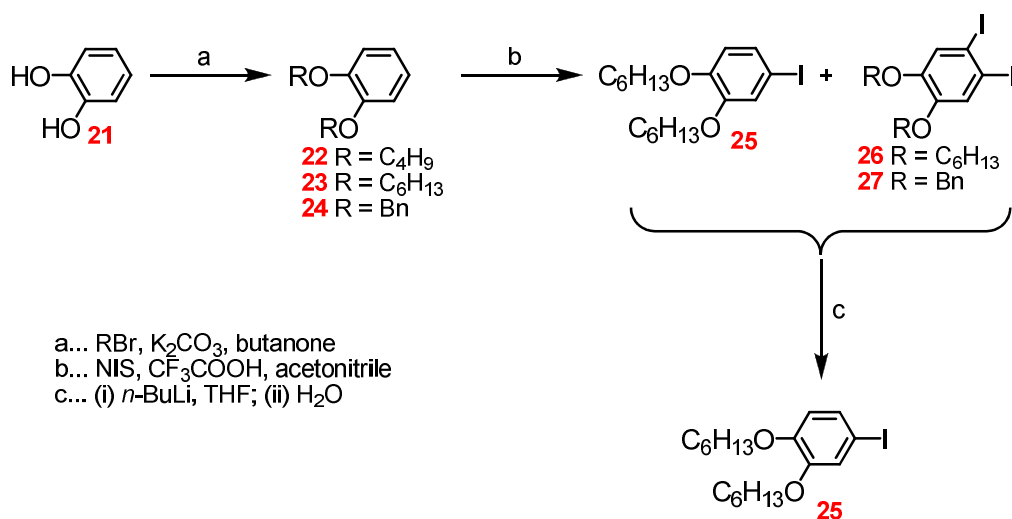
3.2 Schemes



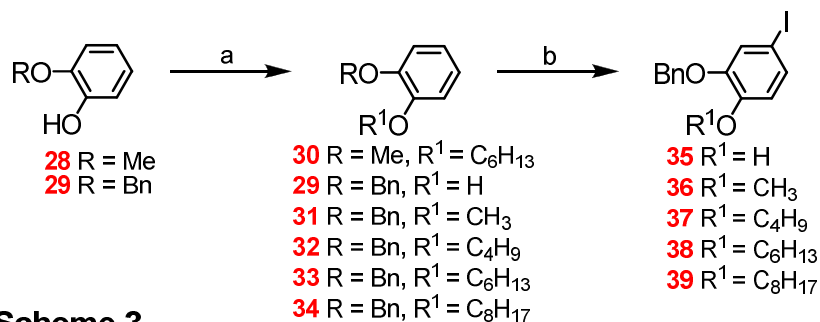


a... $\text{C}_6\text{H}_{13}\text{Br}$, K_2CO_3 , DMF
 b... Br_2 , FeCl_3 , DCM
 c... (i) hept-1-yne, *n*-BuLi, ZnCl_2 , THF; (ii) $\text{Pd}(\text{PPh}_3)_4$
 d... H_2 , 10% Pd/C, THF

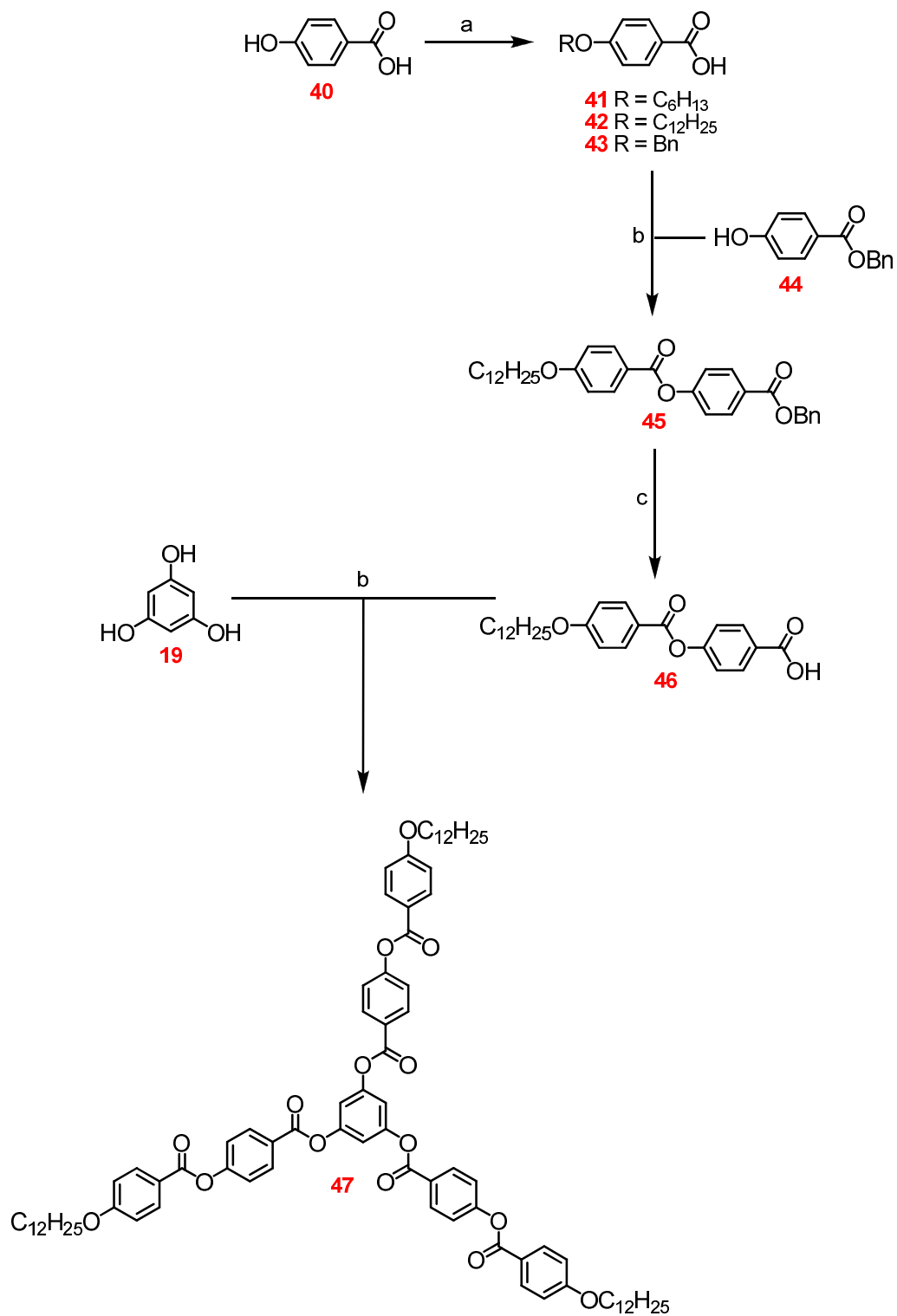
Scheme 2



a... RBr, K_2CO_3 , butanone
 b... NIS, CF_3COOH , acetonitrile
 c... (i) *n*-BuLi, THF; (ii) H_2O

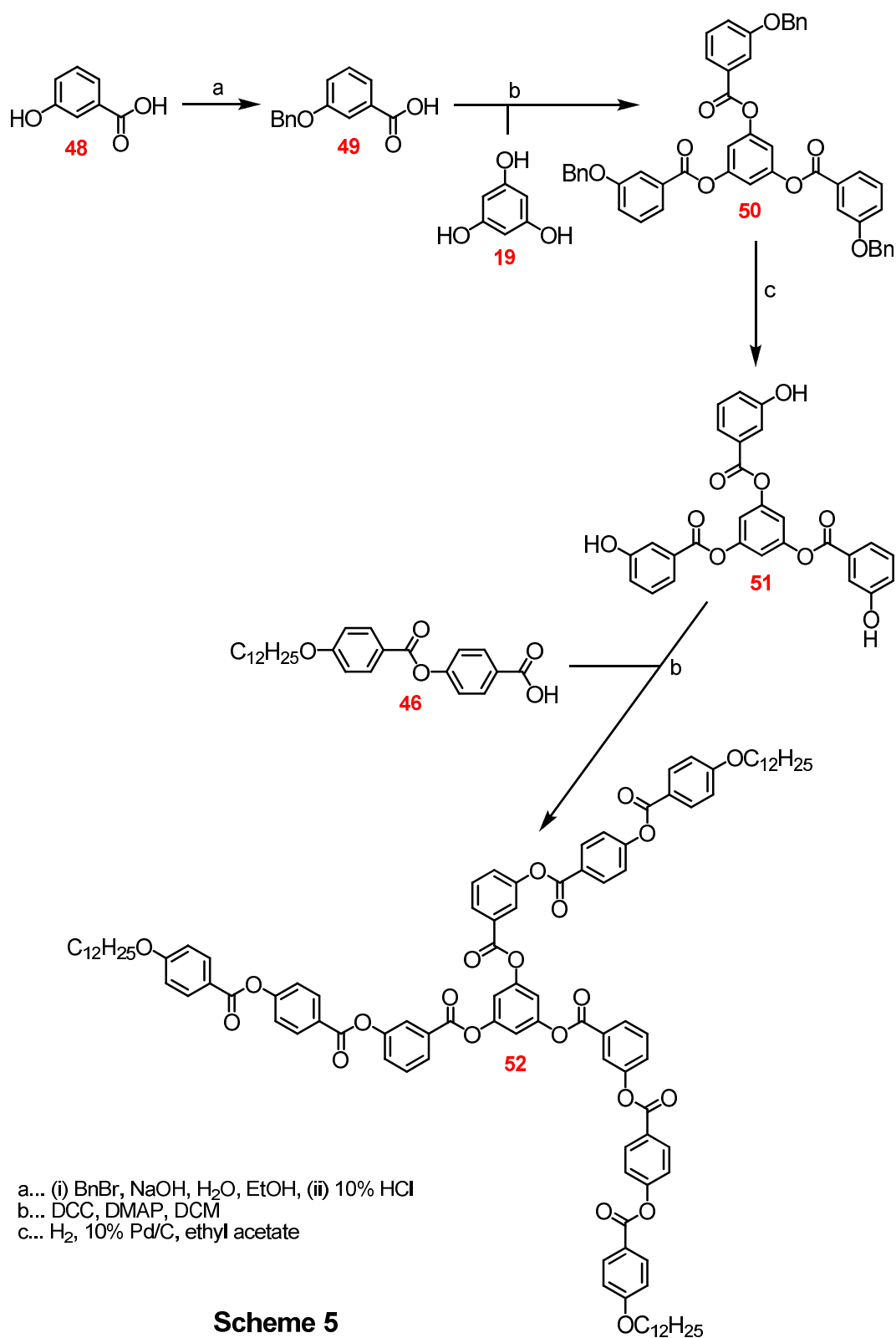


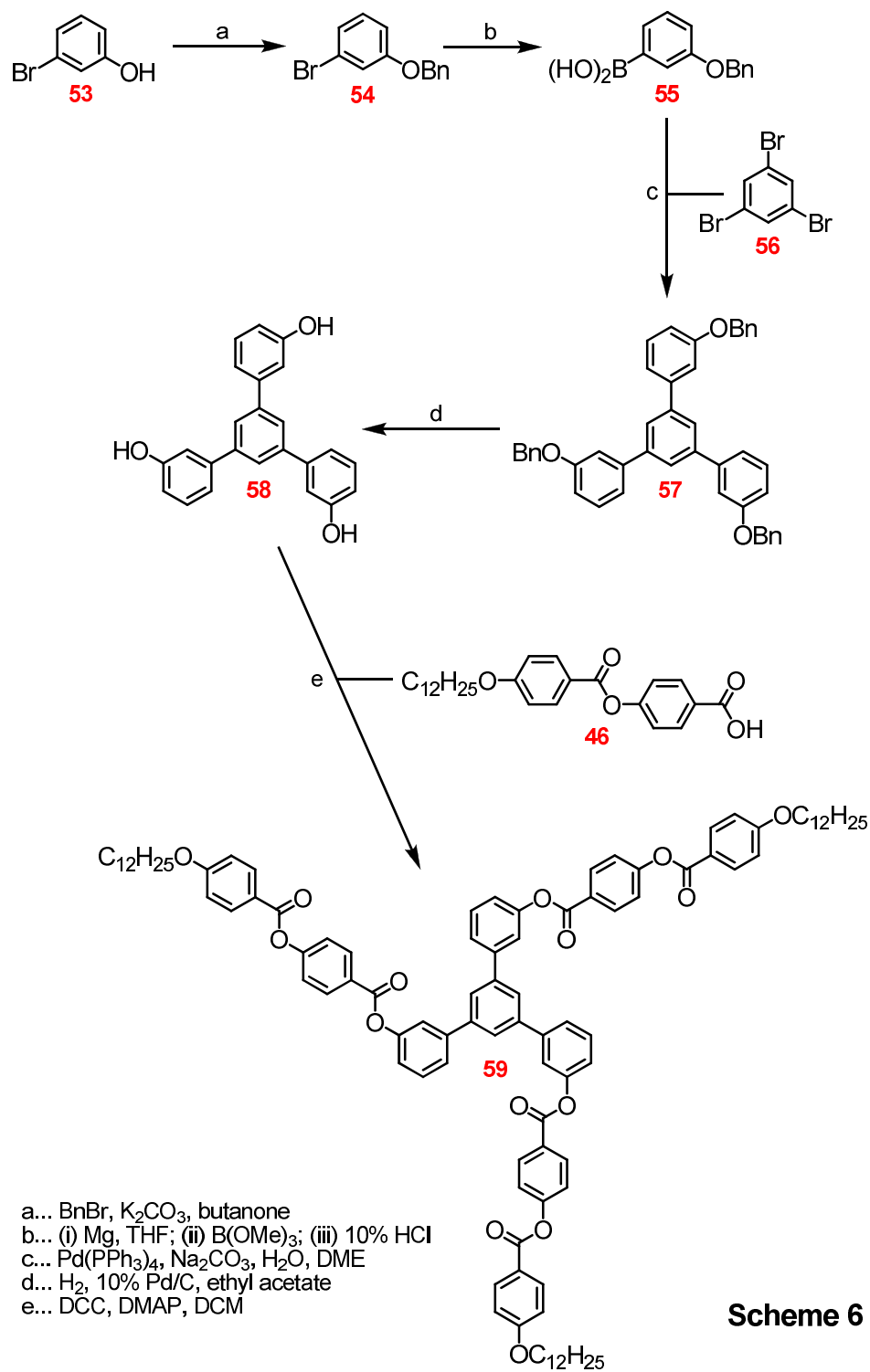
Scheme 3

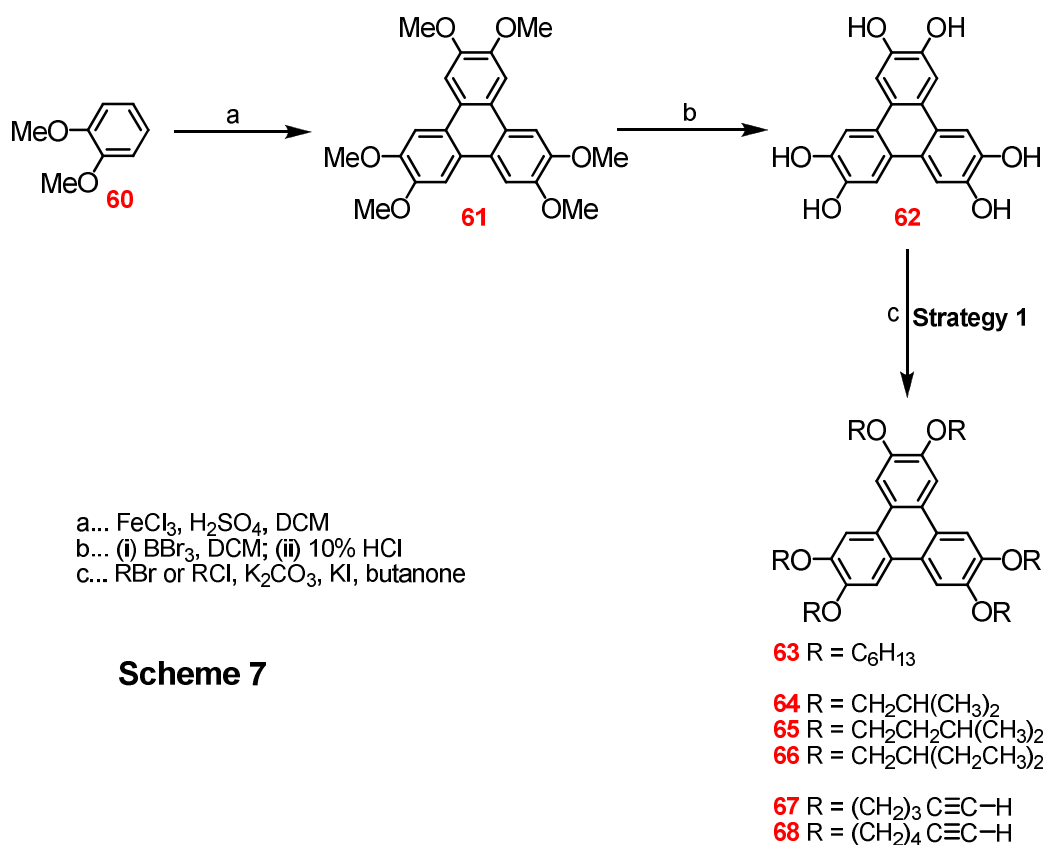


a... (i) RBr, NaOH or KOH, H₂O, EtOH; (ii) 10% HCl
 b... DCC, DMAP, DCM
 c... H₂, 10% Pd/C, THF

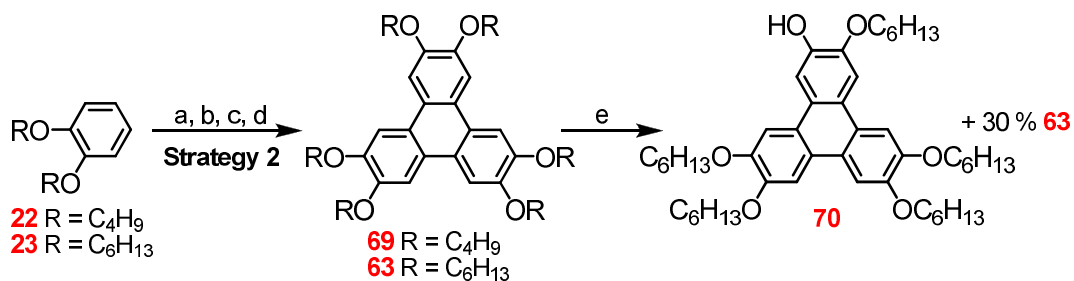
Scheme 4





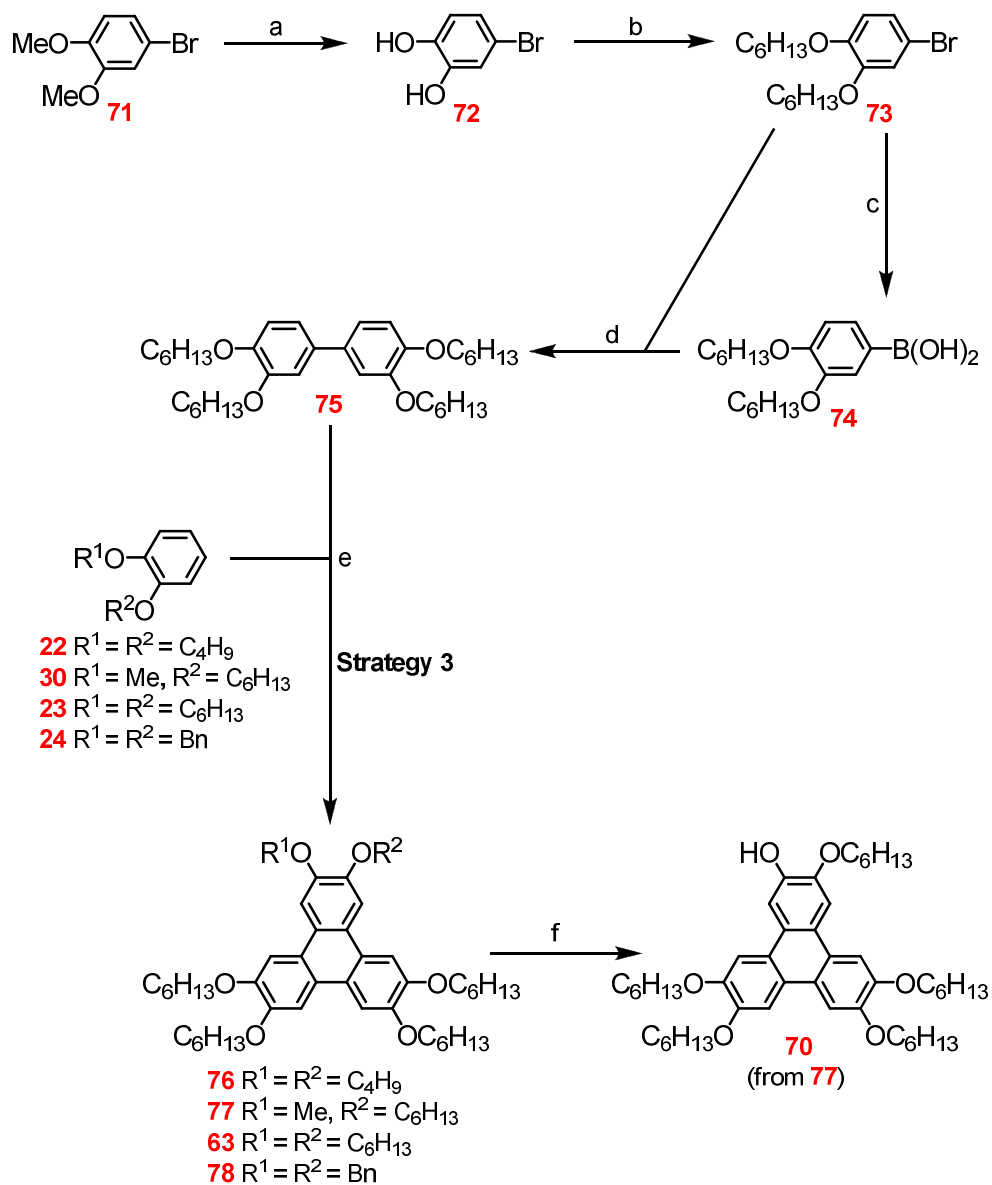


Scheme 7



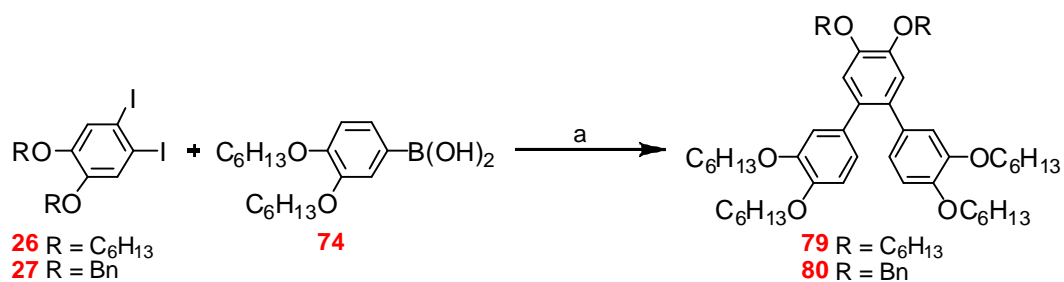
a... FeCl₃, H₂SO₄, DCM
 b... FeCl₃, DCM
 c... MoCl₅, DCM
 d... VOCl₃, DCM
 e... (i) *B*-bromocatecholborane, DCM; (ii) 10% HCl

Scheme 8



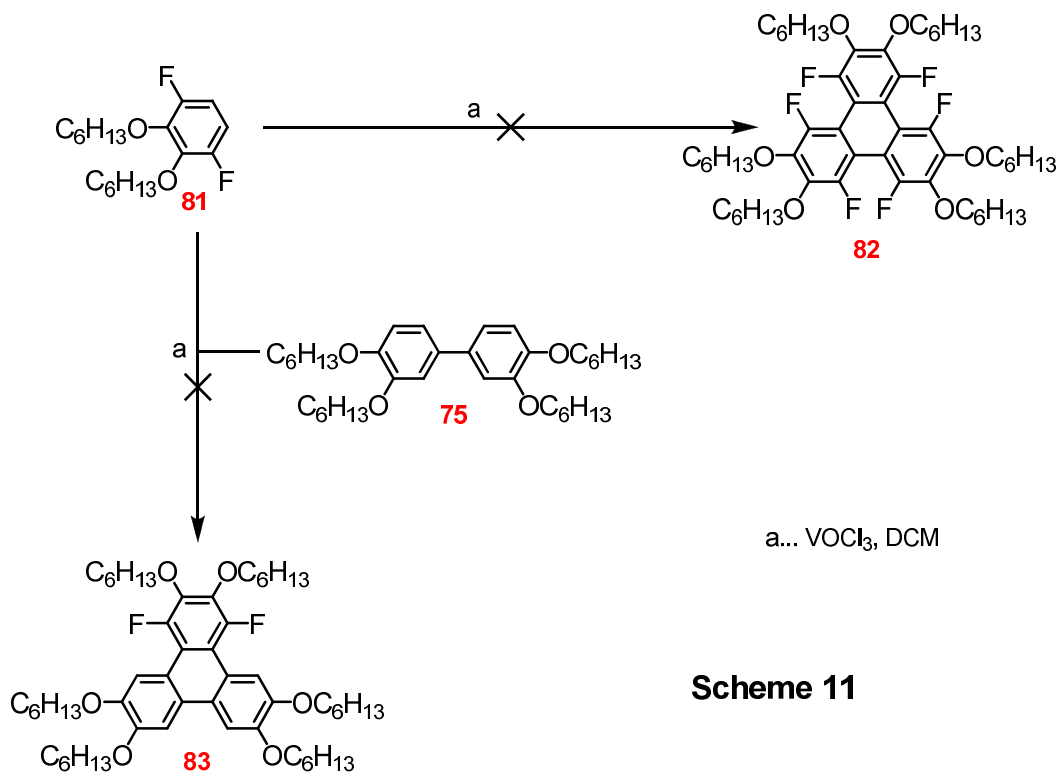
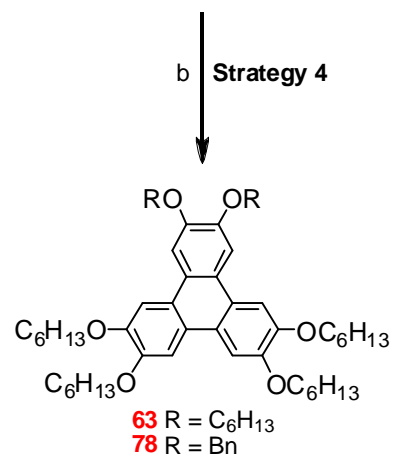
- a... (i) BBr_3 , DCM; (ii) 10% HCl
 b... RBr, K_2CO_3 , butanone
 c... (i) Mg, THF; (ii) $B(OMe)_3$; (iii) 10% HCl
 d... $Pd(PPh_3)_4$, Na_2CO_3 , H_2O , DME
 e... $VOCl_3$ or $MoCl_5$, DCM
 f ... (i) *n*-BuLi, H-PPh₂, THF; (ii) 10% HCl

Scheme 9

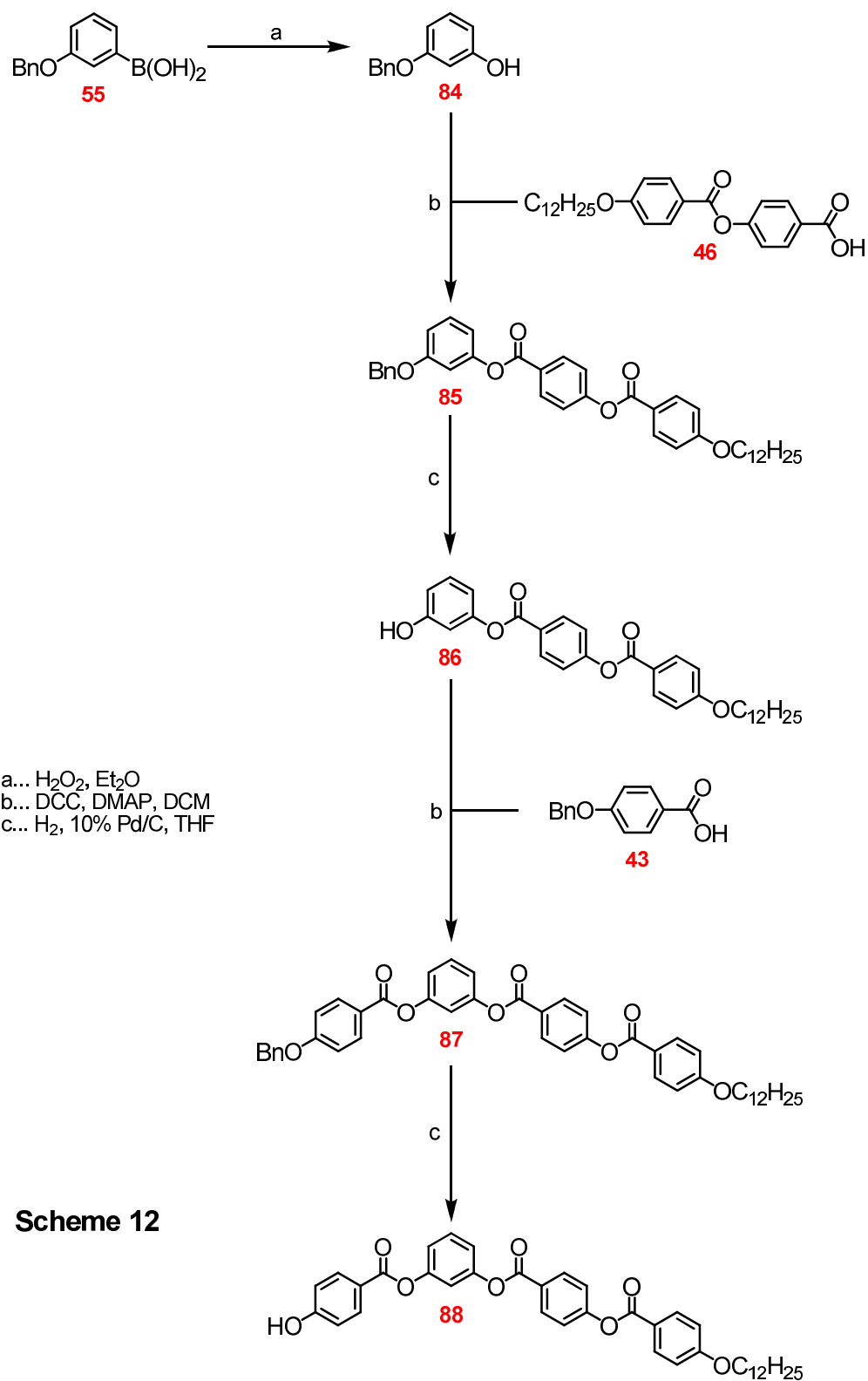


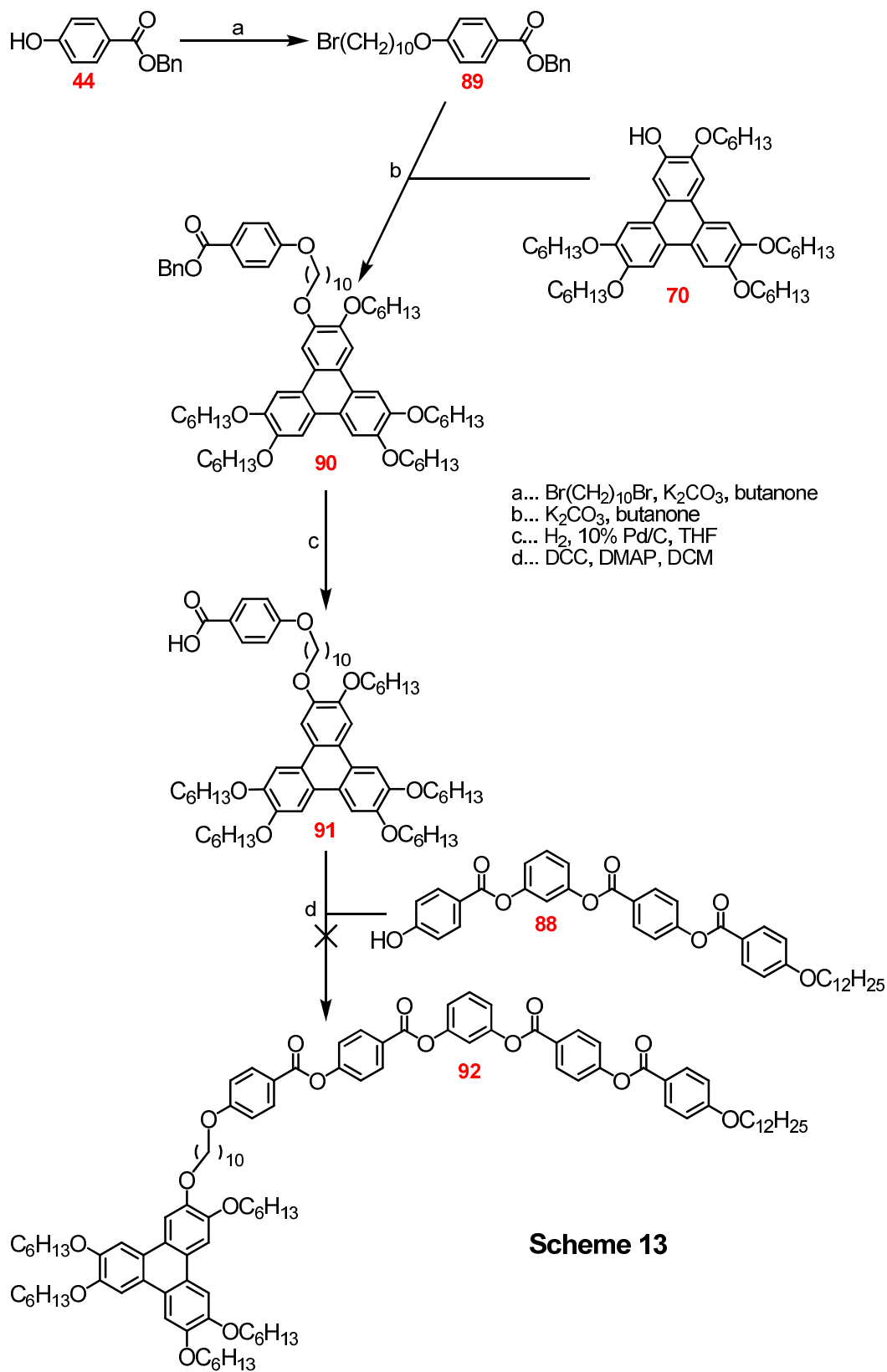
a... Pd(PPh₃)₄, Na₂CO₃, H₂O, DME
 b... VOCl₃ or MoCl₅, DCM

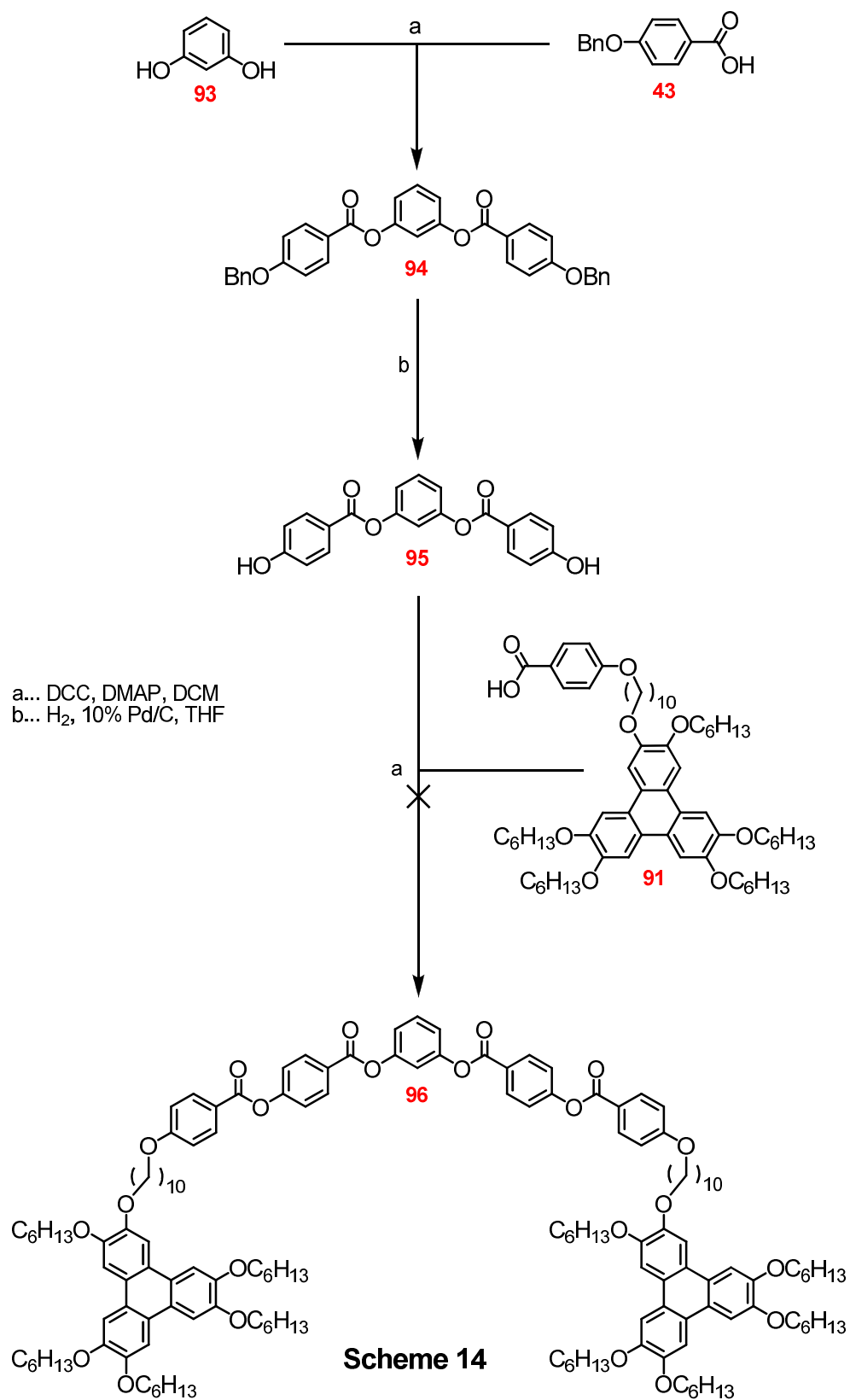
Scheme 10

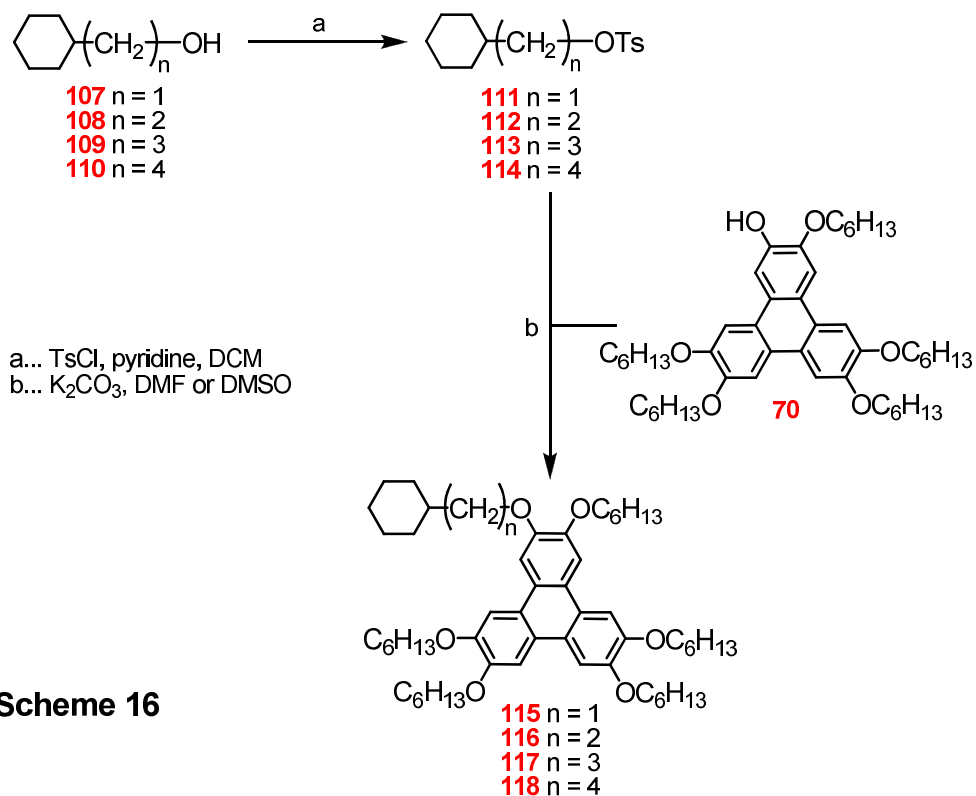
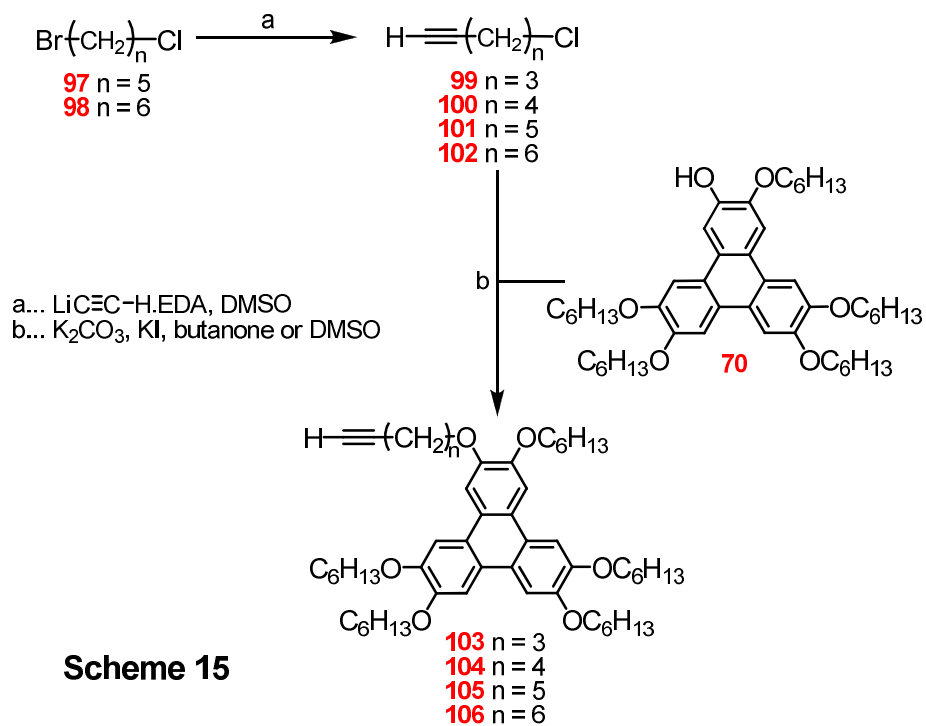


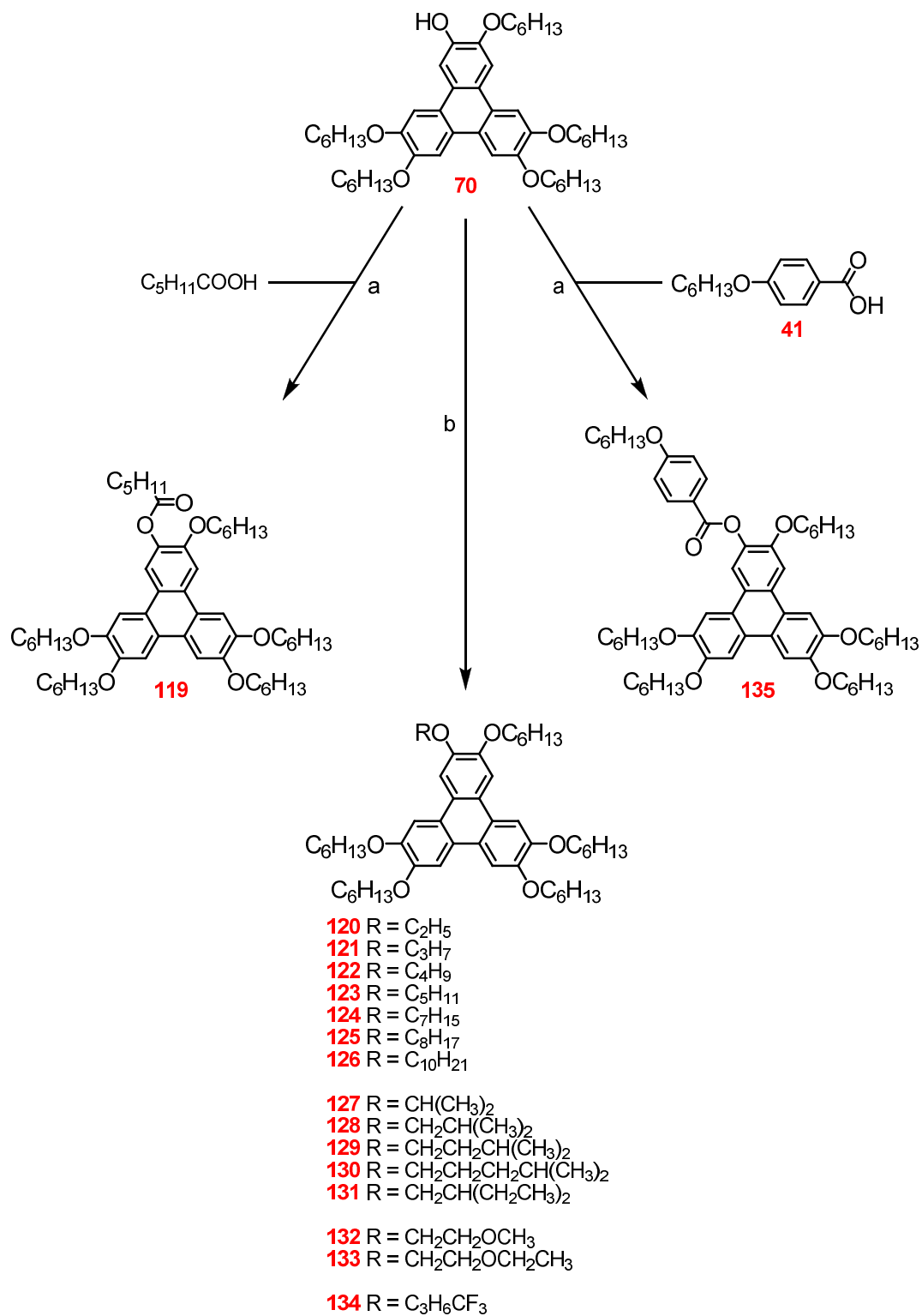
Scheme 11





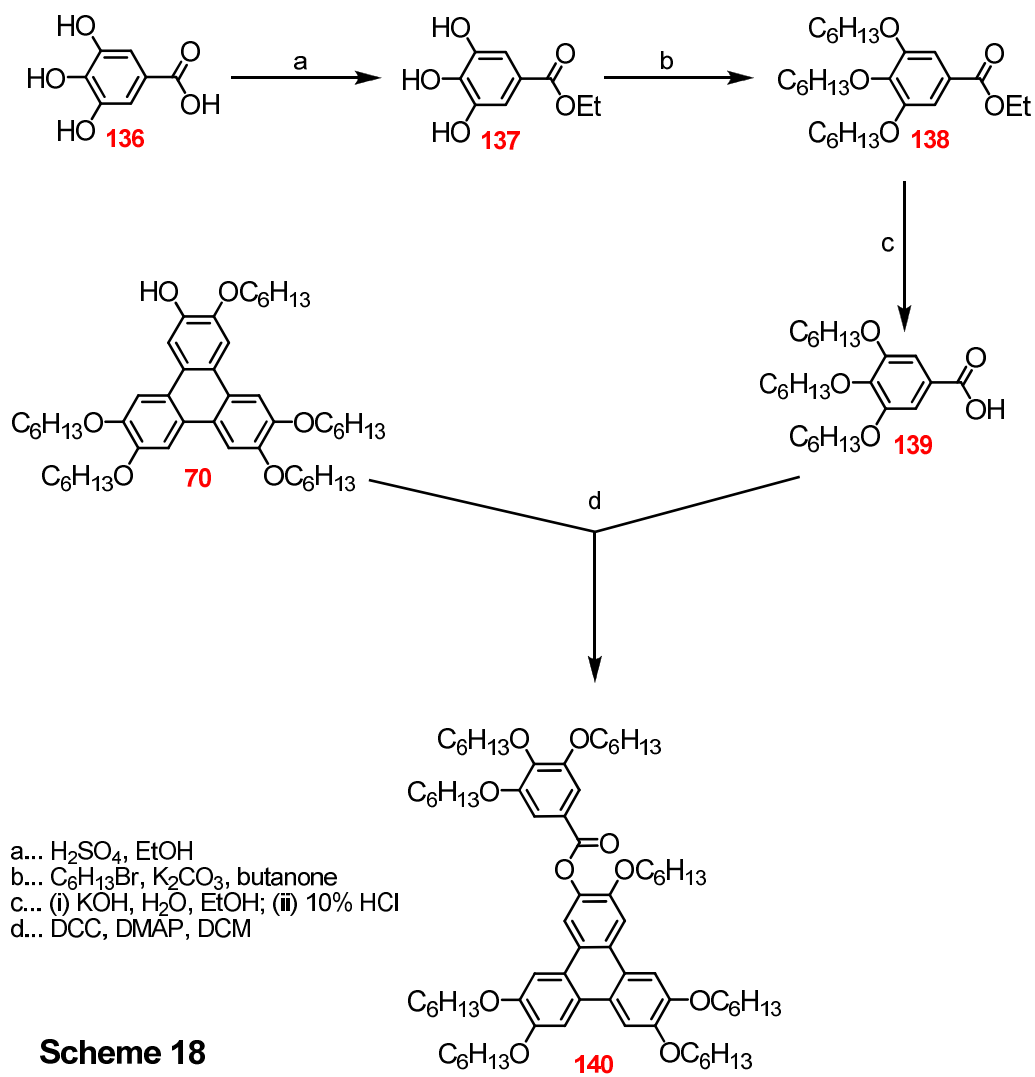


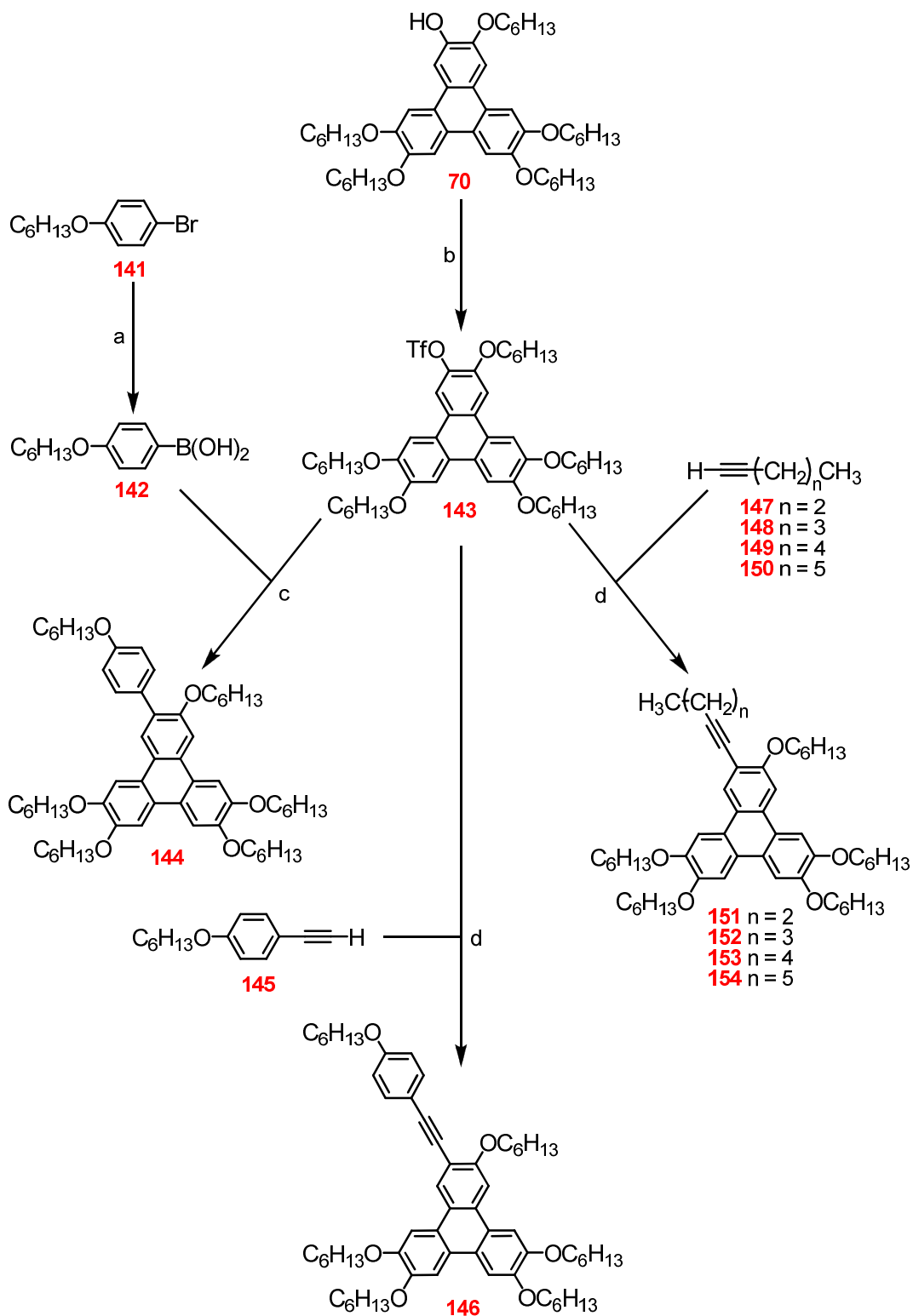




a... DCC, DMAP, DCM
 b... RBr or RI, K₂CO₃, KI, butanone or DMSO

Scheme 17





a... (i) *n*-BuLi, THF; (ii) B(OMe)₃; (iii) 10% HCl
 b... Tf₂O, pyridine
 c... Pd(PPh₃)₄, LiCl, Na₂CO₃, H₂O, DME
 d... (i) *n*-BuLi, THF; (ii) ZnCl₂; (iii) Pd(PPh₃)₄, LiCl

Scheme 19

3.3 Experimental Procedures

1,3,5-Tribromo-2-hexyloxybenzene (3)

A stirred mixture of 2,4,6-tribromophenol (**1**, 50.00 g, 0.152 mol), 1-bromohexane (24.00 g, 0.145 mol) and potassium carbonate (60.00 g, 0.453 mol) in butanone (500 ml) was heated under reflux for 2 days (TLC revealed a complete reaction). The mixture was cooled to room temperature, filtered to remove the potassium carbonate and the solvent was removed *in vacuo*. The product was extracted into diethyl ether, washed with 10 % potassium hydroxide solution and water, the aqueous portions were back extracted with diethyl ether and the ethereal extracts were dried (MgSO₄) and the solvent removed *in vacuo* to yield a colourless oil.

Yield: 52.25 g (86 %), ¹H NMR (CDCl₃) δ: 0.91 (3H, t), 1.31-1.38 (4H, m), 1.51 (2H, quint), 1.85 (2H, quint), 3.97 (2H, t), 7.63 (2H, s), MS *m/z*: 412 (M⁺+1), 414 (M⁺+1), 416 (M⁺+1), 418 (M⁺+1).

1,3,5-Trichloro-2-hexyloxybenzene (4)

The same procedure was carried out as for compound **3** using the following quantities: 2,4,6-trichlorophenol (**2**, 38.70 g, 0.200 mol), 1-bromohexane (29.40 g, 0.178 mol), potassium carbonate (74.00 g, 0.536 mol), and butanone (500 ml). The procedure yielded a colourless oil.

Yield: 50.00 g (100 %), ¹H NMR (CDCl₃) δ: 0.90 (3H, t), 1.31-1.38 (4H, m), 1.50 (2H, quint), 1.82 (2H, quint), 3.98 (2H, t), 7.24 (2H, s), MS *m/z*: 280 (M⁺+1), 282 (M⁺+1), 284 (M⁺+1), 286 (M⁺+1).

2,4,6-Tribromo-3-hexyloxyphenylboronic acid (5)

A solution of *n*-butyllithium (26 ml, 2.5 M in hexanes, 0.0650 mol) was added dropwise to a stirred, cooled (− 78 °C) solution of diisopropylamine (7.00 g, 0.0690 mol) in anhydrous tetrahydrofuran (THF, 500 ml) under dry nitrogen. The mixture was stirred at − 78°C for 1 h before compound **3** was added dropwise and stirred for 2 h. Trimethyl borate (13.50 g, 0.130 mol) was added dropwise to the mixture which was stirred for a further 2 h. The mixture was warmed to room temperature (overnight), then acidified with 10 % hydrochloric acid solution, and stirred for 1 h. The product was extracted into

diethyl ether and washed with water (twice), the aqueous components were backwashed with diethyl ether, the ethereal extracts were dried (MgSO_4), and the solvent removed *in vacuo*. The solid product was purified by stirring in hexane (1 h) to yield an off-white solid.

Yield: 12.89 g (43 %), ^1H NMR (DMSO-D_6) δ : 0.90 (3H, t), 1.31-1.38 (4H, m), 1.50 (2H, quint), 1.83 (2H, quint), 3.98 (2H, t), 4.97 (2H, s), 7.65 (1H, s), MS m/z : 456 (M^+), 458 (M^+), 460 (M^+), 462 (M^+), mp: 98.6-101.2 °C.

2,4,6-Trichloro-3-hexyloxyphenylboronic acid (6)

A solution of *n*-butyllithium (37 ml, 2.5 M in hexanes, 0.0925 mol) was added dropwise to a stirred, cooled (-78 °C) solution of compound **4** (29.00 g, 0.103 mol) in anhydrous THF (500 ml) under dry nitrogen. The mixture was stirred at -78 °C for 1 h and trimethyl borate (19.00 g, 0.183 mol) was added dropwise. The mixture was stirred for 1 h, then warmed to room temperature (overnight), then acidified with 10 % hydrochloric acid solution and stirred for 1 h. The product was extracted into diethyl ether and washed with water (twice), the aqueous components were backwashed with diethyl ether, the combined ethereal extracts were dried (MgSO_4) and the solvent removed *in vacuo* to yield an off-white solid. The crude product was purified by stirring in hexane (1 h) to yield a colourless solid.

Yield: 30.00 g (99 %), ^1H NMR (CDCl_3) δ : 0.91 (3H, t), 1.31-1.38 (4H, m), 1.50 (2H, quint), 1.83 (2H, quint), 3.97 (2H, t), 4.97 (2H, s), 7.29 (1H, s), MS m/z : 324 (M^+), 326 (M^+), 328 (M^+), 330 (M^+), mp: 100.1-103.6 °C.

2,4,6-Tribromo-3-hexyloxyphenol (7)

Hydrogen peroxide (12 %, 63.5 ml, 0.224 mol) was added dropwise to a stirred, heated solution of compound **5** (12.89 g, 0.0281 mol) in diethyl ether (250 ml). The mixture was heated under reflux (overnight) and cooled to room temperature. The product was extracted into dichloromethane (DCM), washed with ammonium ferrous sulphate solution and water (twice), the aqueous components were backwashed with DCM, the combined organic components were dried (MgSO_4), and the solvent removed *in vacuo* to yield a colourless solid.

Yield: 12.07 g, 100 %, ¹H NMR (CDCl₃) δ: 0.92 (3H, t), 1.31-1.38 (4H, m), 1.37 (2H, quint), 1.85 (2H, quint), 3.96 (2H, t), 5.07 (1H, s), 7.64 (1H, s), MS *m/z*: 425 (M⁺+1), 427 (M⁺+1), 429 (M⁺+1), 431 (M⁺+1), mp: 95.9-100.0 °C.

2,4,6-Trichloro-3-hexyloxyphenol (8)

The same procedure was carried out as for compound **7** using the following quantities: compound **6** (30.00 g, 0.0922 mol), hydrogen peroxide (12 %, 209 ml, 0.738 mol) and diethyl ether (500 ml). This procedure yielded an inseparable mixture of the starting material **6**, the de-boronated material, **4**, and the product.

1,3,5-Tribromo-2,4-dihexyloxybenzene (9)

The same procedure was carried out as for compound **3** using the following quantities: compound **7** (12.07 g, 0.0280 mol), 1-bromohexane (5.80 g, 0.0351 mol), potassium carbonate (12.00 g, 0.0870 mol), and butanone (250 ml). The crude product was purified by column chromatography (silica gel, 1:1 hexane / DCM), to yield a colourless oil.

Yield: 12.50 g (87 %), ¹H NMR (CDCl₃) δ: 0.83 (6H, t), 1.22-1.30 (8H, m), 1.31 (4H, quint), 1.75 (4H, quint), 3.89 (2H, t), 7.55 (1H, s), MS *m/z*: 512 (M⁺), 514 (M⁺), 516 (M⁺), 518 (M⁺).

2,4,6-Tribromo-3,5-dihexyloxyphenylboronic acid (11)

The same procedure was carried out as for compound **5** using the following quantities: *n*-butyllithium (7 ml, 2.5 M in hexanes, 0.0220 mol), diisopropylamine (2.30 g, 0.0230 mol), **9** (12.50 g, 0.0240 mol), THF (250 ml), trimethyl borate (7.20 g, 0.0690 mol). The mixture was extracted into diethyl ether and washed with water (twice), the aqueous components were backwashed with diethyl ether, the ethereal extracts were dried (MgSO₄), and the solvent removed *in vacuo* to yield the starting material compound **9**.

1,3,5-Trihexyloxybenzene (20)

A stirred mixture of 1,3,5-trihydroxybenzene (**9**, 10.00 g 0.0794 mol), 1-bromohexane (39.29 g, 0.238 mol) and potassium carbonate (32.86 g, 0.238 mol), potassium iodide (39.52 g, 0.238 mol) in *N,N*-dimethylformamide (DMF, 500 ml) was heated under reflux for 3 days. The mixture was cooled to room temperature, filtered to remove the

potassium carbonate and the solvent was removed *in vacuo*. The product was extracted into diethyl ether, washed with 10 % potassium hydroxide solution and water, the aqueous portions were back extracted with diethyl ether and the ethereal extracts were dried (MgSO₄) and the solvent removed *in vacuo*. The crude product was purified by column chromatography (silica gel, hexane with increasing volume fractions of DCM), to yield a yellow oil.

Yield: 7.73 g (25 %), ¹H NMR (CDCl₃) δ: 0.90 (9H, t), 1.11-1.41 (12H, m), 1.44 (6H, quint), 1.75 (6H, quint), 3.90 (6H, t), 6.06 (3H, s), MS *m/z*: 378 (M⁺).

1,3,5-Tribromo-2,4,6-trihexyloxybenzene (15)

Bromine (9.19 g, 2.9 ml, 0.0574 mol) was added dropwise to a stirred, heated mixture of compound **20** (7.00 g, 0.0185 mol) and iron(III) chloride (0.31 g, 1.85 mmol) in DCM (125 ml). The mixture was heated under reflux for 4 h, cooled to room temperature and stirred together (overnight). Sodium thiosulphate solution was added and the mixture was stirred for a further 2 hours. The organic layer was separated and washed with water, the aqueous components were backwashed with DCM, the combined organic components were dried (MgSO₄) and the solvent removed *in vacuo*. The crude product was purified by column chromatography (silica gel, hexane with increasing volume fractions of DCM) to yield a dark brown oil.

Yield: 6.25 g (55 %), ¹H NMR (CDCl₃) δ: 0.90 (9H, t), 1.28-1.38 (12H, m), 1.44 (6H, quint), 1.88 (6H, quint), 4.40 (6H, t), MS *m/z*: 615 (M⁺), 613 (M⁺), 611 (M⁺), 609 (M⁺).

1,3,5-Trihept-1-ynyl-2,4,6-trihexyloxybenzene (17)

n-Butyllithium (16.3 ml, 2.5 M in hexanes, 0.0408 mol) was added dropwise to a stirred, cooled (0 °C) solution of hept-1-yne (3.90 g, 0.0408 mol) in anhydrous THF (150 ml). The mixture was stirred for 1 h, then zinc(II) chloride (6.66 g, 0.0490 mol) in anhydrous THF (20 ml) was added dropwise. The mixture was stirred for 2 h, slowly warmed to room temperature, and tetrakis(triphenylphosphine)palladium(0) (2 g) and compound **15** (1.00 g, 1.63 mmol) were added. The mixture was heated under reflux (overnight) and then cooled to room temperature. 10 % Hydrochloric acid solution was added to the mixture, which was extracted into diethyl ether, washed with water, sodium hydrogen carbonate solution, and water again. The aqueous components were backwashed with diethyl ether, the combined organic extracts were dried (MgSO₄) and

the solvent removed *in vacuo*. The mixture was subjected to column chromatography (silica gel, hexane with increasing volume fractions of DCM), however no product was isolated.

1,2-Dibutoxybenzene (22)

The same procedure was carried out as for compound **3** using the following quantities: catechol (**21**, 8.00 g, 0.0730 mol), 1-bromobutane (24.00 g, 0.177 mol), potassium carbonate (30.00 g, 0.217 mol) and butanone (250 ml). The crude product was purified by fractional distillation under reduced pressure to yield a colourless oil.

Yield: 14.94 g (92 %), $^1\text{H NMR}$ (CDCl_3) δ : 1.01 (6H, t), 1.54 (4H, sextet), 1.82 (4H, quint), 4.02 (4H, t), 6.89-6.93 (4H, m), MS m/z : 222 (M^+), b.p.: 86-92 °C at 0.01 mmHg.

1,2-Dihexyloxybenzene (23)

The same procedure was carried out as for compound **3** using the following quantities: compound **21** (16.00 g, 0.145 mol), 1-bromohexane (58 g, 0.352 mol), potassium carbonate (60.00 g, 0.435 mol) and butanone (500 ml). The crude product was purified by column chromatography (silica gel, 1:1 hexane / DCM) to yield a colourless oil.

Yield: 39.29 g (98 %), $^1\text{H NMR}$ (CDCl_3) δ : 0.93 (6H, t), 1.30-1.44 (8H, m), 1.50 (4H, quint), 1.83 (4H, quint), 4.00 (4H, t), 6.83-6.88 (4H, m), MS m/z : 278 (M^+).

1,2-Dibenzyloxybenzene (24)

The same procedure was carried out as for compound **3** using the following quantities: compound **21** (6.70 g, 0.0609 mol), benzyl bromide (31.00 g, 0.181 mol), potassium carbonate (25.00 g, 0.183 mol), and butanone (250 ml). The crude product was purified by column chromatography (silica gel, 1:1 hexane / DCM) and recrystallised from ethanol to yield colourless crystals.

Yield: 10.49 g (59 %), $^1\text{H NMR}$ (CDCl_3) δ : 5.15 (4H, s), 6.89 (4H, m), 7.36 (10H, m), MS m/z : 290 (M^+), mp: 56.5-57.2 °C.

1,2-Dihexyloxy-4-iodobenzene (25)

Several methods were employed in preparing this compound.

Method 1

A mixture of compound **23** (10.00 g, 0.0360 mol), *N*-iodosuccinimide (NIS, 9.00 g, 0.0400 mol) and trifluoroacetic acid (1.25 g, 0.0110 mol) in acetonitrile (120 ml) were stirred together at room temperature for 17 h (GC revealed partial reaction). To the mixture, NIS (3.00 g, 0.0133 mol), trifluoroacetic acid (5 ml) and acetonitrile (30 ml) were added and were stirred together for 24 h with gentle heating (30 °C, GC revealed the presence of mono- and di-iodinated material and the absence of starting material). The mixture was extracted into diethyl ether, washed with water, sodium bisulphite solution and water; the aqueous components were backwashed with further portions of diethyl ether. The combined organic extracts were dried (MgSO₄) and the solvent removed *in vacuo*. The crude product was subjected to column chromatography (silica gel, hexane) to yield a yellow / orange oil.

Yield: 12.35 g (85 %), ¹H NMR (CDCl₃) δ: 0.90 (6H, 2×t), 1.23-1.38 (8H, m), 1.40-1.50 (4H, m), 1.74-1.84 (4H, m), 3.92 (4H, 2×t), 6.60 (1H, d), 7.12 (1H, d), 7.15 (1H, dd), (and diiodinated material as: ¹H NMR (CDCl₃) δ: 0.90 (1.95H, t), 1.23-1.38 (2.6H, m), 1.40-1.50 (1.3H, m), 1.74-1.84 (1.3H, m), 3.91 (1.3H, t), 7.24 (0.65H, s)), MS *m/z*: 404 (M⁺), 530 (M⁺).

Method 2

A mixture of compound **23** (10.00 g, 0.0360 mol), NIS (9.00 g, 0.0400 mol) and trifluoroacetic acid (1.25 g, 0.0110 mol) in acetonitrile (120 ml) were stirred together at room temperature for 17 h (GC revealed partial reaction). To the mixture NIS (3.00 g, 0.0133 mol), trifluoroacetic acid (5 ml) and acetonitrile (30 ml) were added and were stirred together for 24 h (GC revealed the presence of mono- and di-iodinated material and the absence of starting material). The mixture was extracted into diethyl ether, washed with water, sodium bisulphite solution and water; the aqueous components were backwashed with further portions of diethyl ether. The combined organic extracts were dried (MgSO₄) and the solvent removed *in vacuo*. The crude product was subjected to column chromatography (silica gel, hexane) to yield a yellow / orange oil.

Yield: 12.41 g (85 %), ¹H NMR (CDCl₃) δ: 0.90 (6H, 2×t), 1.23-1.38 (8H, m), 1.40-1.50 (4H, m), 1.74-1.84 (4H, m), 3.92 (4H, 2×t), 6.60 (1H, d), 7.12 (1H, d), 7.15 (1H, dd), (and diiodinated material as: ¹H NMR (CDCl₃) δ: 0.90 (0.97H, t), 1.23-1.38 (1.3H,

m), 1.40-1.50 (0.65H, m), 1.74-1.84 (0.65H, m), 3.91 (0.65H, t), 7.24 (0.33H, s)), MS *m/z*: 404 (M^+), 530 (M^+).

Method 3

A stirred mixture of compound **23** (3.80 g, 0.0137 mol), NIS (4.86 g, 0.0216 mol) and in acetonitrile (120 ml) was heated under reflux for 48 h. GC indicated only trace levels of product were present.

Method 4

A mixture of compound **23** (10.00 g, 0.0360 mol), NIS (9.00 g, 0.0400 mol) and trifluoroacetic acid (1.25 g, 0.0110 mol) in acetonitrile (120 ml) was stirred together at room temperature for 2 days, and the reaction progress was monitored at regular intervals by GC. The mixture was extracted into diethyl ether, washed with water, sodium bisulphite solution and water; the aqueous components were backwashed with further portions of diethyl ether. The combined organic extracts were dried ($MgSO_4$) and the solvent removed *in vacuo*. The crude product was subjected to column chromatography (silica gel, hexane) to yield a yellow / orange oil.

Yield: 11.26 g (77 %), 1H NMR (CD_2Cl_2) δ : 0.90 (6H, 2xt), 1.27-1.39 (8H, m), 1.60 (4H, 2xquint), 1.86 (4H, 2xquint), 3.98 (4H, 2xt), 6.63 (1H, d), 7.16 (1H, d), 7.19 (1H, dd), MS *m/z*: 404 (M^+).

Method 5

A solution of *n*-butyllithium (6.00 ml, 2.5 M in hexanes, 0.0147 mol) was added dropwise to a stirred, cooled (-78 °C) mixture of 1,2-dihexyloxy-4-iodobenzene and 1,2-dihexyloxy-4,5-diiodobenzene (approximately 4:1, 7.11 g, 0.0134 mol) in dry THF (300 ml) under an atmosphere of dry nitrogen. The mixture was stirred at -78 °C for 1 h and water (30 ml) in THF (70 ml) was added dropwise. The stirred mixture was slowly warmed to room temperature (overnight) and extracted into diethyl ether. The ethereal extracts were washed with 10 % hydrochloric acid solution and water, the aqueous components were backwashed with further portions of diethyl ether, the combined organic components were dried ($MgSO_4$) and the solvent removed *in vacuo*. The crude product was purified by column chromatography (silica gel, hexane) to yield a yellow / orange oil.

Yield: 24.34 g (93 %), ^1H NMR (CD_2Cl_2) δ : 0.90 (6H, 2xt), 1.27-1.39 (8H, m), 1.60 (4H, 2xquint), 1.86 (4H, 2xquint), 3.98 (4H, 2xt), 6.63 (1H, d), 7.16 (1H, d), 7.19 (1H, dd), MS m/z : 404 (M^+).

1,2-Dihexyloxy-4,5-diiodobenzene (26)

A mixture of compound **23** (5.00 g, 0.0180 mol), NIS (10.00 g, 0.0444 mol) and trifluoroacetic acid (1.23 g, 0.0108 mol) in acetonitrile (120 ml) was stirred together at room temperature for 74 h (GC indicated a complete reaction). The mixture was extracted into diethyl ether, washed with water, sodium bisulphite solution and water; the aqueous components were backwashed with further portions of diethyl ether. The combined organic extracts were dried (MgSO_4) and the solvent removed *in vacuo*. The crude product was subjected to column chromatography (silica gel, 1:1 hexane / DCM) to yield a yellow oil.

Yield: 8.00 g (84 %), ^1H NMR (CDCl_3) δ : 0.82 (6H, t), 1.18-1.24 (6H, m), 1.25-1.28 (6H, m), 1.69 (4H, quint), 3.48 (4H, t), 7.16 (2H, s), MS m/z : 530 (M^+).

1,2-Dibenzoyloxy-4,5-diiodobenzene (27)

A mixture of compound **24** (5.35 g, 0.0185 mol), NIS (10.40 g, 0.0463 mol) and trifluoroacetic acid (1.27 g, 0.0111 mol) in acetonitrile (120 ml) was stirred together at room temperature for 9 days and 2 h (GC indicated a complete reaction) and the product formed a solid precipitate. The solid product was filtered, washed with acetonitrile and water and dried (P_2O_5) to yield a solid powder.

Yield: 6.91 g (69 %), ^1H NMR (CDCl_3) δ : 5.10 (4H, s), 7.30-7.41 (12H, m), ^{13}C NMR (CDCl_3) δ : 71.41, 96.82, 125.00, 127.36, 128.12, 128.58, 136.20, 149.47, MS m/z : 542 (M^+), mp: 129.9-133.0 °C.

1-Hexyloxy-2-methoxybenzene (30)

The same procedure was carried out as for compound **3** using the following quantities: 2-methoxyphenol (**28**, 14.90, 0.120 mol), 1-bromohexane (39.65 g, 0.240 mol), potassium carbonate (33.00 g, 0.239 mol) and butanone (500 ml). The excess of 1-bromohexane was removed *in vacuo* to yield a colourless oil.

Yield: 10.26 g (41 %), ^1H NMR (CDCl_3) δ : 0.89 (3H, t), 1.33 (4H, m), 1.44 (2H, quint), 1.83 (2H, quint), 3.83 (3H, s), 3.99 (2H, t), 6.84-6.90 (4H, m) MS m/z : 208 (M^+).

1-Benzyloxy-2-methoxybenzene (31)

The same procedure was carried out as for compound **3** using the following quantities: 2-benzyloxyphenol (**29**, 10.00 g, 0.0500 mol), iodomethane (21.28 g, 0.150 mol), potassium carbonate (20.79 g, 0.150 mol) and butanone (250 ml). The excess of iodomethane was distilled off *in vacuo* to yield a colourless oil.

Yield: 9.67 g (84 %), $^1\text{H NMR}$ (CDCl_3) δ : 3.88 (3H, s), 5.15 (2H, s), 6.83-6.92 (4H, m), 7.22-7.44 (5H, m), MS m/z : 214 (M^+).

1-Benzyloxy-2-butoxybenzene (32)

The same procedure was carried out as for compound **3** using the following quantities: compound **29** (10.00 g, 0.0500 mol), 1-bromobutane (20.50 g, 0.150 mol), potassium carbonate (20.70 g, 0.150 mol) and butanone (250 ml). The excess of 1-bromobutane was distilled off *in vacuo* to yield colourless oil.

Yield: 11.86 g (92 %), $^1\text{H NMR}$ (CDCl_3) δ : 0.96 (3H, t), 1.50 (2H, sext), 1.80 (2H, quint), 4.01 (2H, t), 5.10 (2H, s), 6.77-6.91 (4H, m), 7.24-7.44 (5H, m), MS m/z : 256 (M^+).

1-Benzyloxy-2-hexyloxybenzene (33)

The same procedure was carried out as for compound **3** using the following quantities: compound **29** (10.00 g, 0.0500 mol), 1-bromohexane (20.60 g, 0.125 mol), potassium carbonate (20.70 g, 0.0150 mol) and butanone (250 ml). The crude product was purified by column chromatography (silica gel, 1:1 hexane / DCM) to yield a colourless oil.

Yield: 11.49 g (81 %), $^1\text{H NMR}$ (CDCl_3) δ : 0.90 (3H, t), 1.28-1.38 (4H, m), 1.48 (2H, quint), 1.82 (2H, quint), 4.00 (2H, t), 5.11 (2H, s), 6.81-6.95 (4H, m), 7.19-7.45 (5H, m), MS m/z : 284 (M^+).

1-Benzyloxy-2-octyloxybenzene (34)

The same procedure was carried out as for compound **3** using the following quantities: compound **29** (10.00 g, 0.0500 mol), 1-bromooctane (29.00 g, 0.150 mol), potassium carbonate (20.70 g, 0.150 mol) and butanone (250 ml). The crude product was purified by column chromatography (silica gel, 1:1 hexane / DCM) to yield a colourless oil.

Yield: 12.22 g (78 %), $^1\text{H NMR}$ (CDCl_3) δ : 0.87 (3H, t), 1.24-1.40 (8H, m), 1.46 (2H, quint), 1.81 (2H, quint), 3.99 (2H, t), 5.09 (2H, s), 6.76-6.90 (4H, m), 7.24-7.44 (5H, m), MS m/z : 312 (M^+).

2-Benzyloxy-4-iodophenol (35)

A mixture of compound **29** (3.00 g, 0.0160 mol), NIS (4.08 g, 0.0181 mol) and trifluoroacetic acid (0.51 g, 4.47 mmol) in acetonitrile (100 ml) was stirred at room temperature and monitored by GC. After 8 days no reaction had occurred.

1-Benzyloxy-2-methoxy-5-iodobenzene (36)

A mixture of compound **31** (3.00 g, 0.0150 mol), NIS (3.71 g, 0.0165 mol) and trifluoroacetic acid (0.51 g, 4.47 mmol) in acetonitrile (100 ml) was stirred at room temperature and monitored by GC for 21 h, which indicated 70 % conversion had occurred, with no indication of the presence of the corresponding diiodinated moiety.

1-Benzyloxy-2-butoxy-5-iodobenzene (37)

A mixture of compound **32** (3.00 g, 0.0124 mol), NIS (3.07 g, 0.0136 mol) and trifluoroacetic acid (0.42 g, 3.70 mmol) in acetonitrile (100 ml) was stirred at room temperature and monitored by GC for 26 h, which indicated 92 % conversion had occurred, with no indication of the presence of the corresponding diiodinated moiety.

Yield: 92 % (GC), $^1\text{H NMR}$ (CDCl_3) δ : 0.96 (3H, t), 1.50 (2H, sext), 1.80 (2H, quint), 4.00 (2H, t), 5.10 (2H, s), 6.87-6.92 (3H, m), 7.24-7.44 (5H, m).

1-Benzyloxy-2-hexyloxy-5-iodobenzene (38)

A mixture of compound **33** (3.00 g, 0.0105 mol), NIS (2.61 g, 0.0116 mol) and trifluoroacetic acid (0.36 g, 3.16 mmol) in acetonitrile (100 ml) was stirred at room temperature and monitored by GC for 48 h, which indicated that 92 % conversion had occurred, with no indication of the presence of the corresponding diiodinated moiety.

1-Benzyloxy-2-octyloxy-5-iodobenzene (39)

A mixture of compound **34** (3.00 g, 0.0100 mol), NIS (2.49 g, 0.0110 mol) and trifluoroacetic acid (0.10 g, 0.877 mmol) in acetonitrile (100 ml) was stirred at room

temperature and monitored by GC for 23 h, which indicated that 93 % conversion had occurred, with no indication of the presence of the corresponding diiodinated moiety.

Yield: 93 % (GC), ^1H NMR (CDCl_3) δ : 0.87 (3H, t), 1.23-1.38 (8H, m), 1.45 (2H, quint), 1.80 (2H, quint), 3.97 (2H, t), 5.07 (2H, s), 6.63 (1H, dd), 7.12-7.23 (2H, m), 7.28-7.44 (5H, m).

4-Hexyloxybenzoic acid (41)

1-Bromohexane (120 g, 0.727 mol) was added dropwise to a stirred, heated mixture of 4-hydroxybenzoic acid (**40**, 50.00 g, 0.362 mol), potassium hydroxide (40.72 g, 0.727 mol), water (200 ml) and ethanol (700 ml), which was heated under reflux (overnight). The mixture was cooled to room temperature and a second portion of potassium hydroxide (40.72 g, 0.727 mol) and water (500 ml) were added and the mixture heated for a further 2 h. The mixture was cooled to room temperature, poured onto ice and acidified (congo red) with hydrochloric acid. The resulting precipitate was filtered off, recrystallised from ethanol and dried (P_2O_5) to yield colourless needle-like crystals.

Yield: 37.67 g (47 %), ^1H NMR ($\text{DMSO}-d_6$) δ : 0.85 (3H, t), 1.26-1.30 (4H, m), 1.38 (3H, quint), 1.69 (2H, quint), 4.00 (2H, t), 6.97 (2H, d), 7.85 (2H, d), MS m/z : 222 (M^+), transition temperatures ($^\circ\text{C}$): Cr 106.7 N 157.5 I, lit. transition temperatures ($^\circ\text{C}$): Cr 106.2 N 154.8 I¹⁰⁷.

4-Dodecyloxybenzoic acid (42)

The same procedure was carried out as detailed for compound **41** using sodium hydroxide in place of potassium hydroxide and using the following quantities: 1-bromododecane (32.60 g, 0.131 mol), compound **40** (9.03 g, 0.0654 mol), sodium hydroxide (5.23 g, 0.131 mol), water (100 ml), ethanol (400 ml), sodium hydroxide (5.23 g, 0.131 mol), water (200 ml). The precipitate was recrystallised from ethanol / ethyl acetate (5:1) and dried (P_2O_5) to yield colourless needle-like crystals.

Yield: 16.81 g (84 %), ^1H NMR (CDCl_3) δ : 0.88 (3H, t), 1.21-1.37 (18H, m), 1.47(18H, m) 1.47 (2H, quint), 1.81 (2H, quint), 4.01 (2H, t), 6.93 (2H, d), 8.05 (2H, d), MS m/z : 306 (M^+), transition temperatures ($^\circ\text{C}$): Cr 92.4 SmC 131.5 N 142.0 I, lit. transition temperatures ($^\circ\text{C}$): Cr 88 SmC 130 N 137 I¹⁰⁸.

4-Benzoyloxybenzoic acid (43)

The same procedure was carried out as detailed for compound **41** using sodium hydroxide in place of potassium hydroxide and using the following quantities: benzyl bromide (81.60 g, 0.477 mol), compound **40** (30.00 g, 0.217 mol), sodium hydroxide (19.10 g, 0.478 mol), water (200 ml), ethanol (600 ml), sodium hydroxide (19.10 g, 0.478 mol), water (500 ml). The precipitate was recrystallised from ethanol and dried (P_2O_5) to yield colourless crystals.

Yield: 40.07 g (81 %), 1H NMR (DMSO- D_6) δ : 5.05 (2H, s), 6.87 (2H, d), 7.23-7.40 (5H, m), 7.80 (2H, d), 8.18 (1H, s), MS m/z : 228 (M^+), mp: 187.7-189.9 °C, lit. mp: 188-190 °C¹⁰⁹.

Benzyl 4-(4-dodecyloxyphenylcarbonyloxy)benzoate (45)

Dicyclohexylcarbodiimide (DCC, 14.81 g, 0.0719 mol) was added slowly to a stirred solution of benzyl 4-hydroxybenzoate (**44**, 16.39 g, 0.719 mol), compound **42** (20.00 g, 0.0634 mol) and 4-*N,N*-dimethylaminopyridine (DMAP, 2.92 g, 0.0240 mol) in DCM (200 ml). The mixture was stirred together (overnight) and filtered to remove the insoluble traces of *N,N'*-dicyclohexylurea (DCU) that had formed. The crude product was purified by column chromatography (silica gel, 1:1 hexane / DCM), recrystallised from ethanol / ethyl acetate (9:1) and dried (P_2O_5) to yield colourless crystals.

Yield: 32.43 g (99 %), 1H NMR ($CDCl_3$) δ : 0.88 (3H, t), 1.28-1.38 (16H, m), 1.47 (2H, quint), 1.82 (2H, quint), 4.04 (2H, t), 5.38 (2H, s), 6.97 (2H, d), 7.29 (2H, d), 7.33-7.46 (5H, m), 8.12 (2H, d), 8.15 (2H, d), MS m/z : 516 (M^+), mp: 62.5-63.0 °C, lit. mp: 62-63 °C¹¹⁰.

4-(4-Dodecyloxyphenylcarbonyloxy)benzoic acid (46)

A mixture of compound **45** (15.46 g, 0.0300 mol), 10 % palladium-on-carbon (Pd/C, 3 g) and THF (500 ml) were stirred together under an atmosphere of hydrogen (overnight). The mixture was filtered to remove the palladium catalyst, the solvent removed *in vacuo*. The product was recrystallised from ethanol and dried (P_2O_5) to yield colourless needle-like crystals.

Yield: 12.65 g (99 %), 1H NMR (DMSO- D_6) δ : 0.78 (3H, t), 1.19 (16H, m), 1.36 (2H, quint), 1.96 (2H, quint), 4.03 (2H, t), 7.06 (2H, d), 7.35 (2H, d), 7.97 (2H, d), 8.02 (2H,

d), MS m/z : 426 (M^+), transition temperatures ($^{\circ}C$): Cr 119.4 SmC 204.3 N 219.4 I, lit. transition temperatures ($^{\circ}C$): Cr 120.0 SmC 209.0 N 220.5 I¹⁰.

1,3,5-Tri(4-(4-dodecyloxyphenylcarbonyloxy)phenylcarbonyloxy)benzene (47)

The same procedure was carried out as detailed for compound **45** using the following quantities: 1,3,5-trihydroxybenzene (**19**, 0.28 g, 2.22 mmol), compound **46** (3.12 g, 7.30 mmol), DCC (1.50 g, 7.30 mmol), DMAP (0.28 g, 2.30 mmol) and DCM (120 ml). The crude product was purified by column chromatography (silica gel, 1:1 hexane / DCM and silica gel, hexane with increasing volume fractions of DCM), recrystallised from ethanol / ethyl acetate (10:1) to yield colourless crystals.

Yield: 1.14 g (38 %), 1H NMR ($CDCl_3$) δ : 0.88 (9H, t), 1.24-1.41 (18H, m), 1.49 (6H, quint), 1.83 (6H, quint), 4.06 (6H, t), 6.99 (6H, d), 7.19 (3H, s), 7.38 (6H, d), 8.16 (6H, d), 8.29 (6H, d), ^{13}C NMR ($CDCl_3$) δ : 8.53, 14.12, 22.68, 25.96, 29.07, 29.35, 29.56, 29.58, 29.62, 29.65, 31.91, 68.38, 114.41, 120.89, 122.19, 126.32, 131.91, 132.43, 134.45, 148.72, 151.51, 155.56, 163.82, 164.28, MS m/z : 1374 (M^+Na), elemental analysis for $C_{84}H_{102}O_{15}$ requires 74.64 % C, 7.61 % H; found 74.89 % C, 7.89 % H, purity (HPLC): 98 %, transition temperatures ($^{\circ}C$): Cr 79.9 B₁ 87.7 I.

3-Benzyloxybenzoic acid (49)

The same procedure was carried out as detailed for compound **41** using the following quantities: benzyl bromide (30.00 g, 0.175 mol), 3-hydroxybenzoic acid (**48**, 12.00 g, 0.0870 mol), potassium hydroxide (9.80 g, 0.175 mol), water (20 ml), ethanol (250 ml), potassium hydroxide (9.80 g, 0.175 mol), water (40 ml). The precipitate was recrystallised from ethanol and dried (P_2O_5) to yield colourless crystals.

Yield: 14.08 g (71 %), 1H NMR ($CDCl_3$) δ : 5.13 (2H, s), 7.23 (1H, ddd), 7.32-7.47 (6H, m), 7.71-7.75 (2H, m), MS m/z : 228 (M^+), mp: 131.4-134.6 $^{\circ}C$, lit. mp: 134 $^{\circ}C$ ¹¹.

1,3,5-Tri(3-benzyloxyphenylcarbonyloxy)benzene (50)

The same procedure was carried out as detailed for compound **45** using the following quantities: 1,3,5-trihydroxybenzene (**19**, 2.40 g, 0.0191 mol), compound **49** (13.72 g, 0.0602 mol), DCC (12.40 g, 0.0602 mol), DMAP (2.2 g, 0.0181 mol), DCM (250 ml). The crude product was purified by column chromatography (silica gel, 1:1 hexane /

DCM and silica gel, hexane with increasing volume fractions of DCM) to yield colourless crystals.

Yield: 12.50 g (87 %), ^1H NMR (CDCl_3) δ : 5.13 (6H, s), 7.15 (3H, s), 7.25 (3H, ddd), 7.34-7.47 (18H, m), 7.79 (3H, dd), 7.80 (3H, dd), MS m/z : 780 (M^+Na), mp: 126.5-131.4 °C.

1,3,5-Tri(3-hydroxyphenylcarbonyloxy)benzene (51)

The same procedure was carried out as detailed for compound **46** using the following quantities: compound **50** (9.70 g, 0.0128 mol), 10 % Pd/C (1.50 g) and THF (400 ml). This procedure yielded a colourless solid.

Yield: 6.02 g (97 %), ^1H NMR (CDCl_3) δ : 6.50 (3H, ddd), 6.52 (3H, s), 6.74 (4H, dd), 6.97-7.02 (6H, m), 9.00 (3H, s), ^{13}C NMR (CDCl_3) δ : 112.15, 115.36, 119.50, 120.08, 128.40, 150.17, 156.48, 162.97, mp: 221.7-222.8 °C.

1,3,5-Tri(3-(4-(4-dodecyloxyphenylcarbonyloxy)phenylcarbonyloxy)phenylcarbonyloxy)benzene (52)

The same procedure was carried out as detailed for compound **45** using the following quantities: compound **51** (0.57 g, 1.17 mmol), compound **46** (1.65 g, 3.87 mmol), DCC (0.80 g, 3.88 mmol), DMAP (0.14 g, 1.17 mmol) and DCM (100 ml). The crude product was purified by column chromatography (silica gel 5:1 hexane / ethyl acetate and silica gel, hexane with increasing volume fractions of ethyl acetate), recrystallised from ethanol / ethyl acetate (2:1) and dried (P_2O_5) to yield colourless crystals.

Yield: 0.98 g (49 %), ^1H NMR (CDCl_3) δ : 0.88 (9H, t), 1.23-1.41 (48H, m), 1.48 (6H, quint), 1.83 (6H, quint), 4.05 (6H, t), 6.99 (6H, d), 7.20 (3H, s), 7.39 (6H, d), 7.54 (3H, ddd), 7.60 (3H, dd), 8.09 (3H, ddd), 8.15 (6H, d), 8.30 (6H, d), ^{13}C NMR (CDCl_3) δ : 14.12, 22.68, 25.96, 29.06, 29.34, 29.54, 29.57, 29.62, 29.64, 31.91, 68.38, 113.30, 114.40, 120.88, 122.19, 123.61, 126.37, 127.48, 127.82, 129.85, 130.60, 131.92, 132.43, 151.01, 151.40, 155.58, 163.46, 163.82, 164.23, 164.29, MS m/z : 1735 (M^+Na), elemental analysis for $\text{C}_{105}\text{H}_{114}\text{O}_{21}$ requires 73.66 % C, 6.71 % H; found 73.58 % C, 6.92 % H, purity (HPLC): 91 %, transition temperatures (°C): Cr 132.2 (X 96) I.

1-Benzyloxy-3-bromobenzene (54)

The same procedure was carried out as detailed for compound **3** using the following quantities: 3-bromophenol (**53**, 20.00 g, 0.116 mol), benzyl bromide (18.00 g, 0.105 mol), potassium carbonate (32.00 g, 0.232 mol), and butanone (500 ml). The crude product was purified by column chromatography (silica gel, 1:1 hexane / DCM) recrystallised from ethanol and dried (P_2O_5) to yield colourless crystals.

Yield: 29.42 g (96 %), 1H NMR ($CDCl_3$) δ : 5.03 (2H, s), 6.91 (1H, ddd), 7.09 (1H, ddd), 7.12-7.16 (2H, m), 7.31-7.43 (5H, m), MS m/z : 264 (M^+), 262 (M^+), mp: 60.3-61.4 °C, lit. mp: 61-62 °C¹¹².

3-Benzyloxyphenylboronic acid (55)

A solution of compound **54** (34.16 g, 0.130 mol) in THF (200 ml) was added dropwise to a stirred mixture of magnesium (4.00 g, 0.169 mol) in THF (300 ml) under an atmosphere of dry nitrogen. The mixture was stirred until the exothermic reaction ceased (approximately 1 h), then the mixture was cooled (-78 °C) and trimethyl borate (27.00 g, 0.260 mol) was added dropwise. The mixture was stirred at -78 °C for 1 h, then warmed to room temperature (overnight), acidified with 10 % hydrochloric acid solution and stirred for 1 h. The product was extracted into diethyl ether, washed with water (twice), the aqueous components were backwashed with diethyl ether, the ethereal extracts were dried ($MgSO_4$), and the solvent removed *in vacuo*. The solid product was purified by stirring in hexane (1 h) to yield an off-white solid.

Yield: 21.61 g (73 %), 1H NMR ($DMSO-D_6$) δ : 5.07 (2H, s), 7.02 (1H, ddd), 7.23 (1H, dd), 7.30-7.44 (7H, m), 8.03 (2H, s), MS m/z : 630 (M^+ of trimeric anhydride), mp: 139.2-141.3 °C.

1,3,5-Tri(3-benzyloxyphenyl)benzene (57)

Compound **55** (12.00 g, 0.0528 mol) was added to a stirred, heated mixture of 1,3,5-tribromobenzene (**56**, 5.04 g, 0.0160 mol), sodium carbonate (11.24 g, 0.106 mol), tetrakis(triphenylphosphine)palladium(0) (0.90 g, 0.80 mmol), water (60 ml) and 1,2-dimethoxyethane (DME, 180 ml) under an atmosphere of dry nitrogen. The mixture was heated under reflux for 48 h, cooled to room temperature and filtered to remove traces of palladium catalyst. The mixture was extracted into diethyl ether, washed with water and brine, the aqueous components were backwashed with diethyl ether, the combined

organic extracts were dried (MgSO₄), and the solvent removed *in vacuo*. The crude product was purified by column chromatography (silica gel, 1:1 hexane / DCM), recrystallised from ethanol / ethyl acetate (2:1) and dried (P₂O₅) to yield a cream coloured solid.

Yield: 9.00 g (90 %), ¹H NMR (CD₂Cl₂) δ: 5.07 (6H, s), 6.94 (3H, ddd), 7.24-7.41 (24H, m), 7.70 (3H, s), MS *m/z*: 624 (M⁺), mp: 98.8-102.0 °C.

1,3,5-Tri(3-hydroxyphenyl)benzene (58)

The same procedure was carried out as detailed for compound **46** using the following quantities: compound **50** (8.80 g, 0.0141 mol), 10 % Pd/C (2 g) and THF (400 ml) yielding a cream coloured solid.

Yield: 4.74 g (95 %), ¹H NMR (CDCl₃ & DMSO-D₆) δ: 6.30 (3H, ddd), 6.56-6.59 (6H, m), 6.74 (3H, dd), 7.17 (3H, s), ¹³C NMR (CDCl₃ & DMSO-D₆) δ: 112.88, 113.55, 116.69, 123.24, 128.59, 140.69, 140.78, 156.66, MS *m/z*: 377 (M⁺+Na), mp: 280.5-283.4 °C.

1,3,5-Tri(3-(4-(4-dodecyloxyphenylcarbonyloxy)phenylcarbonyloxy)phenyl)benzene (59)

The same procedure was carried out as detailed for compound **45** using the following quantities: compound **58** (0.45 g, 1.27 mmol), compound **46** (1.79 g, 4.20 mmol), DCC (0.87 g, 4.22 mmol), DMAP (0.15 g, 1.23 mmol) and DCM (170 ml). The crude product was purified by column chromatography (silica gel, hexane with increasing volume fractions of DCM), recrystallised (twice) from ethanol / ethyl acetate (2:1) and dried (P₂O₅) to yield a colourless solid.

Yield: 0.88 g (44 %), ¹H NMR (CDCl₃) δ: 0.89 (9H, t), 1.26-1.38 (48H, m), 1.48 (6H, quint), 1.82 (6H, quint), 4.05 (6H, t), 6.98 (6H, d), 7.28 (3H, ddd), 7.38 (6H, d), 7.75 (3H, dd), 7.56 (3H, dd), 7.63 (3H, ddd), 7.82 (3H, s), 8.15 (6H, d), 8.31 (6H, d), ¹³C NMR (CDCl₃) δ: 14.11, 22.67, 25.95, 29.06, 29.33, 29.54, 29.57, 29.61, 29.64, 31.90, 68.34, 114.36, 120.64, 120.93, 122.08, 124.91, 125.52, 126.79, 129.90, 131.81, 132.39, 141.45, 142.48, 151.35, 155.37, 163.77, 164.26, 164.49, MS *m/z*: 1602 (M⁺+Na), elemental analysis for C₁₀₂H₁₁₄O₁₅ requires 77.54 % C, 7.27 % H; found 77.69 % C, 7.17 % H, purity (HPLC): 85 %, transition temperatures (°C): Cr 184.1 I.

2,3,6,7,10,11-Hexamethoxytriphenylene (61)

Iron(III) chloride (40.00 g, 0.242 mol) and sulfuric acid (50 ml, 98 %) were added to a solution of veratrole (**60**, 30.00 g, 0.217 mol) in DCM (500 ml). The mixture was stirred for 18 h before methanol (200 ml) and water (200 ml) were added. A purple precipitate formed, which was filtered off and washed with methanol and water and dried (P_2O_5) to yield a purple solid.

Yield: 7.85 g (26 %), 1H NMR ($CDCl_3$) δ : 4.08 (18H, s), 7.74 (6H, s), ^{13}C NMR ($CDCl_3$) δ : 56.01, 104.2, 123.14, 148.71, MS m/z : 408 (M^+), mp: >300 °C, lit. mp: 314.5-316 °C¹¹³.

2,3,6,7,10,11-Hexahydroxytriphenylene (62)

Boron tribromide (60.00 g, 0.239 mol), was added dropwise to a stirred, cooled (– 78 °C) solution of compound **61** (12.19 g, 0.0299 mol) in DCM (900 ml) under an atmosphere of dry nitrogen. The mixture was stirred at – 78 °C for 2 h, and then warmed to room temperature (overnight). Ice was added slowly to the mixture, which was acidified with 10% hydrochloric acid to give a dark precipitate. The dark precipitate was filtered off, washed with water and dried (P_2O_5) to yield a dark grey solid.

Yield: 8.94 g (95 %), 1H NMR (DMSO- D_6) δ : 7.60 (6H, s), 9.32 (6H, s), MS m/z : 324 (M^+), mp: >300 °C, lit. mp: >310 °C¹¹³.

2,3,6,7,10,11-Hexahexyloxytriphenylene (63)

Several strategies and methods were used to synthesise this compound.

Strategy 1, Functionalisation, Scheme 7

The same procedure was carried out as for compound **3** using the following quantities: compound **62** (2.30 g, 0.007 mol), 1-bromohexane (20.80 g, 0.126 mol), potassium carbonate (52.20 g, 0.378 mol) and butanone (500 ml). The crude product was purified by column chromatography (silica gel, DCM, followed by 3:1 hexane / DCM) to yield a yellow solid. The product was dissolved in DCM and boiled in the presence of activated charcoal (2 mins) and the solvent was removed *in vacuo*. The yellow waxy solid was recrystallised from ethanol / ethyl acetate (3:1) and dried (P_2O_5) to yield a colourless waxy solid.

Yield: 2.6 g (46 %), ^1H NMR (CDCl_3) δ : 0.94 (18H, t), 1.34-1.45 (24H, m), 1.58 (12H, quint), 1.94 (12H, quint), 4.23 (12H, t), 7.83 (6H, s), ^{13}C NMR (CDCl_3) δ : 14.04, 22.65, 25.84, 29.41, 31.68, 69.69, 107.31, 123.58, 148.95, MS m/z : 829 (M^+), elemental analysis for $\text{C}_{54}\text{H}_{84}\text{O}_6$ requires 78.26 % C, 10.14 % H; found 78.50 % C, 10.36 % H, purity (HPLC): 97 %, transition temperatures ($^\circ\text{C}$): C 66.0 Col_h 96.5 I.

2,3,6,7,10,11-Hexa(3-methylbutoxy)triphenylene (64)

The same procedure was carried out as for compound **3** using the following quantities: compound **62** (1.00 g, 3.09 mmol), 1-bromo-3-methylbutane (3.73 g, 0.0247 mol), potassium carbonate (4.25 g, 0.0308 mol) and butanone (120 ml). The crude product was purified by column chromatography (silica gel, 4:1 hexane / DCM), recrystallised from ethanol / toluene (10:1) and dried (P_2O_5) to yield a colourless waxy solid.

Yield: 1.13 g (49 %), ^1H NMR (CDCl_3) δ : 1.01 (36H, d), 1.82 (12H, quart), 1.94 (6H, non), 4.25 (12H, t), 7.82 (6H, s), ^{13}C NMR (CDCl_3) δ : 22.72, 25.20, 38.04, 67.99, 107.07, 123.50, 148.88, MS m/z : 744 (M^+), elemental analysis for $\text{C}_{48}\text{H}_{72}\text{O}_6$ requires 77.38% C, 9.74% H; found 77.34% C, 9.90 % H, purity (HPLC): 98 %, transition temperatures ($^\circ\text{C}$): Cr 132.0 I.

2,3,6,7,10,11-Hexa(4-methylpentylloxy)triphenylene (65)

The same procedure was carried out as for compound **3** using the following quantities: compound **62** (1.00 g, 3.09 mmol), 1-bromo-4-methylpentane (4.60 g, 0.0279 mol), potassium carbonate (4.25 g, 0.0308 mol) and butanone (120 ml). The crude product was purified by column chromatography (silica gel, 4:1 hexane / DCM), recrystallised from ethanol / toluene (10:1) and dried (P_2O_5), to yield a colourless waxy solid.

Yield: 0.60 g (23 %), ^1H NMR (CDCl_3) δ : 0.96 (36H, d), 1.43-1.49 (12, m), 1.68 (6H, non), 1.91-1.98 (12H, m), 4.21 (12H, t), 7.83 (6H, s), ^{13}C NMR (CDCl_3) δ : 22.63, 27.32, 27.91, 35.31, 69.93, 107.20, 123.56, 148.89, MS m/z : 828 (M^+), elemental analysis for $\text{C}_{54}\text{H}_{84}\text{O}_6$ requires 78.21 % C, 10.21 % H; found 77.97 % C, 10.28 % H, purity (HPLC): 95 %, transition temperatures ($^\circ\text{C}$): Cr 91.8 Col_h 122.1 I.

2,3,6,7,10,11-Hexa(2-ethylbutoxy)triphenylene (66)

The same procedure was carried out as for compound **3** using the following quantities: compound **62** (0.50 g, 1.54 mmol), 1-bromo-2-ethylbutane (2.29 g, 0.0139 mol),

potassium carbonate (2.00 g, 0.0145 mol) and butanone (120 ml). The crude product was purified by column chromatography (silica gel, 1:1 hexane / DCM and silica gel, 4:1 hexane / DCM), recrystallised from ethanol / toluene (10:1) and dried (P_2O_5) to yield a colourless waxy solid.

Yield: 0.06 g (5 %), 1H NMR ($CDCl_3$) δ : 1.01 (36H, t), 1.49-1.65 (24H, quart), 1.84 (6H, sept), 4.12 (12H, d), 7.82 (6H, s), ^{13}C NMR ($CDCl_3$) δ : 11.34, 23.61, 41.10, 71.63, 106.90, 123.43, 149.18, MS m/z : 829 ($M^+ + 1$), elemental analysis for $C_{54}H_{84}O_6$ requires 78.21 % C, 10.21 % H; found 78.49 % C, 10.46 % H, purity (HPLC): 100 %, transition temperatures ($^{\circ}C$): Cr 29.8 Col_h 120.0 I.

2,3,6,7,10,11-Hexapent-4-ynyloxytriphenylene (67)

A stirred mixture of compound **62** (0.50 g, 1.54 mmol), 5-chloropent-1-yne (1.42 g, 0.0139 mol), potassium carbonate (1.90 g, 0.0138 mol), potassium iodide (2.29 g, 0.0138 mol) and butanone (120 ml) was heated under reflux for 9 days. The mixture was cooled to room temperature, filtered to remove the potassium carbonate, extracted into diethyl ether washed with water (twice). The aqueous components were backwashed with diethyl ether, the combined organic extracts were dried ($MgSO_4$) and the solvent removed *in vacuo*. The crude product was purified by column chromatography (silica gel, 4:1 hexane / DCM and alumina, hexane with increasing volume fractions of DCM), recrystallised from ethanol / toluene (10:1) and dried (P_2O_5) to yield a colourless solid.

Yield: 0.23 g (21 %), 1H NMR ($CDCl_3$) δ : 2.03 (6H, t), 2.16 (12H, quint), 2.54 (12H, dt), 4.35 (12H, t), 7.87 (6H, s), ^{13}C NMR ($CDCl_3$) δ : 15.29, 28.36, 67.99, 68.99, 83.65, 107.67, 123.80, 148.82, MS m/z : 721 ($M^+ + 1$), elemental analysis for $C_{48}H_{46}O_6$ requires 79.97 % C, 6.71 % H; found 79.87 % C, 7.00 % H, purity (HPLC): 100 %, transition temperatures ($^{\circ}C$): Cr 130.2 I.

2,3,6,7,10,11-Hexahex-5-ynyloxytriphenylene (68)

The same procedure was carried out as for compound **67** using the following quantities: compound **62** (0.50 g, 1.54 mmol), 6-chlorohex-1-yne (1.62 g, 0.0139 mol), potassium carbonate (1.90 g, 0.0138 mol), potassium iodide (2.29 g, 0.0138 mol) and butanone (120 ml). The crude product was purified by column chromatography (silica gel, 4:1

hexane / DCM and alumina, hexane with increasing volume fractions of DCM), recrystallised from ethanol / toluene (10:1) and dried (P_2O_5) to yield a colourless solid
Yield: 0.80 g (66 %), 1H NMR ($CDCl_3$) δ : 1.85 (12H, quint), 1.99 (6H, t), 2.07 (12H, quint), 2.37 (12H, dt), 4.27 (12H, t), 7.82 (6H, s), ^{13}C NMR ($CDCl_3$) δ : 18.26, 25.29, 28.42, 68.65, 68.99, 84.26, 107.18, 123.62, 148.85, MS m/z : 805 (M^+), elemental analysis for $C_{54}H_{60}O_6$ requires 80.56 % C, 7.51 % H; found 80.45 % C, 7.78 % H, purity (HPLC): 100 %, transition temperatures ($^{\circ}C$): Cr 120.9 I.

2,3,6,7,10,11-Hexabutoxytriphenylene (69)

A mixture of compound **22** (4.00 g, 0.0180 mol), molybdenum(V) chloride (3.65 g, 0.0180 mol) and DCM (100 ml) was stirred together under an atmosphere of dry nitrogen overnight. Methanol (30 ml) and water (60 ml) were added to the mixture and the crude product was extracted into DCM (twice), washed with water and brine, and the combined organic extracts were dried ($MgSO_4$). The solvent was removed *in vacuo* to yield a pink waxy solid, which was purified by column chromatography (silica gel, 4:1 hexane / DCM), and the resulting waxy solid was recrystallised from ethanol and dried (P_2O_5) to yield a pink solid.

Yield: 0.80 g (7 %), 1H NMR (CD_2Cl_2) δ : 0.95 (18H, t), 1.51 (12H, sext), 1.83 (12H, quint), 4.15 (12H, t), 7.75 (6H, s), ^{13}C NMR (CD_2Cl_2) δ : 14.10, 19.73, 31.88, 69.55, 107.30, 123.70, 149.39, MS m/z : 660 (M^+), elemental analysis for $C_{42}H_{60}O_6$ requires 76.33 % C, 9.15 % H; found 75.74 % C, 9.93 % H, purity (HPLC): 95 %, transition temperatures ($^{\circ}C$): Cr 87.3 Col_h 137.5 I, lit. transition temperatures ($^{\circ}C$): Cr 88 Col_h 144 I⁵⁷.

2,3,6,7,10,11-Hexahexyloxytriphenylene (63)

Several strategies and methods were employed in preparing this compound.

Strategy 2, Oxidative Trimerisation, Method A (iron(III) chloride and sulphuric acid), Scheme 8

A mixture of compound **23** (5.00 g, 0.018 mol), iron (III) chloride (9.90 g, 0.0600 mol), sulfuric acid (20 ml), and DCM (100 ml) was stirred together under an atmosphere of dry nitrogen overnight. Methanol (30 ml) and water (60 ml) were added to the mixture and the crude product was extracted into DCM (twice), washed with water and brine,

and the combined organic extracts were dried (MgSO₄). The solvent was removed *in vacuo* to yield a brown solid, which was purified by column chromatography (silica gel, 4:1 hexane / DCM), and the resulting waxy solid was recrystallised from ethanol and dried (P₂O₅) to yield a light purple solid.

Yield: 1.83 g (37 %), ¹H NMR (CDCl₃) δ: 0.94 (18H, t), 1.34-1.45 (24H, m), 1.58 (12H, quint), 1.94 (12H, quint), 4.23 (12H, t), 7.83 (6H, s), ¹³C NMR (CDCl₃) δ: 14.04, 22.65, 25.84, 29.41, 31.68, 69.69, 107.31, 123.58, 148.95, MS *m/z*: 829 (M⁺+1), elemental analysis for C₅₄H₈₄O₆ requires 78.26 % C, 10.14 % H; found 78.40 % C, 10.41 % H, purity (HPLC): 84 %, transition temperatures (°C): Cr 61.4 Col_h 100.1 I.

Strategy 2, Oxidative Trimerisation, Method B (iron(III) chloride), Scheme 8

A mixture of compound **23** (33.61 g, 0.121 mol), iron (III) chloride (6.68 g, 0.0404 mol) and DCM (250 ml) was stirred together under an atmosphere of dry nitrogen overnight. Methanol (70 ml) and water (90 ml) were added to the mixture and the crude product was extracted into DCM (twice), washed with water and brine, and the combined organic extracts were dried (MgSO₄). The solvent was removed *in vacuo* to yield a brown solid, which was purified by column chromatography (silica gel, 4:1 hexane / DCM), and the resulting waxy solid was recrystallised from ethanol and dried (P₂O₅) to yield a light purple solid.

Yield: 7.45 g (22 %), ¹H NMR (CDCl₃) δ: 0.94 (18H, t), 1.34-1.45 (24H, m), 1.58 (12H, quint), 1.94 (12H, quint), 4.23 (12H, t), 7.83 (6H, s), ¹³C NMR (CDCl₃) δ: 14.04, 22.65, 25.84, 29.41, 31.68, 69.69, 107.31, 123.58, 148.95, MS *m/z*: 828 (M⁺), elemental analysis for C₅₄H₈₄O₆ requires 78.26 % C, 10.14 % H; found 78.48 % C, 10.37 % H, purity (HPLC): 75 %, transition temperatures (°C): Cr 66.8 Col_h 95.8 I.

Strategy 2, Oxidative Trimerisation, Method C (molybdenum(V) chloride), Scheme 8

A mixture of compound **23** (5.00 g, 0.0180 mol), molybdenum(V) chloride (3.65 g, 0.0180 mol) and DCM (100 ml) was stirred together under an atmosphere of dry nitrogen overnight. Methanol (30 ml) and water (60 ml) were added to the mixture and the crude product was extracted into DCM (twice), washed with water and brine, and the combined organic extracts were dried (MgSO₄). The solvent was removed *in vacuo* to yield a pink waxy solid, which was purified by column chromatography (silica gel,

4:1 hexane / DCM), and the resulting waxy solid was recrystallised from ethanol and dried (P_2O_5) to yield a light pink solid.

Yield: 1.65 g (33 %), 1H NMR ($CDCl_3$) δ : 0.94 (18H, t), 1.34-1.45 (24H, m), 1.58 (12H, quint), 1.94 (12H, quint), 4.23 (12H, t), 7.83 (6H, s), ^{13}C NMR ($CDCl_3$) δ : 14.04, 22.65, 25.84, 29.41, 31.68, 69.69, 107.31, 123.58, 148.95, MS m/z : 829 ($M^+ + 1$), elemental analysis for $C_{54}H_{84}O_6$ requires 78.26 % C, 10.14 % H; found 77.82 % C, 10.55 % H, purity (HPLC): 62 %, transition temperatures ($^{\circ}C$): Cr 66.0 Col_h 69.6 I.

Strategy 2, Oxidative Trimerisation, Method D (vanadium(V) oxytrichloride), Scheme 8

A mixture of compound **23** (5.00 g, 0.0180 mol), vanadium(V) oxytrichloride (5.24 g, 0.0360 mol) and DCM (100 ml) was stirred together under an atmosphere of dry nitrogen overnight. Methanol (30 ml) and water (60 ml) were added to the mixture and the crude product was extracted into DCM (twice), washed with water and brine, and the combined organic extracts were dried ($MgSO_4$). The solvent was removed *in vacuo* to yield a purple waxy solid, which was purified by column chromatography (silica gel, 4:1 hexane / DCM), and the resulting waxy solid was recrystallised from ethanol and dried (P_2O_5) to yield a light purple solid.

Yield: 3.09 g (62 %), 1H NMR ($CDCl_3$) δ : 0.94 (18H, t), 1.34-1.45 (24H, m), 1.58 (12H, quint), 1.94 (12H, quint), 4.23 (12H, t), 7.83 (6H, s), ^{13}C NMR ($CDCl_3$) δ : 14.04, 22.65, 25.84, 29.41, 31.68, 69.69, 107.31, 123.58, 148.95, MS m/z : 829 ($M^+ + 1$), elemental analysis for $C_{54}H_{84}O_6$ requires 78.26 % C, 10.14 % H; found 78.06 % C, 10.42 % H, purity (HPLC): 88 %, transition temperatures ($^{\circ}C$): Cr 65.8 Col_h 94.1 I.

2,3,6,7,10-Pentahexyloxy-11-hydroxytriphenylene (70)

Two methods were used in synthesising this compound.

Dealkylation Method, Scheme 8

B-Bromocatecholborane (1.59 g, 7.99 mmol) was added to a cooled ($0^{\circ}C$), stirred solution of compound **63** (5.50 g, 6.64 mmol) in DCM (125 ml) under an atmosphere of dry nitrogen. The mixture was slowly warmed to room temperature and stirred for 48 h. The mixture was acidified using 10 % hydrochloric acid solution and stirred for 1 h. The mixture was extracted into diethyl ether and washed with water (twice), the aqueous components were backwashed with diethyl ether, the combined organic

components were dried (MgSO_4) and the solvent removed *in vacuo*. The crude product was purified by column chromatography (silica gel, 1:1 hexane / DCM), to yield a purple waxy solid consisting of the product and approximately 30 % of compound **63**.

Yield: 4.80 g (47 %), $^1\text{H NMR}$ (CDCl_3) δ : 0.93 (15H, 2 \times t), 1.31-1.47 (20H, m), 1.54-1.61 (10H, m), 1.94 (10H, quint), 4.21 (8H, 2 \times t), 4.29 (2H, t), 7.77 (1H, s), 7.81-7.83 (4H, m), 7.96 (1H, s), MS m/z : 745 ($\text{M}^+ + 1$), mp: 64.8-67.3 $^\circ\text{C}$, lit. mp: 45-46 $^\circ\text{C}^{114}$.

4-Bromocatechol (72)

The same procedure was carried out as for compound **62** using the following quantities: 4-bromoveratrole (**71**, 100.5 g, 0.463 mol), boron tribromide (350 g, 1.39 mol), DCM (1000 ml). In this case no precipitate formed, so the mixture was extracted into diethyl ether and washed with water (twice) and the aqueous components backwashed with diethyl ether. The combined organic components were dried (MgSO_4), and the solvent removed *in vacuo* to yield a yellow powder. The powder was stirred in hexane / DCM (10:1) mixture for 2 h and filtered to yield a colourless powder.

Yield: 60.72 g (69 %), $^1\text{H NMR}$ (CDCl_3) δ : 5.22 (1H, s), 5.37 (1H, s), 6.74 (1H, d), 6.92 (1H, dd), 7.01 (1H, d), MS m/z : 188 (M^+), 190 (M^+), mp: 85-89 $^\circ\text{C}$, lit. mp: 85-86 $^\circ\text{C}^{114}$.

4-Bromo-1,2,-dihexyloxybenzene (73)

The same procedure was carried out as for compound **3** using the following quantities: compound **72** (5.20 g, 0.398 mol), 1-bromohexane (198.0 g, 1.2 mol), potassium carbonate (165.5 g, 1.20 mol) and butanone (900 ml). The product was purified by column chromatography (silica gel, 1:1 hexane / DCM) to yield an orange oil.

Yield: 124.27 g (87 %), $^1\text{H NMR}$ (CDCl_3) δ : 0.90 (6H, 2 \times t), 1.33 (6H, m), 1.46 (6H, m), 1.78 (4H, 2 \times sext), 3.94 (4H, 2 \times t), 6.71 (1H, d), 6.96 (1H, d), 6.97 (1H, dd), MS m/z : 358 ($\text{M}^+ + 1$), 356 ($\text{M}^+ + 1$).

3,4-Dihexyloxyphenylboronic acid (74)

The same procedure was carried out as for compound **55** using the following quantities: compound **73** (93.00 g, 0.261 mol), magnesium (8.14 g, 0.339 mol), trimethyl borate (54.30 g, 5.22 mol) and THF (1500 ml). The cream coloured solid was dissolved in ethyl acetate and hexane was added to precipitate out the colourless powder.

Yield: 44.70 g (53 %), ¹H NMR (DMSO-D₆) 0.83 (6H, 2×t), 1.22-1.29 (8H, m), 1.34-1.42 (4H, m), 1.64 (4H, quint), 3.88 (4H, 2×t), 6.84 (1H, d), 7.29 (1H, dd), 7.30 (1H, d), 7.79 (2H, s), MS *m/z*: 912 (M⁺ of trimeric anhydride), mp: 129.0-129.5 °C.

3,3',4,4'-Tetrahexyloxybiphenyl (75)

The same procedure was carried out as for compound **57** using the following quantities: compound **73** (10.50 g, 0.0294 mol), compound **74** (11.36 g, 0.0353 mol), sodium carbonate (6.24 g, 0.0588 mol), tetrakis(triphenylphosphine)palladium(0) (1.70 g, 0.00147 mol), water (30 ml) and DME (500 ml). The crude product was purified by column chromatography (silica gel, 1:1 dichloromethane / hexane), recrystallised from ethanol / ethyl acetate (2:1) and dried (P₂O₅) to yield colourless crystals.

Yield: 14.84 g (98 %), ¹H NMR (CDCl₃) δ: 0.90 (12H, 2×t), 1.32-1.36 (16H, m), 1.45-1.50 (8H, m), 1.83 (8H, 2×quint), 4.03 (8H, 2×t), 6.92 (2H, d), 7.04-7.07 (4H, m), MS *m/z*: 554 (M⁺), mp: 76.4-78.1 °C, lit. mp: 75-76 °C¹¹⁴.

2,3-Dibutoxy-6,7,10,11-Tetrahexyloxytriphenylene (76)

A mixture of compound **22** (1.15 g, 5.18 mmol), compound **75** (2.87 g, 5.18 mmol), vanadium(V) oxytrichloride (0.57 g, 3.29 mmol) and DCM (100 ml) was stirred together under an atmosphere of dry nitrogen (overnight). Methanol (30 ml) and water (60 ml) were added to the mixture and the crude product was extracted into DCM (twice), washed with water and brine. The combined organic extracts were dried (MgSO₄), the solvent was removed *in vacuo* to yield a purple waxy solid, which was purified by column chromatography (silica gel, 4:1 hexane / DCM), and the resulting waxy solid was recrystallised from ethanol and dried (P₂O₅) to yield a purple solid.

Yield: 1.47 g (37 %), ¹H NMR (CDCl₃) δ: 0.93 (12H, t), 1.04 (6H, t), 1.34-1.44 (12H, m), 1.52-1.63 (12H, m), 1.89-1.97 (16H, m), 4.23 (12H, 2×t), 7.84 (6H, s), ¹³C NMR (CDCl₃) δ: 13.96, 14.05, 19.35, 22.62, 22.65, 25.83, 29.35, 29.41, 31.46, 31.60, 31.68, 69.37, 69.70, 107.31, 123.58, 148.95, MS *m/z*: 772 (M⁺), elemental analysis for C₅₀H₇₆O₆ requires 77.72 % C, 9.84 % H; found 77.98 % C, 10.43 % H, purity (HPLC): 90 %, transition temperatures (°C): Cr 67.8 Col_h 92.3 I, lit. transition temperatures (°C): Cr 59 Col_h 90 I¹¹⁵.

2,3,6,7,10-Pentahexyloxy-11-methoxytriphenylene (77)

A mixture of compound **30** (10.75 g, 0.0517 mol), compound **75** (28.64 g, 0.0517 mol), iron(III) chloride (17.11 g, 0.103 mol) and DCM (200 ml) were stirred together under an atmosphere of dry nitrogen (overnight). Methanol (70 ml) and water (100 ml) were added to the mixture and the crude product was extracted into DCM (twice), washed with water and brine, and the combined organic extracts were dried (MgSO₄). The solvent was removed *in vacuo* to yield a purple waxy solid, which was purified by column chromatography (silica gel, 4:1 hexane / DCM), and the resulting waxy solid was recrystallised from ethanol / toluene (10:1) and dried (P₂O₅) to yield a light purple solid.

Yield: 23.75 g (61 %), ¹H NMR (CDCl₃) δ: 0.94 (12H, t), 1.36-1.41 (24H, m), 1.56-1.61 (10H, m), 1.95 (10H, 2×quint), 4.10 (3H, s), 4.24 (10H, t), 7.82 (1H, s), 7.84 (1H, s), 7.85 (1H, s), 7.85 (2H, s), 7.86 (1H, s), MS *m/z*: 758 (M⁺), transition temperatures (°C): Cr 47.1 I.

2,3,6,7,10,11-Hexahexyloxytriphenylene (63)

Strategy 3, Oxidative 'Dimerisation', Scheme 9

A mixture of compound **23** (1.01 g, 3.62 mmol), compound **75** (2.01 g, 3.62 mmol), vanadium(V) oxytrichloride (0.94 g, 5.43 mmol) and DCM (100 ml) was stirred together under an atmosphere of dry nitrogen (overnight). Methanol (30 ml) and water (60 ml) were added to the mixture and the crude product was extracted into DCM (twice), washed with water and brine, and the combined organic extracts were dried (MgSO₄). The solvent was removed *in vacuo* to yield a waxy solid, which was purified by column chromatography (silica gel, 4:1 hexane / DCM), and the resulting waxy solid was recrystallised from ethanol and dried (P₂O₅) to yield a light purple solid.

Yield: 1.46 g (49 %), ¹H NMR (CDCl₃) δ: 0.94 (18H, t), 1.34-1.45 (24H, m), 1.58 (12H, quint), 1.94 (12H, quint), 4.23 (12H, t), 7.83 (6H, s), ¹³C NMR (CDCl₃) δ: 14.04, 22.65, 25.84, 29.41, 31.68, 69.69, 107.31, 123.58, 148.95, MS *m/z*: 829 (M⁺+1), elemental analysis for C₅₄H₈₄O₆ requires 78.26 % C, 10.14 % H; found 77.12 % C, 10.45 % H, purity (HPLC): 94 %, transition temperatures (°C): Cr 68.1 Col_h 98.5 I.

2,3-Dibenzyloxy-6,7,10,11-tetrahexyloxytriphenylene (78)

A mixture of compound **24** (1.73 g, 5.97 mmol), compound **75** (3.30 g, 5.96 mmol), molybdenum(V) chloride (2.42 g, 0.120 mol) and DCM (200 ml) under an atmosphere of dry nitrogen was stirred together (overnight). The mixture was poured onto a mixture of cold methanol (100 ml) and water (200 ml). This procedure yielded an intractable black mass that was impossible to purify further.

2,3,6,7,10-Pentahexyloxy-11-hydroxytriphenylene (70)

Demethylation Method, Scheme 9

n-Butyllithium (21.96 ml, 2.5 M in hexanes, 0.0549 mol), was added dropwise to a stirred, cooled (− 5 °C) solution of diphenylphosphine (10 ml, 9.29 g, 0.0499 mol) in THF (200 ml), under an atmosphere of dry nitrogen. The mixture was stirred for 30 mins, then a solution of compound **77** (13.45 g, 0.0177 mol) in THF (300 ml) was added dropwise. After 30 mins the mixture was warmed to room temperature and heated under reflux (overnight). The mixture was acidified with 10 % hydrochloric acid, and stirred for 2 h. The product was extracted into diethyl ether (twice) and washed with water (twice). The ethereal extracts were dried (MgSO₄) and the solvent removed *in vacuo*. The crude product was purified by column chromatography (silica gel, hexane with increasing volume fractions of DCM), to yield a dark purple waxy solid.

Yield: 10.01 g (76 %), ¹H NMR (CDCl₃) δ: 0.93-0.96 (15H, m), 1.34-1.45 (20H, m), 1.54-1.63 (10H, m), 1.92-1.96 (10H, m), 4.23 (8H, 2×t), 4.29 (2H, t), 7.78 (1H, s), 7.82-7.83 (4H, m), 7.97 (1H, s), mp: 47.7-50.1 °C, lit. mp: 45-46 °C¹¹⁴.

3,4,4',5',3'',4''-Hexahexyloxy[1,1':2',1'']terphenyl (79)

The same procedure was carried out as for compound **57** using the following quantities: compound **26** (5.00 g, 9.43 mmol), compound **74** (6.83 g, 0.0212 mol), tetrakis(triphenylphosphine)palladium(0) (0.54 g, 0.468 mmol), sodium carbonate (4.49 g, 0.0424 mol), water (40 ml) and DME (220 ml). The crude product was purified by column chromatography (silica gel, 1:1 hexane / DCM) to yield an orange oil.

Yield: 7.75 g (99 %), ¹H NMR (CDCl₃) δ: 0.90 (18H, m), 1.28-1.39 (28H, m), 1.42-1.51 (8H, m), 1.65 (4H, quint), 1.77-1.86 (8H, m), 3.68 (4H, t), 3.94 (4H, t), 4.05 (4H, t), 6.58 (2H, d), 6.74 (2H, d), 6.75 (2H, s), 6.94 (2H, s), MS *m/z*: 854 (M⁺+Na).

4',4''-Dibenzyloxy-3,4,3'',4''-tetrahexyloxy[1,1':2',1'']terphenyl (80)

The same procedure was carried out as for compound **58** using the following quantities: compound **27** (6.60 g, 0.0122 mol), compound **74** (8.23 g, 0.0256 mol), tetrakis(triphenylphosphine)palladium(0) (94.48 g, 1.28 mmol), sodium carbonate (5.17 g, 0.0488 mol), water (60 ml) and DME 200 ml). The crude product was purified by column chromatography (silica gel, 1:1 hexane / DCM), recrystallised from ethanol / ethyl acetate (8:1) and dried (P₂O₅), to yield a colourless solid.

Yield: 9.27 g (90 %), ¹H NMR (CD₂Cl₂) δ: 0.91 (12H, t), 1.26-1.35 (20H, m), 1.46 (4H, quint), 1.61 (4H, quint), 1.77 (4H, quint), 3.64 (4H, t), 3.91 (4H, t), 5.17 (4H, s), 6.53 (2H, d), 6.66 (2H, dd), 6.74 (2H, d), 6.99 (2H, s), 7.29-7.48 (10H, m), MS *m/z*: 843 (M⁺+1), mp: 43.1-45.1 °C.

2,3,6,7,10,11-Hexahexyloxytriphenylene (63)

Strategy 4, Oxidative Cyclisation, Scheme 10

A mixture of compound **79** (6.00 g, 7.23 mmol), vanadium(V) oxytrichloride (1.25 g, 7.23 mmol) and DCM (100 ml) was stirred together under an atmosphere of dry nitrogen (overnight). Methanol (60 ml) and water (60 ml) were added to the mixture and the crude product precipitated out. The crude purple solid was purified by column chromatography (silica gel, 4:1 hexane / dichloromethane), and the resulting waxy solid was recrystallised from ethanol to yield a purple solid.

Yield: 2.71 g (42 %), ¹H NMR (CDCl₃) δ: 0.94 (18H, t), 1.34-1.45 (24H, m), 1.58 (12H, quint), 1.94 (12H, quint), 4.23 (12H, t), 7.83 (6H, s), ¹³C NMR (CDCl₃) δ: 14.04, 22.65, 25.84, 29.41, 31.68, 69.69, 107.31, 123.58, 148.95, MS *m/z*: 829 (M⁺+1), elemental analysis for C₅₄H₈₄O₆ requires 78.26% C, 10.14% H; found 77.88 % C, 10.43 % H, purity (HPLC): 99 %, transition temperatures (°C): C 66.5 Col_h 100.0 I.

2,3-Dibenzyloxy-6,7,10,11-tetrahexyloxytriphenylene (78)

A mixture of compound **80** (5.01g, 5.95 mmol), molybdenum(V) chloride (1.21 g, 5.98 mmol) and DCM (200 ml) under an atmosphere of dry nitrogen was stirred together (overnight). The mixture was poured onto a mixture of cold methanol (100 ml) and water (200 ml) was added. This procedure yielded an intractable black mass that was impossible to purify further.

1,4,5,8,9,12-Hexafluoro-2,3,6,7,10,11-hexahexyloxytriphenylene (82)

A mixture of 1,4-difluoro-2,3-dihexyloxybenzene (**81**, 3.00 g, 9.55 mmol), vanadium(V) oxytrichloride (1.82 ml, 3.32 g, 0.0191 mol), and DCM (120 ml) were stirred together under an atmosphere of dry nitrogen (overnight). Methanol (100 ml) and water (100 ml) were added to the mixture which was extracted into DCM (twice), washed with water and brine, and the combined organic extracts were dried (MgSO₄). The solvent was removed *in vacuo* to yield an oil, which was subjected to column chromatography (silica gel, 4:1 hexane / dichloromethane) which yielded only the starting material, **81**.

1,4-Difluoro-2,3,6,7,10,11-hexahexyloxytriphenylene (83)

A mixture of compound **81** (0.78 g, 2.49 mmol), compound **75** (1.38 g, 2.49 mmol), vanadium(V) oxytrichloride (0.355 ml, 0.648 g, 3.74 mmol) and DCM (120 ml) were stirred together under an atmosphere of dry nitrogen (overnight). Methanol (100 ml) and water (100 ml) were added to the mixture which was extracted into DCM (twice), washed with water and brine, and the combined organic extracts were dried (MgSO₄). The solvent was removed *in vacuo* the crude mixture was purified by column chromatography (silica gel, hexane with increasing volume fractions of DCM) to yield the starting materials **81** and **75**.

3-Benzyloxyphenol (84)

The same procedure was carried out as for compound **7** using the following quantities: compound **55** (9.70 g, 0.0425 mol), hydrogen peroxide (138 ml, 12 %, 0.489 mol), diethyl ether (400 ml) to yield a brown solid.

Yield: 7.98 g (94 %), ¹H NMR (CDCl₃) δ: 5.09 (2H, s), 6.43 (1H, ddd), 6.48 (1H, dd), 6.57 (1H, ddd), 7.13 (1H, dd), 7.27-7.46 (5H, m), MS *m/z*: 200 (M⁺), mp: 46.1-48.7 °C, lit. mp: 50-51 °C¹¹⁶.

1-Benzyloxy-3-(4-(4-dodecyloxyphenylcarbonyloxy)phenylcarbonyloxy)benzene (85)

The same procedure was carried out as for compound **45** using the following quantities: compound **84** (3.00 g, 0.0150 mol), compound **46** (5.75 g, 0.0135 mol), DCC (2.78 g, 0.0135 mol), DMAP (0.55 g, 4.50 mmol) and DCM (120 ml). The crude product was

purified by column chromatography (silica gel, 1:1 hexane / DCM) to yield an off white solid.

Yield: 4.62 g (56 %), $^1\text{H NMR}$ (CDCl_3) δ : 0.90 (3H, t), 1.27-1.38 (16H, m), 1.48 (2H, quintet), 1.83 (2H, quintet), 4.05 (2H, t), 5.07 (2H, s), 6.85 (1H, ddd), 6.88 (1H, dd), 6.91 (1H, ddd), 6.99 (2H, d), 7.31-7.48 (8H, m), 8.16 (2H, d), 8.28 (2H, d), MS m/z : 608 (M^+), mp: 95.0-96.7 °C, lit. mp: 97-98 °C¹¹⁰.

3-(4-(4-Dodecyloxyphenylcarbonyloxy)phenylcarbonyloxy)phenol (86)

The same procedure was carried out as for compound **46** using the following quantities: compound **85** (4.30 g, 7.07 mmol), 10 % Pd/C (3 g) and THF (400 ml). This procedure yielded a colourless solid.

Yield: 1.40 g (38 %), $^1\text{H NMR}$ (CDCl_3) δ : 0.87 (3H, t), 1.24-1.39 (16H, m), 1.49 (2H, quint), 1.85 (2H, quint), 4.05 (2H, t), 5.65 (1H, s), 6.69 (1H, dd), 6.78 (1H, ddd), 6.77 (1H, ddd), 6.99 (2H, d), 7.25 (1H, dd), 7.36 (2H, d), 8.14 (2H, d), 8.26 (2H, d), MS m/z : 518 (M^+), mp: 122.8-124.2 °C, lit. mp: 124.5-125.5 °C¹¹⁰.

1-(4-benzyloxyphenylcarbonyloxy)-3-(4-(4-dodecyloxyphenylcarbonyloxy)phenylcarbonyloxy)benzene (87)

The same procedure was carried out as for compound **45** using the following quantities: compound **86** (1.70 g, 3.28 mmol), compound **46** (0.76 g, 3.58 mmol), DCC (0.74 g, 3.59 mmol), DMAP (0.13 g, 1.09 mmol) and DCM (100 ml). The crude product was purified by column chromatography (silica gel, 1:1 hexane / DCM) to yield a colourless solid.

Yield: 1.50 g (63 %), $^1\text{H NMR}$ (CD_2Cl_2) δ : 0.80 (3H, t), 1.18-1.34 (16H, m), 1.39 (2H, quint), 1.74 (2H, quint), 3.98 (2H, t), 5.09 (2H, s), 6.92 (2H, d), 7.01 (2H, d), 7.08-7.10 (3H, m), 7.26-7.44 (8H, m), 8.06 (2H, d), 8.07 (2H, d), 8.19 (2H, d), MS m/z : 729 ($\text{M}^+ + 1$), mp: 116.5-118.0 °C, lit. mp: 119-120 °C¹¹⁰.

1-(4-(4-dodecyloxyphenylcarbonyloxy)phenylcarbonyloxy)-3-(4-hydroxyphenylcarbonyloxy)benzene (88)

The same procedure was carried out as for compound **46** using the following quantities: compound **87** (5.00 g, 6.87 mmol), 10 % Pd/C (2 g) and THF (600 ml). This procedure yielded a colourless solid.

Yield: 4.30 g (98 %), ^1H NMR (DMSO- D_6) δ : 0.80 (3H, t), 1.18-1.33 (16H, m), 1.36 (2H, quint), 1.70 (2H, quint), 4.05 (2H, t), 6.88 (2H, d), 7.08 (2H, d), 7.19 (1H, ddd), 7.23 (1H, ddd), 7.27 (1H, dd), 7.49 (2H, d), 7.51 (1H, dd), 7.95 (2H, d), 8.05 (2H, d), 8.19 (2H, d), MS m/z : 662 (M^+Na), mp: 182.5-184.1 °C, lit. mp: 182-183 °C¹¹⁰.

Benzyl 4-(10-bromodecyloxy)benzoate (89)

A stirred mixture of compound **44** (7.66 g 0.0336 mol), 1,10-dibromodecane (40.00 g, 1.33 mol) and potassium carbonate (9.27 g, 0.0672 mol) in butanone (300 ml) was heated under reflux for 24 h (TLC revealed a complete reaction). The mixture was cooled to room temperature, filtered to remove the potassium carbonate and the solvent was removed *in vacuo*. The product was extracted into diethyl ether, washed water, the aqueous component was back extracted with diethyl ether, the organic extracts were dried (MgSO_4) and the solvent removed *in vacuo*. The crude product was purified by column chromatography (silica gel, 1:1 hexane / DCM), to yield a colourless solid.

Yield: 14.00 g (93 %), ^1H NMR (CD_2Cl_2) δ : 1.31-1.47 (12H, m), 1.78 (2H, quint), 1.82 (2H, quint), 3.40 (2H, t), 4.00 (2H, t), 5.31 (2H, s), 6.91 (2H, d), 7.32-7.45 (5H, m), 7.99 (2H, d), MS m/z : 448 (M^++1), 446 (M^++1), mp: 44.9-46.2 °C.

2-(10-(4-Benzoyloxycarbonylphenoxy)decyloxy)-3,6,7,10,11-pentahexyloxytriphenylene (90)

The same procedure was carried out as for compound **3** using the following quantities: compound **70** (2.00 g, 2.69 mmol), compound **89** (1.41 g, 2.69 mmol), potassium carbonate (1.11 g, 8.04 mmol) and butanone (125 ml). The crude product was purified by column chromatography (silica gel, 5:1 hexane / DCM) to yield a colourless solid.

Yield: 2.39 g (80 %), ^1H NMR (CDCl_3) δ : 0.92 (15H, 2 \times t), 1.23-1.41 (16H, m), 1.57 (14H, quint), 1.70 (2H, quint), 1.91 (14H, quint), 3.85 (2H, t), 4.20 (12H, t), 5.27 (2H, s), 6.81 (2H, d), 7.25-7.83 (5H, m), 7.79 (6H, s), 7.99 (2H, d) MS m/z : 1021 (M^++1), mp: 25.0-27.8 °C.

2-(10-(4-Hydroxycarbonylphenoxy)decyloxy)-3,6,7,10,11-pentaheptyloxytriphenylene (91)

The same procedure was carried out as for compound **46** using the following quantities: compound **90** (2.00 g, 1.80 mmol), 10 % Pd/C (1.5 g) and THF (500 ml). This procedure yielded a colourless solid.

Yield: 1.70 g (93 %), ¹H NMR (CDCl₃) δ: 0.95 (15H, t), 1.33-1.45 (28H, m), 1.56 (14H, quint), 1.93 (14H, quint), 4.00 (2H, t), 4.23 (12H, t), 6.90 (2H, d), 7.84 (6H, s), 8.02 (2H, d), MS *m/z*: 1021 (M⁺+1), mp: 54.9-58.4 °C.

2-(10-(4-(4-(3-(4(4-Dodecyloxyphenylcarbonyloxy)phenylcarbonyloxy)phenoxy)phenoxy)phenoxy)decyloxy)-3,6,7,10,11-triphenylene (92)

The same procedure was carried out as for compound **45** using the following quantities: compound **91** (0.50 g, 0.490 mmol), compound **88** (0.34 g, 0.533 mmol), DCC (0.11 g, 0.534 mmol), DMAP (0.02 g, 0.164 mmol) and DCM (120 ml). The mixture was subjected to column chromatography (silica gel, hexane with increasing volume fractions of DCM), however, only the starting materials were isolated.

1,3-Di(4-benzyloxyphenylcarbonyloxy)benzene (94)

The same procedure was carried out as for compound **45** using the following quantities: resorcinol (**93**, 4.15 g, 0.0377 mol), compound **43** (19.36 g, 0.0849 mol), DCC (17.49 g, 0.0849), DMAP (3.11 g, 0.0255 mol) and DCM (350 ml). The crude product was purified by column chromatography (silica gel, 1:1 hexane / DCM), recrystallised from ethanol / ethyl acetate (9:1) and dried (P₂O₅) to yield a colourless solid.

Yield: 5.64 g (28 %), ¹H NMR (CDCl₃) δ: 5.09 (4H, s), 6.98 (4H, d), 7.05-7.08 (3H, m), 7.26-7.41 (11H, m), 8.08 (4H, d), MS *m/z*: 530 (M⁺), mp: 197.4-198.2 °C, lit. mp: 195-196 °C¹¹⁷.

1,3-Di(4-hydroxyphenylcarbonyloxy)benzene (95)

The same procedure was carried out as for compound **46** using the following quantities: compound **94** (5.56 g, 0.0105 mol), 10 % Pd/C (2 g) and THF (500 ml). This procedure yielded a colourless solid.

Yield: 3.59 g (98 %), ^1H NMR (DMSO- D_6) δ : 6.98 (4H, d), 7.24 (2H, dd), 7.27 (1H, t), 7.57 (1H, t), 8.04 (4H, d), 10.61 (2H, s), MS m/z : 350 (M^+), mp: 231.7-235.5 °C, lit mp: 237-238 °C¹¹⁷.

1,3-Di(4-(4-(10-(3,6,7,10,11-pentahexyloxytriphenylene-2-yloxy)decyloxy)phenylcarbonyloxy)phenylcarbonyloxy)benzene (96)

The same procedure was carried out as for compound **45** using the following quantities: compound **91** (0.50 g, 0.490 mmol), compound **95** (0.08 g, 0.229 mmol), DCC (0.11 g, 0.534 mmol), DMAP (0.02 g, 0.164 mmol) and DCM (120 ml). The mixture was subjected to column chromatography (silica gel, hexane with increasing volume fractions of DCM), however only the starting materials were isolated.

7-Chlorohept-1-yne (101)

1-Bromo-5-chloropentane (**97**, 10.00g, 0.0539 mol) was added dropwise to a stirred, cooled (0 °C) mixture of lithiumacetylide ethylene diamine complex (6.12 g, 0.0665 mol) and anhydrous DMSO (150 ml). The mixture was stirred for 1 h (GC revealed a complete reaction), then water (100 ml) was added cautiously to quench the reaction. The mixture was then extracted into pentane, washed with water (twice) and the aqueous components were back extracted with pentane (twice), the combined organic extracts were dried (MgSO_4) and the solvent was carefully distilled off to yield a colourless oil.

Yield: 6.60 g (94 %), ^1H NMR (CDCl_3) δ : 1.53-1.58 (4H, m), 1.76-1.82 (2H, m), 1.96 (1H, t), 2.21 (2H, dt), 3.54 (2H, t), MS m/z : 133 ($\text{M}^+ + 1$), 130 (M^+).

8-Chlorooct-1-yne (102)

1-Bromo-6-chlorohexane (**98**, 5.00 g, 0.0251 mol) was added dropwise to a stirred, cooled (0 °C) mixture of lithiumacetylide ethylene diamine complex (2.88 g, 0.0313 mol) and anhydrous DMSO (150 ml). The mixture was stirred for 1 h (GC revealed a complete reaction), and then water (100 ml) was added cautiously to quench the reaction. The mixture was then extracted into pentane, washed with water (twice) and the aqueous components were back extracted with pentane (twice), the combined organic extracts were dried (MgSO_4) and the solvent was carefully distilled off *in vacuo* to yield a colourless oil.

Yield: 3.26 g (90 %), ^1H NMR (CDCl_3) δ : 1.41-1.46 (4H, m), 1.54 (2H, quint), 1.78 (2H, quint), 1.94 (1H, t), 2.19 (2H, dt), 3.53 (2H, t), MS m/z : 146 (M^+), 144 (M^+).

2,3,6,7,10-Pentahexyloxy-11-pent-4-ynyloxytriphenylene (103)

A stirred mixture of compound **70** (0.50 g, 0.672 mmol), 5-chloropent-1-yne (**99**, 0.30 g, 2.68 mmol), potassium carbonate (0.46 g, 3.35 mmol), and potassium iodide (0.20 g, 120 mmol) in butanone (120 ml) was heated under reflux for 7 days (TLC revealed a complete reaction). The mixture was cooled to room temperature, filtered to remove the potassium carbonate and the solvent was removed *in vacuo*. The product was extracted into diethyl ether, washed with water, the aqueous component was back extracted with diethyl ether and the combined ethereal extracts were dried (MgSO_4) and the solvent removed *in vacuo*. The crude product was purified by column chromatography (silica gel, 1:1 hexane / DCM and alumina, hexane with increasing volume fractions of DCM), recrystallised from ethanol / toluene (10:1) and dried (P_2O_5) to yield a colourless waxy solid.

Yield: 0.32 g (59 %), ^1H NMR (CDCl_3) δ : 0.93 (15H, t), 1.34-1.41 (18H, m), 1.58 (10H, quint), 1.85 (2H, quint), 1.94 (10H, quint), 1.98 (1H, t), 2.07 (2H, quint), 2.36 (2H, dt), 4.23 (10H, 5 \times t), 4.26 (2H, t), 7.84 (6H, s), ^{13}C NMR (CDCl_3) δ : 14.05, 18.07, 18.25, 22.65, 25.27, 25.84, 31.68, 69.59, 69.05, 69.59, 69.71, 107.13, 107.31, 107.32, 107.37, 107.38, 123.52, 123.54, 123.56, 123.58, 123.64, 123.73, 148.74, 148.95, 148.99, 149.01, MS m/z : 810 (M^+), elemental analysis for $\text{C}_{53}\text{H}_{78}\text{O}_6$ requires 78.47 % C, 9.69 % H; found 78.70 % C, 9.90 % H, purity (HPLC): 94 %, transition temperatures ($^\circ\text{C}$): Cr 53.3 Col_h 97.6 I.

2,3,6,7,10-Pentahexyloxy-11-hex-5-ynyloxytriphenylene (104)

The same procedure was carried out as for compound **103** using the following quantities: compound **70** (0.50 g, 0.672 mmol), 6-chlorohex-1-yne (**100**, 0.30 g, 2.59 mmol), potassium carbonate (0.46 g, 3.35 mmol), and potassium iodide (0.20 g, 120 mmol) in butanone (120 ml). The crude product was purified by column chromatography (silica gel, 1:1 hexane / DCM, and alumina, hexane with increasing volume fractions of DCM), recrystallised from ethanol / toluene (10:1) and dried (P_2O_5) to yield a colourless waxy solid.

Yield: 0.33 g (60 %), ^1H NMR (CDCl_3) δ : 0.94 (15H, t), 1.31-1.48 (22H, m), 1.57 (10H, quint), 1.94 (10H, quint), 2.01 (1H, t), 2.15 (2H, quint), 2.53 (2H, dt), 4.22 (10H, 2 \times t), 4.34 (2H, t), 7.83 (5H, s), 7.86 (1H, s), ^{13}C NMR (CDCl_3) δ : 14.05, 15.28, 22.65, 25.85, 28.44, 29.39, 29.41, 31.66, 31.68, 68.03, 68.80, 69.61, 69.68, 69.69, 69.74, 107.20, 107.29, 107.34, 107.37, 107.73, 123.52, 123.54, 123.61, 123.68, 123.87, 148.63, 148.96, 148.96, 148.98, 149.00, 149.05, MS m/z : 825 (M^+), elemental analysis for $\text{C}_{54}\text{H}_{80}\text{O}_6$ requires 78.60 % C, 9.77 % H; found 78.48 % C, 9.87 % H, purity (HPLC): 94 %, transition temperatures ($^\circ\text{C}$): Cr 62.8 Col_h 84.0 I.

2-Hept-6-ynyloxy-3,6,7,10,11-pentahexyloxytriphenylene (105)

The same procedure was carried out as for compound **103** using the following quantities: compound **70** (0.50 g, 0.672 mmol), compound **101** (0.26 g, 1.99 mmol), potassium carbonate (0.28 g, 2.03 mmol), and potassium iodide (0.20 g, 120 mmol) in DMSO (100 ml). The crude product was purified by column chromatography (silica gel, 4:1 hexane / DCM and alumina, hexane with increasing volume fractions of DCM), recrystallised from ethanol / toluene (10:1), and dried (P_2O_5) to yield a colourless solid.

Yield: 0.12 g (21 %), ^1H NMR (CDCl_3) δ : 0.93 (15H, t), 1.35-1.45 (20H, m), 1.58 (10H, quintet), 1.64 (4H, 2 \times quint), 1.94 (12H, quint), 1.96 (1H, t), 2.27 (2H, dt), 4.22 (10H, t), 4.24 (2H, t), 7.83 (6H, s), ^{13}C NMR (CDCl_3) δ : 14.06, 18.43, 22.67, 25.42, 25.86, 28.33, 28.99, 29.43, 29.72, 31.69, 68.36, 69.49, 69.66, 69.72, 69.74, 107.26, 107.36, 107.39, 107.44, 123.58, 123.62, 123.65, 123.71, 148.85, 148.96, 148.98, 149.00, MS m/z : 839 (M^++1), elemental analysis for $\text{C}_{55}\text{H}_{82}\text{O}_6$ requires 78.71 % C, 9.85 % H; found 78.58 % C, 10.04 % H, purity (HPLC): 91 %, transition temperatures ($^\circ\text{C}$): Cr 51.5 Col_h 67.1 I.

2,3,6,7,10-Pentahexyloxy-11-oct-7-ynyloxytriphenylene (106)

The same procedure was carried out as for compound **103** using the following quantities: compound **70** (0.50 g, 0.672 mmol), compound **102** (0.30 g, 2.08 mmol), potassium carbonate (0.28 g, 2.03 mmol), and potassium iodide (0.20 g, 120 mmol) in DMSO (100 ml). The crude product was purified by column chromatography (silica gel, 4:1 hexane / DCM and alumina, hexane with increasing volume fractions of DCM), recrystallised from ethanol / toluene (10:1), and dried (P_2O_5) to yield a colourless solid.

Yield: 0.31 g (54 %), ^1H NMR (CDCl_3) δ : 0.93 (15H, 5 \times t), 1.35-1.45 (22H, m), 1.51-1.63 (14H, m), 1.94 (12H, quint), 1.95 (1H, t), 2.22 (2H, dt), 4.23 (12H, t), 7.83 (6H, t),

^{13}C NMR (CDCl_3) δ : 14.05, 18.35, 22.66, 25.69, 25.85, 28.43, 28.55, 29.35, 29.42, 31.68, 68.22, 69.55, 69.66, 69.70, 69.73, 107.34, 107.35, 107.39, 123.54, 123.58, 123.62, 148.89, 148.97, 148.99, MS m/z : 853 ($\text{M}^+ + 1$), elemental analysis for $\text{C}_{56}\text{H}_{84}\text{O}_6$ requires 78.83 % C, 9.92 % H; found 78.59 % C, 9.69 % H, purity (HPLC): 93 %, transition temperatures ($^\circ\text{C}$): Cr 52.4 Col_h 68.3 I.

Cyclohexylmethyl tosylate (**111**)

Tosyl chloride (12.53 g, 0.0659 mol) was added slowly to a stirred, cooled (0 $^\circ\text{C}$) mixture of cyclohexylmethanol (**107**, 5.00 g, 0.0439 mol) and pyridine (6.93 g, 0.0877 mol) in dry DCM (100 ml) under an atmosphere of dry nitrogen. The stirred mixture was warmed to room temperature (overnight), then extracted into diethyl ether, washed with 10 % hydrochloric acid solution, sodium hydrogen carbonate solution and water, the aqueous components were back extracted with diethyl ether, the combined organic components were dried (MgSO_4) and the solvent removed *in vacuo* to yield the crude product as a colourless oil. The crude product was used without further purification in subsequent reactions despite the continued presence of tosyl chloride, as it was determined to be of sufficient purity.

Yield: 14.44 g (123 %), ^1H NMR (CDCl_3) δ : 0.75-0.84 (2H, m), 0.95-1.17 (3H, m), 1.47-1.65 (6H, m), 2.35 (3H, s), 3.71 (2H, d), 7.26 (2H, d), 7.68 (2H, d), (and tosyl chloride as: 2.36 (1.2H, s), 7.33 (0.8H, d), 7.85 (0.8H, d)), MS m/z : 268 (M^+).

2-Cyclohexylethyl tosylate (**112**)

The same procedure was carried out as is detailed in the preparation of compound **111**, using the following quantities: tosyl chloride (10.27 g, 0.0539 mol), 2-cyclohexylethanol (**108**, 4.60 g, 0.0359 mol), pyridine (5.68 g, 0.0719 mol) and DCM (120 ml). The crude product was used without further purification in subsequent reactions despite the continued presence of tosyl chloride, as it was determined to be of sufficient purity.

Yield: 13.73 g (136 %), ^1H NMR (CDCl_3) δ : 0.76-0.87 (2H, m), 1.03-1.33 (4H, m), 1.58-1.64 (7H, m), 2.49 (3H, s), 4.05 (2H, t), 7.34 (2H, d), 7.78 (2H, d), (and tosyl chloride as: 2.36 (1.1H, s), 7.33 (0.8H, d), 7.85 (0.8H, d)), MS m/z : 283 ($\text{M}^+ + 1$).

3-Cyclohexylpropyl tosylate (113)

The same procedure was carried out as is detailed in the preparation of compound **111**, using the following quantities: tosyl chloride (14.50 g, 0.0761 mol), 3-cyclohexylpropan-1-ol (**109**, 7.21 g, 0.0508 mol), pyridine (8.03 g, 0.102 mol) and DCM (100 ml). The crude product was used without further purification in subsequent reactions despite the continued presence of tosyl chloride, as it was determined to be of sufficient purity.

Yield: 11.64 g (123 %), ^1H NMR (CDCl_3) δ : 0.69-0.84 (2H, m), 0.97-1.20 (6H, m), 1.50-1.64 (7H, m), 2.38 (3H, s), 3.93 (2H, t), 7.28, (2H, d), 7.72 (2H, d), (and tosyl chloride as: 2.36 (1.2H, s), 7.33 (0.8H, d), 7.85 (0.8H, d)), MS m/z : 297 ($\text{M}^+ + 1$).

4-Cyclohexylbutyl tosylate (114)

The same procedure was carried out as is detailed in the preparation of compound **111**, using the following quantities: tosyl chloride (9.16 g, 0.0481 mol), 4-cyclohexylbutan-1-ol (**110**, 5.00 g, 0.0321 mol), pyridine (5.06 g, 0.0641 mol) and DCM (120 ml). The crude product was used without further purification in subsequent reactions despite the continued presence of tosyl chloride, as it was determined to be of sufficient purity.

Yield: 12.61 g (127 %), ^1H NMR (CDCl_3) δ : 0.75-0.85 (2H, m), 1.04-1.32 (8H, m), 1.57-1.71 (7H, m), 2.45 (3H, s), 4.02 (2H, t), 7.34 (2H, d), 7.78 (2H, d), (and tosyl chloride as: 2.36 (1.2H, s), 7.33 (0.8H, d), 7.85 (0.8H, d)), MS m/z : 311 ($\text{M}^+ + 1$).

2-(Cyclohexylmethoxy)-3,6,7,10,11-pentaheptyloxytriphenylene (115)

The same procedure was carried out as detailed for compound **103** using DMF in place of butanone and using the following quantities: compound **111** (0.50 g, 1.87 mmol), compound **70** (0.50 g, 0.672 mmol), potassium carbonate (0.28 g, 2.03 mmol) and DMF (100 ml). The crude product was purified by column chromatography (silica gel, 1:1 hexane / DCM and silica gel, hexane with increasing volume fractions of DCM), preparatory HPLC, recrystallised from ethanol and dried (P_2O_5) to yield a colourless solid.

Yield: 0.31 g (55 %), ^1H NMR (CDCl_3) δ : 0.93 (15H, t), 1.11-1.45 (25H, m), 1.58 (10H, quint), 1.71-1.83 (3H, m), 1.94 (10H, quint), 1.95-2.04 (3H, m), 4.02 (2H, d), 4.23 (10H, t), 7.81 (1H, s), 7.83 (4H, s), 7.84 (1H, s), ^{13}C NMR (CDCl_3) δ : 14.04, 17.99, 25.65, 25.84, 25.87, 25.89, 26.60, 29.41, 29.47, 30.06, 31.68, 37.97, 49.04, 69.67,

69.71, 69.74, 69.77, 69.83, 107.22, 107.31, 107.34, 107.54, 107.57, 123.51, 123.55, 123.64, 123.65, 148.92, 148.95, 148.97, 148.99, 149.27, MS m/z : 841 (M^+ +1), elemental analysis for $C_{55}H_{84}O_6$ requires 78.52 % C, 10.06 % H; found 78.61 % C, 10.16 % H, purity (HPLC): 100 %, transition temperatures ($^{\circ}C$): Cr 52.3 Col_h 103.3 I.

2-(2-Cyclohexylethoxy)-3,6,7,10,11-pentahexyloxytriphenylene (116)

The same procedure was carried out as detailed for compound **103** using DMF in place of butanone and using the following quantities: compound **112** (0.21 g, 0.745 mmol), compound **70** (0.50 g, 0.672 mmol), potassium carbonate (0.28 g, 2.03 mmol) and DMF (100 ml). The crude product was purified by column chromatography (silica gel, 1:1 hexane / DCM and silica gel, hexane with increasing volume fractions of DCM), preparatory HPLC, recrystallised from ethanol and dried (P_2O_5) to yield a colourless solid.

Yield: 0.21 g (37 %), 1H NMR ($CDCl_3$) δ : 0.93 (15H, t), 0.98-1.10 (2H, m), 1.13-1.44 (22H, m), 1.58 (10H, quint), 1.60-1.91 (9H, m), 1.94 (10H, quint), 4.23 (10H, t), 4.28 (2H, t), 7.84 (6H, s), MS m/z : 855 (M^+ +1), elemental analysis for $C_{56}H_{86}O_6$ requires 78.64 % C, 10.14 % H; found 78.51 % C, 10.04 % H, purity (HPLC): 100 %, transition temperatures ($^{\circ}C$): Cr 61.3 Col_h 90.0 I.

2-(3-Cyclohexylpropoxy)-3,6,7,10,11-pentahexyloxytriphenylene (117)

The same procedure was carried out as detailed for compound **103** using DMSO in place of butanone and using the following quantities: compound **113** (1.19 g, 4.02 mmol), compound **70** (1.00 g, 1.34 mmol), potassium carbonate (1.00 g, 7.25 mmol) and DMSO (110 ml). The crude product was purified by column chromatography (silica gel, 1:1 hexane / DCM and silica gel, hexane with increasing volume fractions of DCM), recrystallised from ethanol / toluene (10:1) and dried (P_2O_5) to yield a colourless solid.

Yield: 0.51 g (44 %), 1H NMR ($CDCl_3$) δ : 0.93 (15H, t), 0.93-0.99 (2H, m), 1.09-1.30 (3H, m), 1.30-1.44 (23H, m), 1.57 (10H, quint), 1.61-1.82 (5H, m), 1.94 (12H, quint), 4.23 (12H, 2 \times t), 7.83 (6H, s), ^{13}C NMR ($CDCl_3$) δ : 14.05, 22.65, 25.84, 26.38, 26.68, 26.84, 29.41, 31.68, 33.40, 33.82, 37.54, 69.70, 70.04, 107.33, 123.59, 148.95, MS m/z : 869 (M^+), elemental analysis for $C_{57}H_{88}O_6$ requires 78.75 % C, 10.20 % H; found 79.01

% C, 10.16 % H, purity (HPLC): 92 %, transition temperatures (°C): Cr 64.0 Col_h 91.4 I.

2-(4-Cyclohexylbutoxy)-3,6,7,10,11-pentahexyloxytriphenylene (118)

The same procedure was carried out as detailed for compound **103** using DMSO in place of butanone and using the following quantities: compound **114** (1.25 g, 4.03 mmol), compound **70** (1.00 g, 1.34 mmol), potassium carbonate (1.00 g, 7.25 mmol) and DMSO (110 ml). The crude product was purified by column chromatography (silica gel, 1:1 hexane / DCM and silica gel, hexane with increasing volume fractions of DCM), recrystallised from ethanol / toluene (10:1) and dried (P₂O₅) to yield a colourless solid.

Yield: 0.56 g (47 %), ¹H NMR (CDCl₃) δ: 0.86-1.92 (2H, m), 0.93 (15H, t), 1.09-1.45 (27H, m), 1.56 (10H, quint), 1.61-1.78 (6H, m), 1.94 (12H, 2×quint), 4.23 (12H, t), 7.84 (6H, s), ¹³C NMR (CDCl₃) δ: 14.05, 22.65, 23.43, 25.85, 26.43, 26.73, 29.41, 29.76, 31.68, 33.40, 37.31, 37.64, 69.70, 107.33, 123.59, 148.95, MS *m/z*: 883 (M⁺+1), elemental analysis for C₅₈H₉₀O₆ requires 78.86 % C, 10.27 % H; found 79.11 % C, 10.38 % H, purity (HPLC): 94 %, transition temperatures (°C): Cr 57.5 Col_h 81.5 I.

2-Pentylcarbonyloxy-3,6,7,10,11-pentahexyloxytriphenylene (119)

The same procedure was carried out as for compound **45** using the following quantities: compound **70** (0.20 g, 0.269 mmol), hexanoic acid (0.05 g, 0.431 mmol), DCC 0.07 g, 0.340 mmol), DMAP (0.01 g, 0.820 mmol) and DCM (80 ml). The crude product was purified by column chromatography (silica gel, 1:1 hexane / DCM), recrystallised from ethanol / toluene (10:1) and dried (P₂O₅) to yield a light purple solid.

Yield: 0.18 g (80 %), ¹H NMR (CDCl₃) δ: 0.94 (15H, 5×t), 0.97 (3H, t), 1.34-1.50 (22H, m), 1.54-1.62 (12H, m), 1.81-1.97 (12H, m), 2.66 (2H, t), 4.23 (10H, 5×t), 7.78 (1H, s), 7.81 (1H, s), 7.82 (1H, s), 7.86 (2H, 2×s), 8.06 (1H, s), ¹³C NMR (CDCl₃) δ: 13.96, 14.04, 22.40, 22.65, 24.80, 25.78, 25.82, 25.83, 25.85, 29.32, 29.34, 29.38, 29.41, 29.43, 31.42, 31.64, 31.68, 34.14, 68.33, 69.23, 69.50, 69.80, 69.92, 105.96, 106.56, 106.91, 107.30, 107.91, 108.05, 116.70, 122.94, 123.16, 148.79, 148.92, 149.21, 149.50, 153.03, 164.94, 172.09, MS *m/z*: 843 (M⁺+1), elemental analysis for C₅₄H₈₂O₆ requires 76.92 % C, 9.80 % H; found 76.67 % C, 9.77 % H, purity (HPLC): 93 %, transition temperatures (°C): Cr 42.0 Col_h 156.0 I.

2-Ethoxy-3,6,7,10,11-pentahexyloxytriphenylene (120)

The same procedure was carried out as detailed in the synthesis of compound **103**, using the following quantities: compound **70** (0.2 g, 0.269 mmol), 1-bromoethane (0.04 g, 0.367 mmol), potassium carbonate (0.11 g, 0.797 mmol) and butanone (110 ml). The product was purified by column chromatography (silica gel, 4:1 hexane / DCM), recrystallised from ethanol / toluene (10:1) and dried (P₂O₅) to yield a colourless waxy solid.

Yield: 0.12 g (58 %), ¹H NMR (CDCl₃) δ: 0.93 (15H, t), 1.35-1.42 (20H, m), 1.53-1.61 (13H, m), 1.94 (10H, quint), 4.22 (2H, t), 4.23 (6H, t), 4.25 (2H, t), 4.31 (2H, quart), 7.83 (5H, s), 7.84 (1H, s), ¹³C NMR (CDCl₃) δ: 14.05, 15.01, 22.65, 25.80, 25.83, 29.33, 29.41, 31.67, 107.12, 107.19, 107.33, 107.41, 123.54, 123.63, 123.66, 123.70, 148.65, 148.85, 148.89, 148.95, 148.98, MS *m/z*: 773 (M⁺), elemental analysis for C₅₀H₇₆O₆ requires 77.68 % C, 9.91 % H; found 77.49 % C, 9.72 % H, purity (HPLC): 91 %, transition temperatures (°C): Cr 57.3 Col_h 79.1 I.

2,3,6,7,10-Pentahexyloxy-11-propoxytriphenylene (121)

The same procedure was carried out as detailed in the synthesis of compound **103**, using the following quantities: compound **70** (0.2 g, 0.269 mmol), 1-bromopropane (0.04 g, 3.25 mmol), potassium carbonate (0.11 g, 0.797 mmol) and butanone (120 ml). The product was purified by column chromatography (silica gel, 4:1 hexane / DCM), recrystallised from ethanol / toluene (10:1) and dried (P₂O₅) to yield a colourless waxy solid.

Yield: 0.13 g (61 %), ¹H NMR (CDCl₃) δ: 0.93 (15H, t), 1.14 (3H, t), 1.35-1.45 (10H, m), 1.58 (10H, quint), 1.93 (10H, quint), 1.97 (2H, quint), 4.19 (2H, t), 4.22 (10H, t), 7.83 (6H, s), ¹³C NMR (CDCl₃) δ: 10.66, 14.06, 22.67, 22.82, 25.87, 29.44, 31.70, 69.74, 107.38, 123.63, 148.99, MS *m/z*: 787 (M⁺), elemental analysis for C₅₁H₇₈O₆ requires 77.82 % C, 9.99 % H; found 77.76 % C, 10.18 % H, purity (HPLC): 91 %, transition temperatures (°C): Cr 60.6 Col_h 84.8 I.

2-Butoxy-3,6,7,10,11-pentahexyloxytriphenylene (122)

The same procedure was carried out as detailed in the synthesis of compound **103**, using the following quantities: compound **70** (0.50 g, 0.672 mmol), 1-bromobutane (0.20 g, 1.46 mmol), potassium carbonate (0.28 g, 2.03 mmol) and butanone (120 ml). The

product was purified by column chromatography (silica gel, 4:1 hexane / DCM), recrystallised from ethanol / toluene (10:1) and dried (P₂O₅) to yield a colourless waxy solid.

Yield: 0.34 g (63 %), ¹H NMR (CDCl₃) δ: 0.94 (15H, t), 1.04 (3H, t), 1.34-1.44 (18H, m), 1.54-1.65 (14H, m), 1.94 (12H, quint), 4.23 (10H, t), 4.24 (2H, t), 7.84 (6H, s), ¹³C NMR (CDCl₃) δ: 13.98, 14.05, 19.38, 22.66, 25.84, 29.41, 31.48, 31.68, 68.34, 69.68, 107.28, 123.58, 148.93, MS *m/z*: 801 (M⁺), elemental analysis for C₅₂H₈₀O₆ requires 77.5 % C, 10.06 % H; found 77.82 % C, 10.35 % H, purity (HPLC): 91 %, transition temperatures (°C): Cr 59.7 Col_h 95.1 I.

2,3,6,7,10-Pentahexyloxy-11-pentyloxytriphenylene (123)

The same procedure was carried out as detailed in the synthesis of compound **103**, using the following quantities: compound **70** (0.20 g, 0.269 mmol), 1-iodopentane (0.10 g, 0.505 mmol), potassium carbonate (0.11 g, 0.797 mmol) and butanone (120 ml). The product was purified by column chromatography (silica gel, 4:1 hexane / DCM), recrystallised from ethanol / toluene (10:1) and dried (P₂O₅) to yield a colourless waxy solid.

Yield: 0.04 g (18 %), ¹H NMR (CDCl₃) δ: 0.92 (15H, t), 0.97 (3H, t), 1.35-1.50 (22H, m), 1.58 (12H, quint), 1.94 (12H, quint), 4.23 (12H, t), 7.84 (6H, s), ¹³C NMR (CDCl₃) δ: 14.06, 22.66, 25.84, 29.40, 31.68, 69.68, 107.28, 123.57, 148.93, MS *m/z*: 815 (M⁺), elemental analysis for C₅₃H₈₂O₆ requires 78.09 % C, 10.14 % H; found 77.83 % C, 10.31 % H, purity (HPLC): 91 %, transition temperatures (°C): Cr 57.7 Col_h 94.5 I.

2-Heptyloxy-3,6,7,10,11-pentahexyloxytriphenylene (124)

The same procedure was carried out as detailed in the synthesis of compound **103**, using the following quantities: compound **70** (0.20 g, 0.269 mmol), 1-bromoheptane (0.06 g, 0.335 mmol), potassium carbonate (0.11 g, 0.797 mmol) and butanone (120 ml). The product was purified by column chromatography (silica gel, 4:1 hexane / DCM), recrystallised from ethanol / toluene (10:1) and dried (P₂O₅) to yield a colourless waxy solid.

Yield: 0.09 g (40 %), ¹H NMR (CDCl₃) δ: 0.91 (3H, t), 0.92 (15H, t), 1.33-1.44 (24H, m), 1.58 (12H, quint), 1.84 (2H, quint), 1.93 (12H, quint), 4.22 (12H, t), 7.83 (6H, s), ¹³C NMR (CDCl₃) δ: 14.07, 22.64, 22.67, 25.87, 29.19, 29.43, 31.70, 31.87, 107.34,

123.61, 148.97, MS m/z : 843 (M^+), elemental analysis for $C_{55}H_{86}O_6$ requires 78.34 % C, 10.28 % H; found 78.64 % C, 10.56 % H, purity (HPLC): 92 %, transition temperatures ($^{\circ}C$): Cr 58.0 Col_h 94.7 I.

2,3,6,7,10-Pentahexyloxy-11-octyloxytriphenylene (125)

The same procedure was carried out as detailed in the synthesis of compound **103**, using the following quantities: compound **70** (0.20 g, 0.269 mmol), 1-bromooctane (0.06 g, 0.310 mmol), potassium carbonate (0.11 g, 0.797 mmol) and butanone (120 ml). The product was purified by column chromatography (silica gel, 4:1 hexane / DCM), recrystallised from ethanol / toluene (10:1) and dried (P_2O_5) to yield a colourless waxy solid.

Yield: 0.20 g (56 %), 1H NMR ($CDCl_3$) δ : 0.89 (3H, t), 0.93 (15H, t), 1.29-1.43 (28H, m), 1.58 (12H, quint), 1.95 (12H, quint), 4.23 (12H, t), 7.83 (6H, s), ^{13}C NMR ($CDCl_3$) δ : 14.07, 22.67, 25.87, 26.21, 29.34, 29.43, 31.70, 31.86, 107.34, 123.61, 148.97, MS m/z : 857 (M^++1), elemental analysis for $C_{56}H_{88}O_6$ requires 78.46 % C, 10.35 % H; found 78.57 % C, 10.40 % H, purity (HPLC): 90 %, transition temperatures ($^{\circ}C$): Cr 52.0 Col_h 86.0 I.

2-Decyloxy-3,6,7,10,11-pentahexyloxytriphenylene (126)

The same procedure was carried out as detailed in the synthesis of compound **103**, using the following quantities: compound **70** (0.20 g, 0.269 mmol), 1-bromodecane (0.07 g, 0.317 mmol), potassium carbonate (0.11 g, 0.797 mmol) and butanone (120 ml). The product was purified by column chromatography (silica gel, 4:1 hexane / DCM), recrystallised from ethanol / toluene (10:1) and dried (P_2O_5) to yield a colourless waxy solid.

Yield: 0.19 g (80 %), 1H NMR ($CDCl_3$) δ : 0.88 (3H, t), 0.93 (15H, t), 1.25-1.42 (32H, m), 1.57 (12H, quint), 1.93 (12H, quint), 4.22 (12H, t), 7.83 (6H, s), ^{13}C NMR ($CDCl_3$) δ : 14.06, 14.11, 22.67, 22.70, 25.86, 26.21, 29.38, 29.48, 29.43, 29.54, 29.61, 29.69, 31.70, 31.92, 69.72, 107.35, 123.61, 148.97, MS m/z : 885 (M^+), elemental analysis for $C_{58}H_{92}O_6$ requires 78.68 % C, 10.47 % H; found 78.87 % C, 10.69 % H, purity (HPLC): 91 %, transition temperatures ($^{\circ}C$): Cr 45.4 Col_h 59.0 I.

2,3,6,7,10-Pentahexyloxy-11-(1-methylethoxy)triphenylene (127)

The same procedure was carried out as detailed in the synthesis of compound **103**, using the following quantities: compound **70** (0.50 g, 0.672 mmol), 2-bromopropane (0.25 g, 2.03 mmol), potassium carbonate (0.28 g, 2.03 mmol) and butanone (110 ml). The product was purified by column chromatography (silica gel, 4:1 hexane / DCM), recrystallised from ethanol / toluene (10:1) and dried (P₂O₅) to yield a colourless waxy solid.

Yield: 0.44 g (91 %), ¹H NMR (CDCl₃) δ: 0.93 (15H, t), 1.40 (2H, quint), 1.32-1.44 (18H, m), 1.45 (6H, d), 1.58 (10H, quint), 1.93 (10H, quint), 4.22 (10H, t), 4.71 (1H, septet), 7.81-1.84 (5H, m), 7.93 (1H, s), ¹³C NMR (CDCl₃) δ: 14.05, 22.32, 22.65, 25.3, 25.84, 25.86, 29.36, 29.38, 29.40, 31.64, 31.68, 69.36, 69.52, 69.62, 69.79, 73.11, 107.01, 107.20, 107.41, 107.48, 112.69, 123.40, 123.45, 123.50, 123.59, 123.62, 124.59, 148.87, 149.04, 149.09, 150.35, MS *m/z*: 786 (M⁺), elemental analysis for C₅₁H₇₈O₆ requires 77.82 % C, 9.99 % H; found 78.00 % C, 10.14 % H, purity (HPLC): 91 %, transition temperatures (°C): Cr 54.6 I.

2,3,6,7,10-Pentahexyloxy-11-(2-methylpropoxy)triphenylene (128)

The same procedure was carried out as detailed in the synthesis of compound **103**, using the following quantities: compound **70** (0.96 g, 1.29 mmol), 1-bromo-2-methylpropane (0.50 g, 3.65 mmol), potassium carbonate (0.50 g, 3.62 mmol) and butanone (120 ml). The product was purified by column chromatography (silica gel, 4:1 hexane / DCM), recrystallised from ethanol / toluene (10:1) and dried (P₂O₅) to yield a colourless waxy solid.

Yield: 0.77 g (75 %), ¹H NMR (CDCl₃) δ: 0.93 (15H, t), 1.13 (6H, d), 1.41 (20H, quint), 1.58 (10H, quint), 1.94 (10H, quint), 2.26 (1H, non), 4.00 (2H, d), 4.21-4.25 (10H, m), 7.82-7.84 (6H, m), ¹³C NMR (CDCl₃) δ: 14.05, 19.41, 22.65, 25.84, 28.57, 29.41, 29.47, 31.68, 69.6, 69.69, 69.71, 69.84, 76.02, 107.25, 107.25, 107.32, 107.34, 107.50, 107.57, 123.55, 123.59, 123.63, 123.65, 148.92, 148.94, 148.97, 148.98, 149.00, 149.19, MS *m/z*: 801 (M⁺+1), elemental analysis for C₅₂H₈₀O₆ requires 77.95 % C, 10.06 % H; found 77.74 % C, 10.14 % H, purity (HPLC): 97 %, transition temperatures (°C): Cr 59.4 Col_h 85.4 I.

2,3,6,7,10-Pentahexyloxy-11-(3-methylbutoxy)triphenylene (129)

The same procedure was carried out as detailed in the synthesis of compound **103**, using the following quantities: compound **70** (0.50 g, 0.672 mmol), 1-bromo-3-methylbutane (0.20 g, 1.32 mmol), potassium carbonate (0.28 g, 2.02 mmol) and butanone (70 ml). The product was purified by column chromatography (silica gel, 4:1 hexane / DCM) and preparatory HPLC, recrystallised from ethanol and dried (P₂O₅) to yield a colourless waxy solid.

Yield: 0.12 g (22 %), ¹H NMR (CDCl₃) δ: 0.94 (15H, t), 1.04 (6H, d), 1.36-1.43 (21H, m), 1.54-1.61 (10H, quint), 1.83 (2H, quart) 1.94 (10H, quint), 4.22 (10H, t), 4.27 (2H, t), 7.84 (6H, s), ¹³C NMR (CDCl₃) δ: 14.05, 22.66, 22.74, 25.84, 29.41, 31.68, 69.65, 69.70, 107.12, 107.33, 123.59, 148.91, 148.93, 148.97, MS *m/z*: 815 (M⁺+1), elemental analysis for C₅₃H₈₂O₆ requires 78.09 % C, 10.14 % H; found 77.98 % C, 10.24 % H, purity (HPLC): 100 %, transition temperatures (°C): Cr 54.5 Col_h 105.0 I.

2,3,6,7,10-Pentahexyloxy-11-(4-methylpentyloxy)triphenylene (130)

The same procedure was carried out as detailed in the synthesis of compound **103**, using the following quantities: compound **70** (0.50 g, 0.672 mmol), 1-bromo-4-methylpentane (0.22 g, 1.33 mmol), potassium carbonate (0.28 g, 2.02 mmol) and butanone (120 ml). The product was purified by column chromatography (silica gel, 4:1 hexane / DCM), recrystallised from ethanol / toluene (10:1) and dried (P₂O₅) to yield a colourless waxy solid.

Yield: 0.34 g (61 %), ¹H NMR (CDCl₃) δ: 0.93 (15H, t), 0.96 (6H, d), 1.38-1.40 (22H, m), 1.54-1.62 (10H, m), 1.68 (1H, sept), 1.93 (12H, quint), 4.21 (2H, t), 4.22 (10H, t), 7.83 (6H, s), ¹³C NMR (CDCl₃) δ: 14.05, 22.62, 22.65, 25.84, 27.33, 27.90, 29.41, 31.68, 35.30, 69.69, 69.99, 107.28, 107.32, 123.58, 148.92, 148.95, MS *m/z*: 828 (M⁺), elemental analysis for C₅₄H₈₄O₆ requires 78.21 % C, 10.21 % H; found 77.71 % C, 11.1 % H, purity (HPLC): 97 %, transition temperatures (°C): Cr 61.5 Col_h 105.3 I.

2-(2-Ethylbutoxy)-3,6,7,10,11-pentahexyloxytriphenylene (131)

The same procedure was carried out as detailed in the synthesis of compound **103**, using the following quantities: compound **70** (0.50 g, 0.672 mmol), 1-bromo-2-ethylbutane (1.50 g, 9.09 mmol), potassium carbonate (0.28 g, 2.03 mmol) and butanone (110 ml). The product was purified by column chromatography (silica gel, 4:1 hexane / DCM),

recrystallised from ethanol / toluene (10:1) and dried (P₂O₅) to yield a colourless waxy solid.

Yield: 0.34 g (61 %), ¹H NMR (CDCl₃) δ: 0.93 (15H, t), 1.01 (6H, t), 1.38-1.42 (24H, m), 1.51-1.64 (10H, m), 1.85 (1H, septet), 1.93 (10H, quint), 4.12 (2H, d), 4.22 (10H, t), 7.82-7.84 (6H, m), ¹³C NMR (CDCl₃) δ: 11.36, 14.06, 22.67, 23.63, 25.87, 29.44, 29.51, 31.70, 41.11, 69.70, 69.73, 69.82, 71.76, 106.99, 107.34, 107.37, 107.51, 107.53, 123.48, 123.57, 123.63, 123.66, 148.95, 148.99, 149.23, MS *m/z*: 829 (M⁺+1), elemental analysis for C₅₄H₈₄O₆ requires 78.21 % C, 10.21 % H; found 78.09 % C, 10.47 % H, purity (HPLC): 99 %, transition temperatures (°C): Cr 44.4 Col_h 78.1 I.

2,3,6,7,10-Pentahexyloxy-11-(2-methoxyethoxy)triphenylene (132)

The same procedure was carried out as detailed in the synthesis of compound **103**, using the following quantities: compound **70** (0.50 g, 0.672 mmol), 2-bromoethyl methylether (0.19 g, 1.37 mmol), potassium carbonate (0.28 g, 2.03 mmol) and butanone (100 ml). The product was purified by column chromatography (silica gel, 4:1 hexane / DCM), recrystallised from ethanol and dried (P₂O₅) to yield a colourless waxy solid.

Yield: 0.12 g (22 %), ¹H NMR (CDCl₃) δ: 0.94 (15H, 2×t), 1.33-1.44 (20H, m), 1.54-1.58 (10H, m), 1.94 (10H, 2×quint), 3.53 (3H, s), 3.88 (2H, t), 4.23 (10H, 3×t), 4.39 (2H, t), 7.83 (5H, s), 7.94 (1H, s), ¹³C NMR (CDCl₃) δ: 14.01, 22.62, 25.80, 29.32, 29.36, 31.64, 69.40, 69.55, 69.66, 69.70, 71.32, 106.78, 106.90, 107.11, 107.23, 107.34, 109.05, 123.36, 123.44, 123.55, 123.74, 124.23, 148.27, 148.80, 148.82, 149.02, 149.12, MS *m/z*: 802 (M⁺), elemental analysis for C₅₁H₇₈O₇ requires 76.27 % C, 9.74 % H; found 76.49 % C, 9.96 % H, purity (HPLC): 100 %, transition temperatures (°C): Cr 54.9, Col_h 86.7 I.

2-(2-Ethoxyethoxy)-3,6,7,10,11-pentahexyloxytriphenylene (133)

The same procedure was carried out as detailed in the synthesis of compound **103**, using the following quantities: compound **70** (0.50 g, 0.672 mmol), 2-bromoethyl ethylether (0.21 g, 1.37 mmol), potassium carbonate (0.28 g, 2.03 mmol) and butanone (100 ml). The product was purified by column chromatography (silica gel, 4:1 hexane / DCM), recrystallised from ethanol / toluene (10:1) and dried (P₂O₅) to yield a colourless waxy solid.

Yield: 0.12 g (22 %), ^1H NMR (CDCl_3) δ : 0.93 (15H, 2 \times t), 1.29 (3H, t), 1.33-1.48 (20H, m), 1.58 (10H, quint), 1.94 (10H, quint), 3.68 (2H, quart), 3.92 (2H, t), 4.23 (10H, 3 \times t), 4.69 (2H, t), 7.83 (5H, s), 7.94 (1H, s), ^{13}C NMR (CDCl_3) δ : 14.04, 15.27, 22.58, 22.65, 25.77, 25.83, 29.41, 31.58, 31.68, 66.95, 69.19, 69.52, 69.56, 69.64, 69.72, 69.76, 106.92, 107.12, 107.21, 107.37, 107.40, 108.85, 123.43, 123.53, 123.61, 123.75, 124.17, 148.44, 148.88, 148.89, 149.06, 149.08, 149.12, MS m/z : 816 (M^+), elemental analysis for $\text{C}_{52}\text{H}_{80}\text{O}_6$ requires 76.43 % C, 9.87 % H; found 76.20 % C, 9.89 % H, purity (HPLC): 99 %, transition temperatures ($^\circ\text{C}$): Cr 51.3 Col_h 77.4 I.

2-(4,4,4-Trifluorobutoxy)-3,6,7,10,11-pentahexyloxytriphenylene (134)

The same procedure was carried out as detailed in the synthesis of compound **103**, using DMSO in place of butanone and using the following quantities: compound **70** (0.50 g, 0.672 mmol), 1-bromo-4,4,4-trifluorobutane (0.15 g, 0.785 mmol), potassium carbonate (0.28 g, 2.03 mmol) and DMSO (120 ml). The product was purified by column chromatography (silica gel, 1:1 hexane / DCM), recrystallised from ethanol / toluene / acetonitrile (17:2:1) and dried (P_2O_5) to yield a colourless waxy solid.

Yield: 0.14 g (24 %), ^1H NMR (CDCl_3) δ : 0.93 (15H, t), 1.36-1.43 (20H, m), 1.54-1.56 (10H, m), 1.94 (10H, quint), 2.18 (2H, m), 2.47 (2H, m), 4.23 (10H, 4 \times t), 4.29 (2H, t), 7.81 (1H, s), 7.83 (4H, 4 \times s), 7.84 (1H, s), ^{13}C NMR (CDCl_3) δ : 13.98, 14.05, 19.37, 22.66, 25.84, 29.40, 31.47, 31.68, 69.68, 107.29, 123.57, 148.93, MS m/z : 855 (M^+), elemental analysis for $\text{C}_{52}\text{H}_{77}\text{O}_6\text{F}_3$ requires 73.03 % C, 9.08 % H; found 72.84 % C, 9.35 % H, purity (HPLC): 91 %, transition temperatures ($^\circ\text{C}$): Cr 59.4 Col_h 128.4 I.

2-(4-Hexyloxyphenylcarbonyloxy)-3,6,7,10,11-pentahexyloxytriphenylene (135)

The same procedure was carried out as detailed for compound **45** using the following quantities: compound **70** (0.50 g, 0.672 mmol), compound **41** (0.18 g, 0.811 mmol), DCC (0.19 g, 0.825 mmol), DMAP (0.02 g, 0.164 mmol) and DCM (80 ml). The crude product was purified by column chromatography (silica gel, 1:1 hexane / DCM), recrystallised from ethanol / toluene (10:1) and dried (P_2O_5) to yield a colourless waxy solid.

Yield: 0.40 g (63 %), ^1H NMR (CDCl_3) δ : 0.82 (3H, t), 0.91-0.93 (15H, m), 1.19-1.28 (4H, m), 1.31-1.43 (22H, m), 1.43-1.68 (10H, m), 1.76 (2H, quint), 1.84 (2H, quint), 1.92 (8H, quint), 4.07 (2H, t), 4.17-4.26 (10H, 5 \times t), 7.00 (2H, d), 7.79 (1H, s), 7.82 (1H,

s), 7.83 (1H, s), 7.88 (1H, s), 7.90 (1H, s), 8.19 (1H, s), 8.23 (2H, d), ¹³C NMR (CDCl₃) δ: 13.93, 14.02, 14.05, 22.51, 22.62, 22.65, 25.78, 25.84, 29.42, 31.55, 31.62, 31.68, 68.30, 69.50, 69.80, 69.85, 106.41, 106.95, 107.29, 107.95, 114.24, 116.96, 121.59, 123.08, 123.11, 123.28, 123.57, 124.60, 127.89, 132.38, 140.32, 148.77, 149.22, 149.67, 163.46, 164.92, MS *m/z*: 949 (M⁺), elemental analysis for C₆₁H₈₈O₈ requires 77.17 % C, 9.34 % H; found 77.14 % C, 9.58 % H, purity (HPLC): 91 %, transition temperatures (°C): Cr 45.2 N_D 58.2 I.

Ethyl 3,4,5-trihydroxybenzoate (137)

Sulfuric acid (10 ml, 98 %) was added to a stirred, heated mixture of 3,4,5-trihydroxybenzoic acid (**136**, 100 g, 0.588 mol) in ethanol (500 ml). The stirred mixture was heated under reflux for 48 h, cooled to room temperature slowly and the solvent removed *in vacuo*. The organic component was extracted into diethyl ether and washed with water (twice), the aqueous components were backwashed with further portions of diethyl ether, the combined organic extracts were dried (MgSO₄) and the solvent removed *in vacuo* to yield a cream coloured solid.

Yield: 114 g (98 %), ¹H NMR (DMSO-D₆) δ: 1.23 (3H, t), 4.16 (2H, quart), 6.90 (2H, s), 8.89 (1H, s), 9.24 (2H, s), MS *m/z*: 198 (M⁺), mp: 154.8-158.9 °C.

Ethyl 3,4,5-trihexyloxybenzoate (138)

The same procedure was carried out as for compound **3** using the following quantities: compound **137** (15.00 g, 0.0758 mol), 1-bromohexane (50.00 g, 0.303 mol), potassium hydroxide (41.80 g, 0.303 mol) and butanone (500 ml). Excess 1-bromohexane was removed *in vacuo* to yield a yellow oil.

Yield: 25.80 g (76 %), ¹H NMR (CDCl₃) δ: 0.90 (9H, 2×t), 1.32-1.37 (12H, m), 1.38 (2H, t), 1.47 (6H, quint), 1.75 (2H, quint), 1.81 (4H, quint), 4.02 (6H, 2×t), 4.35 (2H, q), 7.26 (2H, s), MS *m/z*: 450 (M⁺).

3,4,5-Trihexyloxybenzoic acid (139)

Potassium hydroxide (6.40 g, 0.114 mol) was dissolved in water (200 ml) and added dropwise to a stirred, heated mixture of compound **138** (22.00 g, 0.0489 mol) in ethanol (400 ml). The stirred mixture was heated under reflux (overnight), then poured onto ice

and acidified (congo red) with 36 % hydrochloric acid solution. The solid precipitate was filtered off and recrystallised from hexane to yield colourless crystals.

Yield: 8.90 g (43 %), ^1H NMR (DMSO- D_6) δ : 0.82 (9H, 2 \times t), 1.24-1.27 (12H, m), 1.37-1.39 (6H, m), 1.58 (2H, quint), 1.67 (4H, quint), 3.86 (2H, t), 3.93 (4H, t), 7.14 (2H, s), MS m/z : 422 (M^+), mp: 42.9-44.8 °C, lit. mp: 41 °C¹¹⁸.

2,3,6,7,10-Pentahexyloxy-11-(3,4,5-trihexyloxyphenylcarbonyloxy)triphenylene (140)

The same procedure was carried out as detailed for compound **45** using the following quantities: compound **70** (0.50 g, 0.672 mmol), compound **139** (0.57 g, 1.35 mmol), DCC (0.15 g, 7.26 mmol), DMAP (0.03 g, 0.246 mmol) and DCM (120 ml). The crude product was purified by column chromatography (silica gel, 1:1 hexane / DCM and silica gel, 3:1 hexane / DCM) recrystallised from ethanol / toluene (10:1) and dried (P_2O_5) to yield a colourless solid.

Yield: 0.60 g (78 %), ^1H NMR (CDCl_3) δ : 0.81 (3H, t), 0.90-0.94 (21H, m), 1.24 (2H, sext), 1.33-1.44 (30H, m), 1.45-1.61 (16H, m), 1.78 (2H, quint), 1.84 (4H, quint), 1.94 (10H, quint), 4.07 (4H, t), 4.08 (2H, t), 4.19 (2H, t), 4.21-4.26 (8H, 4 \times t), 7.50 (2H, s), 7.79 (1H, s), 7.83 (1H, s), 7.84 (1H, s), 7.89 (1H, s), 7.91 (1H, s), 8.19 (1H, s), ^{13}C NMR (CDCl_3) δ : 13.93, 14.02, 14.03, 14.05, 14.09, 22.54, 22.62, 22.65, 22.69, 25.65, 25.72, 25.76, 25.79, 25.83, 25.85, 29.23, 29.28, 29.29, 29.37, 29.41, 29.43, 30.31, 31.50, 31.55, 31.62, 31.68, 31.74, 69.03, 69.15, 69.22, 69.50, 69.80, 69.88, 73.56, 106.40, 106.95, 107.27, 107.29, 107.95, 108.56, 116.90, 123.04, 123.14, 123.53, 123.98, 124.63, 127.96, 140.25, 142.80, 148.81, 148.89, 149.24, 149.65, 149.73, 152.96, 164.97, MS m/z : 1149 ($\text{M}^+ + 1$), elemental analysis for $\text{C}_{73}\text{H}_{112}\text{O}_{10}$ requires 76.26 % C, 9.82 % H; found 76.03 % C, 10.10 % H, purity (HPLC): 99 %, transition temperatures (°C): Cr 41.1 Col_h 101.4 I.

4-Hexyloxyphenylboronic acid (142)

A solution of *n*-butyllithium (17.1 ml, 2.5 M in hexanes, 0.0482 mol) was added dropwise to a stirred, cooled (− 78 °C) mixture of 1-bromo-4-hexyloxybenzene (**141**, 10.00 g, 0.0389 mol) in THF (400 ml) under an atmosphere of dry nitrogen. Trimethyl borate (12.00 g, 0.115 mol) was added dropwise to the mixture which was stirred for a further 2 h. The mixture was warmed to room temperature (overnight), then acidified

with 10 % hydrochloric acid solution, and stirred for 1 h. The product was extracted into diethyl ether and washed with water (twice), the aqueous components were backwashed with diethyl ether, the ethereal extracts were dried (MgSO₄), and the solvent removed *in vacuo*. The solid product was purified by stirring in hexane (1 h) to yield an off-white solid.

Yield: 4.01 g (46 %), ¹H NMR (DMSO-D₆) δ: 0.84 (3H, t), 1.25-1.28 (4H, m), 1.37 (2H, quint), 1.66 (2H, quint), 3.92 (2H, t), 6.81 (2H, d), 7.66 (2H, d), 7.79 (2H, s), MS *m/z*: 612 (M⁺ of trimeric anhydride), mp: 93.6-95.2 °C.

2-Trifluoromethylsulfonato-3,6,7,10,11-pentahexyloxytriphenylene (143)

Triflic anhydride (3.75 g, 0.133 mol) was added dropwise to a stirred, cooled (0 °C) mixture of compound **70** (8.10 g, 0.109 mol) in anhydrous pyridine (200 ml) under an atmosphere of dry nitrogen. The mixture was slowly warmed to room temperature (overnight) then poured into water. The mixture was extracted into diethyl ether and washed with 10 % hydrochloric acid solution, water and brine, the aqueous components were backwashed with further portions of diethyl ether, the combined organic extracts were dried (MgSO₄) and the solvent removed *in vacuo*. The crude product was purified by column chromatography (silica gel, hexane with increasing volume fractions of DCM) to yield a dark blue waxy solid.

Yield: 7.04 g (74 %), ¹H NMR (CDCl₃) δ: 0.94 (15H, 5×t), 1.32-1.46 (20H, m), 1.54-1.60 (10H, m), 1.95 (10H, 5×quint), 4.23 (8H, 4×t), 4.28 (2H, t), 7.73 (1H, s), 7.81 (2H, 2×s), 7.90 (1H, s), 8.21 (1H, s), ¹³C NMR (CDCl₃) δ: 14.06, 22.67, 25.86, 28.96, 29.12, 29.43, 29.48, 31.69, 67.71, 107.34, 123.61, 148.97, ¹⁹F NMR (CDCl₃) δ: -73.53, MS *m/z*: 877 (M⁺+1), purity (HPLC): 90 %, transition temperatures (°C): Col_h 168.0 I.

2,3,6,7,10-Pentahexyloxy-11-(4-hexyloxyphenyl)triphenylene (144)

Compound **142** (0.25 g, 1.13 mmol) was added to a stirred, heated mixture of compound **143** (0.75 g, 8.56 mmol), sodium carbonate (0.22 g, 2.08 mmol), lithium chloride (0.05 g, 4.76 mmol) tetrakis(triphenylphosphine)palladium(0) (0.07 g, 0.0607 mmol), water (20 ml) and DME (180 ml) under an atmosphere of dry nitrogen. The mixture was heated under reflux for 24 h, cooled to room temperature and filtered to remove traces of palladium catalyst. The mixture was extracted into diethyl ether, washed with water and brine, the aqueous components were backwashed with diethyl

ether, the combined organic extracts were dried (MgSO₄), and the solvent removed *in vacuo*. The crude product was purified by column chromatography (silica gel, hexane with increasing volume fractions of DCM), recrystallised from ethanol / toluene (10:1) and dried (P₂O₅) to yield a colourless solid.

Yield: 0.34 g (44 %), ¹H NMR (CDCl₃) δ: 0.91-0.94 (18H, m), 1.31-1.46 (20H, m), 1.47-1.61 (14H, m), 1.83 (4H, quint), 1.93 (10H, quint), 4.04 (2H, t), 4.18 (4H, 2×t), 4.22 (4H, 2×t), 4.25 (2H, t), 7.01 (2H, d), 7.63 (2H, d), 7.82 (1H, s), 7.84 (1H, s), 7.86 (1H, s), 7.92 (1H, s), 7.93 (1H, s), 8.33(1H, s), ¹³C NMR (CDCl₃) δ: 14.04, 22.63, 22.65, 25.78, 25.80, 25.84, 25.85, 29.23, 29.32, 29.36, 29.38, 29.39, 29.44, 31.52, 31.61, 31.65, 31.68, 68.05, 68.73, 69.36, 69.51, 69.85, 104.98, 106.56, 106.61, 106.76, 107.01, 107.53, 107.89, 114.00, 122.98, 123.08, 123.25, 124.5, 124.72, 125.19, 129.12, 130.45, 130.91, 130.99, 148.73, 148.78, 149.26, 149.70, 155.01, 158.39, MS *m/z*: 904 (M⁺), elemental analysis for C₆₀H₈₈O₆ requires 79.60 % C, 9.80 % H; found 79.75 % C, 9.88 % H, purity (HPLC): 91 % transition temperatures (°C): Cr 25.6 Col_h 89.1 I.

2,3,6,7,10-Pentahexyloxy-11-(4-hexyloxyphenylethynyl)triphenylene (146)

A solution of *n*-butyllithium (1.4 ml, 2.5 M in hexanes, 3.5 mmol) was added dropwise to a stirred, cooled (− 78 °C) mixture of 1-ethynyl-4-hexyloxybenzene (**145**, 2.30 g, 0.0114 mol) in anhydrous THF (100 ml) under an atmosphere of dry nitrogen and stirred together for 1 h. Zinc(II) chloride (0.53 g, 3.90 mmol) was dissolved in THF (100 ml) and added to the mixture, which was slowly warmed to room temperature. The mixture was stirred for 1 h and tetrakis(triphenylphosphine)palladium(0) (0.07 g, 0.0607 mmol), lithium chloride (0.05 g, 4.76 mmol), and compound **143** (1.00 g, 1.14 mmol) in anhydrous THF (50 ml) were added and the mixture was heated under reflux for 16 h. The mixture was cooled to room temperature, the product was extracted into diethyl ether and washed with water (twice), the aqueous components were backwashed with diethyl ether and the combined organic components were dried (MgSO₄) and the solvent removed *in vacuo*. The crude product was purified by column chromatography (silica gel, hexane with increasing volume fractions of DCM, and alumina, hexane with increasing volume fractions of DCM), recrystallised from ethanol / toluene (10:1) and dried (P₂O₅) to yield a yellow solid.

Yield: 0.66 g (62 %), ¹H NMR (CDCl₃) δ: 0.90-0.96 (18H, m), 1.31-1.51 (24H, m), 1.56 (10H, quint), 1.66 (2H, quint), 1.80 (2H, quint), 1.90-2.02 (10H, quint), 3.99 (2H, t),

4.24 (8H, 4×t), 4.29 (2H, t), 6.98 (2H, d), 7.55 (2H, d), 7.78 (1H, s), 7.81 (2H, s), 7.87 (1H, s), 7.90 (1H, s), 8.55 (1H, s), ¹³C NMR (CDCl₃) δ: 14.05, 14.07, 22.60, 22.65, 22.68, 25.71, 25.83, 25.89, 29.19, 29.35, 29.41, 29.43, 31.58, 31.67, 31.68, 31.71, 68.06, 68.08, 69.12, 69.23, 69.48, 69.89, 69.86, 93.78, 104.68, 106.35, 106.86, 107.39, 112.89, 114.51, 122.78, 122.94, 122.95, 123.45, 128.01, 130.00, 133.02, 133.08, 146.78, 148.79, 148.84, 149.40, 159.18, MS *m/z*: 929 (M⁺+1), elemental analysis for C₆₂H₈₈O₆ requires 80.13 % C, 9.54 % H; found 80.12 % C, 9.62 % H, purity (HPLC): 100 %, transition temperatures (°C): Cr 48.3 Col_h 113.8 I.

2,3,6,7,10-Pentahexyloxy-11-pent-1-ynyltriphenylene (151)

A solution of *n*-butyllithium (1.4 ml, 2.5 M in hexanes, 3.5 mmol) was added dropwise to a stirred, cooled (0 °C) mixture of pent-1-yne (**147**, 1.00 g, 0.0147 mol) in anhydrous THF (100 ml) under an atmosphere of dry nitrogen and stirred together for 1 h. Zinc(II) chloride (0.53 g, 3.90 mmol) was dissolved in anhydrous THF (100 ml) and added to the mixture, which was slowly warmed to room temperature. The mixture was stirred together for 1 h and tetrakis(triphenylphosphine)palladium(0) (0.07 g, 0.0607 mmol), lithium chloride (0.05 g, 4.76 mmol), and compound **143** (1.00 g, 1.14 mmol) in anhydrous THF (50 ml) were added and the mixture was heated under reflux for 16 h. The mixture was cooled to room temperature, the product was extracted into diethyl ether and washed with water (twice), the aqueous components were backwashed with diethyl ether and the combined organic components were dried (MgSO₄) and the solvent removed *in vacuo*. The crude product was purified by column chromatography (silica gel, hexane with increasing volume fractions of DCM, and alumina, hexane with increasing volume fractions of DCM), recrystallised from ethanol / toluene (10:1) and dried (P₂O₅) to yield a yellow solid.

Yield: 0.28 g (31 %), ¹H NMR (CDCl₃) δ: 0.92-0.96 (15H, m), 1.14 (3H, t), 1.36-1.62 (20H, m), 1.57 (10H, quint), 1.73 (2H, sext), 1.89-1.98 (10H, m), 2.54 (2H, t), 4.23 (10H, 5×t), 7.75 (1H, s), 7.80 (1H, s), 7.81 (1H, s), 7.86 (1H, s), 7.88 (1H, s), 8.46 (1H, s), ¹³C NMR (CDCl₃) δ: 13.65, 14.06, 17.86, 21.89, 22.36, 22.67, 25.84, 25.87, 29.35, 29.37, 29.38, 29.43, 31.70, 31.72, 69.09, 69.28, 69.52, 69.85, 69.88, 94.62, 104.61, 106.42, 107.43, 107.95, 113.27, 122.71, 122.96, 123.02, 123.50, 125.09, 128.19, 129.65, 148.81, 149.37, 149.95, 153.81, 157.69, MS *m/z*: 794 (M⁺), elemental analysis

for C₅₃H₇₈O₅ requires 80.05 % C, 9.89 % H; found 80.13 % C, 9.70 % H, purity (HPLC): 95 %, transition temperatures (°C): Cr 49.2 Col_h 134.1 I.

2,3,6,7,10-Pentahexyloxy-11-hex-1-ynyltriphenylene (152)

The same procedure was carried out as detailed for compound **151** using the following quantities: *n*-butyllithium (1.4 ml, 2.5 M in hexanes, 3.5 mmol), hex-1-yne (compound **148**, 1.00 g, 0.0122 mol), zinc(II) chloride (0.53 g, 3.90 mmol) tetrakis(triphenylphosphine)palladium(0) (0.07 g, 0.0607 mmol), lithium chloride (0.05 g, 4.76 mmol), compound **143** (1.00 g, 1.14 mmol) and THF (250 ml). The crude product was purified by column chromatography (silica gel, hexane with increasing volume fractions of DCM, and alumina, hexane with increasing volume fractions of DCM), recrystallised from ethanol / toluene (10:1) and dried (P₂O₅) to yield a colourless solid.

Yield: 0.09 g (10 %), ¹H NMR (CDCl₃) δ: 0.92-0.96 (15H, m), 0.99 (3H, t), 1.32-1.44 (20H, m), 1.53-1.61 (4H, m), 1.68 (2H, sext), 1.91-1.98 (10H, m), 2.56 (2H, t), 4.23 (10H, 5×t), 7.75 (1H, s), 7.80 (1H, s), 7.81 (1H, s), 7.86 (1H, s), 7.88 (1H, s), 8.46 (1H, s), ¹³C NMR (CDCl₃) δ: 13.72, 14.06, 19.60, 22.08, 22.67, 22.69, 25.84, 25.87, 29.35, 29.37, 29.38, 29.43, 29.71, 30.99, 31.72, 69.09, 69.28, 69.53, 69.85, 69.84, 94.77, 104.61, 106.43, 106.94, 107.42, 107.96, 113.28, 121.82, 122.71, 122.96, 123.02, 123.38, 123.50, 128.18, 129.65, 148.75, 149.37, 149.95, 157.69, MS *m/z*: 809 (M⁺+1), elemental analysis for C₅₄H₈₀O₅ requires 80.15 % C, 9.96 % H; found 80.01 % C, 9.85 % H, purity (HPLC): 100 %, transition temperatures (°C): Cr 51.9 Col_h 134.2 I.

2-Hept-1-ynyl-3,6,7,10,11-pentahexyloxytriphenylene (153)

The same procedure was carried out as detailed for compound **151** using the following quantities: *n*-butyllithium (1.4 ml, 2.5 M in hexanes, 3.5 mmol), hept-1-yne (compound **149**, 1.00 g, 0.0104 mol), zinc(II) chloride (0.53 g, 3.90 mmol) tetrakis(triphenylphosphine)palladium(0) (0.07 g, 0.0607 mmol), lithium chloride (0.05 g, 4.76 mmol), compound **143** (1.00 g, 1.14 mmol) and THF (200 ml). The crude product was purified by column chromatography (silica gel, hexane with increasing volume fractions of DCM, and alumina, hexane with increasing volume fractions of DCM), recrystallised from ethanol / toluene (10:1) and dried (P₂O₅) to yield a colourless solid.

Yield: 0.55 g (59 %), ^1H NMR (CDCl_3) δ : 0.93 (15H, 3xt), 0.95 (3H, t), 1.32-1.46 (20H, m), 1.49-1.65 (14H, m), 1.70 (2H, sext), 1.89-1.99 (10H, m), 2.55 (2H, t), 4.23 (10H, 4xt), 7.75 (1H, s), 7.80 (1H, s), 7.81 (1H, s), 7.86 (1H, s), 7.88 (1H, s), 8.46 (1H, s), ^{13}C NMR (CDCl_3) δ : 14.00, 19.85, 22.28, 22.62, 22.64, 25.81, 28.61, 29.33, 29.40, 31.17, 31.66, 68.97, 69.13, 69.38, 69.73, 69.76, 94.68, 104.48, 106.22, 106.75, 107.27, 107.79, 113.16, 122.61, 122.85, 122.90, 123.39, 124.98, 128.11, 129.53, 148.69, 149.25, 149.83, 157.56, MS m/z : 823 ($\text{M}^+ + 1$), elemental analysis for $\text{C}_{55}\text{H}_{82}\text{O}_5$ requires 80.24 % C, 10.04 % H; found 80.26 % C, 10.17 % H, purity (HPLC): 99 %, transition temperatures ($^\circ\text{C}$): Cr 48.1 Col_h 125.5 I.

2,3,6,7,10-Hexyloxy-11-oct-1-ynyltriphenylene (154)

The same procedure was carried out as detailed for compound **151** using the following quantities: *n*-butyllithium (1.4 ml, 2.5 M in hexanes, 3.5 mmol), oct-1-yne (compound **150**, 1.00 g, 9.09 mmol), zinc(II) chloride (0.53 g, 3.90 mmol) tetrakis(triphenylphosphine)palladium(0) (0.07 g, 0.0607 mmol), lithium chloride (0.05 g, 4.76 mmol), compound **143** (1.00 g, 1.14 mmol) and THF (250 ml). The crude product was purified by column chromatography (silica gel, hexane with increasing volume fractions of DCM, and alumina, hexane with increasing volume fractions of DCM), recrystallised from ethanol / toluene (10:1) and dried (P_2O_5) to yield a colourless solid.

Yield: 0.49 g (51 %), ^1H NMR (CDCl_3) δ : 0.91-0.96 (18H, m), 1.33-1.45 (24H, m), 1.53-1.61 (12H, m), 1.70 (2H, sext), 1.89-1.98 (10H, m), 2.55 (2H, t), 4.23 (10H, 4xt), 7.75 (1H, s), 7.80 (1H, s), 7.81 (1H, s), 7.86 (1H, s), 7.88 (1H, s), ^{13}C NMR (CDCl_3) δ : 14.05, 14.12, 19.92, 22.62, 22.65, 22.68, 25.83, 28.71, 28.90, 29.35, 29.41, 31.48, 31.68, 69.09, 69.22, 69.49, 69.82, 69.86, 94.81, 104.63, 106.34, 106.89, 107.38, 107.90, 113.27, 122.70, 122.93, 122.99, 123.46, 125.06, 128.20, 129.62, 148.78, 149.34, 149.92, 157.63, MS m/z : 837 ($\text{M}^+ + 1$), elemental analysis for $\text{C}_{56}\text{H}_{84}\text{O}_5$ requires 80.33 % C, 10.11 % H; found 80.03 % C, 10.05 % H, purity (HPLC): 94 %, transition temperatures ($^\circ\text{C}$): Cr 39.3 Col_h 108.3 I.

3.4 Discussion of Synthetic Routes and Methodologies

3.4.1 Benzene-based Disc-shaped Systems

Schemes 1 and 2 outline the attempted synthesis of hexa-substituted benzene-based discotic materials. Scheme 1 outlines the attempt to form the hexa-substituted benzene core by sequential removal of the acidic proton in between the halogen units. Scheme 2 details the attempt to form the hexa-substituted benzene core by *O*-alkylation reactions on the three hydroxyl groups of 1,3,5-trihydroxybenzene (**19**), followed by bromination of the remaining 2,4,6- positions. Whilst both Schemes 1 and 2 attempt to generate a 1,3,5-trialkoxy-2,4,6-trihalogenobenzene moiety the synthetic methodologies are significantly different. Scheme 1 was followed initially since the synthetic procedure allows for different alkyl halides to be used in the *O*-alkylation steps, thus symmetrical and unsymmetrical examples of the key material could be generated. The tribromide moiety was used first since bromides offer improved yields over chlorides in coupling reactions,¹⁰⁴ which would follow subsequently. Initial attempts to synthesise a trialkoxytribenzenebenzene moiety (such as compound **15**) failed. This failure to generate compound **15** using the method illustrated in Scheme 1 is perhaps due to the steric hindrance within the system, whereby the acidic proton site of the dialkoxytribromobenzene moiety (**9**) could be sterically hindered by the two alkoxy chains (Figure 3.1). The use of lithiumdiisopropylamide (LDA), which must be used to abstract the acidic proton, is well recognised as a sterically hindered base, hence further disadvantaging the generation of the boronic acid (compound **11**).

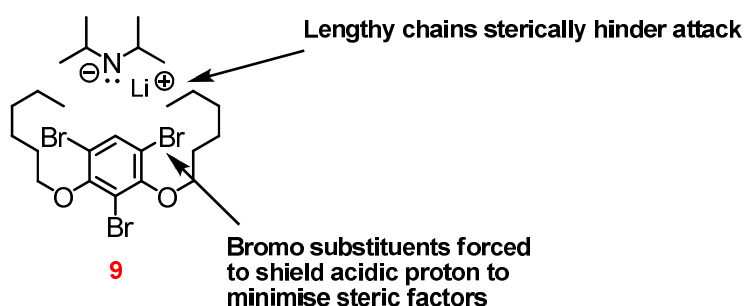


Figure 3.1: Steric hindrance from the alkoxy chains of compound **9, and from LDA**

The abstraction of the first acidic proton is relatively easy, since there are two acidic proton sites and just one alkoxy chain. When abstracting the second acidic proton (as

illustrated in Figure 3.1), however, the bulky LDA has less probability of reacting since there is only one acidic proton with which the LDA can react, plus there is increased steric hindrance from the alkoxy chains which shield the acidic proton, and force the bromo substituents closer together to help alleviate steric factors. Hence, switching from bromo to chloro substituents (Scheme 1) reduces this problem, since a chloro substituent is not only smaller than a bromo substituent, but it is stable to *n*-butyllithium, thus this stronger and less sterically hindered base can be used to abstract the acidic proton. It was found, however, that this route was still challenging since no product was isolated, which is possibly due to the overall reduction in steric factors in the reaction being insufficient. Thus to attempt to generate symmetrical materials an alternative route was employed, utilising the alkylation of 1,3,5-trihydroxybenzene (**19**) and subsequently halogenating the trialkoxy intermediate, as illustrated in Scheme 2. This second method of trying to form the trialkoxy trihalogenated species (**17**) has a number of disadvantages over the method outlined in Scheme 1; firstly the method only allows for the synthesis of symmetrical compounds, and secondly the free hydroxyl groups are all vinylogous to a carbon-carbon double bond of the benzene ring, and unsubstituted in the *ortho* positions of the ring, hence increasing the risk of *C*-alkylation occurring in the Williamson procedure (illustrated in Figure 3.2).

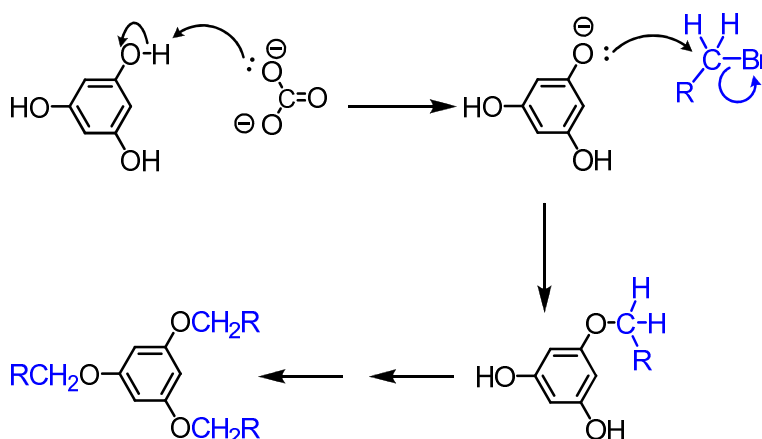


Figure 3.2: Williamson ether synthesis

The major by-products of the synthesis outlined in Scheme 2 were *C*-alkylated products, the formation of which are outlined in Figure 3.3. These products form owing to the keto-enol and conjugate stabilised carbanion intermediates, thus, further reactions from those indicated in Figure 3.3 are possible, since the materials shown also contain

additional conjugated units. These C-alkylated by-products accounted for a significant portion of the crude material when synthesising compound **20**, which caused a low yield (25 %). Further to the low yield of the alkylation step in Scheme 2, the subsequent bromination of compound **20**, to form compound **15**, also had a low yield owing to steric hindrance in the material. The steric hindrance perhaps accounts for the failure of the coupling reaction in the next stage of Scheme 2; however, the successful bromination of compound **20** suggests that it would be possible to perform the coupling reaction even though in this case it was unsuccessful.

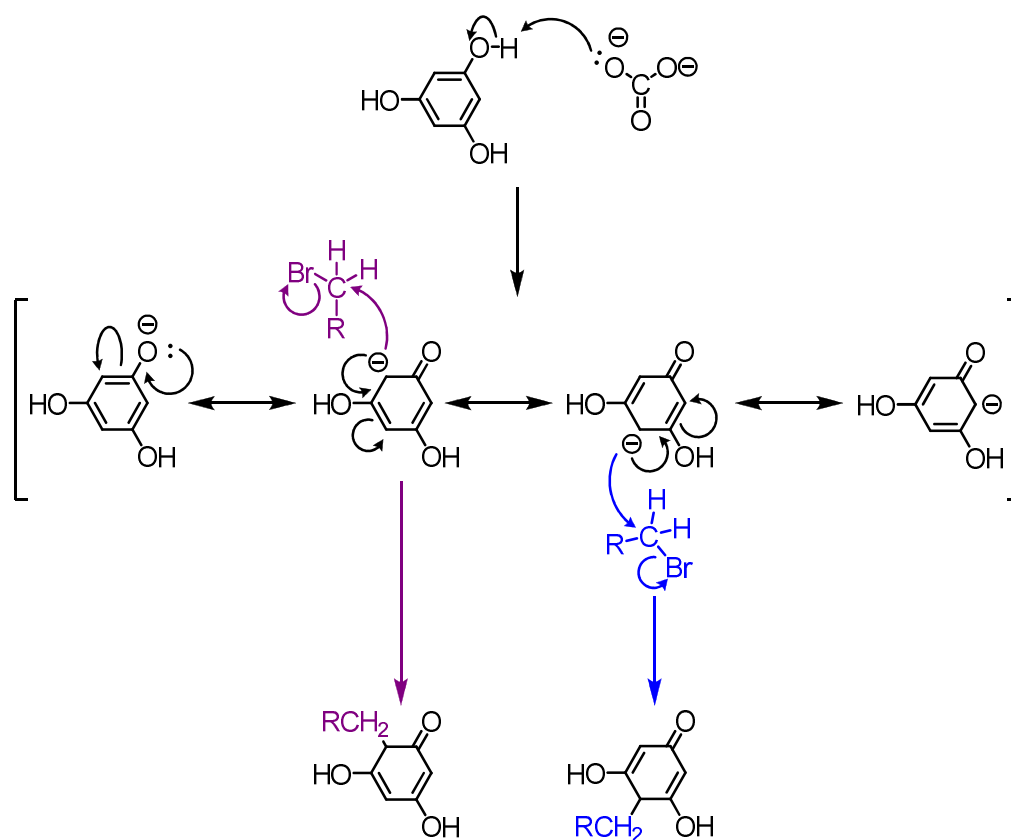


Figure 3.3: C-Alkylation of 1,3,5-trihydroxybenzene

3.4.2 Iodination Reactions to Generate Valuable Intermediates

Halogenation reactions are valuable in organic chemistry, Schemes 1 and 2, for example, include several reactions that utilise halogenated intermediates, so reliable methods of halogenating intermediates are extremely important. Further to the failure of the reaction illustrated in Scheme 2 to perform the coupling reaction and synthesise compound **17**, the coupling reaction may have been aided by the use of an iodinated

intermediate as opposed to a brominated intermediate since it is known that iodides react at a faster rate than bromides in coupling reactions.¹⁰⁴ There are a large variety of methods that could be used to iodinate, for example: iodine and tetrabutylammonium peroxydisulfate¹¹⁹, organolithiums and 2,2,2-trifluoro-1-iodoethane¹²⁰, iodine and nitrogen dioxide¹²¹, NIS¹²², bis(*sym*-collidine)iodine(I) hexafluorophosphate¹²³, iodine monochloride¹²⁴, bis(pyridine)iodonium(I) tetrafluoroborate¹²⁵, NIS and trifluoromethanesulfonic acid¹²⁶, iodine and silver sulfate¹²⁷, iodine with mercury salts¹²⁸, sodium hypochlorite and sodium iodide¹²⁹, *N,N'*-diiodo-*N,N'*-1,2-ethanediybis(*p*-toluenesulfonamide)¹³⁰ and NIS with trifluoroacetic acid¹³¹. NIS with trifluoroacetic acid was the method chosen for 1,2-dialkoxybenzene substrates since it offers excellent selectivity, high yields and is a mild reaction, requiring low temperatures and inexpensive materials. It was noted when utilising Method 1 (see Section 3.3) of the iodination of compound **23** (illustrated in Scheme 3), that the reaction proceeds slowly, and that the diiodinated material, **26**, begins to form before all of the starting material has been converted to the product, **25**. This lack of selectivity is a significant drawback, so Method 2 involved more careful monitoring of the reaction by GC, so that a reaction profile could be built up (see Section 4.1.1).

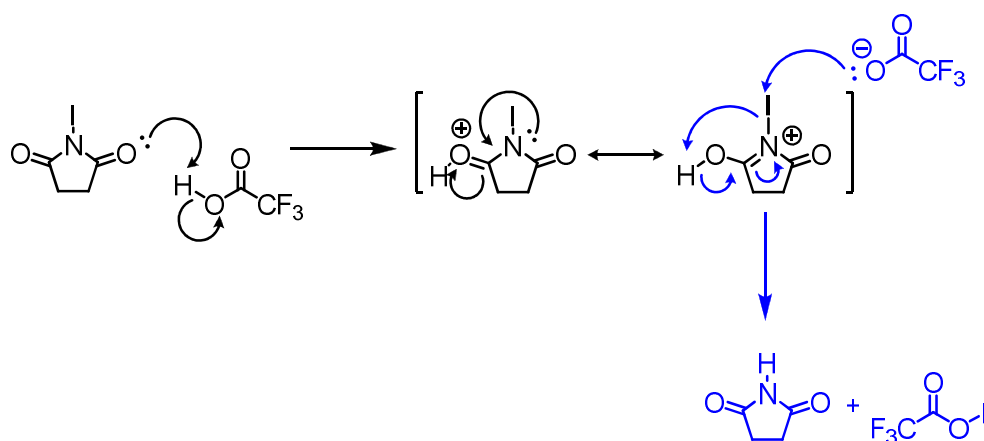


Figure 3.4: Mechanism for the generation of the reactive species for iodination

In an effort to improve the selectivity of the iodination reaction in Method 3, the trifluoroacetic acid catalyst was removed and the mixture heated, which had a detrimental effect upon the reaction (only trace amounts of product generated). This result is not entirely unexpected given the unusual nature of the mechanism of the reaction, whereby the reactive species is not the NIS but rather the more reactive 2,2,2-

trifluoroacetic hypiodous anhydride¹³¹, the formation of which is shown in Figure 3.4, and naturally, is absent when the trifluoroacetic acid is not present.

Method 5 attempts to “purify” a mixture of compounds **25** and **26** (approximately 4:1 mixture) by selectively removing the “second” iodo substituent from compound **26** whilst leaving the “first” iodo substituent in place utilising *n*-butyllithium and quenching the reaction with water (Scheme 3). This method was successful in purifying the material, as GC and NMR indicated a significant reduction in the amount of compound **26** present (only *ca* 2 % remaining) without the regeneration of the starting material, compound **24**. However, whilst this method is useful, since it makes it possible to purify the material, it is somewhat impractical to repeatedly perform the iodination step and then to purify the material by removing the extraneous iodo substituent.

The results of the iodination reactions, especially related to Methods 2 and 4, involving both symmetrical and unsymmetrical dialkoxybenzene moieties are described in greater detail in Section 4.1.1.

3.4.3 Spiral-shaped Systems

Schemes 4-6 illustrate the synthesis of three spiral-shaped molecules (**47**, **52** and **59**). These systems were targeted since their unusual shape could give rise to columnar, banana, nematic or combinations of these mesomorphic behaviours. It was expected that the peripheral “arms” attached to the central disc in these spiral-shaped molecules would have sufficient flexibility to fill space around the central disc, which would promote intermolecular self organisation. The routes illustrated in Schemes 4-6 make extensive use of the Steglich esterification reaction¹³²⁻¹³⁴ since it offers excellent yields and selectivity, but additionally it is a mild reaction in comparison with the more traditional Fischer esterification¹³⁵ which utilises the acid catalysed condensation of an acid and an alcohol (see Section 3.4.8). The mild nature of the Steglich method is important for the esterifications in Schemes 4-6 since the presence of acid, which is used in alternate methods, would cleave the ester groups present in the starting carboxylic acids and phenols. By contrast with the Fischer esterification, the protons liberated in the Steglich esterification procedure are taken in by the DCC to eventually form the DCU by-product as can be seen in Figure 3.5.

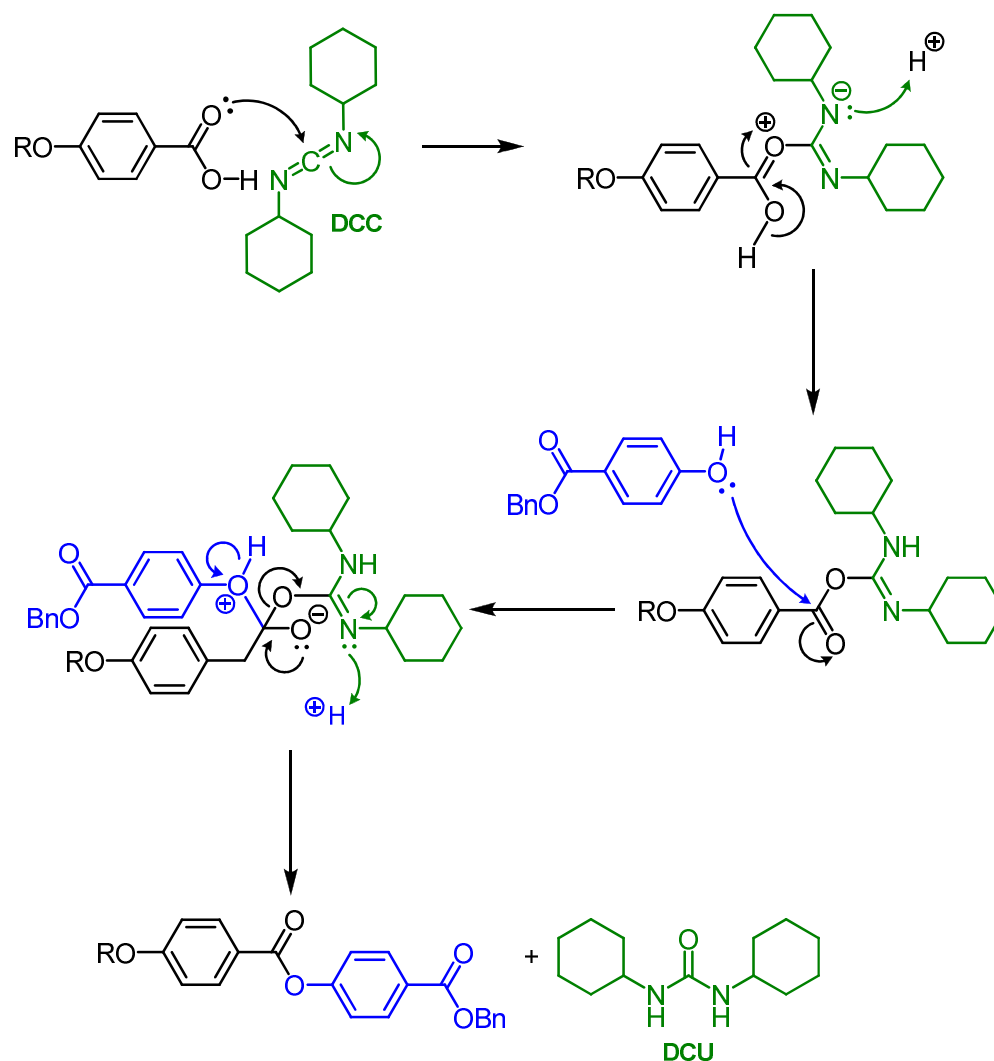


Figure 3.5: Steglich esterification mechanism

The Steglich reaction does not work very efficiently in the presence of just DCC, in practice 3-10 mol % of DMAP is required to achieve high yields, which is attributable to the high efficiency of dialkylaminopyridine catalysts in group transfer reactions, since it is a stronger nucleophile than the corresponding alcohol.^{132-134, 136} Thus, DMAP modifies the final stages of the reaction from the point of the nucleophilic attack of the phenol as is illustrated in Figure 3.6. It is this “DMAP acceleration” coupled with the mild conditions that makes this reaction so valuable to use in these circumstances.

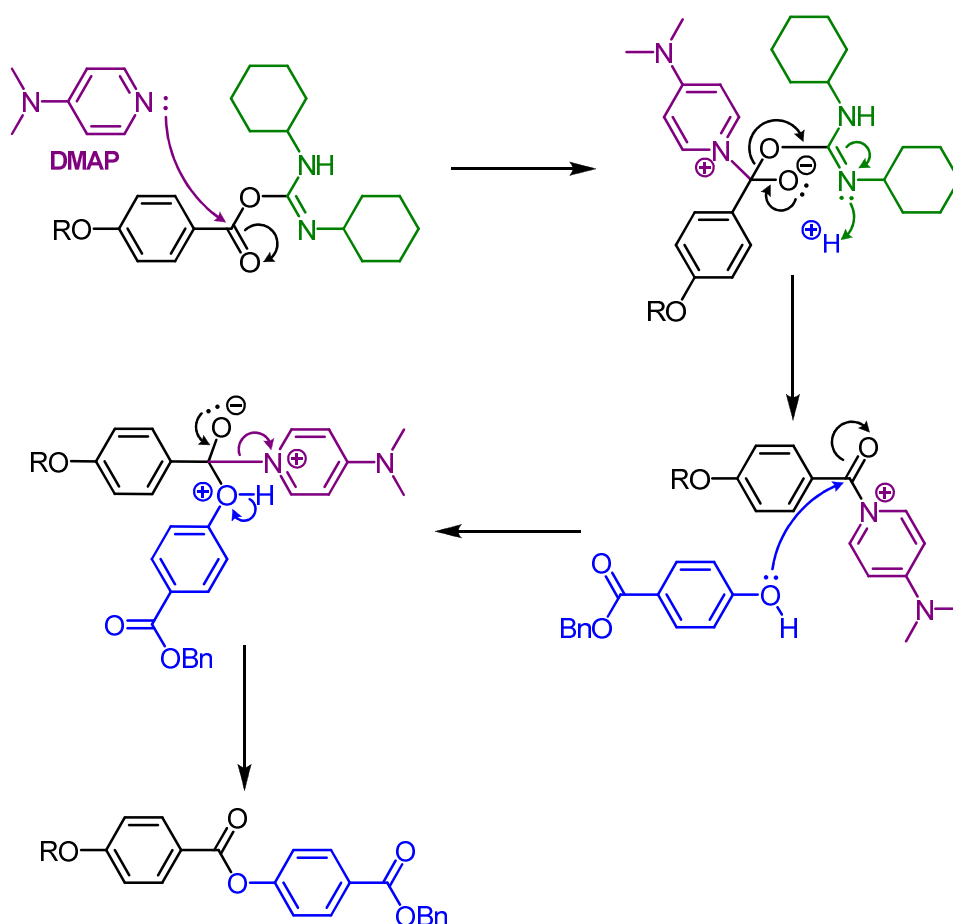


Figure 3.6: DMAP acceleration of Steglich esterification

One of the major difficulties encountered in the cases of the final steps in Schemes 4-6 was in the purification of the materials, there are several reasons for this: firstly as a material increases in size, the polarity increases; secondly trans-esterification can occur leading to impurities with “arms” of the spiral-shaped units being longer or shorter than in the desired product (trans-esterification is discussed in greater detail later). The similar chemical nature of these impurities to the desired product means that column chromatography using silica or alumina provides little scope for purification. Whilst compounds **47** and **52** are relatively pure by HPLC (98 % and 91 % respectively), compound **59** contains 15 % impurities, which is mostly attributable to one substance. Since it was impossible to separate this impurity from the desired product, it was not possible to determine the structure. However, it is likely that the impurity is a trans-esterified product, since it was inseparable by column chromatography and the signals for the protons and carbons by NMR coincided with those of the desired product. Even

by HPLC analysis the two components have virtually the same retention factor, despite using a wide range of eluent combinations.

3.4.4 Synthesis of Alkoxytriphenylenes

Several strategies have been investigated for the synthesis of triphenylene-based liquid crystals (the results of which are discussed in Section 4.1.2), beginning with the etherification of a preformed hexahydroxytriphenylene (Scheme 7). This etherification method is only viable for the synthesis of symmetrical triphenylenes and thus the scope is somewhat limited, however it does provide a benchmark for the comparative study of various oxidative strategies and methods of the synthesis of triphenylene derivatives. In order to facilitate the comparison of these various strategies and methods, a single product, 2,3,6,7,10,11-hexahexyloxytriphenylene (HAT6, **63**), was selected. HAT6 is an ideal choice for this comparison since the material has been fully characterised, and its mesomorphic properties have been well established previously.^{62, 69, 137, 138} Scheme 8 details the oxidative trimerisation strategy for the synthesis of compound **63** using various different Lewis acids. The trimerisation step was performed using a common set of conditions: a consistent time for the trimerisation process, DCM as purchased from suppliers (containing less than 0.05% water), and simple purification techniques (single silica gel column chromatography using 4:1 hexane / DCM, and a single recrystallisation from ethanol). The selected conditions are perhaps not ideal for the oxidative process, which is a variation of the Scholl reaction. For example, although the mechanism of the Scholl reaction is not well understood, it is believed to be a mixture of an electrophilic and a radical process occurring simultaneously^{139, 140} and since water is known to be detrimental to radical processes, the use of non-anhydrous DCM as a solvent is not ideal. Once the “best” and “worst” oxidative trimerisation agents had been determined through the reactions shown in Scheme 8, compound **69** was synthesised using the method that was determined to be “the worst”, *i.e.* the method that gave the lowest yield and lowest purity material, although greater care was taken in the column chromatography purification step. This process was performed in order to prove that it is possible to isolate materials of higher purity (95 %, as opposed to 62 % in the concurrent preparation of compound **63**) with only minor adjustments to the purification procedure, even when “the worst” methods were utilised.

Scheme 9 outlines the synthesis of triphenylenes using the ‘dimerisation’ strategy whereby a tetraalkoxybiphenyl unit (**75**) is oxidatively ‘dimerised’ with a

dialkoxybenzene unit. In order for this oxidative strategy to be compared with the other strategies (shown in Schemes 7, 8 and 10), the same synthetic procedures were used as shown in Scheme 8, with the exception that only one Lewis acid was used in the ‘dimerisation’ process. The Lewis acid that was selected for the ‘dimerisation’ process was vanadium(V) oxytrichloride since it gave the highest yield and greatest purity in the strategy shown in Scheme 8. This ‘dimerisation’ strategy offers significant benefits over the previous two strategies as it easily allows for the generation of unsymmetrical materials which can be further functionalised as required. One issue with creating a symmetrical material *via* this method is that it is impossible to determine if the material produced is formed *via* the ‘dimerisation’ of the biphenyl with the single ring unit, or if the single ring unit is also being trimerised to form the product. To clarify the situation, an unsymmetrical material (**76**) was synthesised by the same ‘dimerisation’ strategy and methodology to determine if any of compound **69** was generated in the reaction, which would have indicated the trimerisation reaction occurring. There was no evidence from either the NMR or the HPLC to suggest that any compound **69** had formed, thus indicating that the ‘dimerisation’ reaction had occurred exclusively. This observation fits with literature data which indicates that the trimerisation product is rarely, if ever, seen due to the reaction kinetics whereby the more favourable reaction, the ‘dimerisation’, occurs almost exclusively at the expense of the less favourable, trimerisation, reaction.¹⁴¹ This exclusivity is most likely due to the four alkoxy chains making the biphenyl unit very electron rich, and thus much more reactive than a dialkoxybenzene unit.

Scheme 10 illustrates the oxidative cyclisation strategy of forming a triphenylene, whereby an *ortho*-terphenyl (such as compounds **79** or **80**) is synthesised through a double Suzuki coupling, which is then cyclised using the same oxidative methods as used in the trimerisation and ‘dimerisation’ strategies examined previously in Schemes 8 and 9. This strategy offers the greatest synthetic flexibility in the synthesis of unsymmetrical triphenylenes since although Scheme 10 shows the involvement of two simultaneous Suzuki couplings, it would be simple to adapt the methodology to involve selective couplings to generate multi-functionalised triphenylenes. Compound **73**, for example, could be iodinated utilising the iodination methods highlighted in Scheme 3 to give 1,2-dihexyloxy-4-bromo-5-iodobenzene, which would undergo selective Suzuki couplings, which has been well-established previously.^{104, 142, 143}

Scheme 11 outlines attempts to generate fluorinated triphenylene species utilising a difluorodialkoxybenzene and performing either the oxidative trimerisation or ‘dimerisation’ procedures as shown in Schemes 8 or 9 respectively. The failure of the trimerisation, to form compound **82**, was not unexpected even though the most successful trimerisation method (utilising vanadium(V) oxytrichloride) was used. It is likely that the steric and polar nature of the fluoro substituents hinder the trimerisation process. However, perhaps the major reason why the trimerisation reaction failed is due to the electron withdrawing nature of the fluorine unit, since the generation of triphenylenes *via* oxidative strategies is best achieved in an electron rich environment (see ‘dimerisation’ process). It was expected that the formation of a 1,4-difluorotriphenylene species, such as compound **83**, would perhaps be successful since the steric and polarity factors are reduced as there are only two fluorines as opposed to six in the previous reaction, and it was also expected that the electron rich nature of the biphenyl unit would help to counter the electron withdrawing effect of the fluoro substituents on compound **81**. Nevertheless no reaction occurred, which shows that the oxidative strategies for the generation of triphenylenes are not very general and success is substituent dependent. However, a monofluorotriphenylene liquid crystal has been synthesised previously through the ‘dimerisation’ strategy⁶⁹, indicating that it may be possible to synthesise other fluorinated triphenylene liquid crystals, albeit with perhaps a lower yield.

Several attempts were made to synthesise hydroxytriphenylenes to allow for the synthesis of a range of more elaborate systems, which could then be compared in terms of their effect upon mesophase stabilities and morphologies with the parent compound HAT6 (**63**), which was selected for comparison for its well-established physical properties.^{62, 69, 137, 138} The first attempts to synthesise such hydroxytriphenylenes involved the attempted synthesis of the benzyl-protected analogue **78** (Schemes 9 and 10). Unfortunately, the attempt to synthesise the desired 2,3-dibenzyloxytriphenylene failed in both cases because the Lewis acid nature of the vanadium(V) oxytrichloride cleaved the labile benzyloxy bond, from this point it is unclear what occurred as the material formed an intractable black mass that could not be characterised. These failed attempts fit with the literature, which indicates that labile groups (*e.g.* isopropoxy groups) are cleaved in the oxidative conditions required for the synthesis of the triphenylene¹⁴⁴, and the results from other research groups that indicate that this process

is somewhat unpredictable¹⁴⁵. Other, more successful, attempts at generating hydroxytriphenylenes are also detailed in Schemes 8 and 9 where the synthesis of compound **70** is outlined. Compound **70** was synthesised firstly from compound **63** using *B*-bromocatechol borane (Scheme 8) and then from compound **77** using diphenylphosphine and *n*-butyllithium (Scheme 9). The use of *B*-bromocatechol borane (Scheme 8) is similar to the use of boron tribromide (Schemes 7 and 9), in that it is rather unselective, and tends to dealkylate any alkoxy chains present.

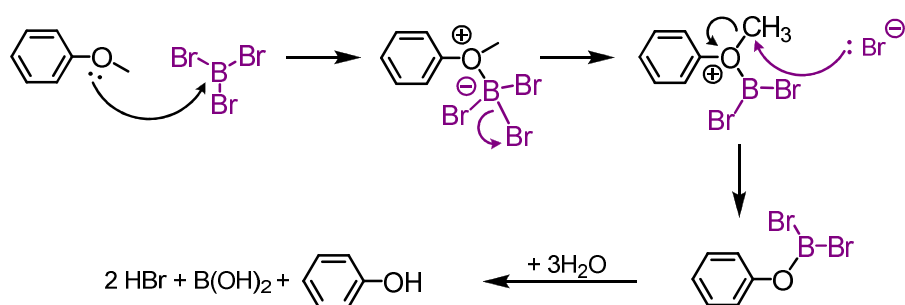


Figure 3.7: Mechanism of boron tribromide dealkylation

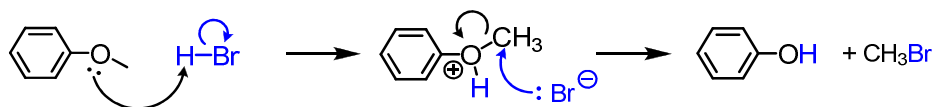


Figure 3.8: Mechanism of HBr dealkylation

As can be seen from Figure 3.7 and Figure 3.8, the dealkylation methods utilising boron tribromide and hydrogen bromide have no selectivity since they react with the oxygen in the ether bond in the initial step. Additionally the small size of the substances in these mechanisms means that steric factors will not aid selectivity, thus the use of large or bulky groups will not aid in the selectivity of the reaction. The only possibility of steric factors aiding selectivity would have been with the boron tribromide mechanism (Figure 3.7), however, since this method generates hydrobromic acid as a by-product when the reaction is quenched with water, it would mean that the mechanism highlighted in Figure 3.8 would also occur, thus eliminating the possibility that it could be used selectively.

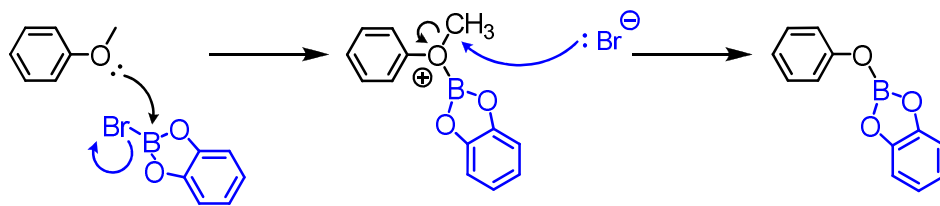


Figure 3.9: Mechanism of *B*-bromocatecholborane dealkylation

As can be seen in Figure 3.9 the mechanism of dealkylation using *B*-bromocatechol borane is very similar to the boron tribromide and hydrobromic acid methods (*cf.* Figure 3.7 and Figure 3.8). Thus, the *B*-bromocatechol borane method of dealkylation suffers from similar selectivity problems as the other methods mentioned previously. In the case of the *B*-bromocatechol borane method of dealkylation, the steric bulk of the bromocatechol borane unit reduces the possibility of dealkylation of large substituents. However, the +I effect of the alkyl chain counters and negates the charge on the oxygen in the intermediate transition state (see Figure 3.9). Hence, the longer the alkyl chain, the greater the stability of the intermediate transition state, and hence, the more likely it is that the reaction will occur. Thus, the selectivity introduced by the steric effect of the *B*-bromocatechol borane unit is offset by the increased stability of the intermediate transition state when large alkyl chains are present.

The lack of selectivity during dealkylation processes presents a particular problem when attempting to dealkylate one or two positions, as was attempted in Scheme 8, as it means that precisely the correct amount of *B*-bromocatechol borane must be used to perform the dealkylation step. Whilst the *B*-bromocatechol borane method does offer the benefit that a symmetrical triphenylene such as compound **63** can be used, which is easy to synthesise in high yield, it means that if any of the *B*-bromocatechol borane has hydrolysed it will not be as effective, and thus the correct amount will not actually be used. This proved a particular problem when attempting to synthesise compound **70** by using the method illustrated in Scheme 8 as approximately 30 % of the starting material, **63**, had remained unreacted. This fact proved extremely detrimental as it made purification on a multi-gram scale difficult as the steric effect of the product (**70**) shielded the free hydroxyl group from interacting with the silica during column chromatography, thus giving both substances **63** and **70** a very similar retention factor, and thus making separation difficult. In order to overcome this problem a different procedure was employed (Scheme 9), where the unsymmetrical compound **77** was

successfully demethylated using diphenylphosphine and *n*-butyllithium. This method, although it requires a more complex procedure to generate the unsymmetrical intermediate triphenylene, proved to be the better method, since the procedure was more selective, higher yielding (76 %), and easier to purify (due to the higher purity of the crude product).

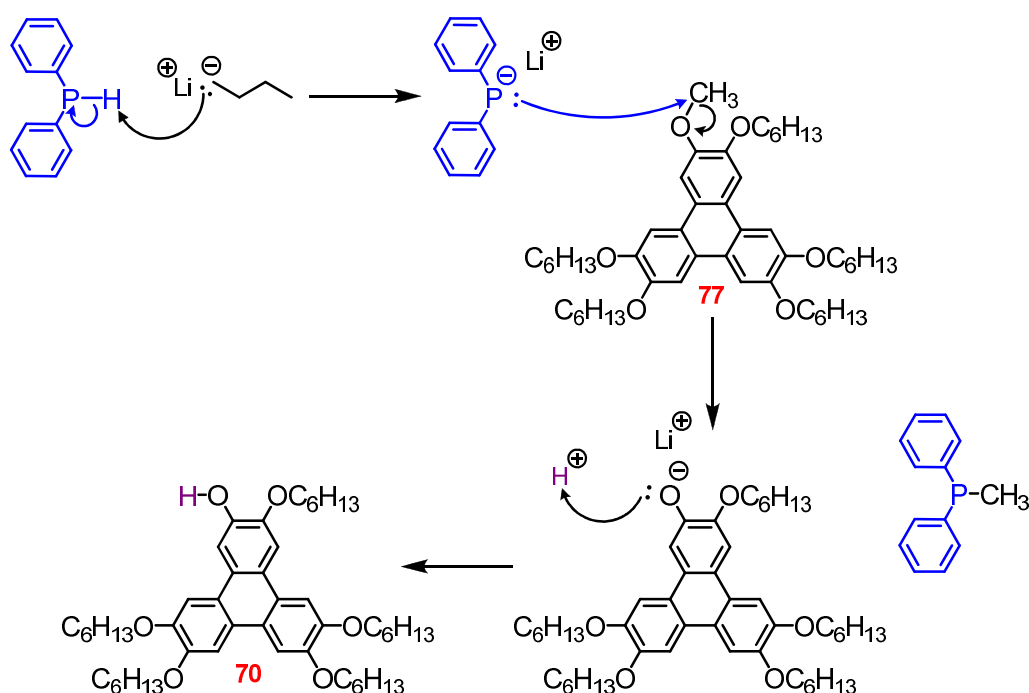


Figure 3.10: Mechanism of demethylation using diphenylphosphine

The reason for the selectivity of the reaction is obvious from the reaction mechanism, as illustrated in Figure 3.10. The steric bulk of the diphenylphosphine unit prevents the anion from reacting with the lengthy alkoxy chains, meaning that the methoxy unit is the only substituent small enough for the reagent to successfully attack. An additional factor that reduces the probability that the phospho-anion will attack the lengthy alkoxy chain is that the inductive effect of the chain will mean that the $-I$ effect of the oxygen will affect the neighbouring carbon to a lesser degree than in the case of the methoxy group, which is in contrast to the boron tribromide, hydrobromic acid and *B*-bromocatechol borane mechanisms (Figure 3.7, Figure 3.8 and Figure 3.9), where the $+I$ effect of the alkyl chain stabilises the charged intermediate species.

3.4.5 Triphenylene-banana Combinations

The successful isolation of the monohydroxytriphenylene species (compound **70**, Scheme 9), facilitated the synthesis of a wide range of more elaborate unsymmetrical triphenylenes. One of the most elaborate systems investigated was the linked triphenylene-banana combinations. These systems build upon the areas of both discotic and bent-core liquid crystals and the spiral-shaped systems investigated earlier. The synthesis of intermediates for the generation of triphenylene-banana combinations illustrated in Schemes 12-14 make extensive use of the Steglich esterification just as the spiral-shaped systems did previously. This method of esterification did, however, lead to trans-esterification (see Figure 3.11 for mechanism) occurring in the synthesis of intermediate compound **87**.

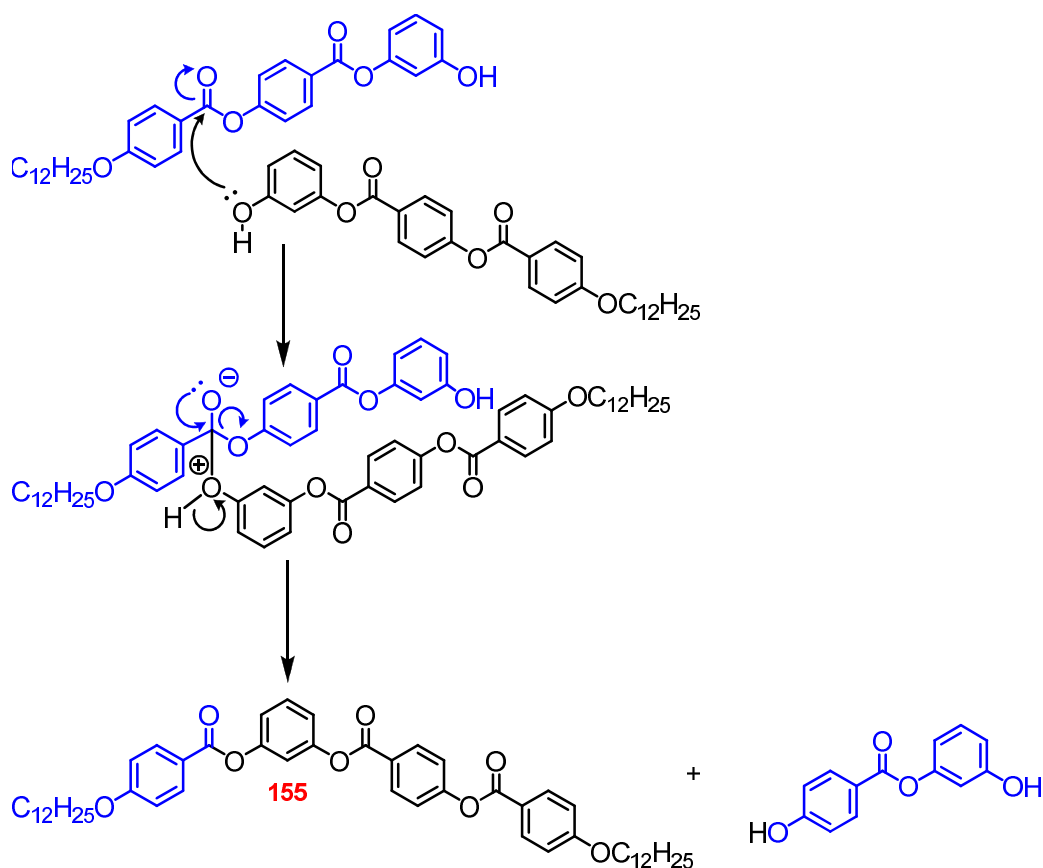


Figure 3.11: Mechanism of trans-esterification

In one attempt to synthesise compound **87** utilising the method outlined previously, 1-(4-dodecyloxyphenylcarbonyloxy)3-(4-(4-dodecyloxyphenylcarbonyloxy)phenylcarbonyloxy)benzene (**155**) was generated in

quantitative yield, which was characterised as follows: ^1H NMR (CDCl_3) δ : 0.88 (6H, t), 1.22-1.38 (32H, m), 1.48 (4H, quint), 1.82 (4H, 2 \times quint), 4.05 (4H, 2 \times t), 6.96 (2H, d), 6.98 (2H, d), 7.15-1.78 (3H, m), 7.37 (2H, d), 7.48 (1H, ddd), 8.13 (2H, d), 8.16 (2H, d), 8.27 (2H, d), ^{13}C NMR (CDCl_3) δ : 14.13, 22.70, 25.98, 29.10, 29.37, 29.56, 29.59, 29.65, 29.66, 68.35, 68.40, 114.35, 114.43, 115.91, 119.03, 122.15, 129.81, 131.86, 132.35, 132.44, 151.36, 163.84, MS m/z : 830 ($\text{M}^+ + \text{Na}$), elemental analysis for $\text{C}_{51}\text{H}_{66}\text{O}_8$ requires 75.90 % C, 8.24 % H; found 75.65 % C, 8.49 % H, purity (HPLC): 99 %, transition temperatures ($^\circ\text{C}$): Cr 80.0 I, lit. transition temperatures ($^\circ\text{C}$): Cr 80.0 I¹⁴⁶.

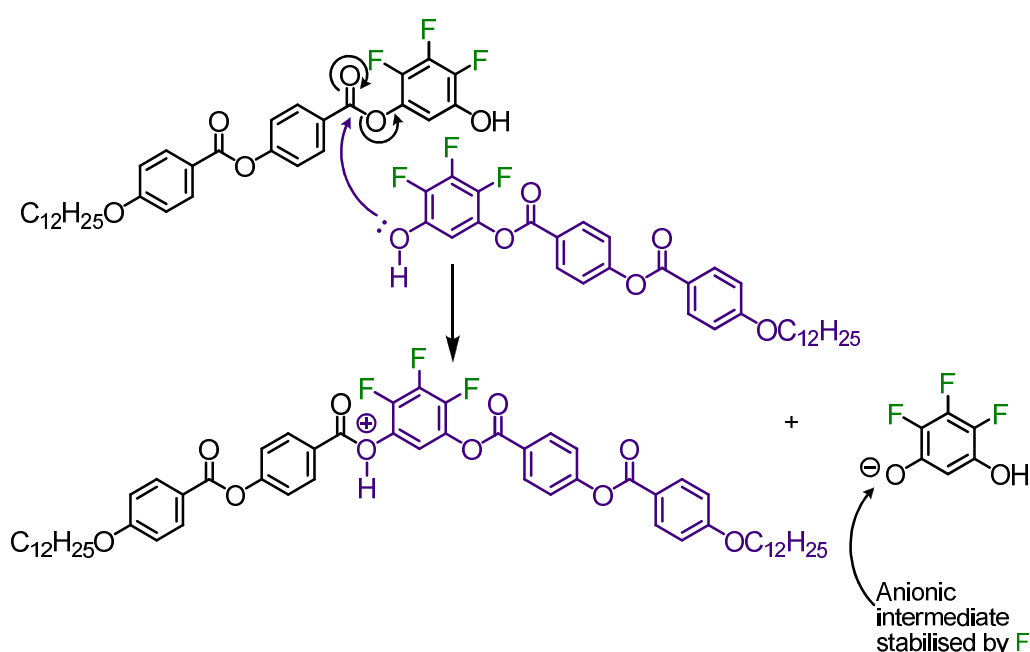


Figure 3.12: Stabilisation of trans-esterification

Whilst this type of side reaction is not rare, it is unexpected that it should proceed with such a high yield, and is inconsistent with other results, which suggest that the process of trans-esterification is more likely to occur when fluoro substituents are present.^{77, 147,}

¹⁴⁸ During the process of trans-esterification the presence of electron withdrawing units, such as fluoro substituents, stabilises intermediate anions (Figure 3.12), thus increasing the probability that the trans-esterification side reaction will occur.¹⁴⁷ Thus, it is somewhat unclear as to why in this case the process of trans-esterification was so selective and proceeded with such a high yield; the most likely explanation is that just as the presence of the fluoro substituents in the compounds shown in Figure 3.12

stabilise the intermediate anion, the ester *para* to the intermediate anion in Figure 3.11 stabilises the corresponding anion, thus facilitating the cleavage of the appropriate bond. Whilst this argument serves to explain the selectivity of the side reaction, it fails to explain the high yield of the side reaction, for which there is no satisfactory explanation. All reactions shown in Schemes 12-14 proceeded without difficulty with the exceptions of the final steps in Schemes 13 and 14 both of which failed to yield the final products. Possibly this failure is attributable to steric factors, since the long flexible spacer unit in compound **91** could cause the reaction site to be obscured by the spacer unit itself, or by the nearby hexyloxy chains of the hexasubstituted triphenylene or by the triphenylene core, thus the mechanistic steps (highlighted in Figure 3.5 and Figure 3.6) would be extremely disadvantaged.

3.4.6 Terminal Acetylenes

Whilst compounds **99** and **100** are commercially available, the synthesis of compounds **101** and **102** (Scheme 15) was essential for the generation of a meaningful series of triphenylene-based liquid crystals. Initial attempts at the synthesis of such materials occurred with materials of shorter chain length, which underwent double coupling and elimination reactions and thus were difficult to isolate. Subsequent attempts to generate materials for the synthesis of triphenylenes with terminal acetylenes (compounds **105** and **106**), were performed utilising longer chains (compounds **97** and **98**) and under several different conditions. Early attempts to synthesise compounds **101** and **102** utilised THF as a solvent; however the reactions failed to yield any product which, it was determined, was due to the polarity of the THF being insufficient. Hence, since DMSO is significantly more polar than THF¹⁴⁹, it is a far better solvent for the acetylation reaction. The use of a solvent with a greater polarity also causes the lithium acetylide bond to dissociate to a greater degree, since the polar solvent can stabilise the lithium ion and acetylide anion, thus enhancing the reactivity of the acetylide anion. The synthesis of compounds **101** and **102** was further complicated by constraints that had to be placed on the work-up procedure used. The removal of the DMSO, lithium bromide and ethylene diamine, was straight forward, requiring simple separation procedures involving large quantities of water, however the organic solvent used in the separation procedure had to be extremely hydrophobic to ensure complete removal of the water soluble matter and the solvent had to have a low boiling point, since compounds **101** and **102** possess low boiling points. The choice of solvent was also influenced by the

next synthetic step, an *O*-alkylation reaction, thus dictating that the solvent did not possess a unit susceptible to the etherification procedure such as a carbon-halogen bond (*e.g.* DCM was not suitable). Thus, pentane was selected as the only solvent that possesses a sufficiently low boiling point that was sufficiently hydrophobic and does not possess any structural features that would be susceptible to an etherification procedure. Despite these possible difficulties in the synthesis, however, high yields (94 % and 90 %, for compounds **101** and **102** respectively) were returned for these materials. Additionally, there was no evidence for the presence of the double-coupled or elimination products. However, not all traces of pentane could successfully be removed from compound **101**, due to the similarity in boiling points of the materials; however only trace amounts of pentane remained at the end of the procedure.

3.4.7 Cyclohexanes

The preparation of several cyclohexane-containing tosylates is outlined in Scheme 16. During the preparation of compounds **111-114** tosyl chloride was used which remained as an impurity in the synthesised materials. This is highly unusual, since the work-up procedure that was used should have removed any traces of the tosyl chloride, and indeed, when the tosylation reaction is performed using chloroform as the solvent instead of DCM, the remaining unreacted tosyl chloride is lost during the work-up procedure. Possibly the greater acidity of the chloroform over the DCM affects the work-up procedure, aiding the removal of the tosyl chloride by aiding the dissociation of the sulfur-chlorine bond. This explanation, however, is somewhat unsatisfactory, since the hydrochloric acid and sodium hydrogen carbonate used during the work-up procedure should be sufficient to facilitate the removal of the tosyl chloride. Further attempts to remove the tosyl chloride by crystallisation procedures and column chromatography failed to yield pure samples of compounds **111-114**, however the tosylates themselves were pure enough to use in the subsequent alkylation reaction. The tosyl chloride which remained in the materials, however, also reacts with the hydroxytriphenylene under the same alkylation conditions.

Figure 3.13 shows how tosyl chloride reacts with compound **70** as a side reaction during the *O*-alkylation process using compounds **111-114** contaminated with tosyl chloride. This side reaction, however, proved to be only a minor component in the reaction mixture, and the material was easily removed by preparatory HPLC to yield the pure hexa-substituted triphenylenes (compounds **115-118**).

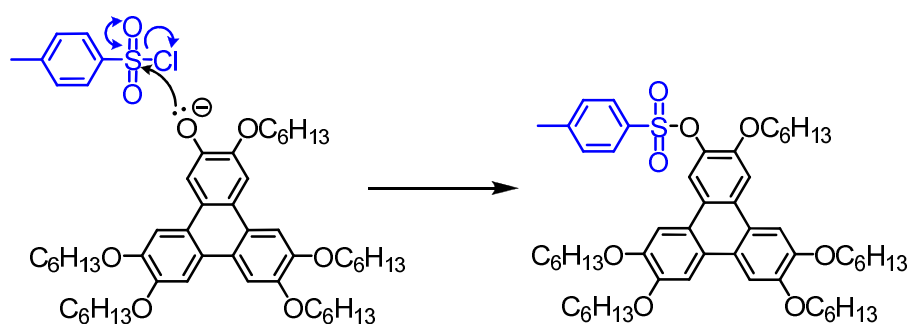


Figure 3.13: Reaction of tosyl chloride under alkylation conditions

3.4.8 Esters and Ethers of Triphenylene

Schemes 17 and 18 detail the synthesis of several unsymmetrical ethers and esters of triphenylene from the hydroxytriphenylene derivative, compound **70**. The synthesis of the unsymmetrical hexaesters of triphenylene was relatively straightforward, just as the synthesis of the symmetrical triphenylene derivatives were in Scheme 7. Whilst the majority of the etherification reactions proceeded in good yield, some procedures were disadvantaged by the presence of electron withdrawing groups within the chain which where required substituents in the final products (*e.g.* oxygen in compounds **132** and **133**, or the fluoro substituents in compound **134**). In such cases potassium iodide was added to the reaction mixture in order to facilitate the Finkelstein reaction *in situ* (Figure 3.14). In the Finkelstein reaction the bromo or chloro substituent is replaced by the more reactive iodo substituent, thus facilitating the etherification reaction, and hence generating a higher yield of the product.¹⁵⁰ In such cases where the etherification procedure was challenging, an alternative solvent to butanone was selected (typically either DMF or DMSO). These alternative solvents were used due to their high boiling points, which allowed higher reaction temperatures to be reached, and also allowing for greater solubilisation of the potassium carbonate, thus facilitating the generation of higher yields of products.

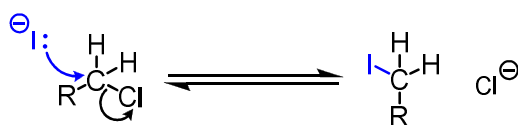


Figure 3.14: Mechanism of the Finkelstein reaction

The synthesis of compound **140** involved a different methodology to the formation of other ester-containing compounds described in this thesis. The synthesis of compound **139**, which is analogous to compounds **41-43** and **49**, could not be prepared by the same methodology, since during initial attempts to generate the material directly *C*-alkylation occurred, just as occurred with compound **20** previously (see Figure 3.3). Thus additional protection and deprotection steps (of the acid group) were added to the synthetic strategy, which allowed for milder alkylation conditions to be used, which reduced the probability of *C*-alkylation occurring. The protection of the acid group was accomplished by utilisation of the Fischer esterification method (Figure 3.15), and the deprotection step utilised was simply the same base-catalysed deprotection step used when synthesising alkoxybenzoic acids **41-43** and **49** previously.

As indicated in Figure 3.15, all of the steps in the Fischer reaction mechanism are reversible, thus the mechanism also indicates how the cleavage of the ester can occur under acidic conditions, since the mechanism is simply reversed. This fact reinforces the need for mild conditions for esterification and etherification reactions in the cases of materials with ether or ester groups already present, such as the spiral-shaped and banana-triphenylene compounds described previously.

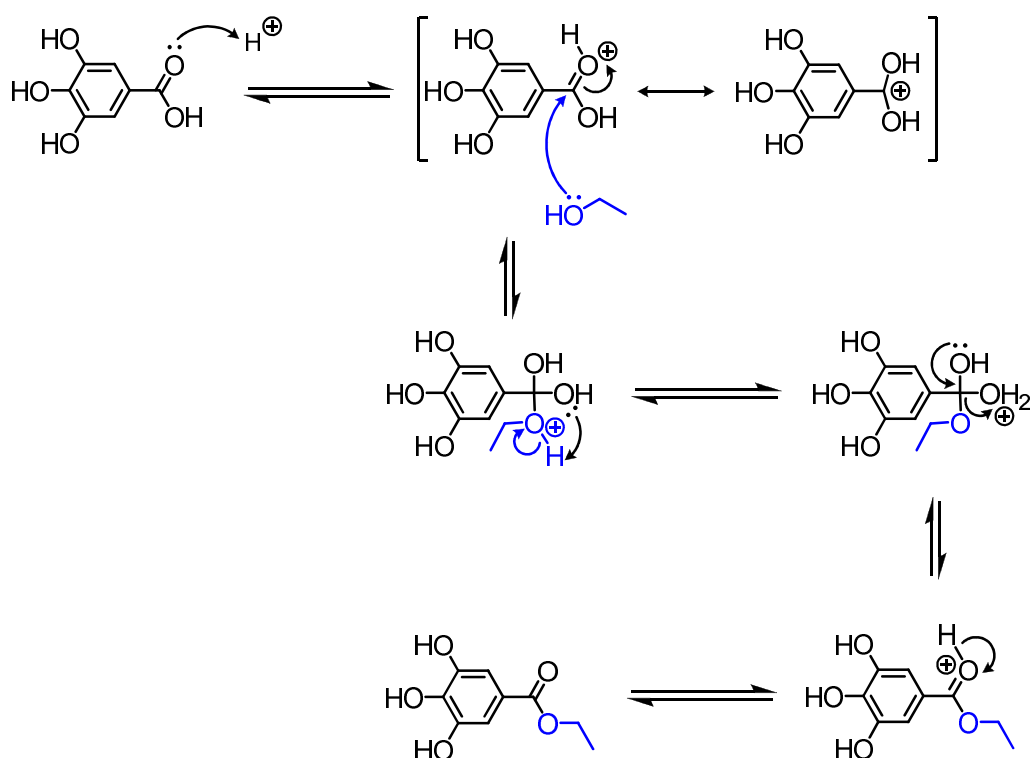


Figure 3.15: Mechanism of the Fischer esterification

3.4.9 Coupling Reactions

Scheme 19 outlines the synthesis of several acetylene-containing and directly linked benzene-containing triphenylene-based materials. Access to these materials was made possible through palladium-catalysed cross-coupling reactions with the triphenylene based triflate, compound **143**. The triflate was utilised in the reactions illustrated in Scheme 19 since it could be synthesised directly from compound **70** (prepared previously) in reasonable yields and high purity (74 % and 90 % respectively) and since in cross-coupling reactions triflate groups react in a similar manner to halides, with a similar reactivity to the corresponding bromo-substituted material. Thus, compound **143** facilitated the subsequent cross-coupling reactions without the need for reductive and halogenation steps which would otherwise have been necessary and could potentially have been problematic.

The synthesis of compound **144** which contains a benzene ring directly linked to the triphenylene core, was achieved *via* a standard Suzuki-type palladium catalysed cross-coupling reaction between the triflate (**143**), and the corresponding boronic acid (**142**).¹⁴² The Suzuki coupling reaction was selected as the ideal reaction to access compound **144**, since the Suzuki reaction is typically high yielding even in sterically hindered conditions, offers little homocoupling, and tolerates a wide range of functional groups all of which were essential for the successful synthesis of compound **144**.¹⁴²

The synthesis of compounds **151-154** and **146**, as illustrated in Scheme 19, makes use of Negishi¹⁵¹ coupling reactions between the triflate (**143**) and the appropriate acetylene-containing compound (compounds **147-150** and **145**).¹⁵¹ Two possibilities exist for the synthesis of compounds **151-154** and **146**, the zinc coupling method that was utilised (Scheme 19) and the Sonogashira¹⁵² coupling reaction, which is similar, but does not utilise the organo-zinc intermediate species¹⁵². One of the drawbacks of the Sonogashira reaction, however, is that purification can sometimes be complex, thus the zinc-coupling method was attempted first, and achieved excellent results (in terms of both yield and purity) when synthesising compound **146** (62 % yield and 100 % purity). Thus, the zinc-coupling method was adhered to for the subsequent reactions (compounds **151-154**) with reasonable success.

4 Results and Discussion

4.1 Investigation of Synthetic Methodologies

4.1.1 Iodination Reactions

The importance of halogenated intermediate compounds has been highlighted previously (Section 3.4.2), thus the halogenation of 1,2-dialkoxybenzene species (*e.g.* compound **23**), important in the systematic synthesis of unsymmetrical hexaalkoxytriphenylenes, was studied in order to generate a mono-iodinated compound (*e.g.* compound **25**) and/or a diiodinated compound (*e.g.* compound **26**). Iodination reactions were selected in preference to bromination or chlorination reactions since iodinations proceed slower than chlorination or bromination reactions, and hence offer the greatest scope for the desired regioselectivity.⁴⁹ In addition to the expected enhanced selectivity of iodination reactions, the enhanced reactivity of the iodo substituent over bromo and chloro alternatives is important as it allows for higher yields and improved methodologies through the possibility of selective reactions (*e.g.* Suzuki coupling reactions) which are invaluable in synthetic chemistry.¹⁰⁴

Initial attempts to generate 1,2-dialkoxy-4-iodobenzene, **25** (Scheme 3), were partially successful using Methods 1 and 2, however the diiodinated material, compound **26**, was also generated in the same processes. These methods for the formation of compound **25** involved the addition of second portions of the iodinating agents NIS and trifluoroacetic acid to aid the completion of the reaction since there had been less than 50 % conversion after 24 hours. Method 1 also involved the heating of the sample at 30 °C after the addition of the second portion of NIS and trifluoroacetic acid, whereas Method 2 did not. This process of adding additional NIS and trifluoroacetic acid, whilst speeding up the reaction, also speeded up the side reaction, thus generating a relatively high proportion of the diiodinated material, **26**. In order to overcome the problem of diiodination, and hence generate compound **25** without the concurrent formation of compound **26**, the reaction was attempted without the presence of the trifluoroacetic acid catalyst, although the reaction was heated in order to compensate for the absence of the catalyst (Method 3). Removal of the trifluoroacetic acid catalyst, however, proved to be too detrimental, and the reaction did not proceed to any significant degree in Method 3. In order to overcome the difficulties encountered with the previous methodologies a fourth method was employed to generate compound **25**, which involved careful control

of the amount of trifluoroacetic acid catalyst used and careful monitoring of the reaction by GC.

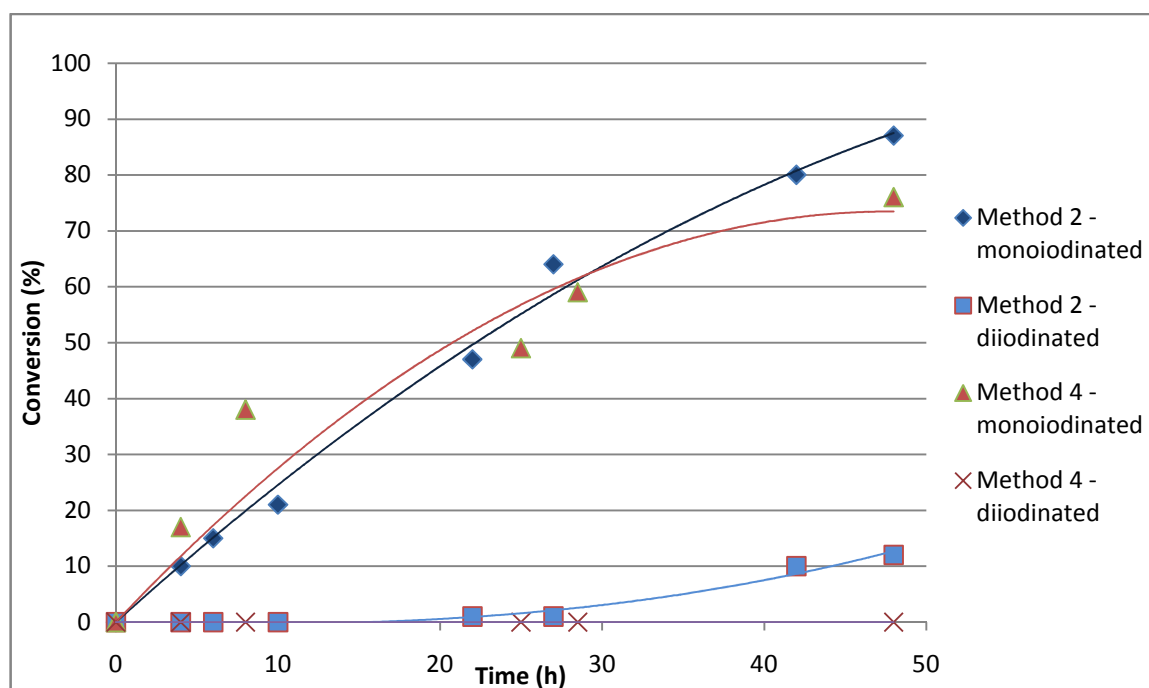
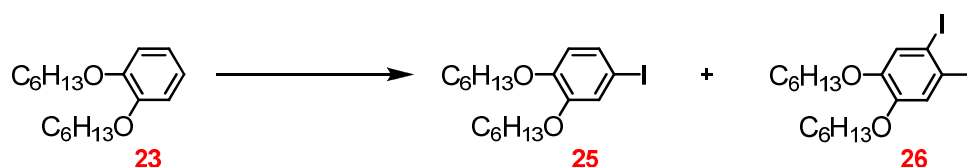


Figure 4.1: Iodination reaction progression for the formation of compounds 25 and 26 through Methods 2 and 4 (Scheme 3)

Method 3 is not included in the comparison of the results shown in Figure 4.1, since the reaction did not proceed to any measurable degree, and Method 1 is omitted from this comparison since the diiodinated material was generated to such a high degree as to make any comparison meaningless. Comparisons of the GC results from Methods 2 and 4, shown in Figure 4.1, indicates that at the end of the 48 h time frame, there are significant differences in the results of the two methods; Method 2, for example, generates more product (25) than Method 4 (87 % for Method 2 versus 76 % for Method 4) and the level of diiodinated by-product (26), which is a significant portion of the material in Method 2 (12 %), is virtually undetectable in Method 4 (< 0.5 %). Thus the best method for the selective control of the iodination of 1,2-dialkoxybenzene species using NIS and trifluoroacetic acid in acetonitrile is by strictly controlling the

level of catalyst to curb the probabilities of diiodination occurring. However, the yield must be sacrificed in order to maintain the selectivity of the reaction.

Whilst the initial attempts to synthesise 1,2-dialkoxy-4-iodobenzene units took place on symmetrical dialkoxy benzene species, it is often desirable to synthesise materials with different alkoxy chains. Thus, the scope for iodination of unsymmetrical materials was investigated. Several different alkoxy chain lengths were employed, and to allow for an easy and direct comparison it was decided that only one of the alkoxy chains should be varied and the other should remain constant. The benzyloxy group was the constant unit, since it was noticed that iodinations involving the dibenzyloxy moiety to give compound **27** occurred more slowly than those involving the corresponding dihexyloxy moiety to give compound **26**. This slower reaction of the benzyloxy moiety is advantageous, as it means that the driving force for the reaction rate will be the different alkoxy chain as opposed to the benzyloxy group, and thus the results could be compared with greater confidence and also further ensuring selectivity of the position of the iodo substituent.

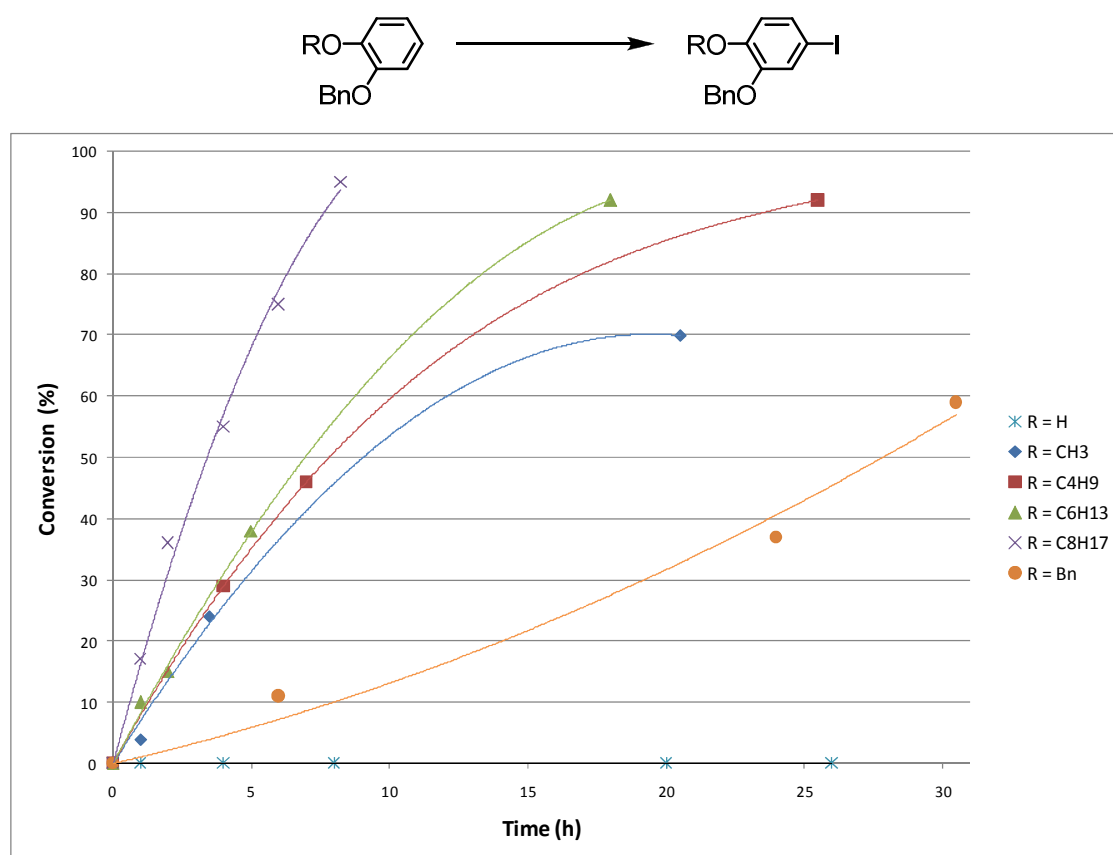


Figure 4.2: The influence of alkoxy chain lengths on conversion to monoiodinated product

Figure 4.2 shows how the speed of the iodination reactions vary with the change in alkoxy chain length and graphically illustrates how the longer the chain length the faster the reaction progresses. This result conforms to earlier assertions that the inductive effect of the alkyl chain influences the rate of reaction, hence longer alkyl chains give a greater +I effect (hence reducing the overall -I effect of the alkoxy group), and hence have a greater +M effect, and thus the reaction progresses faster than that of a shorter alkoxy chain. These results allow for the selective iodination of dialkoxybenzene based systems, as with accurate control of the levels of NIS and trifluoroacetic acid, the reaction that will proceed the fastest is iodination *para* to the longest alkoxy chain, and with careful monitoring and control of the levels of NIS and trifluoroacetic acid, double iodinations and other side reactions can be avoided. These results mean that it is possible to generate functionalised unsymmetrical systems with good selectivity and high yields which can be used to further generate more elaborate systems.

The iodination progression for the dibenzyloxybenzene analogue cannot be directly compared with the other iodination reactions in Figure 4.2, since the aim of that particular reaction was to generate the diiodinated product. Thus, higher levels of NIS and trifluoroacetic acid were present in the reaction, which should have caused the conversion of the starting material to the monoiodinated product to occur significantly faster. As can be observed in Figure 4.2, however, even with the higher levels of the iodinating agents the reaction still proceeded more slowly than the corresponding iodinations of the alkoxy-containing species. Initially it was assumed that due to the slower reaction of the dibenzyloxy moiety to generate a mono or diiodo product, that only one product would be generated in the iodination reactions of the monobenzyloxymonoalkoxybenzene species, as illustrated in Figure 4.2. This assumption appears to be borne out in reality, since there was no evidence of mixed products either from the GC or NMR evidence. Thus, although it is not possible to be certain from this evidence that the iodination has occurred *para* to the alkoxy group as opposed to *para* to the benzyloxy group, it is a reasonable assumption given that the reaction occurs significantly faster when the length of the alkoxy chain increases. The reason why the reaction occurs more slowly when the benzyloxy unit is present as opposed to an alkoxy unit is somewhat unclear, since there is no way for the mesomeric effect of the benzyloxy group to work “backwards”, meaning that the major difference between the two units is that the benzyloxy group lacks the +I effect of the alkyl group.

This effect is somewhat confusing, however, since the inductive effect of the chain would have little effect upon the overall –I effect of the alkoxy group and would only affect the +M effect to a small degree. Nevertheless the lack of mixed products and the faster reaction times of the longer alkoxy chain containing species permits the use of this method for the generation of unsymmetrical systems, and thus this method can be used for the generation of more elaborate systems.

The generation of compound **25**, utilising the most selective methodology (Method 4), generates the iodinated analogue of bromide **73** (Scheme 9). Comparing the lowest yields in the synthetic strategies to generate these materials (76 % to form compound **25**, and 69 % to form compound **72**, from which compound **73** is generated) reveals that the iodination strategy offers higher yielding procedures, to generate a more reactive and more versatile material. The iodination process offers additional benefits in the “clean” nature of the reaction, whereas the generation of compound **73** requires harsh conditions (large quantities of hydrobromic acid, low temperatures *etc.*) to synthesise the required intermediate compound **72**; the formation of compound **25**, however, utilises milder conditions (room temperature, small amounts of acid, minimal work-up procedures *etc.*) in order to generate a more reactive intermediate compound.

4.1.2 Synthesis of Hexaalkoxytriphenylenes

In recent years, several methods have been investigated for the synthesis of triphenylene-based liquid crystals, many of which have involved the use of various oxidising agents, such as chloranil,¹⁵³ or transition metal Lewis acids such as iron(III) chloride,⁶⁸ molybdenum(V) chloride,¹⁵⁴ potassium hexaferrocyanate,¹⁰⁵ or vanadium(V) oxytrichloride¹⁵⁵ to perform a modified version of the Scholl reaction^{139, 140, 156} to oxidatively trimerise, dimerise or cyclise various aryl moieties to form a variety of functionalised triphenylenes.^{68, 105, 139, 153-157} The oxidative methodology for generating triphenylenes using Lewis acids was reinvigorated by the work of Cammidge, Bushby, Boden, Borner and Jesudason who successfully modified the oxidative methodology using iron(III) chloride, and thus established the first viable method for synthesising hexaalkoxytriphenylenes with reasonable yield and purity.^{68, 141, 158} Up until the work of Cammidge *et al.* the only hexasubstituted triphenylene that could be generated in a single step with reasonable yield was 2,3,6,7,10,11-hexamethoxytriphenylene (**61**), which made the study of both symmetrical, and especially unsymmetrical, hexa-substituted triphenylenes significantly more difficult. This pioneering work led to the

work of Watson, Hird, Toyne and Goodby who successfully generated unsymmetrical triphenylenes utilising the ‘dimerisation’ strategy (Strategy 3) using combinations of Suzuki couplings and the above mentioned iron(III) chloride procedure.¹⁵⁹ The oxidative process also led to the work of Borner and Jackson who, at the same time that Watson and co-workers were perfecting the dimerisation strategy, perfected the cyclisation strategy (Strategy 4), utilising multiple Suzuki coupling procedures and the iron(III) chloride oxidative process to generate unsymmetrical triphenylenes.¹⁶⁰ It is these major events that have led to the wide-spread study of hexa-substituted triphenylenes and now various different Lewis acids are used to perform the oxidative step (*e.g.* molybdenum(V) chloride¹⁵⁴ and vanadium(V) oxytrichloride¹⁵⁵). However, all of these methodologies can be traced back to the iron(III) chloride procedure perfected previously.⁶⁸ Whilst there have been several theories and various synthetic methods advanced in this regard, there has been no comparative research of the synthetic methodology, other than the recent generalised review of previously-reported triphenylene syntheses by Pérez and Guitián.¹⁰⁵

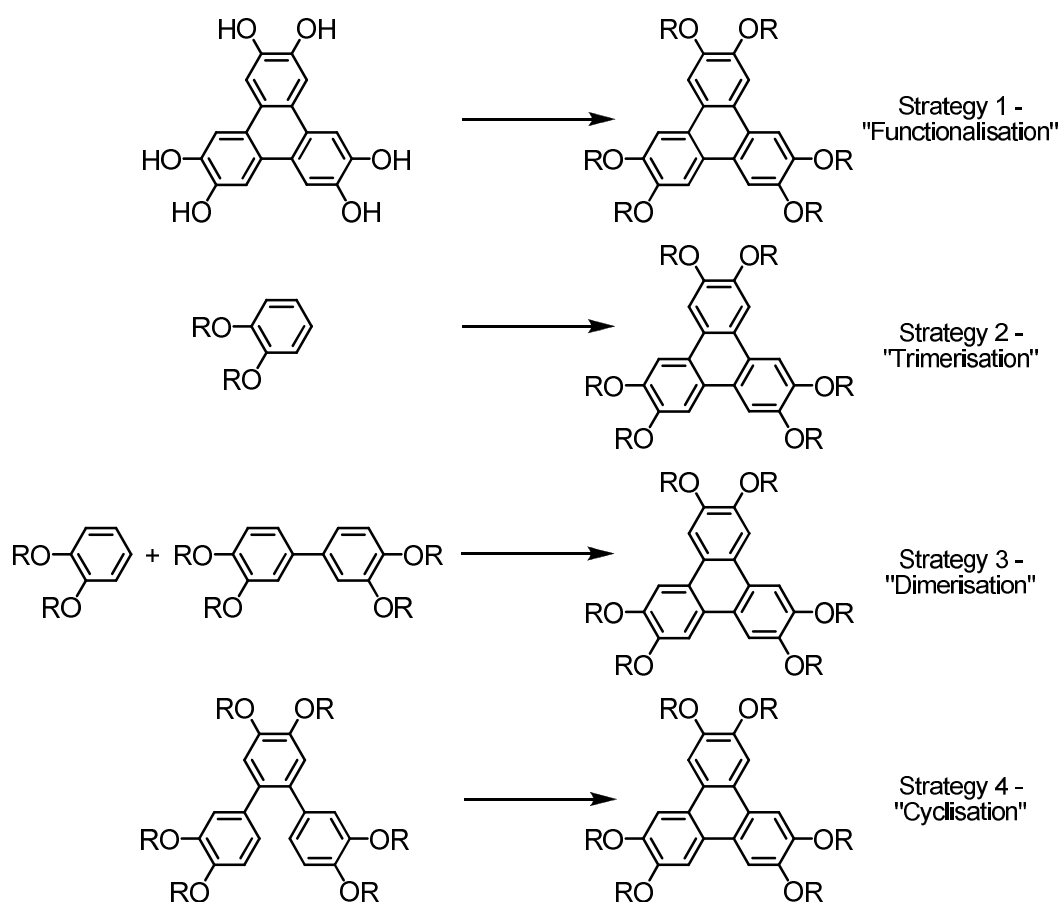


Figure 4.3: Investigated strategies of triphenylene synthesis

This section of research was aimed at evaluating the scope and limitations of four different strategies of synthesising hexa-substituted triphenylene liquid crystals (see Figure 4.3): functionalisation of a pre-formed triphenylene (Strategy 1, Scheme 7), trimerisation of three single ring units (Strategy 2, Scheme 8), ‘dimerisation’ of a single ring unit with a biphenyl unit (Strategy 3, Scheme 9), cyclisation of an *ortho*-terphenyl unit (Strategy 4, Scheme 10). This work also assessed the three most common oxidising agents: iron(III) chloride (Methods A & B), molybdenum(V) chloride (Method C), and vanadium(V) oxytrichloride (Method D) in the trimerisation of single ring units (Scheme 8).

Table 4.1: Yield, purity and transition temperatures of HAT6, 63

Strategy & Method	Lewis Acid	Yield (%)	Purity (% HPLC)	Transition Temperatures (°C)
1	FeCl ₃	46	97	Cr 66.0 Col _h 96.5 I (Cr 68 Col _h 97 I) ¹³⁷
2A	FeCl ₃	37	84	Cr 64.1 Col _h 100.1 I (Cr 67 Col _h 99.5) ⁶⁸ (Cr 70 Col _h 100 I) ⁶²
2B	FeCl ₃	22	75	Cr 66.8 Col _h 95.8 I
2C	MoCl ₅	33	62	Cr 66.0 Col _h 69.6 I
2D	VOCl ₃	62	88	Cr 66.3 Col _h 94.1 I
3	VOCl ₃	49	94	Cr 68.1 Col _h 98.5 I
4	VOCl ₃	42	99	Cr 66.5 Col _h 100.0 I

From the data shown in Table 4.1, the purity and yield of the final product indicates that for the trimerisation step (Strategy 2), vanadium(V) oxytrichloride (2D) gives the best results, and molybdenum(V) chloride (2C) gives the worst results. The vanadium species offers an additional advantage over its competition in its ease of handling; iron(III) chloride, molybdenum(V) chloride and vanadium(V) oxytrichloride are all

moisture sensitive reagents which must be taken into account when handling the materials; molybdenum(V) chloride will react readily in air, as will vanadium(V) oxytrichloride, but iron(III) chloride is significantly more stable. Vanadium(V) oxytrichloride, however, is a liquid and so is more easily handled under anhydrous conditions using standard syringe and needle techniques, thus practical considerations are easily attended to.

The data in Table 4.1 indicates that the worst yield achieved from Methods 2A and 2B comes from Method 2B, which did not include the use of concentrated sulfuric acid during the trimerisation step. This result is consistent with the original literature data which indicates that catalytic amounts of concentrated sulfuric acid enhances the yield of the reaction.⁶⁸ The low yield of Method 2B is somewhat surprising given the results of Method 2A, and the small difference between the two reactions, however this could simply be an anomaly and for the practical purposes of the comparison is irrelevant since it merely serves to reinforce the difference in the yield and purity data between the iron(III) chloride and vanadium(V) oxytrichloride methods.

Comparisons of Strategy 3 with the analogous Strategy 2 are difficult due to the possibility of the trimerisation of the single ring unit occurring along with the ‘dimerisation’ of the single ring and biphenyl units. It is impossible to determine which of the two possible reactions is occurring when the product is a symmetrical unit, thus to determine which reaction is occurring in Strategy 3 an unsymmetrical unit (**76**) was prepared in addition to the symmetrical example (**63**, see Table 4.2).

Table 4.2: Yields, purity and transition temperatures from Strategy 3

Dimerisation of	Product	Yield (%)	Purity (% , HPLC)	Transition Temperatures (°C)
23 + 75	63	49	94	Cr 68.1 Col _h 98.5 I
22 + 75	76	37	90	Cr 63.5 Col _h 92.3 I (Cr 59 Col _h 90 I) ¹¹⁵

Transition temperatures of compound **76** are slightly different from those indicated in the literature (Table 4.2). This discrepancy could be due, in part, to the different methodology used to synthesise the two materials. One of the major differences

between the material prepared in these investigations and the literature material is the Lewis acid used in the oxidative process. In the literature procedure iron(III) chloride was used as the oxidative agent, whereas in this investigation vanadium(V) oxytrichloride was used. It is, however, impossible to be certain as to the cause of this discrepancy in the data, since there could be slight differences in the purity of the materials or in the equipment or methodology used in the determination transition temperatures of the two materials.

A comparison of the data shown in Table 4.2 with that from Table 4.1 indicates that the ‘dimerisation’ strategy (Strategy 3) gives a lower yield than the trimerisation from Strategy 2. It is possible that the drop in efficiency between the two strategies is due to various additional competing reactions. For instance, the trimerisation reaction (as illustrated in Scheme 8) could also occur in Strategy 3 (although this is somewhat unlikely) and the dimerisation of the biphenyl units (**75**) is also possible. The effect on the yield caused by the difference in chain length illustrated in Strategy 3 could also be attributable to these side reactions. In the case of the formation of HAT6 (**63**), trimerisation of compound **23** and dimerisation of compounds **23** and **75**, leads to the same product, whereas in the case of compound **76** the trimerisation of compound **22** would generate HAT4 (**69**) instead of the desired product. This effect, however, is somewhat unlikely, and it is more likely that the yield is somewhat arbitrary in these cases. The purity of the isolated materials from Strategy 3 (Table 4.2), however, is significantly greater than the corresponding results from Strategy 2 (Table 4.1). This result is attributable to the reaction strategy, since in Strategy 3 there are fewer steps to form the product there will therefore be fewer side products in the isolated material. It is interesting to note that in Strategy 3 the trimerisation product is rarely seen due to the reaction kinetics whereby the more favourable reaction, the ‘dimerisation’, occurs almost exclusively at the expense of the less favourable trimerisation reaction,¹⁴¹ most likely due to the four alkoxy chains making the biphenyl unit very electron rich. This effect is extremely useful as it allows great control in the generation of materials, which complements the flexibility that the synthetic strategy offers. In Strategy 2 the use of unsymmetrical 1,2-dialkoxybenzene moieties, or mixtures of different 1,2-dialkoxybenzene moieties, allows for the generation of unsymmetrical triphenylenes, although purification of the resulting mixed products would be difficult. By comparison, Strategy 3 allows greater scope for the generation of unsymmetrical triphenylenes since

selective *O*-alkylations can be employed to generate unsymmetrical biphenyl units and unsymmetrical dialkoxybenzene species, and hence, ultimately generate unsymmetrical triphenylenes, and ensuring easier purification of materials than would be the case in either Strategies 1 or 2.

Strategy 4 (Scheme 10) details the formation of compound **63** by cyclisation of the *ortho*-terphenyl unit (**79**). Strategy 4 has several advantages over previous methods in that formation of symmetrical and unsymmetrical triphenylenes is relatively straight forward given that the framework is in place and the formation of only one bond is required. Whilst in Scheme 10 the two Suzuki couplings were performed simultaneously, it would be simple to adapt the technique to perform selective couplings to generate multi-functionalised triphenylenes in Strategy 4. The same is true of Strategy 3. Compound **73**, for example, could be iodinated using the method perfected earlier (see Section 4.1.1) to give 1,2-dihexyloxy-4-bromo-5-iodobenzene, which would undergo selective Suzuki couplings, which has been well-established previously.^{104, 142,}

¹⁴³ Utilization of this method offers the best opportunity for synthesis of unsymmetrical triphenylenes since it is easy to have multi-functionalised units prior to the Suzuki couplings and the purification of these materials involves simple column chromatography. The purity of the materials generated from the oxidative cyclisation step in Strategy 4 are unsurprisingly high given the results from Strategies 2 and 3, since there are no competing side reactions that may occur, the other than de-alkylation by the Lewis acid.¹⁴⁴ Strategy 4 offered the greatest material purity with a yield comparable with Strategy 3, the only other viable method for generating unsymmetrical triphenylenes, which indicates that Strategy 4 would offer not only the greatest synthetic flexibility, but offers a significantly more favourable oxidative step than in previous methods, which is always the least-favourable step in triphenylene synthesis.

Table 4.1 shows the general significance of material purity on the melting point and transition temperatures of compound **63**, which was prepared by the various different methods. Compound **63** has been reported previously, and although the literature values of the melting point and clearing temperatures vary, they are very similar, and such differences can be explained by different instrumentation and/or different interpretation of the results. However, melting point and transition temperatures depend crucially on material purity, and unfortunately, purity of samples previously reported was not specified. Strategy 1 generated compound **63** with a purity of 97 %, and although quite

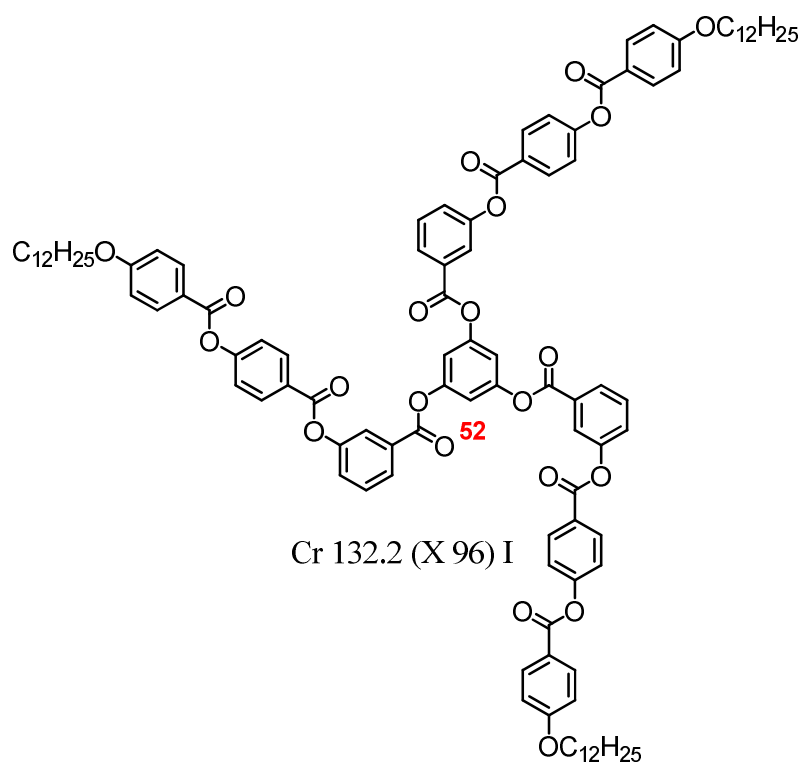
high, a purity of 99 % or better is usually considered essential to provide accurate and meaningful melting point and transition temperature data for comparisons. Nevertheless, the melting point and transition temperatures are very similar to the appropriate literature values, suggesting a similar level of purity. The purity of compound **63** obtained from Method 2A (84 %) is very disappointing, particularly since the synthesis involved in Method 2 is the most simple for symmetrical triphenylenes. However, despite the poor purity, the melting point is only a couple of degrees below that obtained by Strategy 1, and the clearing point is a few degrees higher. Such results suggest that the impurities in this sample of compound **63** could be similar in structure to compound **63**, and hence good promoters of columnar liquid crystal phases. An alternate explanation of these results could be provided by complementary polytopic interactions with other units (*e.g.* dealkylated materials, such as **70**), which have been shown by Bushby *et al.* to enhance columnar phase stabilities^{64, 161} in a similar way to the enhanced melting point that is generated by an equimolar mixture (mp 23.7 °C) of benzene (mp 5.5 °C) and hexafluorobenzene (mp 3.9 °C).¹⁶² However, the metal content of compound **63** prepared by Method 2A is considerably higher than that of Strategy 1, and hence the higher clearing point could be due, in part, to a stabilisation of columnar mesophase structure through coordination of the π -system with the metal ion. It is known that the use of Lewis acids for the synthesis of alkoxy-substituted triphenylenes causes a dealkylation to a slight extent.¹⁴⁴ Any resultant phenolic material should be easily removed by column chromatography, but in these cases just one hydroxyl group between such long alkoxy chains would not be so easily distinguished, and hence purification is not so straightforward. Hence, it is possible that compound **63** obtained from Method 2A is contaminated with dealkylation products such as compound **70**, and the resultant intermolecular hydrogen bonding would be expected to enhance columnar phase stability, thus accounting for the increased clearing point. The worst purity of compound **63** (just 62 %) came from Method 2C, which is the same ‘dimerisation’ strategy as all the Methods 2, but uses molybdenum(V) chloride. Despite the very poor purity from Method 2C, the melting point is identical to that of compound **63** obtained by Method 1, which has a purity of 97 %, and the melting point is 2 °C higher than that obtained by Method 2A with a purity of 84 %. Such a result is difficult to explain given that melting point should always be reduced by the presence of impurities. However, it is possible that this result is simply co-incidental, since there is only one major impurity

in the sample (accounting for 33 % of the impurity), which is likely to be a biphenyl unit (**75**, mp 76.4-78.1 °C, *i.e.* higher than that of the desired product **63**), or a biphenylene moiety. The clearing point, however, is in keeping with the poor level of purity, and is drastically reduced when compared with compound **63** obtained by other methods and literature values. Of the three Lewis acids employed in Strategy 2, vanadium(V) oxytrichloride (Method 2D) provided the highest purity (88 %). Although the melting point obtained from Method 2D is consistent with that obtained from the other methods and the literature values, the clearing point is lower than that obtained from Method 2A, despite the higher purity. It is possible that in this case, the impurities are not the hydroxytriphenylene impurities from Method 2A as discussed above, and hence the clearing point is reduced despite higher purity. This result suggests that vanadium(V) oxytrichloride causes de-alkylation of the resultant triphenylene to a lesser extent than iron(III) chloride. Strategy 3 uses the most efficient Lewis acid (vanadium(V) oxytrichloride) in terms of yield and purity, as determined from Strategy 2, and it would be expected from the style of synthesis that the purity of compound **63** obtained from Strategy 3 would be higher than that from Method 2D, and this is so, with a purity of 94 %. However, the purity is still lower than that obtained from Strategy 1, yet the melting point is 2 °C higher. The clearing point is also 2 °C higher, but still 2 °C lower than that of compound **63** obtained from Method 2A where the purity is much lower, again suggesting, as with Method 2D discussed above, that the impurities do not include any hydroxytriphenylenes. Method 4 employs vanadium(V) oxytrichloride in a strategy that requires the generation of just one carbon-carbon bond, and such simple syntheses would be expected to generate a high purity, and indeed the purity of compound **63** was found to be the highest of all preparations (99 %). However, the melting point is again the usual consistent value of 66 °C and the clearing point is found to be the joint highest at 100 °C. Such results show that this method is clearly the best of those evaluated, and additionally provides much scope for the synthesis of unsymmetrical triphenylenes.

4.2 Mesomorphic Properties of Materials

4.2.1 Spiral-shaped

Three examples of novel molecular architectures (compounds **47**, **52** and **59**) have been investigated in this programme of research which have been designated as ‘spiral-shaped’ architectures. These molecular architectures were investigated since their unusual shape could give rise to columnar, banana, nematic or combinations of these mesomorphic behaviours. It was expected that the peripheral arms attached to the central disc in these spiral-shaped molecules would have sufficient flexibility to fill space around the central disc, which would promote intermolecular self organisation in the form of mesomorphism.



It was initially expected that compound **52** would be the most likely of these spiral-shaped compounds to exhibit such mesomorphism, since it possesses the most flexible molecular architecture (due to the flexible nature of the ester linkages), and it also bends around itself, allowing the greatest potential to fill space around the central disc, and perhaps give rise to interesting mesomorphic properties.

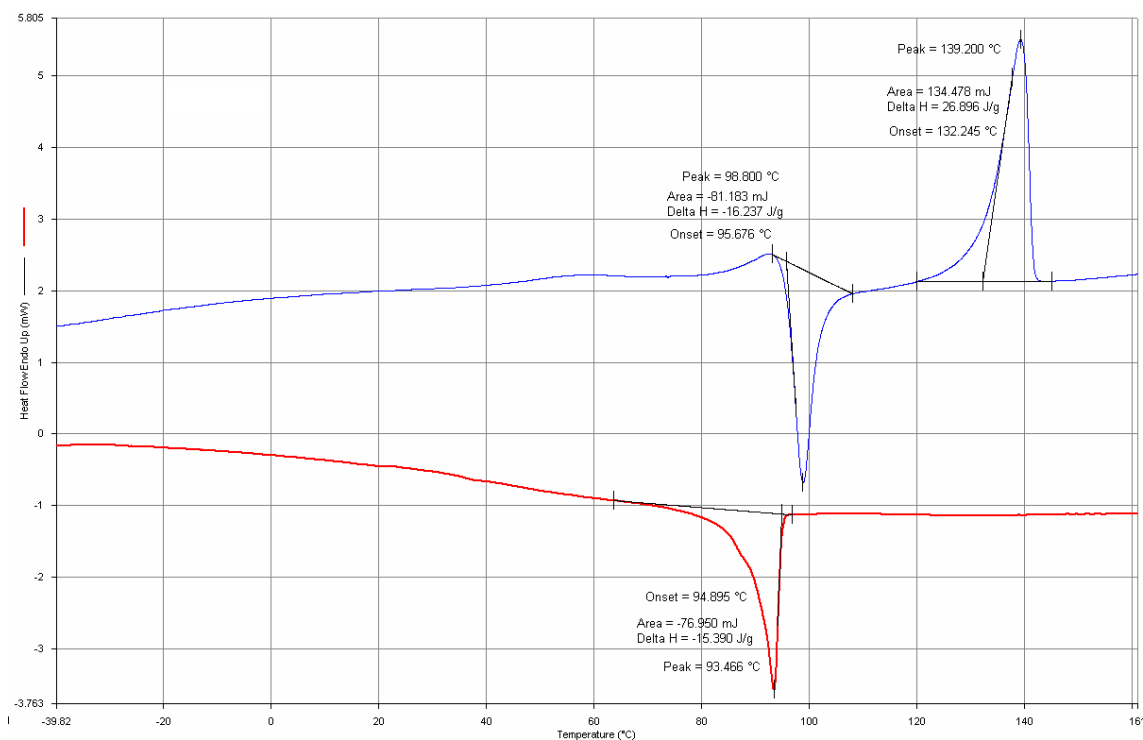
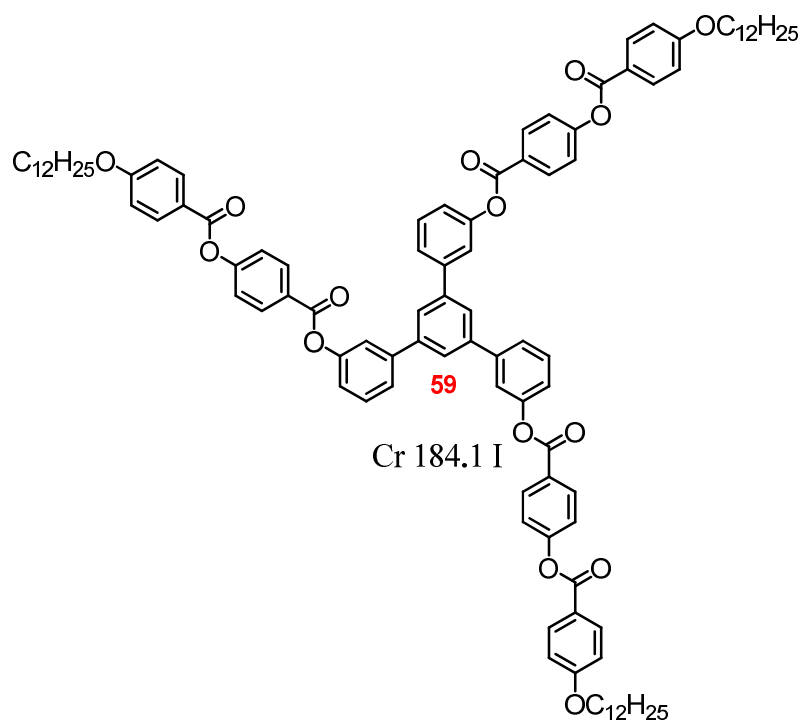


Figure 4.4: DSC thermograph of compound 52

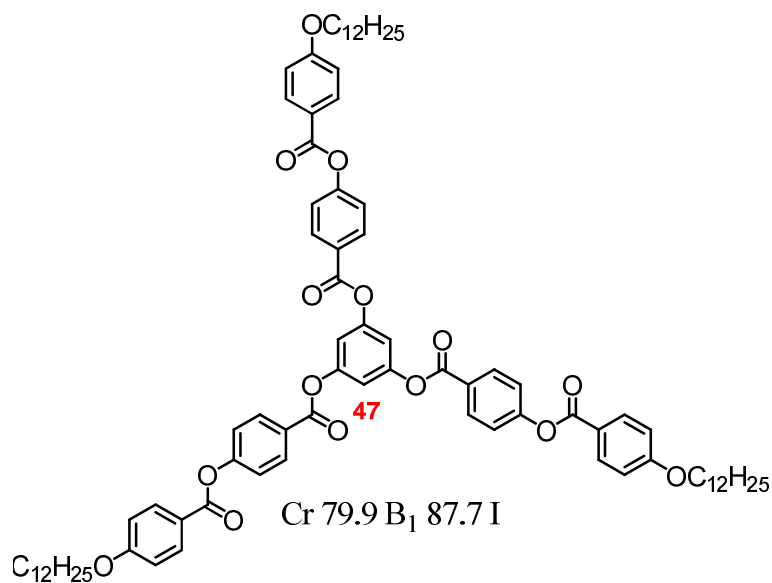
Compound **52** does not, upon first inspection, appear to exhibit mesomorphic behaviour; however, the mesomorphic behaviour of this material is highly unusual. By optical microscopy, an indistinct and reversible monotropic phase transition occurs at 96 °C. This mesomorphic-like behaviour is not easily seen in the DSC thermograph (Figure 4.4) which appears to show the enthalpy of crystallisation (appearing at approximately 94 °C on cooling) as approximately half of the enthalpy of the melt, with the remaining enthalpy change occurring during a “second crystallisation” phase during the next heating cycle of the DSC (Figure 4.4). Given the observations by optical microscopy, the DSC could be indicating that the “first crystallisation” is induced by a monotropic phase transition, which then impedes further crystallisation of the sample until the second heat, whereby the temperature exceeds the energy of the transition, and thus true crystallisation of the sample can occur. This argument further explains the indistinct reversible mesophase observed during microscopy since the gradient of the supercool during microscopy is significantly different than that of the DSC, and thus the superior gradient of the cool during microscopy is sufficient for the transition to be observed. This observation also conforms to previous observations which indicate that disc-shaped systems with highly flexible peripheral units impede crystallisation, which

can often give rise to glassy mesophases, or in this case, a monotropic mesophase that further impedes true crystallisation.^{163, 164}

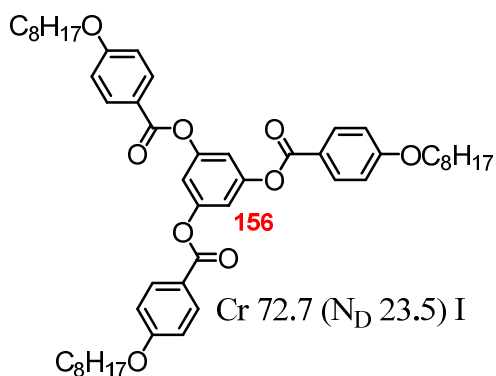


Compound **59** does not exhibit mesomorphic behaviour most likely because of the steric bulk of the closely packed benzene rings directly linked to the central core, which causes interannular twisting at the points of attachment of the benzene rings to the central benzene core. Thus, the non-planar nature of the material at the core makes it unlikely that the material would exhibit columnar mesophase morphology. In addition to this effect, the lack of flexibility at the core attachment reduces the possibility that calamitic or banana mesomorphism would be exhibited.

Compound **47** was created as a “straight-armed” alternative to compound **52**, so that the two materials could be compared for the effect of the bend within the peripheral moiety. The columnar mesophase morphology that was exhibited by compound **47** was perhaps not expected given the large amount of space surrounding the central disc.



Spiral-shaped molecular architectures similar to compound **47** consisting of smaller peripheral arms (such as compound **156**,¹³ Cr 72.7 (N_D 23.5) I) have been previously observed to exhibit the discotic nematic mesophase (monotropically). This monotropic discotic nematic mesophase is exhibited because of the overall compact disc-shaped molecular architecture which cannot generate a columnar mesophase due to the small core area and the large amount of space surrounding the central disc.¹³



The mesophase exhibited by compound **47** was initially difficult to identify by optical microscopy due to the slow nature of the phase transition and texture formation. However, after several attempts at annealing the microscopy sample overnight the mosaic texture of the B₁ phase of compound **47** became readily apparent (Figure 4.5).

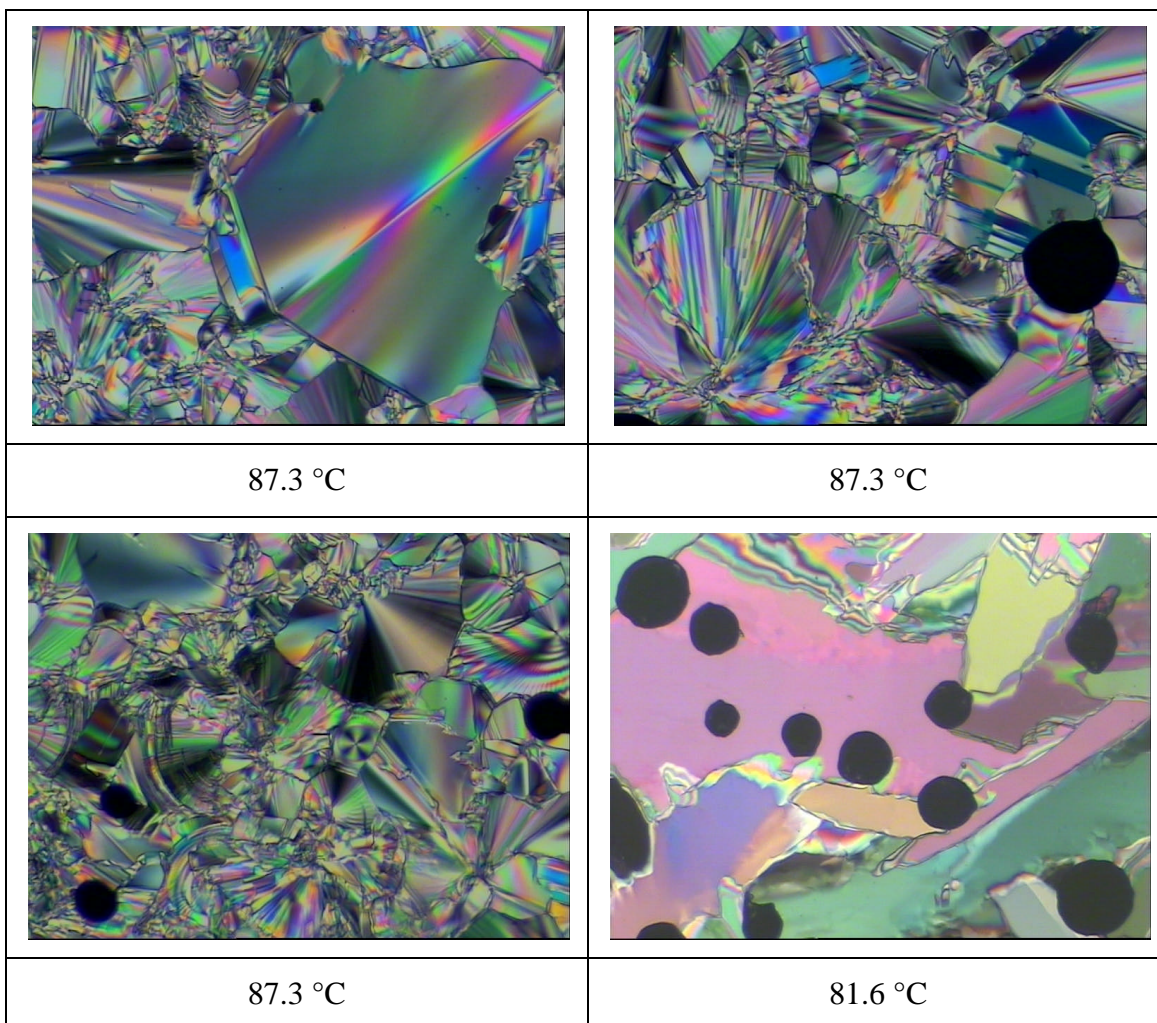


Figure 4.5: Mosaic texture of the B₁ phase of compound 47

The observation of the B₁ phase of compound 47 is interesting; given the large amount of free space around the central disc compound 47 may have not been expected to exhibit a columnar structure just as compound 156 did not. Compound 47, however, is significantly larger than the more compact compound 156 and the reason that the B₁ phase is generated by compound 47 could be due to the large peripheral arms coiling around and filling space around the central disc. A more likely explanation for the formation and stabilisation of the columnar structure of compound 47 is illustrated in Figure 4.6, whereby superimposing one molecule of compound 47 on top of another shows how the material can fill in space around the central disk by overlapping with the layer beneath in such a way that the free space is “filled” by the molecules above and below.

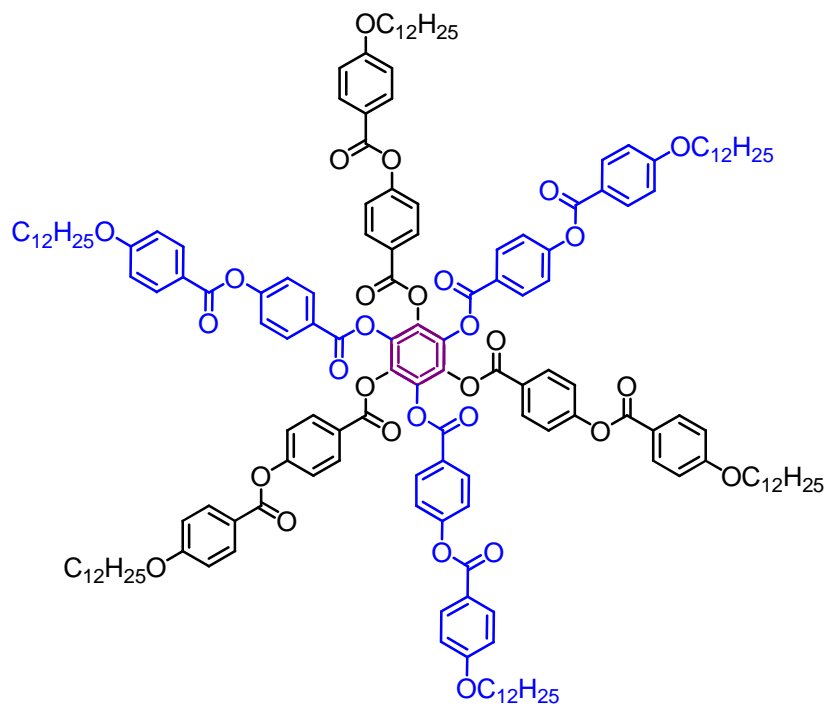


Figure 4.6: Suggested arrangement of molecules in columnar structure of the B₁ phase of compound 47

Figure 4.6 offers additional possible explanations for the generation of a columnar structure, as the ester linkages of compound 47 could also form dipole-dipole interactions between the electron rich oxygen of one arm with the electron deficient carbon of another arm, and when the molecules are arranged in the columnar structure shown in Figure 4.6, it is easy to see how the dipoles in the ester linkages of the “arms” could interact with those on an adjacent molecule.

By applying the same reasoning to compound 52, and superimposing one molecule on top of another as is shown in Figure 4.7, it becomes readily apparent that this structure would not easily give rise to a columnar mesophase in the same manner as described for compound 47. Whilst compound 52 contains a greater number of benzene rings and ester linkages than the comparable compound 47, and thus can fill space around the central disc easier than compound 47. Thus, by logical extension of the argument, compound 52 should possess a more stable columnar mesophase structure than compound 47. However, the increase in flexibility and the presence of the bend increases the steric hindrance within the columnar phase structure. Thus, the “arms” of neighbouring molecules would interact with one another and disrupt molecular packing, which reduces the possibility that a columnar phase structure could form. This

explanation could, however, partially explain how the crystallisation process is impeded during cooling, as the columnar structure could be forming during cooling and the steric hindrance caused by the rotation of the “arms” prevents the columnar structure from properly forming, which in turn, prevents the substance from crystallising properly.

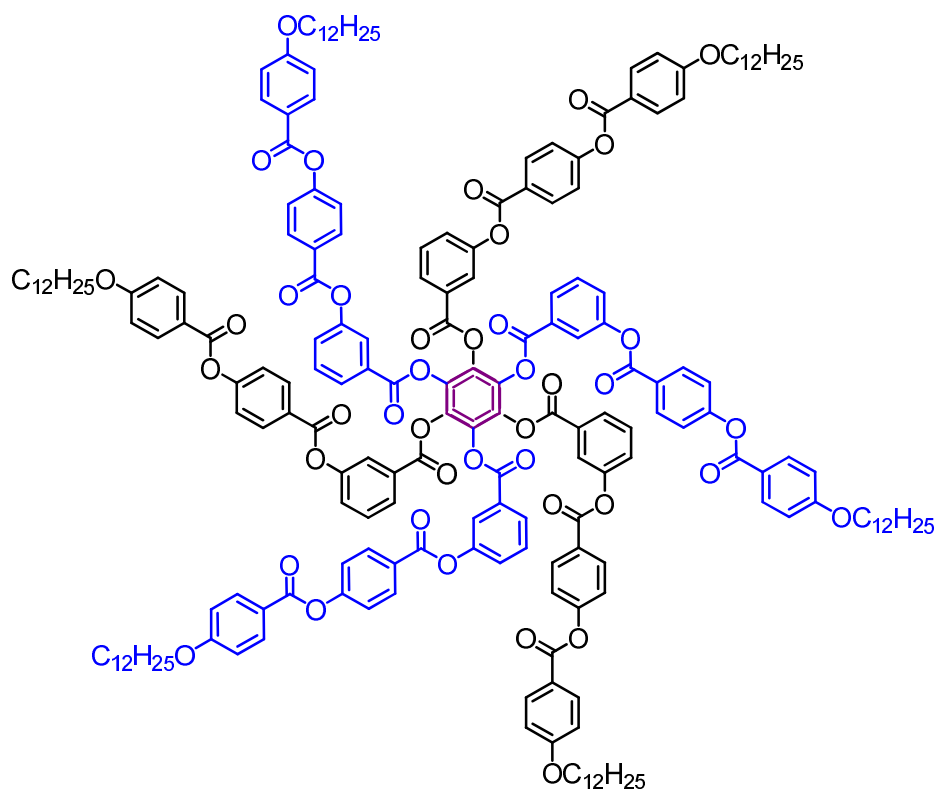


Figure 4.7: Suggested columnar arrangement of compound 52

4.2.2 Triphenylene-based Materials

4.2.2.1 Unbranched Open Alkoxy Chains

Several examples of known triphenylene-based materials were prepared in order for comparisons to be made with novel materials (see later). Table 4.3 shows the known symmetrical triphenylene based liquid crystalline materials: HAT3 (**157**)¹⁶⁵, HAT4 (**69**), HAT5 (**158**)⁶⁰ and HAT6 (**63**); these materials show a trend of decreasing melting and clearing points as the alkoxy chain length increases. This decrease in melting and isotropisation temperatures is due to the introduction of free space into the molecule by the peripheral chains and the decreasing rigidity of the chain as the length increases. Hence, those compounds with very short alkoxy chains (C₂ or below), which are extremely rigid, do not exhibit mesomorphic behaviour since the melting points are so high.¹⁶⁵

Table 4.3: Transition temperatures of symmetrical hexa-n-alkoxytriphenylenes

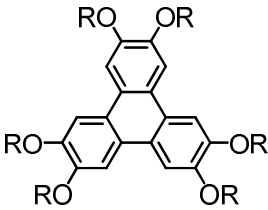
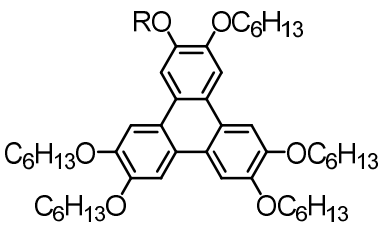
						
Compound	R	Transition Temperatures (°C)				
		Cr		Col _h		I
157 ¹⁶⁵	-C ₃ H ₇	•	100.0	•	174.5	•
69	-C ₄ H ₉	•	87.3	•	137.5	•
158 ⁶⁰	-C ₅ H ₁₁	•	69	•	122	•
63	-C ₆ H ₁₃	•	67.6	•	100.1	•

Table 4.4 shows how the level of symmetry within the molecule is important to melting points and liquid crystal phase stability. Whilst in Table 4.3, the driving force for melting and clearing temperatures was the rigidity of the system, in Table 4.4 the overall rigidity of the molecules is relatively constant, and the minor alterations in the rigidity caused by altering one chain, has little overall effect on the system, which is

mainly driven by symmetry. This effect is evidenced by the generally increasing clearing points (Table 4.4) as the chain length increases from C₂ (**120**) to C₅ (**123**) as the system approaches symmetry which is reached in C₆ (**63**) which gives the highest clearing point. The clearing temperatures then rapidly reduce as the chain length exceeds the optimum six-carbon length (compounds **124-126**), hence distorting the symmetry.

Table 4.4: Transition temperatures of unsymmetrical linear alkoxy chain triphenylenes based on HAT6

						
Compound	R	Transition Temperatures (°C)				
		Cr		Col _h		I
120	-C ₂ H ₅	•	57.3	•	79.1	•
121	-C ₃ H ₇	•	60.6	•	84.8	•
122	-C ₄ H ₉	•	59.7	•	95.1	•
123	-C ₅ H ₁₁	•	57.7	•	94.5	•
63	-C ₆ H ₁₃	•	67.6	•	100.1	•
124	-C ₇ H ₁₅	•	58.0	•	94.7	•
125	-C ₈ H ₁₇	•	52.0	•	86.0	•
126	-C ₁₀ H ₂₁	•	45.4	•	59.0	•

The reason for the destabilisation effect when the molecular shape is distorted from the symmetrical is illustrated in Figure 4.8, which shows the molecular shapes of unsymmetrical triphenylenes **120** and **126** and how the molecular shape is distorted by the short alkoxy chain in compound **120** and the long alkoxy chain in compound **126**. The short alkoxy chain of compound **120**, as is shown in Figure 4.8, essentially creates free space around the central disc, thus disrupting the molecular packing which affects

both the melting and clearing points of the material. The long alkoxy chain of compound **126**, as shown in Figure 4.8, protrudes out of the area of the otherwise symmetrical disc, which disrupts molecular packing, and thus causes depression of melting and clearing temperatures. The destabilising effect of the longer alkoxy chain on melting and clearing temperatures is even greater than that of the shorter alkoxy chains since the longer the alkoxy chain, as is evidenced by compounds **120** and **126**, both of which are separated from the symmetrical unit by 4 carbon units in the unique chain. The reason for the greater disruption by longer alkoxy chains is that the longer the alkoxy chain the greater interdigitation of the chains that occur with other discs, thus the greater the disruption. Thus the effect of the longer alkoxy chains is larger since it affects other molecules in the phase as opposed to the localised effect that is introduced by the reduction in space occupied by the compounds with the shorter alkoxy chains.

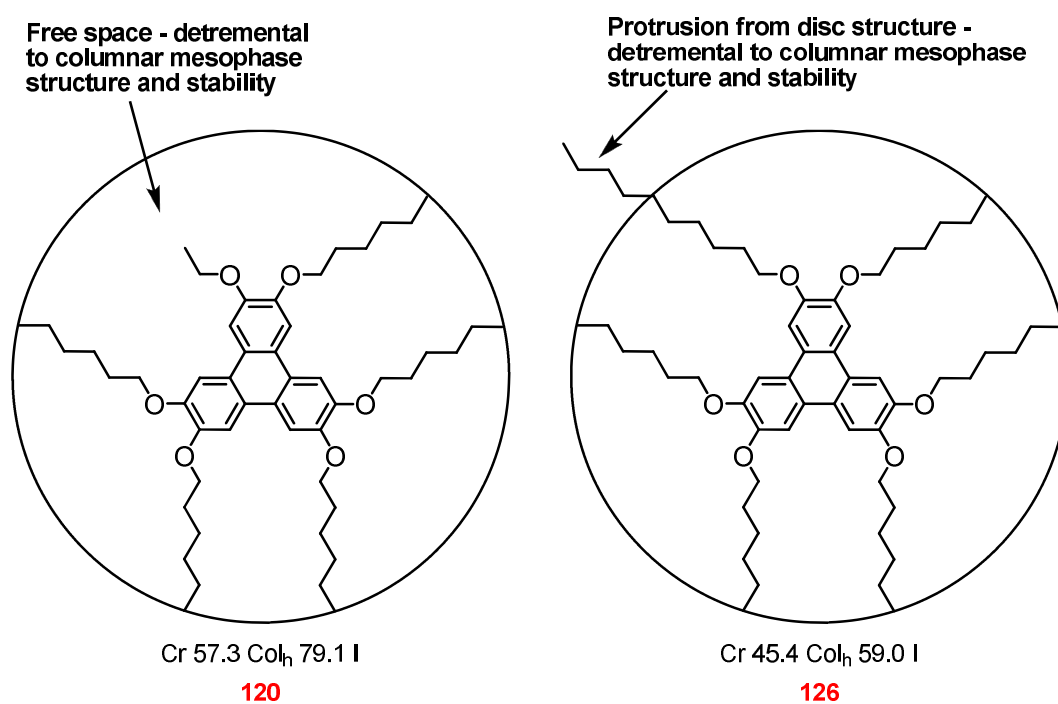
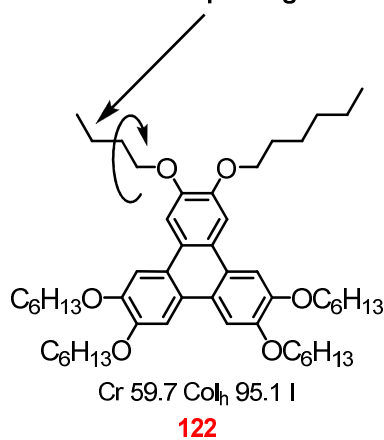


Figure 4.8: Molecular shape of compounds 120 and 126

The major exception to the trend of melting and clearing points increasing up to the values of the symmetrical material as the alkoxy chain length increases, is compound **123**, where the melting and clearing temperatures are slightly lower than that of compound **122**. This reduction in temperatures is caused by a slight odd-even effect of the chain length on the molecular packing.⁶³

Rotation within plane of triphenylene core, hence causes little disruption to inter-molecular columnar packing



Rotation outside of plane of triphenylene core, hence causing disruption to inter-molecular columnar packing

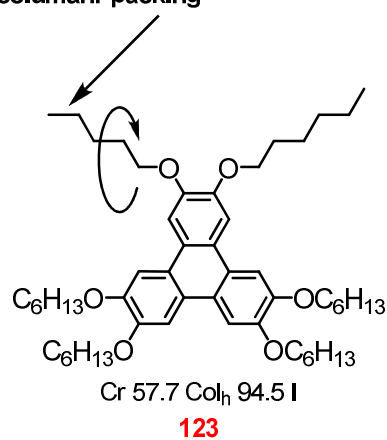


Figure 4.9: Odd-even effect of alkoxy chains

As can be observed in Figure 4.9, the unique alkoxy substituent possesses a different orientation when the carbon chain length is an even number (*e.g.* compound **122**) than when the carbon chain length is an odd number (*e.g.* compound **123**). When the carbon chain length in the unique alkoxy chain is even, the chain is within the plane of the molecule, however when the chain length contains an odd number of carbon units the chain is outside the plane of the molecule (see Figure 4.8). This orientation of the alkoxy chain has an effect upon the cone of rotation of the unit, and thus when the unique unit is within the plane of the molecule the cone of rotation is smaller, and thus causes less disruption to molecular packing than when the carbon chain length is an odd number. Hence, the disruption on molecular packing means that intermolecular forces of attraction will be disrupted to a greater degree when the carbon chain length of the unique chain is odd as opposed to even. This effect is rarely observed in the compounds displayed in Table 4.4, since the odd-even effect plays a minor role in the overall stabilities of these materials since the symmetry of the material (as described earlier) provides the more dominant effect.

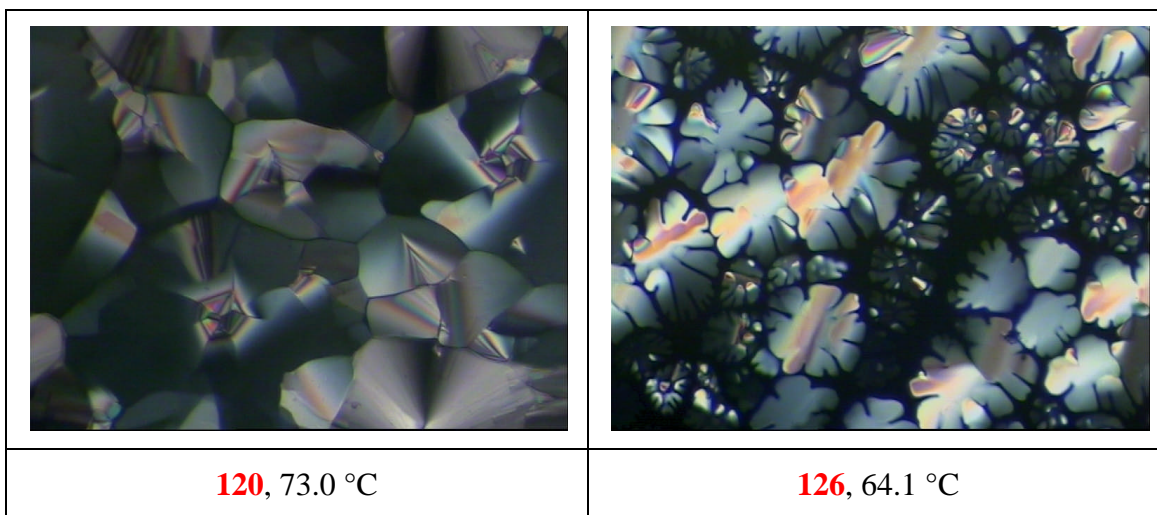


Figure 4.10: Typical POM textures observed for unsymmetrical hexa-n-alkoxytriphenylenes

4.2.3 End-group Modifications of Hexa-substituted Triphenylenes

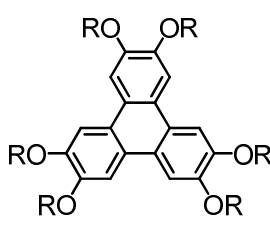
4.2.3.1 Branched Alkoxy Chains

One significant area of structure-property relationships that has been explored in this programme of research is in the comparison of the branched and unbranched nature of the peripheral alkoxy chains in hexaalkoxytriphenylene derivatives. The branching of peripheral chains in discotic liquid crystals has been examined before and has shown promising results; the first room temperature nematic discotic materials, for example, based upon benzene, contained branched peripheral alkyl chains and reported stabilisation of the mesophase.⁷³ Other investigations into the effects of branched chains on coronenes established other beneficial effects of branched peripheral chains, including the enhanced solubility of highly branched materials.^{166, 167} The effects of branched chains on coronenes also reduced the melting and clearing points of the investigated material, which is an effect that is also observed in tricycloquinazoline derivatives and is generally attributed to enhanced or reduced core-core interactions in the respective materials, which can consequently affect charge mobility.¹⁶⁶⁻¹⁷⁰ This reduction in isotropisation temperatures is not entirely consistent with the results from the aforementioned benzene-based systems which exhibited enhanced isotropisation temperatures. Indeed other investigations into benzene, cyclohexane and triphenylene-based materials have shown that the picture is somewhat more complex and it is

possible to widen the mesophase temperature range by appropriate tuning of the branched nature of the peripheral chain.¹⁷¹

As is shown in Table 4.5, compound **64** does not exhibit mesomorphic behaviour, which is unsurprising given the high melting point (132.0 °C) and high re-crystallisation temperature (127.8 °C). The high melting point of compound **64** indicates that the space-filling effect of the branched chain has increased the melting point in comparison to the straight-chain analogue (compound **69**), as predicted. However, given the high melting point and re-crystallisation temperature, it is not possible to determine if there has been an increase in liquid crystal phase stability, but it would seem likely given the unexpected effect upon the clearing points of compounds **65** and **66**. It would perhaps be expected that the transition temperatures would drop significantly, due to the steric effect of the chain, as occurs in calamitic systems, where typically the temperatures can drop by an average value of approximately 30 °C.¹⁰⁴ This significant drop in transition temperatures is not the case in discotic systems however, since the isotropisation temperatures of compounds **65** and **66** remain relatively high compared to the unbranched analogues.

Table 4.5: Transition temperatures of symmetrical triphenylenes with branched peripheral chains

						
Compound	R	Transition Temperatures (°C)				
		Cr		Col _h		I
64	-CH ₂ CH ₂ CH(CH ₃) ₂	•	132.0	-	-	•
65	-CH ₂ CH ₂ CH ₂ CH(CH ₃) ₂	•	91.8	•	122.1	•
66	-CH ₂ CH(CH ₂ CH ₃) ₂	•	29.8	•	120.0	•

Compound **64** can be further compared with HAT4 (**69**, Cr 87.3 Col_h 137.5 I), since the material shares the same carbon chain length, and with HAT5 (**158**, Cr 69 Col_h 122 I),

which possesses the same mass units. The melting point of compound **64**, when compared with that of HAT4 (**69**) and that of HAT5 (**158**), shows that compound **64** has the highest melting point and its melting point is even higher than the clearing point of HAT5 (**158**). This increase in stability shows how the space-filling effect has significantly increased the level of intermolecular attractions.

Moving the branched unit away from the triphenylene core by one CH₂ group, as in compound **65** relative to compound **64**, considerably reduces the melting point, which is not surprising given the additional conformational flexibility of the chain. Hence, the lower melting point permits the observation of the columnar mesophase. In addition to the effect of lowering the melting point, comparisons of the clearing point of compound **65** with the clearing point of HAT6 (**63**) show that the space-filling effect of the branch has drastically enhanced columnar mesophase stability, with an increase in temperature of more than 20 °C, bringing the clearing point back to a similar value as would be exhibited by the straight chain analogue of HAT5 (**158**). This is highly significant since it would be expected that although the chain lengths of the two compounds are the same, the steric effect of the branch would decrease the clearing point of the material which should lead to **65** exhibiting a significantly lower clearing point than HAT5 (**158**). The space filling effect of the branched chain can also be observed in the effect on the melting point of the two compounds, whereby compound **65** has a higher melting point than **158**. It would be expected that due to the steric effect of the branched chain that the melting point of compound **65** should be lower than compound **158**, which is not the case.

Modification of the branched nature of the material, switching from a methyl branch to an ethyl branch, as in compound **66** has drastically reduced the melting point of the material (29.5 °C), yet retains the high clearing point (120.0 °C). Reducing the chain length from compound **65** to that of compound **66** should have increased the melting point and columnar phase stability due to increased rigidity; however the steric effect of the branch has significantly reduced the melting point and has slightly reduced columnar phase stability. Comparing compound **66** with the analogous HAT4 (**69**) and HAT6 (**63**), reveals that the columnar phase stability is reduced compared with HAT4, but enhanced relative to HAT6. The reduction in liquid crystal phase stability (*cf.* **69**) is attributable to the significant steric effect of the branch. The increase in liquid crystal phase stability when compared with compound **63**, is due to a combination of the

increased rigidity offered by shorter chain lengths and the space-filling effect of the branch. The melting point of compound **66** when compared with HAT4 and HAT6, however, reveals that compound **66** has a significantly reduced melting point compared with the analogous compounds **69** (by ~60 °C) and **63** (by ~40 °C) which is due to the significant steric effect of the branch.

The encouraging results obtained from the wholly symmetrical branched-chain hexa-substituted triphenylenes (Table 4.5) prompted the preparation of several unsymmetrical examples of branched alkoxy chain triphenylenes. These compounds were prepared in order to further investigate the relative influences of the steric effect and space filling effect of the branch in the peripheral alkoxy chain, and to allow for the further tuning of the structure-property relationships that have already been highlighted in this section.

Table 4.6: Transition temperatures of unsymmetrical triphenylenes containing a branched peripheral chain

Compound	R	Transition Temperatures (°C)				
		Cr		Col _h		I
127	-CH(CH ₃) ₂	•	54.6	-	-	•
128	-CH ₂ CH(CH ₃) ₂	•	59.4	•	85.4	•
129	-CH ₂ CH ₂ CH(CH ₃) ₂	•	54.5	•	105.0	•
130	-CH ₂ CH ₂ CH ₂ CH(CH ₃) ₂	•	61.5	•	105.3	•
131	-CH ₂ CH(CH ₂ CH ₃) ₂	•	44.4	•	78.1	•

As shown in Table 4.6, compound **127** has a depressed melting point relative to the parent compound (HAT6, **63**). There are two complementary factors for this effect, firstly the molecule has lost C₃ symmetry, which will significantly reduce the level of molecular ordering, and hence reduce the melting point of the material, as was observed previously (Table 4.4) Secondly, the steric effect caused by the introduction to the

molecule of the isopropoxy chain will disrupt molecular packing of the triphenylene cores and thus reduce the melting point. The steric influence of the isopropoxy chain on the packing of the molecules and subsequent reduction in π - π interactions, also accounts for the loss of the liquid crystal phase from compound **127**. It is reasonable, therefore, to assume that by moving the steric bulk away from the triphenylene core, there will be a subsequent reduction of the steric influence on the packing of the molecules, and hence there will be a corresponding increase in both melting point and liquid crystal phase stability. This proves to be the case since in compound **128**, moving the steric bulk away from the triphenylene core by one CH₂ unit increases the melting point of the material, although the melting point is still lower than that of the parent compound **63**. Alleviation of the steric effect on the triphenylene core by moving the steric bulk away from the core allows for closer contact of the core units to one another, which enhances π - π interactions and hence liquid crystalline phase behaviour, which was absent in compound **127**, is seen in compound **128**. Comparing the melting point and clearing point of **128** with those of **121** (Cr 60.6 Col_h 84.8 I), which has the same chain length, and **122** (Cr 59.7 Col_h 98.1 I), which possess the same mass, reveals little difference in melting point. The clearing point of **128**, however, remains similar to the T_{Col-I} value of **121**, despite the increase in mass; this is due to the steric influence of the branched chain.

Further increasing the distance of the branched unit away from the core by an additional CH₂ unit has a significant effect on the transition temperatures of the material. Compound **129** benefits from lower melting points compared with the parent compound (HAT6, **63**), and the analogous compounds **122** and **123**, indicating that the steric effect of the branch is exerting a significant influence on intermolecular forces. By contrast with the effect on the melting point, the clearing point of compound **129** is 5 °C higher than that of the parent compound and 10 °C higher than the analogous straight-chain compounds **122** and **123**. This effect is highly unusual, since the reduction in symmetry and the steric effect of the branch should have significantly reduced columnar liquid crystal phase stability. The increased inter-molecular forces generated by the space-filling effect of the branch in this case are sufficient to overcome these effects, and hence, columnar liquid crystal phase stability is increased. Unlike the decreased melting point observed in **129**, compound **130** possesses a higher melting point than the analogous compound **123**, and a significantly enhanced melting point over **129**. This

unusual reversal of effect on melting point is due to the space-filling effect of the branch and the marginally improved symmetry dominating over the marginally reduced steric effect.

It is perhaps unexpected that the columnar mesophase stabilities of compounds **129** and **130** are virtually identical. The greater steric influence of the branched chain in compound **129** should mean that the $T_{\text{Col-I}}$ value should be significantly lower than for compound **130**. This observation further re-enforces that there are two competing effects of the branch; namely that the steric effects of the branch reduce liquid crystal phase stability, and that the space-filling effects of the branch increases intermolecular attraction, and thus enhances columnar mesophase stability. In the case of compound **129**, the space filling effect of the branch is sufficient to counter the greater steric effect and thus the $T_{\text{Col-I}}$ values of compounds **129** and **130** are almost identical.

Modification of the branched nature of the peripheral chain, switching from a methyl branch to an ethyl branch, as in compound **131**, has had a drastic effect upon the melting and clearing points, just as the symmetrically branched **66** did. Compound **131** has a melting point that is significantly reduced compared with the parent compound (HAT6, **63**) and the straight-chain analogue of **122**. This dramatic reduction in melting point is due to the steric effect of the branch, which also affects the clearing point of the material, which is also reduced relative to compounds **63** and **122**. These observations highlight the “balancing act” between the steric and space-filling effects of the branch as the branched nature changes from compound **130** to compound **131**, the balance of the steric / space-fill moves away from the space-filling effect, and towards the dominance of the steric effect. This overall effect is in contrast to the effect of the branching in compound **66**, where the steric effect enhanced the clearing point relative to HAT6 (**63**), but reduced the clearing point relative to HAT4 (**69**). This observation suggests that the space-filling effect is cumulative, whereby the six branched groups have a larger overall effect on the $T_{\text{Col-I}}$ value than when there is only one branched chain, and the overall effect of the steric factor is less significant.

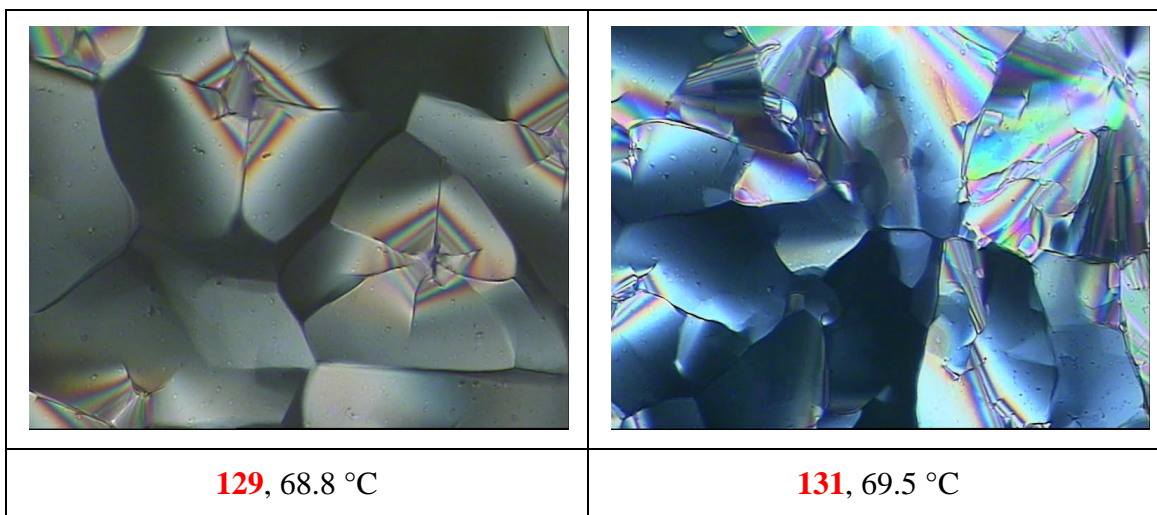


Figure 4.11: Typical POM textures of Col_h mesophase observed for unsymmetrical branched chain triphenylenes

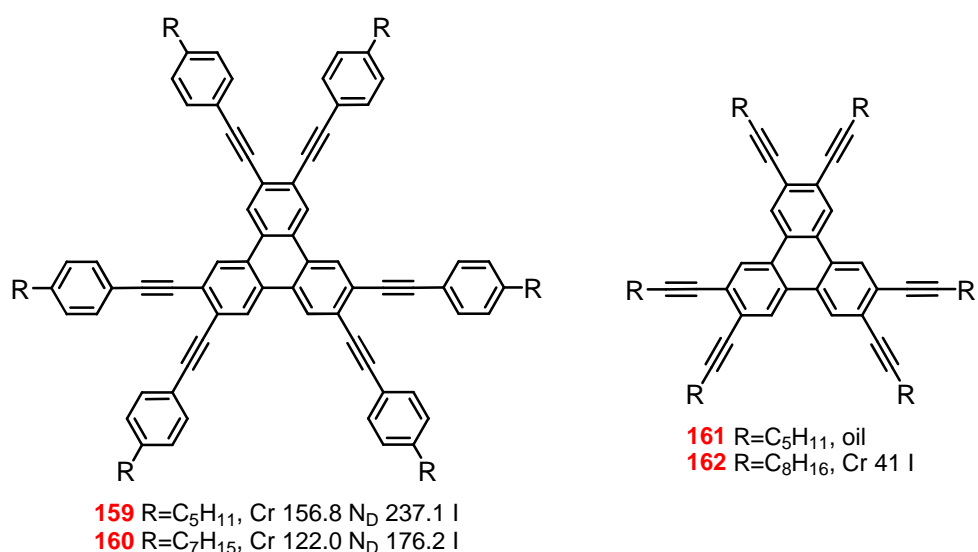
4.2.3.2 Terminal Acetylenes

Triphenylene based materials containing an acetylenic unit are interesting to investigate, since the acetylene unit contains a polarisable unit with considerable electron density. This unique feature of the acetylene bond could exert significant influence on the mesomorphic properties of a triphenylene based structure, since the π -system of the acetylene unit could interact with acetylene-containing chains on other molecules or the triphenylene core of other molecules, enhancing core-core interactions and thus enhancing phase stability. The acetylenic unit, in addition to the significant electronic effects, also exerts a significant steric and space-filling presence, the effect of which upon a columnar mesophase is expected to be highly significant, as has already been discussed with branched alkoxy chains previously (Section 4.2.3.1).

Triphenylene based compounds containing acetylenic units are known to exist, however to date, all such examples of acetylene-containing triphenylenes have had the acetylenic unit close to the triphenylene core, as in compounds **159-162** for example.^{56, 172}

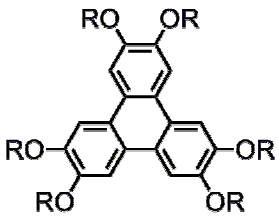
These known acetylene-containing compounds exclusively exhibit the nematic discotic mesophase in structures such as **159** and **160** since the steric influence of the large acetylenic unit and benzene ring prevents columnar packing. The extension of the central disc by the space filling effect of the acetylene and benzene ring units, whilst preventing columnar packing, extend the overall disc shape, thus increasing the area of interaction, and thus such compounds give rise to the discotic nematic phase. Without

the additional benzene rings to extend the core, compounds **161** and **162** lack the enhanced disc size of compounds **159** and **160**, but still possess the steric effect of the six acetylene bonds which prevent columnar packing, and hence no mesomorphism is exhibited. Thus, the inversion of such a structure, positioning the acetylenic unit on the periphery of the molecule may permit the beneficial effects of the acetylenic unit to be exhibited with minimal steric influence from the unit to disrupt the columnar mesomorphism that is often generated by hexaalkoxytriphenylene architectures.



Data shown in Table 4.7 reveals that neither compounds **67** or **68** are mesogenic. However, on rapid cooling compound **67** does exhibit a transient monotropic mesophase (see Figure 4.12). Although the temperature that the transient monotropic phase exhibited by compound **67** could not be recorded, it is possible that crystallisation of the material is promoted by the phase transition, in which case since crystallisation occurs at 113.4 °C, this could indicate the stability of the columnar mesophase. If this explanation is accurate, it explains why compound **68** does not exhibit mesomorphic behaviour, since it also crystallises at approximately 113 °C, and since the reduced rigidity of longer chains is known to reduce clearing temperatures (see Section 4.2.2.1) it is understandable that mesomorphic behaviour is not observed.

Table 4.7: Transition temperatures of symmetrical hexa-substituted triphenylenes with terminal acetylenic peripheral chains

				
Compound	R	Transition Temperatures (°C)		
		Cr		I
67	$-(\text{CH}_2)_3\text{C}\equiv\text{C}-\text{H}$	•	130.2	•
68	$-(\text{CH}_2)_4\text{C}\equiv\text{C}-\text{H}$	•	120.9	•

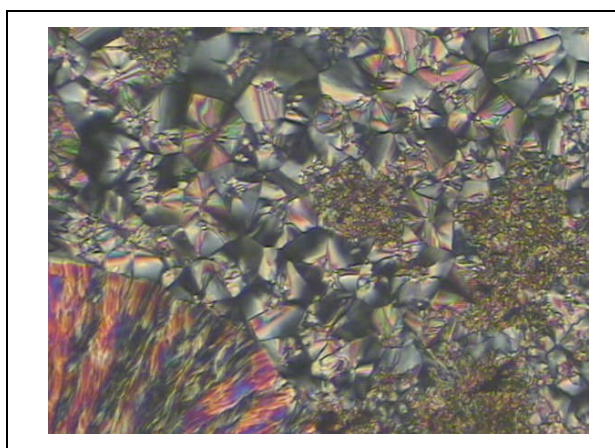


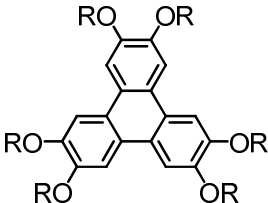
Figure 4.12: Transient monotropic Col_h mesophase exhibited by compound 67

Comparing the melting points of compounds **67** and **68** with their hexaalkoxy counterparts HAT5 (**158**, Cr 69 Col_h 122 I)⁶⁰ and HAT6 (**63**, Cr 67.6 Col_h 100.1 I), reveals that the melting points of **67** and **68** are higher, with a difference of approximately 50-60 °C. This enhanced melting point of the acetylenic-containing species is due to the increased molecular rigidity of compounds **67** and **68**, and space-filling effect caused by the acetylenic unit. Whilst the melting points of compounds **67** and **68** have been enhanced when compared with their hexaalkoxy counterparts, the columnar mesophase stabilities have not been affected in the same manner. This disparity is not unexpected, since melting points and columnar phase stabilities are not affected to the same degree by space filling and steric effects (as noted previously in

Section 4.2.3.1). A typical interdisc distance for hexaalkoxy triphenylene moieties in the columnar phase is approximately 3.6 \AA ⁶³, thus the steric effect of the large cylindrical acetylenic bonds easily disrupts molecular packing and hence columnar phase stability is easily disrupted.

During the preparation of this thesis, work was published by Cammidge, Beddall and Gopee which contained similar symmetrical structures, however instead of terminal alkynes, their work focussed on terminal alkenes.¹⁷³

Table 4.8: Symmetrical triphenylenes with terminal alkenes

						
Compound	R	Transition Temperatures (°C)				
		Cr		Col _h		I
163 ¹⁷³	-(CH ₂) ₃ CH=CH ₂	•	62	•	95	•
164 ¹⁷³	-(CH ₂) ₄ CH=CH ₂	•	64	•	92	•

As can be observed from the data in Table 4.8, compounds **163** and **164**, which are comparable to compounds **67** and **68** from Table 4.7, have depressed melting and clearing temperatures when compared with their symmetrical counterparts HAT5 (**158**, Cr 69 Col_h 122 I)⁶⁰ and HAT6 (**63**, Cr 67.6 Col_h 100.1 I). This depression of melting and clearing temperatures is opposite to the effect of the terminal acetylenes that has been highlighted by work presented in this thesis, whereby the melting points have increased. This difference in the behaviour is interesting, since the terminal units are similar it may have been expected that they would exert a similar influence. However, triphenylene based compounds containing terminal alkenes appear to resist molecular packing, whilst triphenylene based compounds containing terminal alkynes experience enhanced intermolecular attractions due to increased alkoxy chain rigidity, and increased space filling effects, which offsets the steric effect of the acetylenic unit.

In order to better compare the effects of the terminal acetylene group on mesophase morphology and stabilities, the unsymmetrical compounds (**103-106**) were synthesised where five conventional hexyloxy chains are present with only one terminal alkynyloxy chain making up the six peripheral chains. Hence these units could be compared with the entirely symmetrical HAT6 (**63**), and the unsymmetrical units with linear alkoxy chains discussed previously (Table 4.4).

Table 4.9: Transition temperatures of unsymmetrical triphenylenes with terminal acetylene units

Compound	n	Transition Temperatures (°C)				
		Cr		Col _h		I
103	3	•	53.3	•	97.6	•
104	4	•	62.8	•	84.0	•
105	5	•	51.5	•	67.1	•
106	6	•	52.4	•	68.3	•

The data shown in Table 4.9 reveals that the melting points of compounds **103-106** are all significantly reduced compared with HAT6 (**63**, Cr 67.6 Col_h 100.1 I), which is not unexpected, due to the loss of symmetry (highlighted previously, see Table 4.4 and Section 4.2.2.1). This effect upon the melting point can be observed in Figure 4.13, where the melting points of the acetylene-containing compounds following the same trend as their simple alkoxy counterparts (**123-125** and **63**). Figure 4.13 also reveals that the melting points of the terminal acetylene-containing materials are lower than their simple alkoxy counterparts; this is due to the steric disruption caused by the large cylindrical nature of the acetylene bond, and increased disruption of symmetry caused by the acetylenic unit.

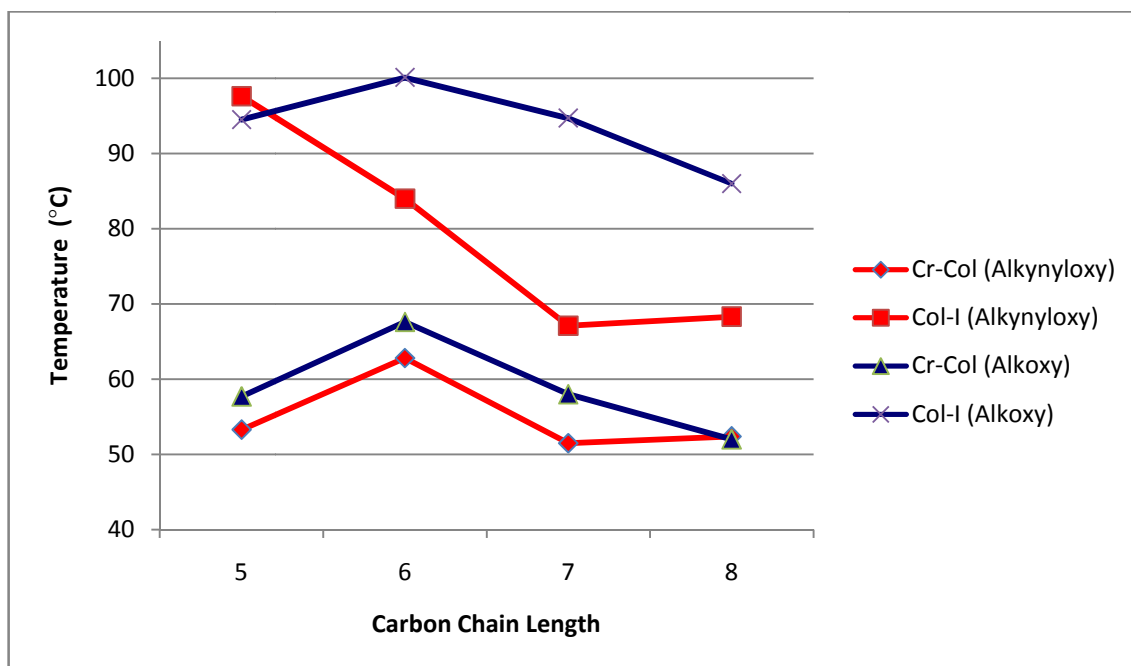


Figure 4.13: Comparison of transition temperatures of unsymmetrical triphenylenes containing terminal acetylenes (103-106) with unsymmetrical triphenylenes containing linear alkoxy chains (123-125 and 63)

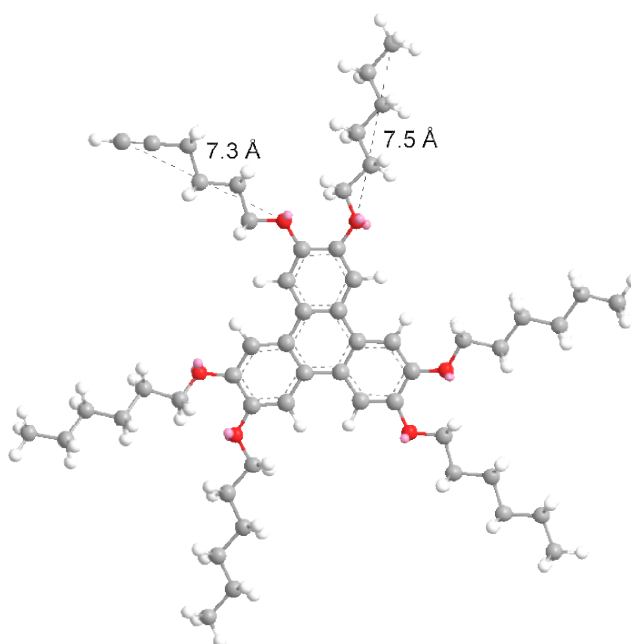


Figure 4.14: Simple model of compound 104, indicating alkoxy chain lengths

The melting points of compounds 103-106 may follow the same trend as their alkoxy counterparts (123-125 and 63), however it is clear from Table 4.9 and Figure 4.13 that other factors are at work with respect to the columnar phase stabilities. Initially it was

expected that compound **104** should have possessed the most stable columnar mesophase since it possesses a carbon chain length similar to that of the otherwise symmetrical material as the simple model illustrated in Figure 4.14 indicates. However, results from compounds **103** and **104**, quickly disproved this and it was then believed, based upon these results, that the cone of rotation of the acetylenic bond was important to the columnar phase stability. This explanation is owing to the sp hybridisation of the carbons of the acetylenic bond, whereby the final carbons in the chain are linear, and thus they possess a different orientation to the sp^3 hybridised carbons that are present in the alkoxy chain without the acetylenic unit. Hence, as can be observed in Figure 4.14, since the acetylenic unit essentially points outside of the central plane of the triphenylene core (in **104**), the cone of rotation of the bond (Figure 4.15) will be larger than if the acetylenic bond were within the plane of the molecule, as it would be when the carbon chain length count were odd (*e.g.* **103**) as opposed to even (*e.g.* **104**). The cone of rotation of the acetylene-containing chain explains why compound **104** has a lower $T_{\text{Col-I}}$ value than compound **103**, however it also explains why the $T_{\text{Col-I}}$ value of compound **103** is higher than the comparable compound **123**. In the case of sp^3 hybridised carbons, as in compound **123**, the terminal bond of alkoxy chains with odd numbered carbon units will be outside the cone of rotation just as the even numbered chains are in the case of the sp hybridised terminal acetylenes, thus compound **123** possesses a lower $T_{\text{Col-I}}$ value than the analogous compound **103**.

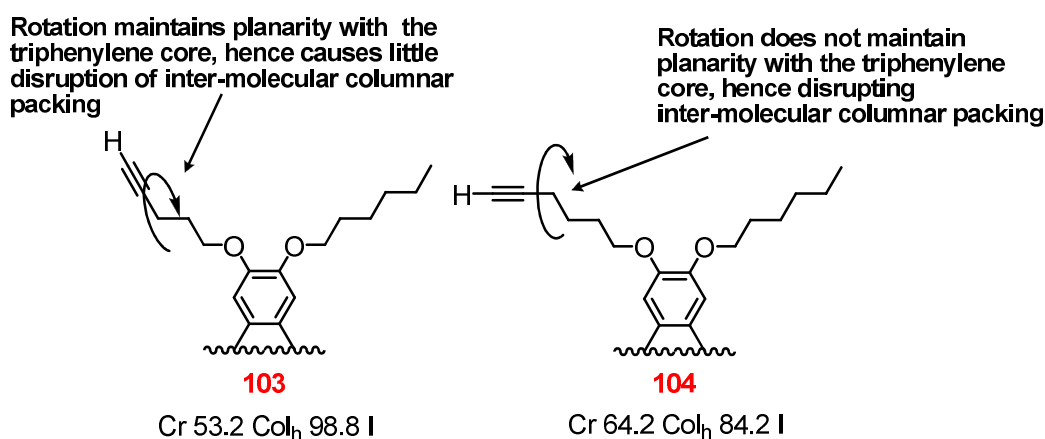


Figure 4.15: Cone of rotation of terminal acetylenes

The explanation regarding the cone of rotation, however, does not account for the significantly lowered columnar phase stability of compound **105**, relative to compound

104 and the similarity of the phase stabilities of compounds **105** and **106**. Perhaps a better explanation of the behaviour of these compounds is based on the enhanced rigidity of the acetylenic unit (mentioned previously), coupled with the space filling and steric effect of the acetylenic unit. The large acetylenic unit is capable of filling space around the periphery of the molecule, which as was shown with branched alkoxy chains previously (Section 4.2.3.1), can enhance the columnar phase stability. At the same time as the space filling effect is enhancing the clearing point, the steric influence of the acetylenic unit impedes columnar packing which destabilises the columnar phase stability and, as has been shown previously (Section 4.2.3.1), there is a balance between these two influences, which ultimately determines the columnar phase stabilities. Thus, for these acetylene containing compounds with short chain lengths (such as compound **103**) the enhanced attractions caused by the increased rigidity and space filling effect of the acetylene unit dominate over the disruptive steric effect and offer an enhancement or maintenance of the columnar phase stability. Increasing the length of the alkynyloxy chains (compounds **104** and **105**) increases the flexibility of the chains, destroying the control and balance between the space filling and steric effects. Thus, once the alkynyloxy chain length surpass this point of disruption there is little further significant flexibility caused by increasing the chain length, which means that the steric effect of the acetylenic unit is reduced as much as possible and the space filling effect again becomes the dominant factor, hence offering a slight increase in columnar phase stability of compound **106** relative to compound **105**.

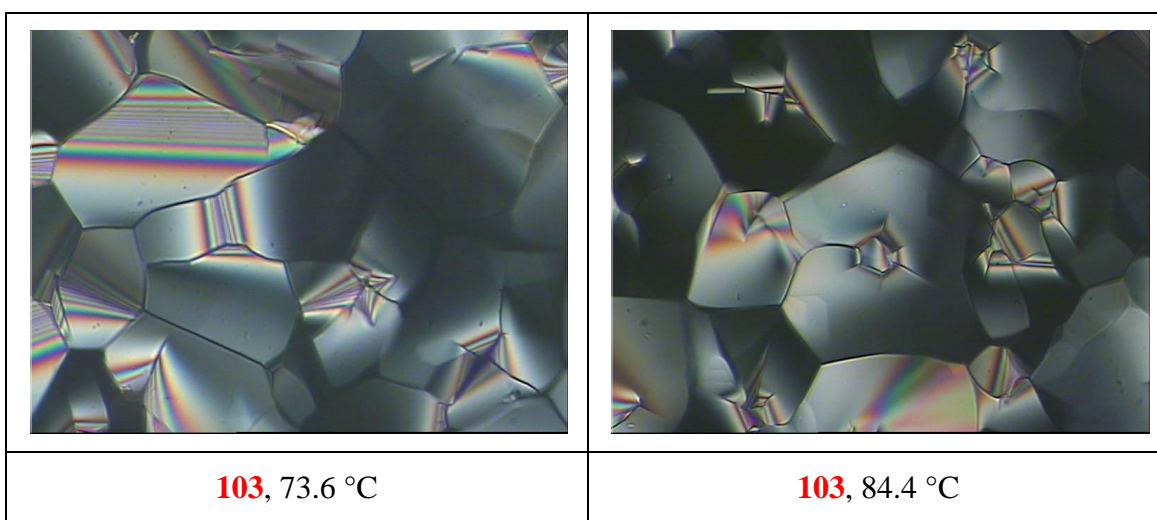


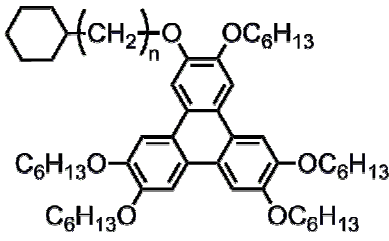
Figure 4.16: Typical POM textures of Col_h mesophase observed for triphenylenes with a terminal acetylene in a peripheral chain

4.2.3.3 Cyclohexanes

Modifications to the peripheral groups of triphenylenes have, thus far, included branched alkoxy chains and terminal acetylenes, both of which it has been shown have exerted a significant effect upon both melting points and columnar mesophase stabilities due to combinations of steric and space filling effects. Thus, a further peripheral unit that has been investigated in this programme of research is that of the cyclohexane ring. The cyclohexane ring is a bulky unit, and as such is expected to exert significant steric influence and space filling effects, which will have an effect on intermolecular packing and consequently melting points and columnar phase stabilities. In addition to these effects, the cyclohexane unit can exist in several conformational forms, which permits excellent stacking possibilities in a disc-shaped environment, which can aid in columnar phase stability. These major influences are, once again, in conflict with one another and thus this conflict was investigated with a focus on the distance of the cyclohexane ring from the central triphenylene core. Unlike the previous investigations in this programme, symmetrical triphenylenes have not been examined since it is expected that the steric influence of six cyclohexane rings would prove too destructive to columnar mesophase formation. This decision was based, in part, on the experience garnered from the materials containing branched chains, where the steric influence is not as great as that of the cyclohexane materials, but the small branched unit had to be moved a significant distance from the central triphenylene core before a stable columnar mesophase could be generated.

The data presented in Table 4.10 reveals a trend in the melting points of the unsymmetrical cyclohexane-containing materials. The trend regarding the melting points of compounds **115-118** closely reflects the length of the unique cyclohexane-containing chain, whereby, as was observed with the linear open-chained materials (Table 4.4 in Section 4.2.2.1), the melting points increase as the length of the unique chain increases, until it reaches the same length as the hexyloxy chains, and then when the chain length exceeds the optimal length the melting point decreases. Thus, the compound with the closest cyclohexane-containing chain length to the optimal 7.5 Å, compound **117** (as the simple model illustrated in Figure 4.17 demonstrates), possesses the highest melting point.

Table 4.10: Transition temperatures of unsymmetrical triphenylenes containing a peripheral cyclohexane unit

						
Compound	n	Transition Temperatures (°C)				
		Cr		Col _h		I
115	1	•	52.3	•	103.3	•
116	2	•	61.3	•	90.0	•
117	3	•	64.0	•	91.4	•
118	4	•	57.5	•	81.5	•

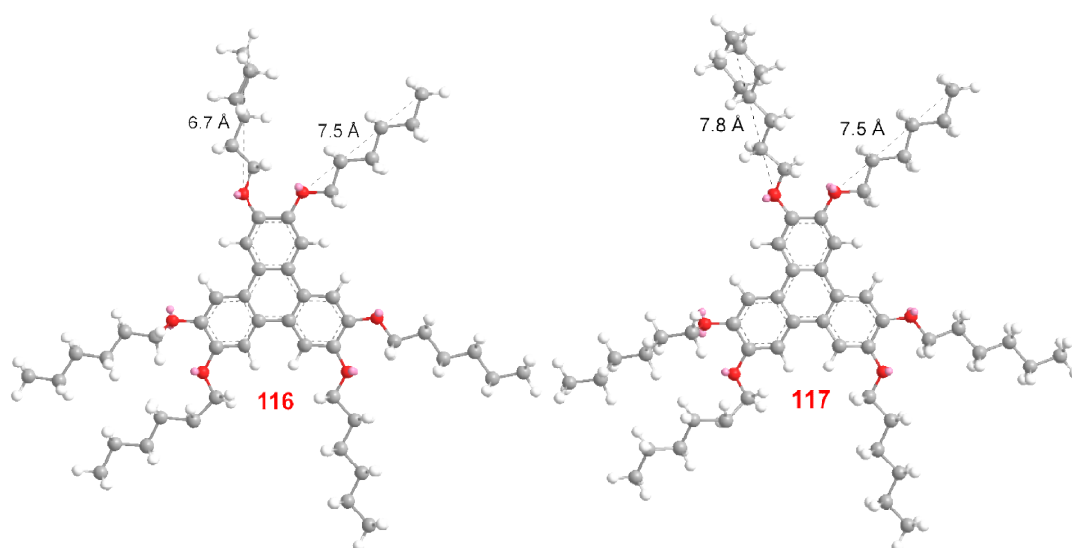


Figure 4.17: Simple model of compounds **116 and **117**, indicating alkoxy chain lengths**

Comparing the data shown in Table 4.10, with the parent compound HAT6 (**63**, Cr 67.6 Col_h 100.1 I) indicates that the first compound in this series of cyclohexane containing compounds, **115**, possesses a higher clearing point. This higher clearing point of compound **115** is caused by the increased space filling that is generated by the large cyclohexane ring and the conformational flexibility of the cyclohexane ring, which

promotes columnar phase stability. These factors, although offset by the steric influence of the cyclohexane unit on the columnar packing, generate enhanced forces of attraction and hence are clearly the dominant effect. Increasing the distance of the cyclohexane unit from the core by one carbon (as in compound **116** relative to compound **117**) decreases the mesophase stability significantly (approximately 13 °C drop in the $T_{\text{Col-I}}$ value). Initially this reduction in columnar phase stability is somewhat unexpected, since the comparable branched chain homologues benefited from enhanced columnar phase stabilities when the steric effect of the bulky unit was reduced by moving it further from the central core of the molecule (see Section 4.2.3.1). Thus different factors are affecting the overall columnar phase stability of these cyclohexane containing materials. One such factor that affects the columnar phase stability is the enhanced packing possibilities of the cyclohexane ring which, just like the space-filling and steric effects of the ring, are greatest when the cyclohexane ring is close to the triphenylene core. Thus, as the distance of the cyclohexane ring from the core increases the decreased rigidity reduces the ability of the cyclohexane ring to pack effectively, as well as reducing the overall space-filling effect and thus the columnar phase stability drops accordingly.

Further examination of the data in Table 4.10, reveals a pattern to the drops in columnar phase stability, and enhanced columnar phase stability of compound **117** when compared with compounds **116** and **118**. This pattern of columnar phase stabilities is caused by an odd-even effect similar to what was described previously with the terminal acetylene containing compounds (Section 4.2.3.2).

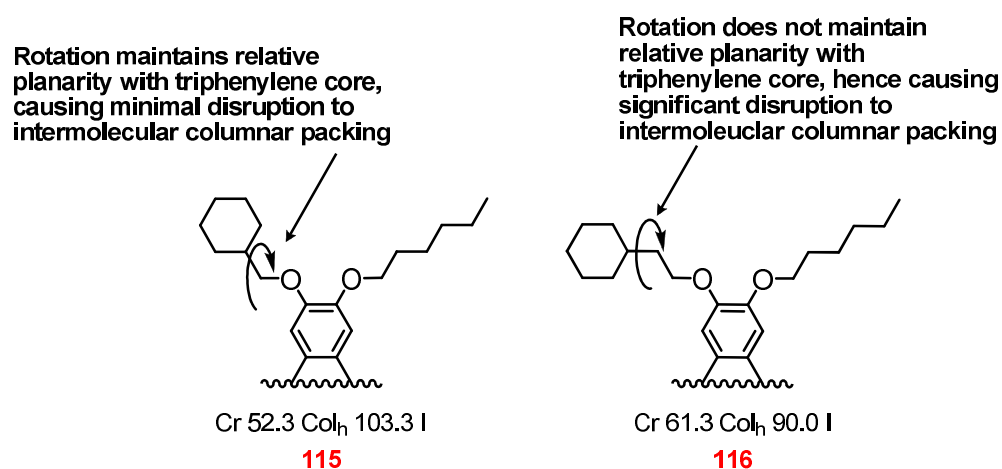


Figure 4.18: Structural features of cyclohexane-containing materials **115 and **116****

Examination of Figure 4.18 indicates that with spacer units containing odd numbers of carbons (such as compound **115**), the cyclohexane unit is within the plane of the molecule and when the spacer unit contains even numbers of carbons (such as compound **116**) the cyclohexane unit is outside the plane of the molecule. Thus, the number of carbons in the spacer chain affects the orientation of the cyclohexane ring, thus the arc of rotation is affected, and thus an odd-even effect is generated. Thus, there is greater disruption of intermolecular forces when the spacer unit contains an even number of carbons than when the spacer unit contains an odd number of carbons, and thus the clearing temperatures for compounds with odd numbers of carbons are higher. Further examination of this pattern of the odd-even effect in Table 4.10 indicates that the effect may be starting to reduce as the distance of the cyclohexane unit increases from the core since the drop in columnar phase stability is less between compounds **117** and **118** than it is between compounds **115** and **116**. It seems likely, therefore, that such odd even effects reduce as the overall chain length increases, thus it may be that at longer chain lengths this effect will not have a significant effect upon the clearing point, just as the effect did not seem to be present in the longer chained terminal acetylene containing compounds. Thus, it is possible that the apparent odd-even effect observed in the terminal acetylene containing compounds could be better observed with shorter chain lengths.

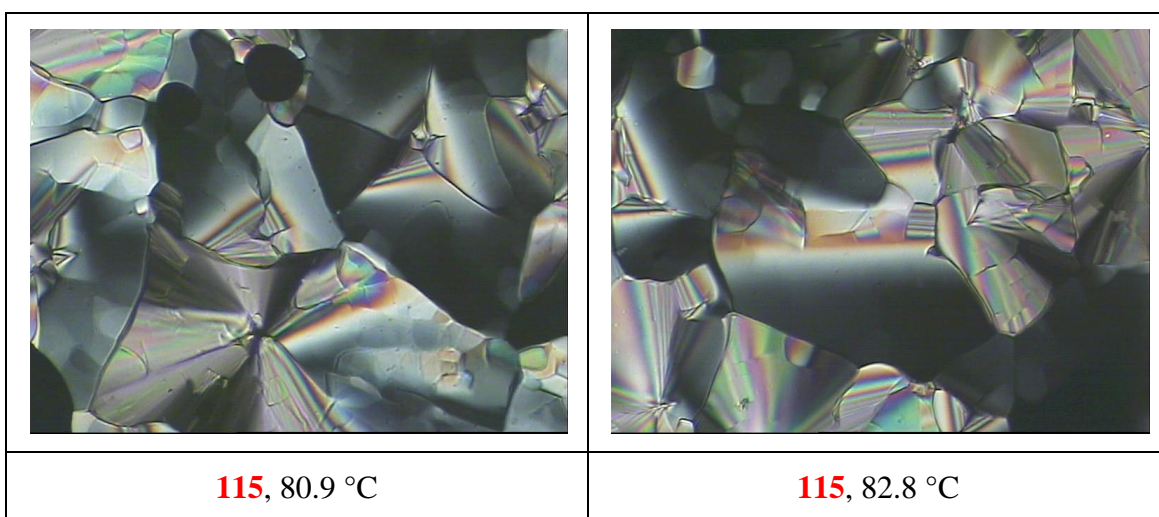


Figure 4.19 Typical POM textures of Col_h mesophase observed for unsymmetrical triphenylenes containing a peripheral cyclohexane group

4.2.3.4 Ethers

This programme of research has, thus far, investigated the effects of bulky peripheral groups on the mesomorphic properties of triphenylene and has shown that there can be a balance between space filling effects of the bulky substituents and the steric effects which they exert. This section examines the inclusion of small ether substituents into the peripheral chains of hexaalkoxy triphenylenes. The addition of the oxygen into one of the peripheral chains, whilst keeping five conventional hexyloxy chains to make up the six peripheral chains, permits the examination of the effect of the inclusion of the oxygen on the melting point and clearing point of the material relative to the parent compound HAT6 (**63**). The inclusion of the additional oxygen atom into one of the peripheral chains of the molecules introduces an additional polar group which can give rise to intermolecular dipole-dipole interactions, which could enhance melting and clearing temperatures.

Table 4.11: Transition temperatures of unsymmetrical triphenylenes containing an ether in a peripheral chain

Compound	R	Transition Temperatures (°C)				
		Cr		Col _h		I
132	-CH ₂ CH ₂ OCH ₃	•	54.9	•	86.7	•
133	-CH ₂ CH ₂ OCH ₂ CH ₃	•	51.3	•	77.4	•

Data displayed in Table 4.11 shows that, rather than enhancing melting and clearing temperatures as may have been expected from the inclusion of a polar group, the inclusion of the oxygen into the peripheral chain of the molecule has reduced the melting and clearing temperatures relative to the parent compound **63** (Cr 67.6 Col_h 100.1 I). Compound **132** can be further compared with **122** (Cr 59.7 Col_h 95.1 I), and compound **133** can be further compared with **123** (Cr 57.7 Col_h 94.5 I), their simple

alkoxy counterparts containing the same overall chain lengths. These comparisons reveal that the melting points of the ether containing species have reduced by approximately 5 °C and that the clearing points have been reduced to an even greater degree, by approximately 10 °C in the case of **132** (relative to **122**), and approximately 20 °C in the case of **133** (relative to **123**).

The reason for the reductions in melting point and mesophase stabilities is due to the altered geometry of the chain caused by the introduction of the oxygen unit. As can be observed in Figure 4.20 the inclusion of the oxygen unit has altered the bond angles within the chain, with typical values of approximately 112° in the typical alkoxy chain which, with the inclusion of the ether unit, is modified in some cases to 109°. This adjustment to the bond angle of the chain, making the angle less obtuse, modifies cone of rotation of the oxygen containing chain. Thus when the bond rotates and the chain sweeps around, it encompasses a greater area and thus causes greater disruption to intermolecular packing, disrupting intermolecular attractions, and thus decreases melting and clearing points. This explanation also explains why the longer ether chain present in compound **133** destabilises the columnar phase to a greater degree than the shorter ether chain of **132**, since the longer the chain the larger the area that will be encompassed by the rotation of the chain around the oxygen of the ether bond. Hence, the longer the ether chain, the greater the disruption to the intermolecular forces of attraction and thus the greater the disruption to columnar phase stability.

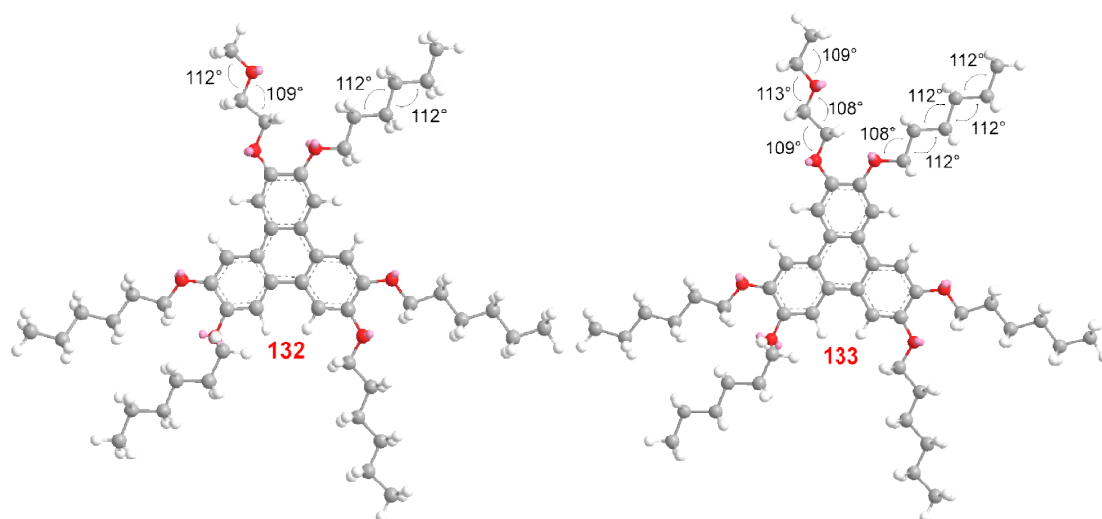


Figure 4.20: Simple models of compounds **132 and **133**, indicating comparable bond angles**

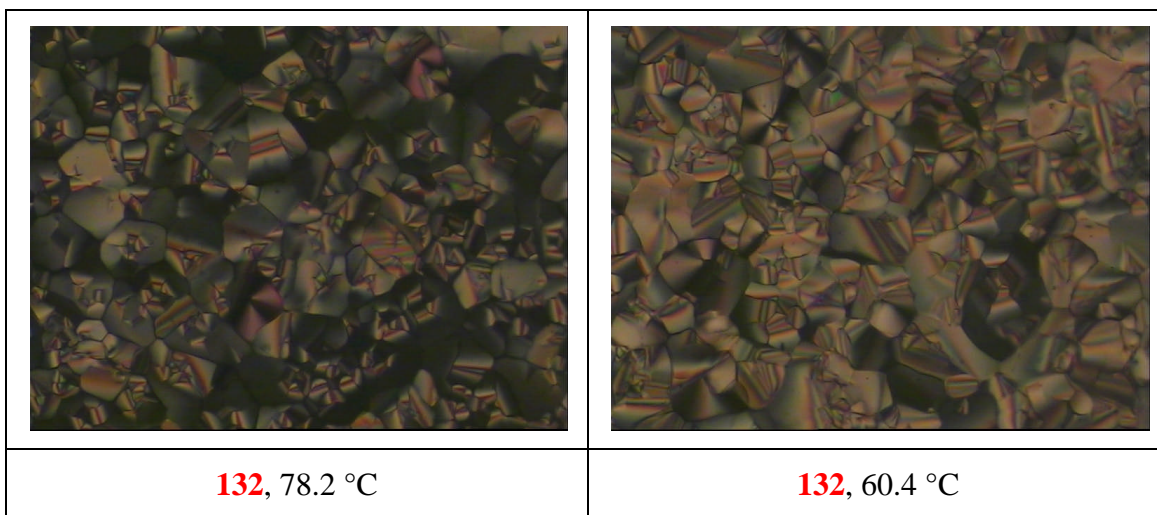
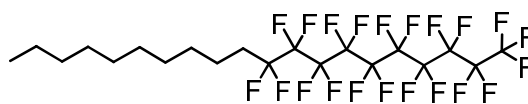


Figure 4.21: Typical POM textures of Col_h mesophase observed for unsymmetrical triphenylenes containing an ether in the unique alkoxy chain

4.2.3.5 Terminal Fluoro Substituents

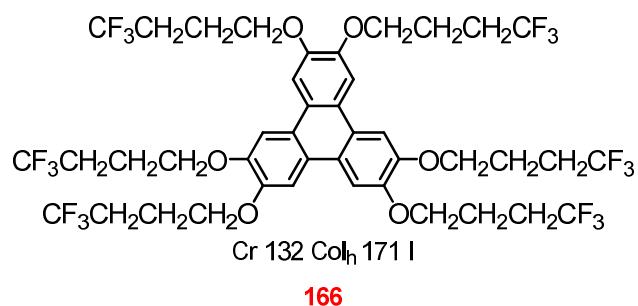
Fluoro substituents in liquid crystals have been widely investigated for their effects upon mesophase stabilities and morphologies. Such investigations into fluorinated liquid crystals is significantly more common in calamitic, rather than discotic, systems, since a lateral fluoro substituent can confer negative dielectric anisotropy and often promote the formation of the SmC mesophase, which are both properties which are useful in the field of ferroelectrics.¹⁶² The significant effects that arise from fluorination, however, is probably best demonstrated by compound **165** which, somewhat unusually, exhibits either a G or J mesophase due to chain stiffening and the fluorophilic effect introduced by the high levels of fluorination.¹⁷⁴



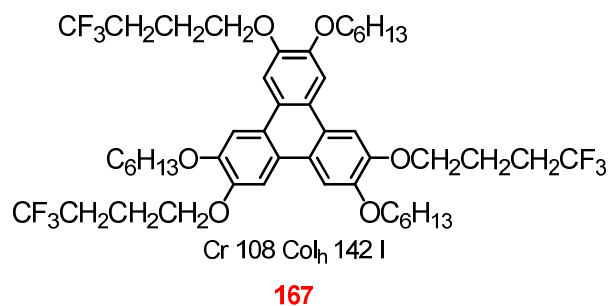
165

Cr 46.9 G or J 63.6 I

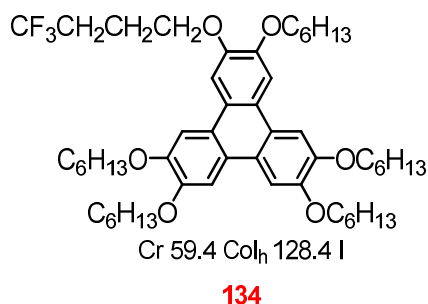
The effect of fluorination in discotic liquid crystals, while not as well established as in calamitic liquid crystals, has furnished some interesting results. The modification of HAT4 (**69**, Cr 87.3 Col_h 137.5 I) by substituting the terminal methyl unit for a trifluoromethyl unit (**166**) for example, has been noted to significantly enhance both the melting point and clearing point of the material (**166**, Cr 132 Col_h 171 I).⁵⁷



This pattern of enhanced melting and isotropisation temperatures in fluoro-substituted discotic liquid crystals is maintained even when the material possesses three fluoroalkylated chains as opposed to all six, as in compound **167** (Cr 108 Col_h 142 I).¹⁷⁵



So far, however, the vast majority of examples of fluorinated compounds in the literature have highly fluorinated chains (perfluorinated or semi-perfluorinated), and the majority of such compounds have been symmetrical in nature.¹⁶² Thus, it was interesting to investigate an example of an unsymmetrical fluorinated compound, in order to determine if the clearing point of the material could be enhanced, whilst maintaining a low melting point as has been observed with unsymmetrical materials already discussed in this thesis.



Compound **134** benefits from a depressed melting point and an enhanced clearing point compared to the parent compound HAT6 (**63**, Cr 67.6 Col_h 100.1 I). The reduction of the melting point of compound **134** is directly attributable to the loss of symmetry within the system, since the melting point is the same as the comparable compound **122** (Cr 59.7 Col_h 95.1 I, Table 4.4), which differs from compound **134** only in terms of the fluoro-substituents. The difference between the clearing points of compounds **134** and **122**, however, is quite large (more than 30 °C), and the clearing point of compound **134** is even higher than the parent compound **63** (Cr 67.6 Col_h 100.1 I) by a similar level. This difference in clearing temperatures is due to the effects of the fluoro-substituents which cause stiffening of the alkoxy chain, increases space-filling, and increased molecular ordering due to the fluorophilic effect. Whilst all of these effects of the fluoro substituent serve to increase the mesophase stability, it is interesting that the stabilisation of the columnar phase occurs to such a large degree. This observation is especially significant since materials already discussed in this thesis which exhibit enhanced columnar phase stabilities due to chain stiffening and space filling effects, such as the cyclohexane-containing compound **115** (Cr 52.3 Col_h 103.3 I), and the branched chain containing compound **130** (Cr 61.5 Col_h 105.3 I), have experienced this columnar phase stabilisation to only a small degree (*ca* 5 °C). Hence the large enhancement of mesophase stability in compound **134** is probably due primarily to the enhanced molecular ordering introduced by the fluorophilic effect as opposed to any space filling effects. This assertion is backed up by evidence from calamitic systems, where the effect is well known, for example Liu and Nohira discovered such an effect when increasing levels of fluorination of alkoxy chains in phenylpyrimidines.¹⁷⁶

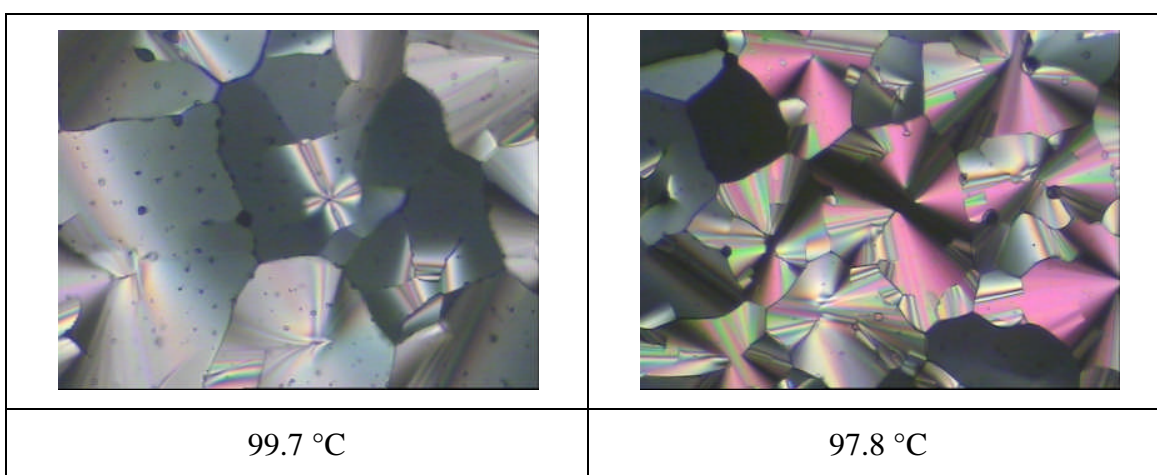
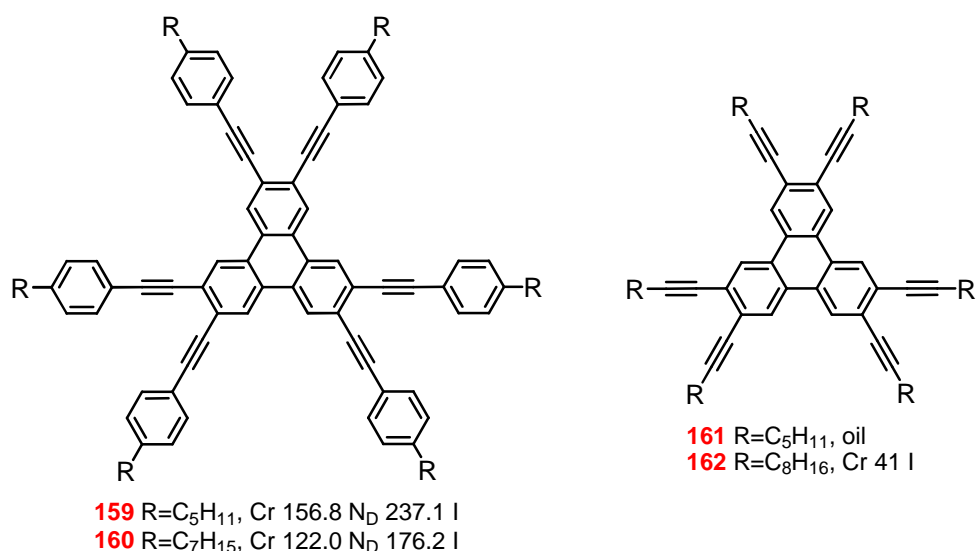


Figure 4.22: POM textures of the Col_h phase of compound **134**

4.2.4 Near-core Modifications of HAT6

4.2.4.1 Acetylenes

As was mentioned previously (Section 4.2.3.2), triphenylene based compounds containing acetylenic units are interesting to investigate since the acetylenic unit exerts significant space-filling and steric effects and the π -system of the acetylene bond can interact with the π -system of the triphenylene, enhancing core-core interactions and consequently columnar phase stabilities. It was shown previously (Section 4.2.3.2) how having the acetylenic unit in a terminal position of a peripheral chain enhanced melting points of symmetrical materials and disrupted mesophase formation. It was also shown that with unsymmetrical materials the significant space-filling effect and steric effect of the acetylenic unit could significantly affect columnar phase stability, both enhancing and disrupting columnar phase stability depending on chain length. It has also been mentioned that some triphenylene-based discotic materials containing an acetylenic unit have been examined before in the literature.



Compounds **159-162**^{56, 172} are known literature materials, compounds **159** and **160** exhibit the nematic discotic phase due to the steric effect of the acetylenic units and the benzene rings which prevent columnar packing and the enhanced disc size which promotes the nematic discotic phase. Compounds **161** and **162**, however, do not exhibit any mesomorphism because the steric effect of the acetylenic units preclude columnar packing, but lack the enhanced disc size required to generate the nematic discotic phase.

Initially it may appear to be counter-intuitive to investigate such structures, since they have been shown not to exhibit mesomorphic behaviour. To date, however, all such triphenylene-based acetylene-containing compounds that have been investigated have been symmetrical in nature (*e.g.* **161** and **162**) and this programme of research has demonstrated how modification of a single peripheral unit of a hexaalkoxytriphenylene structure often permits the retention of the columnar mesophase, which is often owing to a reduction in steric factors due to the presence of fewer bulky units. Thus, the modification of the HAT6 (**63**) structure by introducing one acetylene-containing chain has been investigated in the expectation that the reduction in steric factors by only introducing one bulky and antagonistic (due to π -electron repulsion) unit will permit the generation of a columnar mesophase, whilst the space-filling and possible enhanced π - π interactions introduced by the acetylenic unit will enhance the columnar phase stability relative to the parent system (**63**).

Table 4.12: Transition temperatures of unsymmetrical triphenylenes containing acetylenic units

Compound	R	Transition Temperatures (°C)				
		Cr		Col _h		I
151	CH ₃ CH ₂ CH ₂ -≡	•	49.2	•	134.1	•
152	CH ₃ CH ₂ CH ₂ CH ₂ -≡	•	51.9	•	134.2	•
153	CH ₃ CH ₂ CH ₂ CH ₂ CH ₂ -≡	•	48.1	•	125.5	•
154	CH ₃ CH ₂ CH ₂ CH ₂ CH ₂ CH ₂ -≡	•	39.3	•	108.3	•

Perhaps the most striking aspect revealed by the data displayed in Table 4.12 is that all of the acetylene-containing compounds (**151-154**) not only exhibit the columnar mesophase, but the phase stability is significantly enhanced beyond that of the hexaalkoxy analogues.

Comparing compound **151** with its hexaalkoxy counterpart, compound **122** (Cr 59.7 Col_h 95.1 I), and similarly compound **152** with its hexaalkoxy counterpart, compound **123** (Cr 57.7 Col_h 94.5 I), reveals a difference in columnar phase stabilities of approximately 40 °C. This significant enhancement is due primarily to the increased π - π interactions which arise from the inclusion of the acetylenic unit which is more polarisable than the oxygen which it replaces and possesses significant electron density which enhances π - π interactions between triphenylene cores. It is this effect which significantly enhances the columnar phase stabilities of these compounds since it is known that polarisable groups are required to generate a stable columnar structure, and the more polarisable the unit, the more it will conjugate with the triphenylene core, and thus the more stable the columnar mesophase.^{72, 173} This assertion is further backed up by evidence from this thesis, since when other space filling groups have been present, such as cyclohexane units (*e.g.* compound **115**), or branched alkoxy chains (*e.g.* compounds **129** and **130**), there have only been small increases in the columnar phase stabilities (approximately 5 °C for compounds **115**, **129** and **130**), which is due to the space-filling effect being balanced by the steric effect, and hence can only generate small increases in columnar phase stabilities.

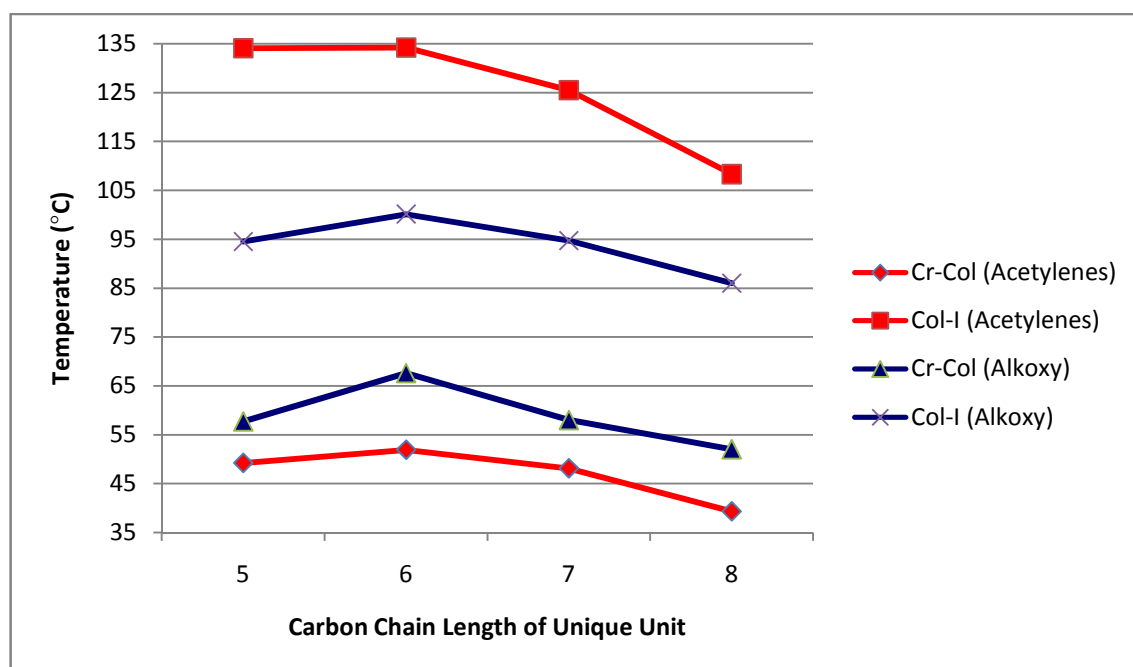


Figure 4.23: Comparison of transition temperatures of triphenylenes containing acetylenes (151-154) with triphenylenes containing six alkoxy chains (123-125 and 63)

The melting points of compounds **151-154** (Table 4.12) are significantly reduced relative to the parent compound **63** and their hexa alkoxy counterparts (illustrated in Table 4.4). There are several factors for this reduction in the melting points of these materials, including the reduction in symmetry and, most significantly in the cases of compounds **151-154**, the steric effect of the acetylenic unit. Since the acetylenic unit is next to the triphenylene core in compounds **151-154** the disruption to the melting temperature is maximised, and hence the melting points of the materials are 10-20 °C lower than the comparable hexa alkoxy systems (see Figure 4.23).

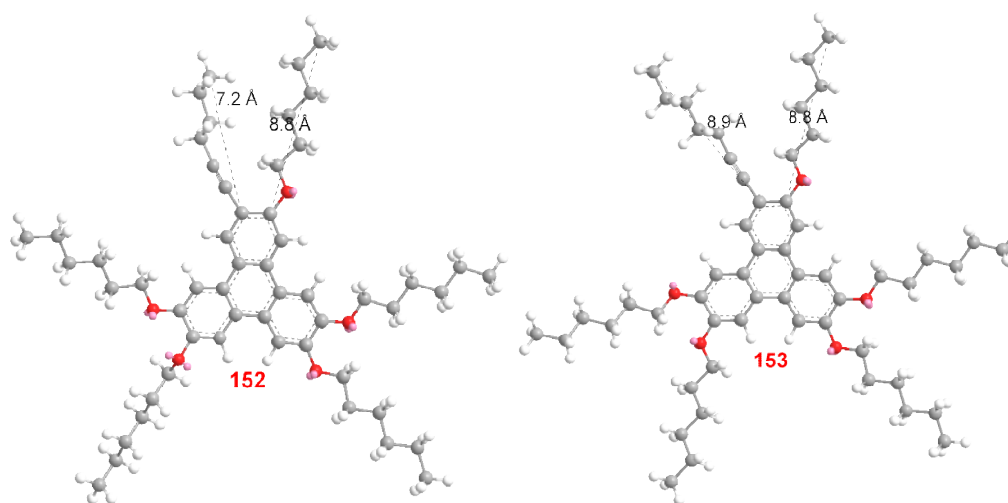


Figure 4.24: Simple model of compounds 152 and 153, indicating chain lengths

As can be observed from the data displayed in Table 4.12 and Figure 4.23, the trend in melting point closely mirrors the trend in clearing temperatures of compounds **151-154**, and show that the compound with the highest melting point and columnar mesophase stability is compound **152** which, like the symmetrical HAT6 (**63**), contains six carbons in all of the peripheral units. When compared with the unsymmetrical triphenylenes containing six linear alkoxy chains (displayed in Table 4.4), these acetylene-containing compounds behave in a similar fashion, with the transition temperatures increasing up to the entirely six carbon chain length, then decreasing rapidly when the chain length exceeds six carbons as is shown in Figure 4.23. This result is interesting since, as can be observed in Figure 4.24, it is compound **153**, not compound **152**, in which the acetylene-containing chain possesses a chain length which is similar to that of the hexyloxy chain, thus it may have been expected that compound **153** would exhibit the highest melting and isotropisation temperatures. Thus, it is not the effect of the

acetylene-containing chain length on the overall area of the disc that is the significant factor in this case, but rather the rigidity of the acetylene-containing chain. Thus, as the rigidity of the chain decreases (due to increasing chain length) the isotropisation temperatures decrease rapidly from compounds **152-154**.

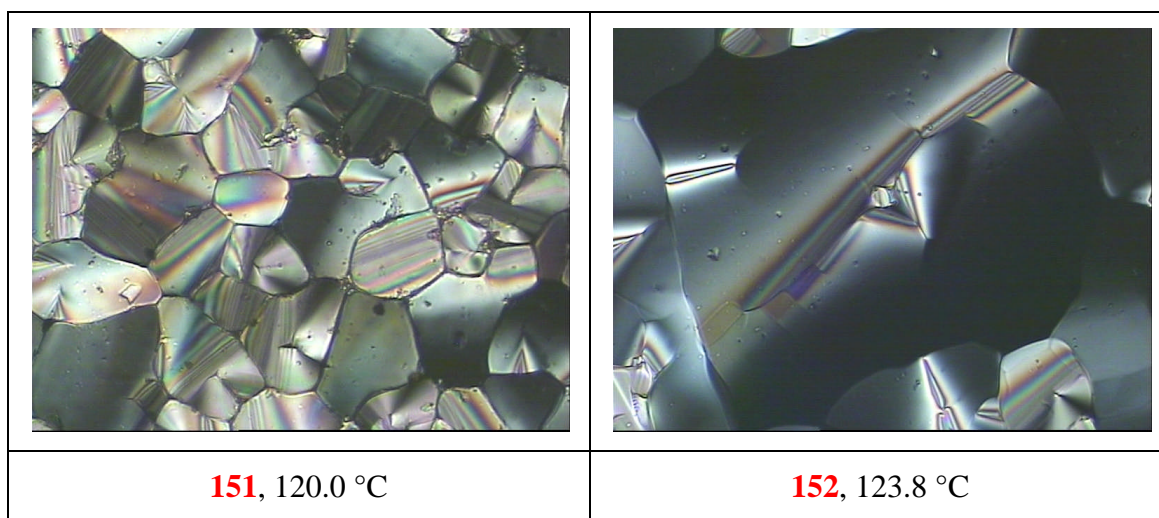
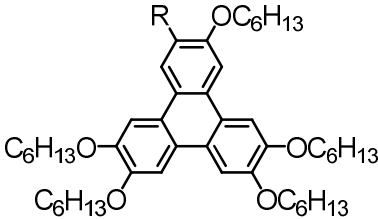
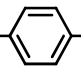
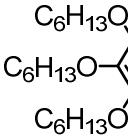
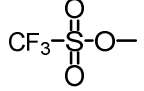
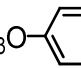
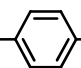


Figure 4.25: Typical POM textures of the Col_h phase exhibited by compounds 151-154

4.2.4.2 Miscellaneous Near-core Modifications

This research programme has thus far demonstrated how modification of a single peripheral unit of a hexasubstituted triphenylene can depress the melting point stabilise the columnar mesophase relative to that of the parent system. This control over melting and isotropisation temperatures has been accomplished by combinations of space-filling, steric, electronic effects, and the fluorophilic effect. This section is dedicated to examining several miscellaneous modifications of the HAT6 structure, to exemplify how near-core modifications affect the transition temperatures and mesophase morphology relative to those of the parent compound.

Table 4.13: Transition Temperatures of Various Unsymmetrical Hexa-substituted Triphenylenes

								
Compound	R	Transition Temperatures (°C)						
		Cr		Col _h		N _D		I
119	C ₅ H ₁₁ COO-	•	42.0	•	156.0	-	-	•
135	C ₆ H ₁₃ O-  -COO-	•	45.2	-	-	•	58.2	•
140	 -COO-	•	41.1	•	101.4	-	-	•
143				•	168.0	-	-	•
144	C ₆ H ₁₃ O-  -	•	25.6	•	89.1	-	-	•
146	C ₆ H ₁₃ O-  -	•	48.3	•	113.8	-	-	•

The most investigated discotic liquid crystalline materials are hexa-esters and hexa-ethers of triphenylene since they have a strong tendency to form ordered columnar mesophases.²⁴ Typically it has been observed that hexa-ethers of triphenylene typically have low melting points, and low clearing points and that that hexa-esters of triphenylenes often exhibit high melting and high clearing points.¹¹³ The reason that hexa-esters and hexa-ethers of triphenylene exhibit columnar mesophases is due to the nature of the peripheral unit whereby it is known that in order to exhibit the columnar mesophase the π -system of the triphenylene core unit must be expanded (in order to enhance π - π interactions), hence conjugated double bonds and peripheral oxygen-containing units are excellent for conferring this property.⁷² As shown in Table 4.13, compound **119**, which possesses one ester linkage and five ether linkages as opposed to

the six ether linkages of the symmetrical parent compound (HAT6, **63**, Cr 67.6 Col_h 100.1 D), benefits from a lowered melting point compared with the parent compound due to the unsymmetrical nature of the material and the steric effect of the ester unit. Compound **119**, in addition to benefiting from a depressed melting point, also has a significantly higher clearing temperature than the parent HAT6 (**63**, Cr 67.6 Col_h 100.1 D). This higher clearing point of compound **119** is attributable to the extended conjugated π system of the ester unit. This enhancement of columnar phase stability and depression of melting point corresponds with previous reports of widened enantiotropic columnar mesophase ranges when mixed ether and ester groups are present.¹⁷⁷

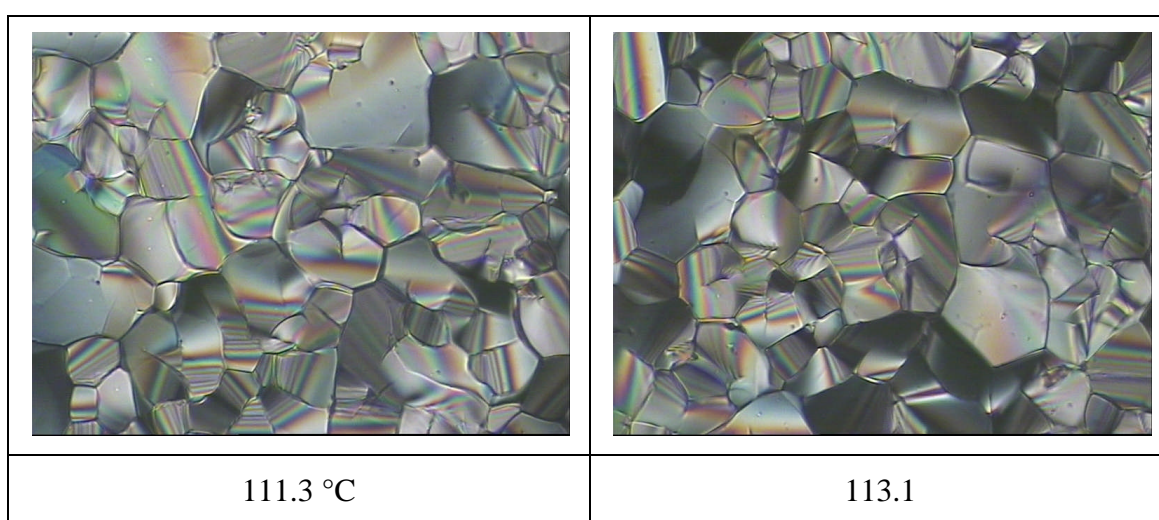


Figure 4.26: Typical POM Textures of the Col_h Mesophase of Compound **119**

Compound **135**, as illustrated in Table 4.13, exhibits a narrow enantiotropic mesophase temperature range, low melting point, low clearing point, and a different mesophase morphology compared with the parent HAT6. Initially this result appears to be counter-intuitive, since it has already been shown how the introduction of units which expand the π -system of the central triphenylene units enhances the mesophase stability, and even, retains the hexagonal columnar morphology (*cf.* **119**). According to this logic, therefore, given that the π -system of compound **135** will be expanded by both the ester unit and the benzene ring it would be expected that the columnar mesophase should be significantly more stable than that of compound **119**, or the parent compound **63**, and maintain the same morphology. However the significant steric influence of the benzene ring and the ester group tends to prevent columnar packing. The highly flexible nature of the ester unit also allows the benzene ring to rotate to and thus intermolecular forces

of attraction are significantly disrupted, and hence the material is prevented from forming a columnar structure. This observation of the nematic mesophase in compound **135** (phase identified by observation of a Schleioren texture displayed in Figure 4.27) is supported by previous work on symmetrical, hexa-substituted materials, whereby when six such benzene-containing units are present the nematic phase tends to be observed, although columnar mesophases are still sometimes observed and the transition temperatures of such materials are typically quite high.⁵⁶

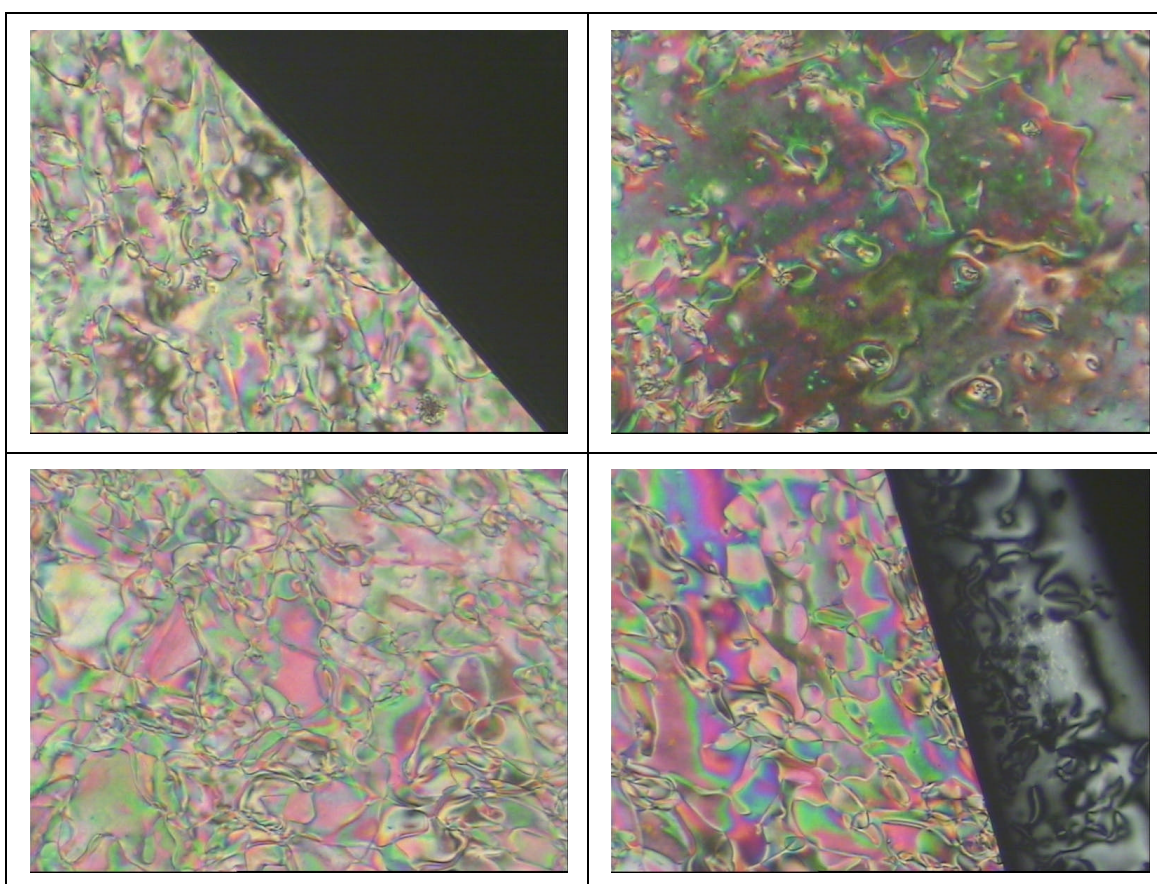


Figure 4.27: POM images of Schleioren texture of the N_D phase of compound **135, at room temperature**

Compound **140**, as displayed in Table 4.13, exhibits a columnar mesophase with a stability similar to that of the parent compound, HAT6 (**63**, Cr 67.6 Col_h 100.1 I). This result is surprising, since the mesophase morphology should be similar to that of compound **135** since the core structure of two compounds is identical. However, compound **140** has three terminal alkoxy chains in the benzoate arm. These additional alkoxy chains will interdigitate with alkoxy chains on neighbouring molecules, which

permits the alkoxy chains to interlock with one another in a similar manner to that of twine or a rope and thus partially stabilise the columnar structure. This explanation also accounts for the stability of the columnar mesophase, which is significantly higher than the nematic phase stability of compound **135**.

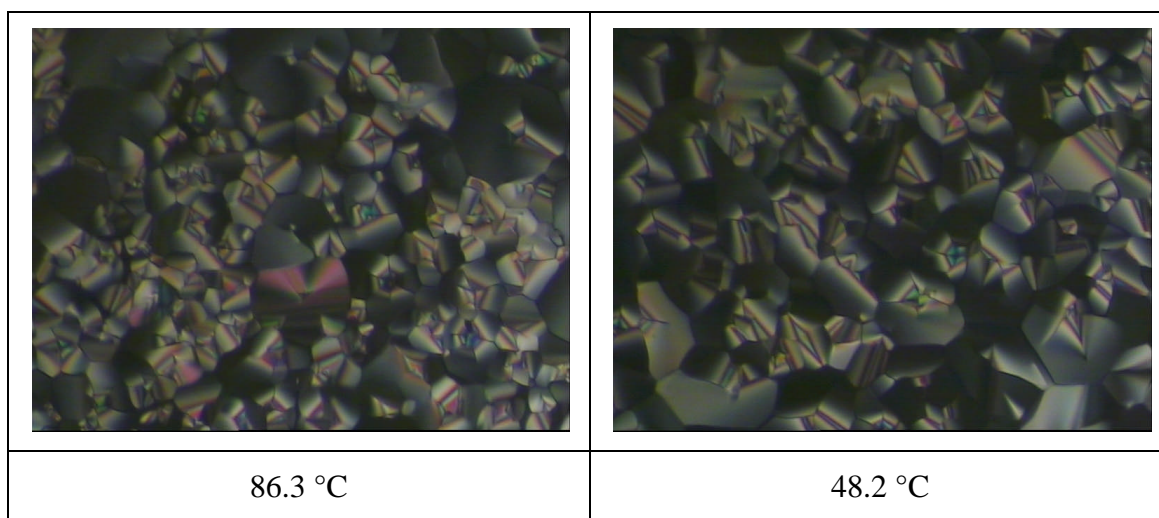


Figure 4.28: Typical POM textures of Col_h mesophase of compound **140**

Compound **143**, as shown in Table 4.13, was synthesised as an intermediate compound for generating several other liquid crystalline materials, and was found to exhibit an extremely stable columnar mesophase when compared with that of the parent compound, **63** (nearly 70 °C higher), and to benefit from a low (and undetermined) melting point. Whilst this discovery may have been serendipitous, it is not exactly unexpected, since the material contains several structural features which have been shown to be beneficial to columnar mesophase formation. One such factor which leads to the high clearing point of **143** is the extension of the π -system due to the sulfonato unit which, as with the carbonyl unit present in compound **119**, leads to the enhancement of columnar phase stability through enhanced π - π interactions. In addition to the effect of the sulfonato unit, compound **143** also possesses a terminal trifluoromethane unit, which was shown in compound **134** to enhance columnar mesophase stability through the fluorophilic effect (which aids molecular ordering). In addition to these effects, the sulfonato unit of compound **143** exerts a space-filling effect since it occupies more space close to the central disc compared with the alkoxy chain of the parent compound which has also been shown to enhance columnar phase stabilities.

Compound **144**, as illustrated in Table 4.13, exhibits reduced melting and clearing temperatures relative to the parent compound HAT6 (**63**, Cr 67.6 Col_h 100.1 I). These reduced temperatures are due to the steric hindrance introduced by the phenyl unit. The addition of the phenyl unit increases space filling and extends the π -system of the material (thus allowing for increased π - π interactions), both of which have been shown to enhance columnar mesophase stability. However, the phenyl ring is linked directly to the core, and the significant steric influence disrupts molecular packing, and thus lowers columnar phase stability and greatly reduces the melting point. Compound **144** is quite unlike compound **135**, because the phenyl unit is linked directly to the triphenylene core and hence the steric disruption is closer to the central core of the molecule, thus the molecules cannot pack as well. Additionally the interannular twisting at the linking bond reduces the polarisability and planarity. The mesophase morphology of compound **144** is columnar, compared with the nematic phase of compound **135**, which is likely due to the greater rigidity of the direct link to the core compared with the flexible ester linkage.

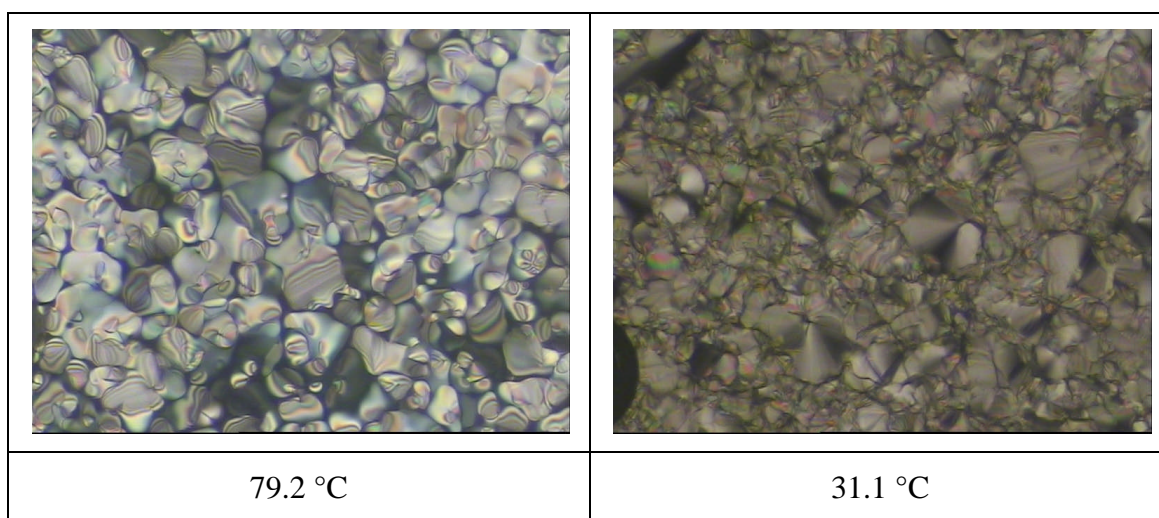


Figure 4.29: Typical POM textures of the Col_h mesophase of compound **144**

Compound **146**, shown in Table 4.13, exhibits an enhanced columnar phase stability compared with the parent compound HAT6 (**63**, Cr 67.6 Col_h 100.1 I), whilst also benefiting from a lower melting point. The reduced melting point of compound **146** is probably due to several complimentary factors including: loss of symmetry, the enhanced steric hindrance introduced by the phenyl unit and the bulky acetylenic linking unit close to the core of the molecule. These conditions serve to disrupt

molecular packing in the crystal phase and thus reduce the melting point of the material. The columnar phase stability of the material, whilst disrupted by the same effects which reduce the melting point, is enhanced through a number of factors: firstly, the space-filling effect of the acetylenic linking unit and the phenyl group; and secondly, the acetylenic unit and the phenyl unit greatly expand the area of the conjugated π -system of the material, thus greatly increasing the π - π interactions that can take place, which has already been shown to significantly enhance columnar phase stability. These effects which enhance the columnar phase stability of compound **146** significantly outweigh the destabilisation effects, and hence the columnar phase stability is increased by almost 14 °C compared with the parent compound. The mesophase morphology of compound **146** is slightly unusual, since the inclusion of acetylenic units close to the triphenylene core of the material usually results in the generation of nematic as opposed to columnar mesophases (*cf.* compounds **159** and **160**). The reason that the columnar phase morphology is maintained in this, and similar compounds, is that the disruption caused by the steric effect of the bulky acetylenic unit being close to the core of the molecule is minimised by only occurring in one of the six positions, as opposed to all of the six positions. This reduction of steric effect permits closer contact between the triphenylene cores and thus enhances π - π interactions; hence the phase behaviour of the otherwise symmetrical unit is maintained, *i.e.* having five out of six positions the alkoxy unit reduces the steric effect, and thus helps to preserve the columnar mesophase which is prevalent in hexa alkoxy substituted triphenylenes.

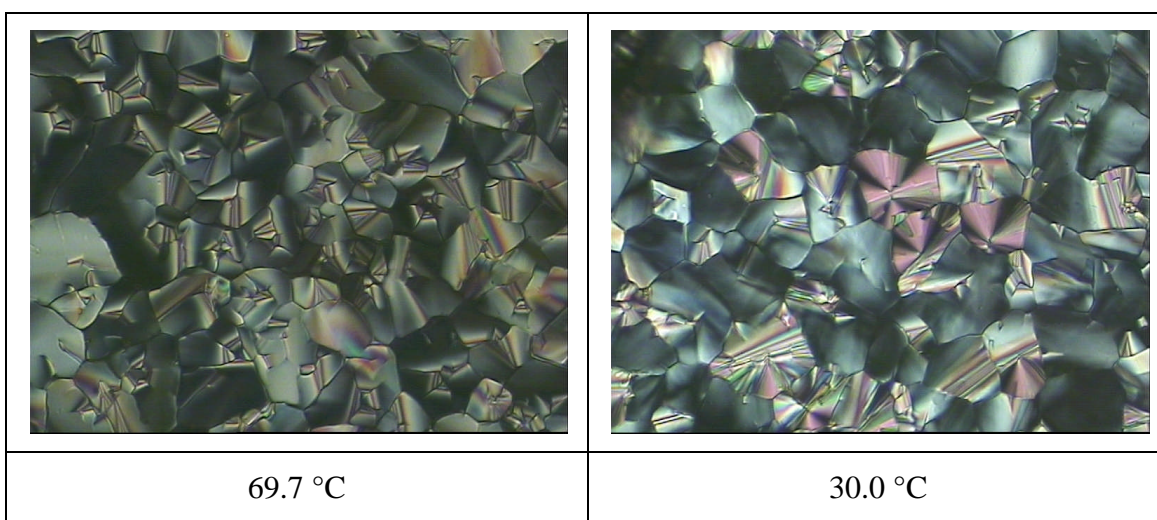


Figure 4.30: Typical POM textures of the Col_h mesophase of compound **146**

5 Conclusions and Summary

5.1 Synthetic Methodologies

5.1.1 Iodination Reactions

Several iodination reactions to generate valuable intermediates were performed. By varying the methodology for the synthesis of symmetrical 1,2-dialkoxy-4-iodobenzene moieties it was revealed that careful control of the levels of iodination agents NIS and trifluoroacetic acid was essential for selective mono-iodination. This process also revealed that high yields must be sacrificed for excellent regioselectivity. However, reasonable yields can still be achieved whilst maintaining excellent selectivity. This selectivity was achieved utilising Method 4, which achieved 76 % yield, with less than 0.5 % of the corresponding diiodinated material being generated. It was also noted that the presence of benzyloxy substituents as opposed to hexyloxy substituents *para* to the position to be iodinated drastically increased the time it took for the reaction to reach completion. Further iodination reactions involving unsymmetrical alkoxybenzenes revealed that the procedure is ineffective when phenols are present, and that the methodology is sensitive to the length of alkoxy chains present. It has been speculated that the inductive effect of the alkyl chain influences the overall mesomeric effect of the alkoxy group which consequently enhances the reactivity of the benzene-based species. Thus it has been demonstrated that by careful control of the iodinating agents (NIS and trifluoroacetic acid), and use of benzyloxy and alkoxy substituents on a benzene ring, iodination reactions can be performed which can selectively generate a 1-alkoxy-2-benzyloxy-4-iodobenzene moiety.

5.1.2 Synthesis of Hexaalkoxytriphenylenes

The most commonly used oxidative strategies and methodologies for generating hexaalkoxytriphenylenes have been investigated by synthesising HAT6 (**63**) *via* the various strategies and methods. This investigation has revealed that of the three most commonly used trimerisation agents (FeCl_3 , MoCl_5 and VOCl_3), molybdenum(V) chloride offered the worst overall results, vanadium(V) oxytrichloride offered the best results, and iron(III) chloride offered results which were marginally worse (in terms of yield and purity) than those of the best trimerisation agent. The synthetic investigation also revealed that the cyclisation strategy (Strategy 4) offered the best results in terms of

purity and a yield comparable to that of the dimerisation strategy (Strategy 3). Synthesis of the unsymmetrical compound **76** *via* the dimerisation strategy (Strategy 3), revealed no evidence of the generation of the trimerisation product (*i.e.* there was no concurrent synthesis of compound **69** during the reaction), which is owing to the electron rich nature of the biphenyl unit. This reasoning also explains the success of the cyclisation strategy, since the terphenyl unit is even more electron rich than the biphenyl unit, thus the reaction is the most favourable. Thus the combination of the cyclisation strategy (Strategy 4) and the vanadium(V) oxytrichloride method is, perhaps, the best for the generation of hexaalkoxytriphenylenes.

5.2 Mesomorphic Properties of Materials

5.2.1 Spiral-shaped

Three spiral-shaped compounds have been prepared (compounds **47**, **52** and **59**). Of these spiral-shaped materials one compound, compound **59**, has been shown to be non-mesogenic which is due to interannular twisting of the benzene rings at the core which prevents effective columnar packing. The remaining two materials, compounds **47** and **52**, however, both exhibit mesomorphic behaviour. Compound **52** (Cr 132.2 (X 96) I) exhibits a monotropic mesophase (possibly columnar) which triggers crystallisation. It was initially hoped that the bend within the peripheral ‘arms’ of the molecule would help to fill space around the central core and thus promote columnar packing. However, whilst this space filling effect may occur in isolation, it appears that in the bulk material the bend is detrimental to columnar phase generation since the rotation of the ‘arms’ interferes with columnar packing of neighbouring molecules, thus destabilising the phase.

Compound **47** (Cr 79.9 B₁ 87.7 I) exhibits a columnar mesophase (B₁ being a Col_r phase) despite large amounts of free space around the central disc, and similar molecular architectures previously having exhibited only the nematic discotic mesophase monotropically. The mesogenic behaviour of compound **47** has been ascribed to the large ‘arms’ of the molecule filling space around the central cores of the molecules above and below in the columnar structure and dipole-dipole interactions between electron rich oxygen atoms and electron deficient carbon atoms in the ester groups of neighbouring molecules in the phase, all of which serve to stabilise the columnar phase structure.

5.2.2 Triphenylene-based Materials

5.2.2.1 Unbranched Open Alkoxy Chains

Two series of simple open unbranched alkoxy chains have been examined, one series of which was symmetrical, and the other series was unsymmetrical and based upon HAT6 (**63**). Comparisons of the known symmetrical materials revealed a trend of decreasing melting and isotropisation temperatures as alkoxy chain lengths increase. This effect is due to increasing molecular flexibility as the chain lengths increase and increasing

overall levels of free space in the disc which is introduced as the chain lengths increase in size.

Unsymmetrical triphenylene-based materials containing unbranched open alkoxy chains that have been prepared have shown that melting points and columnar phase stabilities are driven by the symmetry within the molecule. In the case of the unsymmetrical materials the overall rigidity and flexibility of the molecule is relatively constant is little affected by the change in chain length of one chain, unlike the symmetrical materials described earlier. The reason that symmetrical materials possess the highest melting point and columnar phase stability in these cases is due to the effect of the unique chain upon the overall area of the central disc. In the case of alkoxy chains shorter than the symmetrical length, free space is introduced to the disc, and in the case of chains longer than the symmetrical length the excess protrudes from the area of the disc. Both of these described effects have been demonstrated to be detrimental to columnar phase stability and reduce melting points. In addition, a slight odd-even effect has been noted, particularly with respect to the melting and clearing temperatures of compounds **122** and **123**.

5.2.3 End-group Modifications of Hexa-substituted Triphenylenes

5.2.3.1 Branched Alkoxy Chains

Two series of novel branched alkoxy chain-containing triphenylene-based discotic liquid crystalline materials have been prepared. Comparison of these materials with unbranched analogues has revealed that the delicate balance between steric and space-filling effects of the peripheral branched chains often favours the space filling effect with respect to the clearing point of the material and the steric effect often wins out with respect to the melting point. This information has led to the generation of materials with enhanced isotropisation temperatures, reduced melting points and hence wider temperature ranges of the mesophase compared with their straight chain analogues.

The low melting point of compound **66**, illustrates how the steric effect can reduce the melting point, whilst the space filling effect maintains the high clearing point. This effect is emphasised by compound **131**, where the same branch reduces the melting point, but the clearing point is also reduced, indicating that the space-filling effect of multiple peripheral chains is important. The clearing points of compounds **129** and **130** highlight the importance of the space filling effect, given that both compounds exhibit

enhanced isotropisation temperatures relative to the parent compound **63**, when the steric effect of the branch and reduction in symmetry would have otherwise significantly reduced the clearing point.

5.2.3.2 Terminal Acetylenes

A number of symmetrical and unsymmetrical triphenylene-based materials containing alkynyloxy chains have been prepared. The symmetrical compounds (**67** and **68**) contained six alkynyloxy chains, and exhibited enhanced melting points relative to the comparable hexaalkoxy analogues HAT5 and HAT6. It was noted that the columnar mesophase of the compounds was not enhanced to the same degree as melting point, with only compound **67** exhibiting a columnar mesophase, albeit transiently and monotropically. It is likely that the enhancement of the melting points of the terminal acetylene-containing materials is due to combinations of increased chain rigidity, and increased space filling due to the acetylenic unit, which would not affect the columnar phase stabilities to the same degree as the melting points, as has already been shown (Section 4.2.3.1).

Unsymmetrical alkynyloxy-containing triphenylene-based materials that have been synthesised all have reduced melting points and isotropisation temperatures relative to their hexaalkoxy counterparts. This reduction in melting and clearing temperatures is due to steric disruption of the acetylenic unit and loss of symmetry within the molecule. A possible odd-even effect was noted at small alkynyloxy chain lengths (similar to the alkoxy chain lengths which generated the odd-even effect in compounds highlighted in Section 4.2.2.1), where this effect could be more dominant than other factors governing columnar phase stabilities. It is also possible that at short chain lengths the space filling effect and enhanced rigidity offered by the acetylenic unit enhance (or maintain) columnar phase stability, and that as the alkynyloxy chain length increases the increased flexibility of the chain destroys this control and the steric effect of the acetylenic unit reduces the columnar phase stability. At even longer alkynyloxy chain lengths the increase in flexibility then appears to become less of a factor as the overall increase in flexibility is minimal, thus the steric and space filling effects and increased rigidity and enhanced π - π interactions offered by the acetylenic unit again become more dominant.

5.2.3.3 Cyclohexanes

A series of unsymmetrical triphenylene-based materials containing a singular cyclohexane-containing alkoxy chain (compounds **115-118**) have been synthesised. The melting point of these cyclohexane-containing materials closely reflects the chain length of the unique cyclohexane-containing chain, just as the open unbranched materials highlighted in Section 4.2.2.1 did, with the materials with unique chains longer or shorter than the ideal (*i.e.* close to symmetrical) length distorting the molecular shape and hence reducing the melting point of the material compared with the parent compound (**63**). Columnar phase stabilities, however, do not reflect this pattern, and compound **115**, possesses a clearing point higher than the parent compound. The enhanced clearing point is due to the enhanced packing possibilities of the cyclohexane unit and the space filling effect of the unit. These effects, however, reduce as the cyclohexane unit is moved further from the core due to the increased flexibility offered by the alkoxy chain and the shift in the dominance of space filling and steric effects of bulky units on columnar phase stabilities noted previously (Section 4.2.3.1). An odd-even effect was noted in the columnar phase stabilities of compounds **115-118**, which appeared to become less dominant as the overall chain length of the unique unit increased, thus suggesting that such effects are more noticeable with small alkoxy chain lengths, when the unique unit is close to the triphenylene core of the molecule. Thus, this observation reinforces the possible identification of an odd-even effect in short-chained terminal acetylene-containing triphenylene-based materials.

5.2.3.4 Ethers

Two compounds with ether-containing alkoxy chains (compounds **132** and **133**) have been prepared. Both of these compounds exhibit reduced melting points and isotropisation temperatures compared with their simple alkoxy analogues (compounds **122** and **123**), which has been attributed to the altered geometry of the alkyl chain after the incorporation of the additional oxygen into the chain. The additional atom changes the bond angle of the chain to such a degree that rotation of the chain causes a greater area to be swept by the chain and thus melting points and columnar phase stabilities are reduced accordingly. Increasing the chain length (as in compound **133** relative to compound **132**) causes a greater disruption to melting and isotropisation temperatures due to the larger area swept by the chain with the modified geometry.

5.2.3.5 Terminal Fluoro Substituents

In order to determine the effect of low levels of fluoro substitution upon melting and isotropisation temperatures, a single compound (**134**) was prepared which contained a terminal trifluoromethyl group. Compound **134**, when compared with its non-fluorinated counterpart, compound **122**, revealed that at low levels of fluorination there is very little effect upon the melting point of the material which is still affected mostly by the symmetry of the material. The clearing point of the material, however, is significantly affected by the inclusion of the terminal fluoro substituents and increased by approximately 30 °C relative to the non-fluorinated compound **122**. This increase in clearing temperature is due primarily to the fluorophilic effect which increases molecular ordering within the mesophase, which consequently enhances columnar phase stability.

5.2.4 Near-core Modifications of HAT6

5.2.4.1 Acetylenes

A series of acetylene-containing triphenylene-based compounds (**151-154**) has been synthesised. These compounds all exhibit the hexagonal columnar mesophase, with phase stabilities higher than that of their hexaalkoxy counterparts or even the symmetrical parent compound HAT6 (**63**). This columnar phase enhancement has been demonstrated to be due to combinations of the space filling effect of the acetylenic unit and, more importantly, the enhanced π - π interactions introduced by the acetylenic unit. It has also been noted that the melting and clearing points of these materials do not appear to be influenced by the symmetrical length of the peripheral acetylenic chain to any significant degree. Rather it appears that the overall rigidity of the molecule, as affected by the peripheral chains, is the most significant factor with regards to columnar phase stabilities and melting points in the case of these acetylene-containing materials.

5.2.4.2 Miscellaneous Near-core Modifications

Several miscellaneous compounds based upon the HAT6 architecture have been prepared. These compounds have been compared with HAT6 (**63**, Cr 67.7 Col_h 100.1 I) for their effect upon melting points and mesophase stability and morphology and have revealed several interesting facts:

- The reduction in symmetry within the molecule caused by the introduction of a unique unit always appears to decrease the melting point of the material compared with the parent system.
- The inclusion of modifications which extend the π -system of the core, and thus increase π - π interactions between neighbouring molecules in a columnar mesophase can significantly enhance the columnar phase stability (*e.g.* compounds **119**, **143** and **146**).
- The fluorophilic effect can play a significant role in enhancing columnar phase stability, especially in conjunction with other columnar phase enhancing factors such as enhanced π - π interactions and space filling effects (*e.g.* compound **143**, and *cf.* compound **134** for the effect of the effect of the π - π interactions).
- The unit linking the peripheral group to the central core of the molecule plays a pivotal role in mesophase stability and morphology, for example flexible groups such as ester units when linking a benzene ring to the central core can lead to the nematic discotic phase, but more rigid units such as acetylenes or direct-linking can lead to retention of the columnar morphology (*cf.* compounds **135**, **144** and **146**).
- Interdigitation and intertwining of peripheral alkoxy chains can “lock” flexible peripheral groups into conformations, which can lead to the generation of columnar mesophase morphology in compounds which otherwise may not be expected to generate a columnar phase (*cf.* compounds **135** and **140**).
- Replacing a single peripheral group of the HAT6 structure can lead to the retention of the columnar phase morphology in cases where the replacement of all six peripheral units would ordinarily lead to the generation of the nematic discotic phase or the total loss of mesogenic behaviour, due to the reduction in steric factors (*e.g.* compound **146**).

6 References

1. H. Kelker and P. M. Knoll, *Liq. Cryst.*, 1989, **5**, 19-42.
2. R. Virchow, *Virchows Arch. path. Anat. Physiol.*, 1853, **6**, 571.
3. W. Heintz, *J. Prakt. Chem.*, 1855, **66**, 1.
4. F. Reinitzer, *Monatsh. Chem.*, 1888, **9**, 421-441.
5. F. Reinitzer, *Liq. Cryst.*, 1989, **5**, 7-18.
6. O. Lehmann, *Zeitschrift für Physikalische Chemie*, 1889, **4**, 462-467.
7. G. W. Gray, in *Physical Properties of Liquid Crystals*, eds. D. Demus, J. W. Goodby, G. W. Gray, H. W. Spiess and V. Vill, Wiley-VCH, Weinheim, 1999.
8. T. J. Sluckin, D. A. Dunmur and H. Stegemeyer, *Crystals that Flow*, Taylor and Francis, London & New York, 2004.
9. V. Vill, *Liq. Cryst.*, 1988, **24**, 21-24.
10. D. Vorländer, *Berichte der Deutschen Chemischen Gesellschaft*, 1907, **40**, 1970-1972.
11. G. Pelzl, I. Wirth and W. Weissflog, *Liq. Cryst.*, 2001, **28**, 969-972.
12. G. Friedel, *Annales de Physique*, 1922, **18**, 273-474.
13. P. J. Collings and M. Hird, *Introduction to Liquid Crystals*, Taylor & Francis, London & New York, 1997.
14. M. Barón, *Pure Appl. Chem.*, 2001, **73**, 845-895.
15. M. de Broglie and E. Friedel, *Comptes rendus de l'Académie des Sciences*, 1923, **176**, 738-740.
16. G. W. Gray, K. J. Harrison and J. A. Nash, *Electronic Letters*, 1973, **9**, 130-131.
17. G. W. Gray and D. G. McDonnell, *Electronic Letters*, 1975, **11**, 556-557.
18. J. Billard, *Liq. Cryst.*, 1998, **24**, 99-103.
19. H. J. Backer and S. Van der Baan, *Recl. Trav. Chim. Pays-Bas Belg.*, 1937, **56**, 1160.
20. J. E. Lydon, *British Liquid Crystal Society 21st Annual Conference*, Sheffield, 2007.
21. J. D. Bunning, J. E. Lydon, C. Eaborn, P. M. Jackson, J. W. Goodby and G. W. Gray, *J. Chem. Soc., Faraday Trans. 1*, 1982, **78**, 713-724.
22. S. Chandrasekhar, B. K. Sadashiva and K. A. Suresh, *Pramana*, 1977, **9**, 471-480.

23. S. Chandrasekhar, B. K. Sadashiva, K. A. Suresh, M. N. V., S. Kumar, R. Shashidhar and G. Venkatesh, *J. Phys. (Paris)*, 1979, **40**, 120-124.
24. R. J. Bushby and O. R. Lozman, *Current Opinion in Colloid and Interface Science*, 2002, **7**, 343-354.
25. S. Kumar, *Chem. Soc. Rev.*, 2006, **35**, 83-109.
26. J. W. Goodby, *Liq. Cryst.*, 1998, **24**, 25-38.
27. G. Tiddy, *British Liquid Crystal Society Winter Workshop*, University of Hull, 2004.
28. J. W. Goodby, *British Liquid Crystal Society Winter Workshop*, University of Hull, 2004.
29. J. W. Goodby and G. W. Gray, in *Physical Properties of Liquid Crystals*, eds. D. Demus, J. W. Goodby, G. W. Gray, H. W. Spiess and V. Vill, Wiley-VCH, Weinheim, 1999.
30. S. Chandrasekhar, *Liquid Crystals*, Second edn., Cambridge University Press, Cambridge, 1992.
31. K. M. Fergusson and M. Hird, *Adv. Mater.*, 2007, **19**, 211-214.
32. A. Isaacs, J. Daintith and E. Martin eds., *Oxford Concise Colour Science Dictionary*, Third edn., Oxford University Press, Oxford, 1997.
33. J. Daintith ed., *Oxford Dictionary of Chemistry*, Fourth edn., Oxford University Press, Oxford, 2000.
34. H. F. Gleeson, *British Liquid Crystal Society Winter Workshop*, University of Hull, 2004.
35. <http://plc.cwru.edu/tutorial/enhanced/main.htm>, Accessed 15/05/08.
36. M. Hird, *British Liquid Crystal Society Winter Workshop*, University of Hull, 2004.
37. J. W. Goodby, *J. Mater. Chem.*, 1991, **1**, 307-318.
38. S. Laschat, A. Baro, N. Steinke, F. Giesselmann, C. Hägele, G. Scalia, R. Judele, E. Kapatsina, S. Sauer, A. Schreivogel and M. Tosoni, *Angew. Chem. Int. Ed.*, 2007, **46**, 4832-4887.
39. G. W. Gray and J. W. Goodby, *Smectic Liquid Crystals: Textures and Structures*, Blackie Academic and Professional, 1984.
40. S. Chandrasekhar, *Contemporary Physics*, 1988, **29**, 527-558.

41. L. M. Blinov and V. G. Chigrinov, *Electrooptic Effects in Liquid Crystal Materials*, Springer, New York, 1996.
42. M. Hird, *10th International Conference on Ferroelectric Liquid Crystals*, Stare Jablonki, Poland, 2005.
43. M. Hird, *Liq. Cryst. Today*, 2005, **14**, 9-21.
44. G. Pelzl, S. Diele and W. Weissflog, *Adv. Mater.*, 1999, **11**, 707-724.
45. J. P. Bedel, J. C. Rouillon, J. P. Marcerou, M. Laguerre, H. T. Nguyen and M. F. Achard, *J. Mater. Chem.*, 2002, **12**, 2214-2220.
46. I. Dierking, *Textures of Liquid Crystals*, Wiley-VCH, Weinheim, 2003.
47. R. A. Reddy and C. Tschierske, *J. Mater. Chem.*, 2006, **16**, 907-961.
48. C. Tschierske, *Dendrimer Soft Self-assembly Systems DENSOM Euro-conference* Obernai, France, 2006.
49. T. W. G. Solomons and C. B. Fryhle, *Organic Chemistry*, Wiley, Hoboken, 2004.
50. J. Clayden, N. Greeves, S. Warren and P. Wothers, *Organic Chemistry*, Oxford University Press, Oxford, 2001.
51. K. J. Toyne, *Personal Communication*.
52. S. Chandrasekhar, *Liq. Cryst.*, 1993, **14**, 3-14.
53. S. Chandrasekhar and G. S. Ranganath, *Rep. Prog. Phys.*, 1990, **53**, 57-84.
54. D. Kardas, M. Prehm, U. Baumeister, D. Pocięcha, R. A. Reddy, G. H. Mehl and C. Tschierske, *J. Mater. Chem.*, 2005, **15**, 1722-1733.
55. K. Praefcke, D. Singer, B. Kohne, M. Ebert, A. Liebmann and J. H. Wendorff, *Liq. Cryst.*, 1991, **10**, 147-159.
56. K. Praefcke, in *Physical Properties of Liquid Crystals: Nematics*, eds. D. A. Dunmur, A. Fukuda and G. R. Luckhurst, INSPEC, The Institution of Electrical Engineers, London, 2001.
57. N. Terasawa, H. Monobe, K. Kiyohara and Y. Shimizu, *Chem. Comm.*, 2003, 1678-1679.
58. K. Kawata, *The Chemical Record*, 2002, **2**, 59-80.
59. N. Steinwke, W. Frey, A. Baro, S. Laschat, C. Drees, M. Nimitz, C. Hägele and F. Giesselmann, *Chem. Eur. J.*, 2006, **12**, 1026-1035.
60. M. T. Allen, S. Diele, K. D. M. Harris, T. Hegmann, B. M. Kariuki, D. Lose, J. A. Preece and C. Tschierske, *J. Mater. Chem.*, 2001, **11**, 302-311.

61. A. Fechtenkötter, N. Tchegotareva, M. D. Watson and K. Müllen, *Tetrahedron*, 2001, **57**, 3769-3783.
62. N. Boden, R. J. Bushby and A. N. Cammidge, *Mol. Cryst. Liq. Cryst.*, 1995, **260**, 307-313.
63. I. Paraschiv, P. Delforterie, M. Giesbers, M. A. Posthumus, A. T. M. Marcelis, H. Zuilhof and E. J. R. Sudhölter, *Liq. Cryst.*, 2005, **32**, 977-983.
64. N. Boden, R. J. Bushby, G. Cooke, O. R. Lozman and Z. B. Lu, *J. Am. Chem. Soc.*, 2001, **123**, 7915-7916.
65. P. Henderson, S. Kumar, J. Rego, H. Ringsdorf and P. Schuhmacher, *J. Chem. Soc., Chem. Comm.*, 1995, 1059-1060.
66. H. Heaney and I. T. Millar, *Organic Syntheses*, 1960, **40**, 105.
67. A. N. Cammidge and H. Gopee, *Mol. Cryst. Liq. Cryst.*, 2003, **397**, 117-128.
68. N. Boden, R. C. Borner, R. J. Bushby, A. N. Cammidge and M. V. Jesudason, *Liq. Cryst.*, 1993, **15**, 851-858.
69. N. Boden, R. J. Bushby, A. N. Cammidge, S. Duckworth and G. Headdock, *J. Mater. Chem.*, 1997, **7**, 601-605.
70. N. Boden, R. J. Bushby and A. N. Cammidge, *Liq. Cryst.*, 1995, **18**, 673-676.
71. N. Boden, R. J. Bushby, A. N. Cammidge and G. Headdock, *J. Mater. Chem.*, 1995, **5**, 2275-2281.
72. A. N. Cammidge, *British Liquid Crystal Society 20th Annual Conference*, York, 2006.
73. S. Kumar and S. K. Varshney, *Angew. Chem. Int. Ed.*, 2000, **39**, 3140-3142.
74. J. W. Goodby, *Chem. Soc. Rev.*, 2007, **36**, 1855-1856.
75. J. A. Hunt, *The Pharmaceutical Journal*, 1999, **263**, 985-989.
76. M. Hird, *University of Hull 75th Anniversary*, University of Hull, 2003.
77. M. Hird, *Personal Communication*.
78. G. Lester, *British Liquid Crystal Society Winter Workshop*, University of Hull, 2004.
79. M. Hird, *Royal Society of Chemistry Landmark Achievement Award Ceremony*, University of Hull, 2005.
80. M. Schadt and W. Helfrich, *Applied Physics Letters*, 1971, **18**, 127-128.
81. M. Schadt, *Liq. Cryst.*, 1989, **5**, 57-71.
82. S.-T. Wu and D.-K. Yang, *Reflective Liquid Crystal Displays*, Wiley, 2001.

83. D. Pauluth and K. Tarumi, *J. Mater. Chem.*, 2004, **14**, 1219-1227.
84. D. Pauluth and K. Tarumi, *J. Soc. Inf. Display*, 2005, **13**, 693-702.
85. P. Van de Witte, S. Stallinga and J. A. M. M. Van Haaren, *Japanese Journal of Applied Physics*, 2000, **39**, 101-108.
86. M. Lu and K. H. Yang, *Japanese Journal of Applied Physics*, 2000, **39**, L412-L415.
87. O. V. Kruglova, *Discotic Liquid Crystals: from dynamics to conductivity*, IOS Press, Amsterdam, 2007.
88. N. Boden, R. J. Bushby, O. R. Lozman, Z. B. Lu, A. McNeill and B. Movaghar, *Mol. Cryst. Liq. Cryst.*, 2004, **410**, 541-549.
89. R. J. Bushby and O. R. Lozman, *Current Opinion in Solid State & Materials Science*, 2002, **6**, 569-578.
90. N. Boden, R. J. Bushby, J. Clements and B. Movaghar, *J. Mater. Chem.*, 1999, **9**, 2081-2086.
91. N. Boden, R. J. Bushby and J. Clements, *J. Chem. Phys.*, 1993, **98**, 5920-5931.
92. N. Boden, R. J. Bushby, J. Clements, B. Movaghar, K. J. Donovan and T. Kreouzis, *Phys Rev B*, 1995, **52**, 13274-13280.
93. T. Kreouzis, K. J. Donovan, N. Boden, R. J. Bushby, O. R. Lozman and Q. Liu, *J. Chem. Phys.*, 2001, **114**, 1797-1802.
94. N. Boden, R. J. Bushby, J. Clements, K. Donovan, B. Movaghar and T. Kreouzis, *Phys Rev B*, 1998, **58**, 3063-3074.
95. K. Donovan, *Proc. Int. Symp. Super-Functionality Organic Devices, IPAP Conference Series 6*, 2004, 38-41.
96. A. M. van de Craats and J. M. Warman, *Adv. Mater.*, 2001, **13**, 130-133.
97. Q. Li and L. Li, in *Thermotropic Liquid Crystals: Recent Advances*, ed. A. Ramamoorthy, Springer, 2007.
98. S. Sergeev, W. Pisula and Y. H. Geerts, *Chem. Soc. Rev.*, 2007, **36**, 1902-1929.
99. S. Kumar, *Current Science*, 2002, **82**, 256-257.
100. L. Schmidt-Mende, A. Fechtenkötter, K. Müllen, E. Moons, R. H. Friend and J. D. MacKenzie, *Science*, 2001, **293**, 1119-1122.
101. J. Nelson, *Science*, 2001, **293**, 1059-1060.
102. M. O'Neill and S. M. Kelly, *Adv. Mater.*, 2003, **15**, 1135-1147.
103. J. Nelson, *Current Opinion in Solid State & Materials Science*, 2002, **6**, 87-95.

104. G. W. Gray, M. Hird, D. Lacey and K. J. Toyne, *J. Chem. Soc., Perkin Trans. II*, 1989, 2041-2053.
105. D. Pérez and E. Guitián, *Chem. Soc. Rev.*, 2004, **33**, 274-283.
106. D. R. Coulson, *Inorganic Synthesis*, 1972, **13**, 121-124.
107. D. Chen, L. Wan, J. Fang and X. Yu, *Chemistry Letters*, 2001, **30**, 1156-1157.
108. E. Nishikawa, J. Yamamoto, H. Yokoyama and E. T. Samulski, *Mol. Cryst. Liq. Cryst.*, 2001, **364**, 605-610.
109. P. C. Ferreira, N. Z. Kiyan, Y. Miyata and J. Miller, *J. Chem. Soc., Perkin Trans. II*, 1976, 1648-1651.
110. H. N. S. Murthy and B. K. Sadashiva, *J. Mater. Chem.*, 2004, **14**, 2813-2821.
111. B. Jones, *J. Chem. Soc.*, 1943, 430 - 432.
112. J. Kim, Y. K. Kim, N. Park, J. H. Hahn and K. H. Ahn, *J. Org. Chem.*, 2005, **70**, 7087-7092.
113. D. R. Beattie, P. Hindmarsh, J. W. Goodby, S. D. Haslam and R. M. Richardson, *J. Mater. Chem.*, 1992, **2**, 1261-1266.
114. D. Stewart, G. S. McHattie and C. T. Imrie, *J. Mater. Chem.*, 1998, **8**, 47-51.
115. S. J. Cross, J. W. Goodby, A. W. Hall, M. Hird, S. M. Kelly, K. J. Toyne and C. Wu, *Liq. Cryst.*, 1998, **25**, 1-11.
116. A. O. Fitton and G. R. Ramage, *J. Chem. Soc.*, 1962, 4870 - 4874.
117. R. A. Reddy and B. K. Sadashiva, *J. Mater. Chem.*, 2002, **12**, 2627-2632.
118. K. Borisch, S. Diele, P. Göring, H. Kresse and C. Tschierske, *J. Mater. Chem.*, 1998, **8**, 529-543.
119. S. G. Yang and Y. H. Kim, *Tetrahedron Lett.*, 1999, **40**, 6051-6054.
120. I. J. Blackmore, A. N. Boa, E. J. Murray, M. Dennis and S. Woodward, *Tetrahedron Lett.*, 1999, **40**, 6671-6672.
121. Y. Noda and M. Kashima, *Tetrahedron Lett.*, 1997, **38**, 6225-6228.
122. M. C. Carreno, J. L. G. Ruano, G. Sanz, M. A. Toledo and A. Urbano, *Tetrahedron Lett.*, 1996, **37**, 4081-4084.
123. Y. Brunel and G. Rousseau, *Tetrahedron Lett.*, 1995, **36**, 8217-8220.
124. S. M. Hubig, W. Jung and J. K. Kochi, *J. Org. Chem.*, 1994, **59**, 6233-6244.
125. J. Barluenga, J. M. González, M. A. Garcia-Martin, P. J. Campos and G. Aseniso, *J. Org. Chem.*, 1993, **58**, 2058-2060.

126. G. A. Olah, Q. Wang, G. Sandford and G. K. S. Prakash, *J. Org. Chem.*, 1993, **58**, 3194-3195.
127. W.-W. Sy, *Tetrahedron Lett.*, 1993, **34**, 6223-6224.
128. A. Bachki, F. Foubelo and M. Yus, *Tetrahedron*, 1994, **50**, 5139-5146.
129. K. J. Edgar and S. N. Falling, *J. Org. Chem.*, 1990, **55**, 5287-5291.
130. R. Ghorbani-Vaghei, *Tetrahedron Lett.*, 2003, **44**, 7529-7532.
131. A. S. Castanet, F. Colobert and P. E. Broutin, *Tetrahedron Lett.*, 2002, **43**, 5047-5048.
132. B. Neises and W. Steglich, *Angew. Chem. Int. Ed.*, 1978, **17**, 522-524.
133. <http://www.organic-chemistry.org/namedreactions/steglich-esterification.shtm>, Accessed 24/10/2005.
134. <http://www.orgsyn.org/orgsyn/orgsyn/prepContent.asp?prep=cv7p0093>, Accessed 22/11/2007.
135. <http://www.organic-chemistry.org/namedreactions/fischer-esterification.shtm>, Accessed 4/12/2007.
136. W. Steglich and G. Höfle, *Angew. Chem. Int. Ed.*, 1969, **8**, 981.
137. C. Destrade, N. H. Tinh, H. Gasparoux, J. Malthete and A. M. Levelut, *Mol. Cryst. Liq. Cryst.*, 1981, **71**, 111-135.
138. N. H. Tinh, M. C. Bernaud, G. Sigaud and C. Destrade, *Mol. Cryst. Liq. Cryst.*, 1981, **65**, 307-316.
139. G. A. Clowes, *J. Chem. Soc. C*, 1968, 2519-2526.
140. P. Rempala, J. Kroulik and B. T. King, *J. Org. Chem.*, 2006, **71**, 5067-5081.
141. R. C. Borner, R. J. Bushby and A. N. Cammidge, *Liq. Cryst.*, 2006, **33**, 1439-1442.
142. N. Miyaoura, T. Yanagi and A. Suzuki, *Synth. Commun.*, 1981, **11**, 513-519.
143. D. J. Sinclair and M. S. Sherburn, *J. Org. Chem.*, 2005, **70**, 3730-3733.
144. R. J. Bushby and Z. B. Lu, *Synthesis*, 2001, 763-767.
145. R. J. Bushby, *Personal Communication*.
146. K. M. Fergusson and M. Hird, *British Liquid Crystal Society Annual Meeting*, Exeter, U.K., 2005.
147. M. Hird, Y. Raoul, J. W. Goodby and H. F. Gleeson, *9th International Conference on Ferroelectric Liquid Crystals*, Dublin, Ireland, 2003.
148. K. M. Fergusson, *Personal Communication*.

149. <http://www.phenomenex.com/phen/Doc/z366.pdf>, Accessed 10/12/2007.
150. <http://www.organic-chemistry.org/namedreactions/finkelstein-reaction.shtml>, Accessed 17/04/08.
151. A. O. King, N. Okukado and E.-I. Negishi, *J. Chem. Soc., Chem. Comm.*, 1977, 683-684.
152. K. Sonogashira, Y. Tohda and Hagihara, *Tetrahedron Lett.*, 1975, **16**, 4467-4470.
153. I. M. Matheson, O. C. Musgrave and C. J. Webster, *Chem. Comm.*, 1965, **13**, 278-279.
154. S. Kumar and M. Manickam, *Chem. Comm.*, 1997, 1615-1616.
155. S. Kumar and S. K. Varshney, *Liq. Cryst.*, 1999, **26**, 1841-1843.
156. O. C. Musgrave, *Chemical Reviews*, 1969, **69**, 499-531.
157. S. Kumar, *Liq. Cryst.*, 2004, **31**, 1037-1059.
158. N. Boden, R. C. Borner, R. J. Bushby, A. N. Cammidge and M. V. Jesudason, *Liq. Cryst.*, 2006, **33**, 1443-1448.
159. J. W. Goodby, M. Hird, K. J. Toyne and T. Watson, *J. Chem. Soc., Chem. Comm.*, 1994, 1701-1702.
160. R. C. Borner and R. F. W. Jackson, *J. Chem. Soc., Chem. Comm.*, 1994, 845-846.
161. R. J. Bushby, J. Fisher, O. R. Lozman, S. Langer, J. E. Lydon and S. R. McLaren, *Liq. Cryst.*, 2006, **33**, 653-664.
162. M. Hird, *Chem. Soc. Rev.*, 2007, **36**, 2070-2095.
163. P. Hindmarsh, M. Hird, P. Styring and J. W. Goodby, *J. Mater. Chem.*, 1993, **3**, 1117-1128.
164. P. Hindmarsh, M. J. Watson, M. Hird and J. W. Goodby, *J. Mater. Chem.*, 1995, **5**, 2111-2123.
165. R. J. Bushby, N. Boden, C. A. Kilner, O. R. Lozman, Z. Lu, Q. Liu and M. A. Thornton-Pett, *J. Mater. Chem.*, 2003, **13**, 470-474.
166. W. Pisula, M. Kastler, D. Wasserfallen, M. Mondeshki, J. Piris, I. Schnell and K. Müllen, *Chem. Mater.*, 2006, **18**, 3634-3640.
167. C.-y. Liu, A. Fechtenkötter, M. D. Watson, K. Müllen and A. J. Bard, *Chem. Mater.*, 2003, **15**, 124-130.
168. S. Kumar, D. S. S. Rao and S. K. Prasad, *J. Mater. Chem.*, 1999, **9**, 2751-2754.

169. S. Kumar, J. J. Naidu and D. S. S. Rao, *J. Mater. Chem.*, 2002, **12**, 1335-1341.
170. P. G. Schouten, J. M. Warman, M. P. De Hass, C. F. van Nostrum, G. H. Gelinck, R. J. M. Nolte, M. J. Copyn, J. W. Zwikker, M. K. Engel, M. Hanack, Y. H. Chang and W. T. Ford, *J. Am. Chem. Soc.*, 1994, **116**, 6880-6894.
171. D. M. Collard and C. P. Lillya, *J. Am. Chem. Soc.*, 1991, **113**, 8577-8583.
172. K. Praefcke, B. Kohne and D. Singer, *Angew. Chem. Int. Ed.*, 1990, **29**, 177-179.
173. A. N. Cammidge, A. R. Beddall and H. Gopee, *Tetrahedron Lett.*, 2007, **48**, 6700-6703.
174. M. Hird and K. J. Toyne, *Mol. Cryst. Liq. Cryst.*, 1998, **323**, 1-67.
175. K.-Q. Zhao, B.-Q. Wang, P. Hu, Q. Li and L.-F. Zhang, *Chinese Journal of Chemistry*, 2005, **23**, 764-774.
176. H. Liu and H. Nohira, *Liq. Cryst.*, 1998, **24**, 719-726.
177. K.-Q. Zhao, B.-Q. Wang, P. Hu, C.-Y. Gao, F.-J. Yuan and H.-R. Li, *Chinese Journal of Chemistry*, 2006, **24**, 210-214.